INTERACTIONS BETWEEN NEURONAL INNATE IMMUNE PATTERN RECOGNITION RECEPTOR PATHWAYS AND NEUROTROPIC ARBOVIRUSES: HOST MEASURES, VIRAL COUNTERMEASURES, AND POTENTIAL THERAPEUTICS

by

Daniel C. Peltier

A dissertation submitted in partial fulfillment
of the requirements for the degree of
Doctor of Philosophy
(Microbiology and Immunology)
In the University of Michigan
2010

Doctoral Committee:

Associate Professor David Miller, Chair
Professor Michael J. Imperiale
Professor Richard R. Neubig
Professor Michele S. Swanson
Assistant Professor Sonja R. Gerrard

2010

ACKNOWLEDGMENTS

I'd like to start by thanking everyone who collaborated with me and made these studies possible. Chapter II would not have been possible without the excellent assistance of Allison Simms and Jocelyn Farmer who helped perform the kinase inhibitor screen and helped perform PRR expression analysis respectively. Chapter III would not have been possible without the excellent assistance of Helen McGraw-Lazear and Jocelyn Farmer who provided mouse cortical tissue and HESC-derived neurons respectively. Finally, chapter IV would not have been possible without the excellent assistance of the staff at the Center for Chemical Genomics at the University of Michigan and Weiping Peng who helped validate the antiviral activity of CCG-32091.

I'd like to thank the Miller lab members, both past and present, for putting up with me, teaching me, collaborating with me, hanging out, and just making lab an enjoyable place to work. I'll miss you all and best of luck in your future endeavors.

I'd like to thank my advisor, David Miller, for his mentorship during my dissertation research. Dave allowed me to dream big, make my own mistakes, pursue my own ideas, and somehow gently put me back on course when I strayed. He always made me feel like a colleague, even when I was obviously in

need of a teacher, and I would not be the same independent scientist I feel I am today without his mentorship. Thank you, Dave.

I need to thank my committee members for their critical evaluation of my research and incredibly helpful suggestions. This body of work would not have been possible without your guidance and suggestions.

Importantly, I need to thank all of my friends for their continued love, support, and encouragement. I could not have completed this work without you.

I don't think a thank you can do justice for the love and support my parents and siblings provided, but that is all I can offer on this page. Thanks Mom, Dad, Chad, Joe, Adam, and Carrie. I love you guys. Similarly, I need to thank my new family, the Temmes, for all of their support. I appreciate all that you have done for Marliese and me. Thank you!

Finally, I need to thank my beautiful, talented, and caring wife Marliese. Her support, more than anyone else's, was critical over the last few years. She was my number one fan and sturdiest shoulder to lean on. Thank you, and I love you.

TABLE OF CONTENTS

LIST OF FIGURES

Figure

LIST OF TABLES

Table

ABSTRACT

Neurotropic arboviruses are a group of pathogens capable of causing severe and fatal central nervous system infections for which there are few effective treatments or vaccines. The extent of neurotropic arbovirus-mediated destruction of central nervous system neurons is often an important determinant in the severity and clinical outcome after infection. Early cellular innate immune responses mediated by pattern recognition receptors (PRRs) are often vital for effective pathogen control, and an effective neuronal innate immune response may be crucial to prevent the essentially irreversible loss of critical central nervous system neurons by neurotropic arboviruses. The work presented here describes efforts to preserve neurotropic arbovirus-infected neurons by: a) studying the interactions between neurotropic arboviruses and neuronal PRR pathways in order to indentify novel targets for future therapeutics, and b) identifying potential anti-neurotropic arbovirus medications which target viral replication.

Innate PRR pathways function in both a cell and pathogen-specific manner. However, relatively little is known about the induction and regulation of neuronal PRR signaling. Therefore, I assessed PRR pathway expression and function in neurons and found that neurons possess functional PRR pathways mediated by select receptors and signaling molecules which activate the downstream transcription factors NFκB and IRF3 resulting in the production of genes with putative antiviral activity. Next, I characterized how neuronal PRR pathways interact with neurotropic arboviruses using western equine encephalitis virus (WEEV) as a model neurotropic arbovirus. From these studies I concluded that IRF3 mediates a neuron-protective response to WEEV; however, this response was independent of type-I IFN signaling, which possesses potent antiviral activity and is canonically activated downstream of IRF3 in alternate cell types. Importantly, WEEV inhibited neuronal PRR-mediated induction of antiviral type-I interferons, and this inhibitory capacity was mapped to the WEEV capsid protein. These data indicated that neuronal PRR pathways may be important determinants in neurotropic arbovirus pathogenesis and that neuronal PRR pathways and viral countermeasures to them may be exploited to develop anti-neurotropic arboviral treatments. Finally, I identified a novel class of small molecules which inhibit WEEV replication, protect neuronal cells from WEEV-induced cell death, and may be a useful component of future anti-neurotropic arbovirus therapies.

Chapter I

General Introduction

Early cellular innate immune responses are vital for effective pathogen control, and an effective neuronal innate immune response may be crucial to prevent the essentially irreversible loss of critical central nervous system neurons by neurotropic arboviruses. Neurotropic arboviruses are a group of viral pathogens transmitted by insect vectors, most often mosquitoes, capable of causing severe and potentially fatal central nervous system infections in humans. Unfortunately there are very few effective treatments or vaccines for these viral infections, which are classified as NIAID Category B Priority Pathogens due to their potential misuse as bioterrorism agents. The extent of neurotropic arbovirus-mediated destruction of central nervous system neurons is often an important determinant in the severity and clinical outcome after infection. The work presented here describes efforts to preserve neurotropic arbovirus-infected neurons by: a) studying the interaction between neurotropic arboviruses and the neuronal innate immune response to indentify novel targets for future therapeutics and vaccines; and b) identifying potential anti-neurotropic arbovirus medications which inhibit viral replication. This introductory chapter provides background information on innate cellular immunity and neurotropic arbovirus

pathogenesis with a particular emphasis on the new world alphavirus western equine encephalitis virus which is the model neurotropic arbovirus primarily studied in this body of work.

Neurotropic Arbovirus Epidemiology and Clinical Significance

Neurotropic arboviruses preferentially infect central nervous system (CNS) neurons and include but are not limited to West Nile virus (*Flaviviridae*), St. Louis encephalitis virus (*Flaviviridae*), La Crosse virus (*Bunyaviridae*), and the equine encephalitic alphaviruses (*Togaviridae* genus alphavirus) (**Table 1.1**). Neurotropic arboviruses are transmitted via insect vectors and are responsible for sporadic epidemics of viral encephalitis (71). Many neurotropic arboviruses are endemic to North America including West Nile virus (WNV), St. Louis encephalitis virus (SLEV), La Crosse virus (LACV), Western equine encephalitis virus (WEEV), Eastern equine encephalitis virus (EEEV), and Venezuelan equine encephalitis virus (VEEV) (26). Most infections occur during warmer, moister months due to increased amounts of mosquito vectors and an increased amount of time spent outdoors by the human population in temperate regions (132). There are currently no recommended or approved anti-viral treatments for these viral infections, and the standard of care is purely supportive (132). Ribavirin, an FDA-approved nucleoside analogue, may be beneficial for some neurotropic arboviruses in the *Flaviviridae* family (90), but definitive clinical evidence is lacking (8). Initial studies have identified novel small molecules with

Table 1.1. Neurotropic arboviruses.

Family	Genus	Species	Genome	BSL	Priority
Togaviridae	Alphavirus	– Western equine encephalitis virus – Eastern equine encephalitis virus – Venezuelan equine encephalitis viruses	Positive sense RNA (subgenome structural gene production)	3	B
Flaviviridae	Flavivirus	– St. Louis encephalitis virus – West Nile virus – Japanese encephalitis virus	Positive sense RNA	3	B
Bunyaviridae	Orthobunyavirus	– La Crosse virus – California encephalitis viruses	Segmented negative sense RNA	2	B

BSL-biosafety level, Priority-NIAID Pathogen Category Priority

anti-neurotropic arboviral properties (121, 122, 128), but it is unclear how clinically useful these will be. Vaccines to some neurotropic-arboviruses exist, including WEEV, EEEV, VEEV, and Japanese encephalitis virus (JEV), but with the exception of JEV, which is not endemic to North America, they are all poorly protective, have significant side effects including mild encephalitic symptoms for the VEEV vaccine, and are not available to the general public (155). Development of better vaccines for neurotropic arboviruses is an active area of research, and several promising candidates have been identified (12, 54, 123, 152, 168, 169, 174, 181). To summarize, there is a great need for better vaccines and effective antivirals to treat neurotropic arbovirus infections.

Most neurotropic arboviruses are listed as NIAID priority A, B, or C pathogens due to numerous characteristics that make them potential biological weapons including: a) high clinical morbidity and mortality; b) potential for aerosol transmission; c) lack of effective countermeasures for disease prevention or control; d) public anxiety elicited by CNS infections; e) ease with which large volumes of infectious materials can be produced; and f) potential for malicious introduction of foreign genes designed to increase virulence (23, 155). Unfortunately, it is widely thought that VEEV has been weaponized for aerosol delivery (80). Due to many of the same reasons that contribute to their classification as potential biological weapons, many neurotropic arboviruses require biosafety level 3 containment (33), highlighting the importance of understanding and being able to combat these severe pathogens.

The clinical portrait of neurotropic arbovirus infection can range from moderate constitutional symptoms and uncomplicated resolution to fulminant encephalitis, especially in the young, old, immunocompromised, or chronically ill (64, 72, 132, 142, 151). The incubation period for neurotropic arbovirus encephalitis ranges from 2-21 days, and encephalitis is typically preceded by a prodrome of fever, malaise, headache, stiff neck, and occasionally sore throat and nausea/vomiting. These symptoms can then progress to fulminant encephalitis including changes in mentation, stupor, coma, convulsions, and signs of upper motor neurons lesions such as exaggerated deep tendon reflexes and spastic paralysis. Diagnosis is usually accomplished by identifying pathogen-specific IgM antibodies in the cerebral spinal fluid of symptomatic patients. The acute encephalitic phase lasts from a few days to as long as 2-3 weeks, and full recovery, if achieved, may take months (64, 72, 132, 142, 151). However, survivors, especially children, are often left with significant sequelae including changes in cognition, seizures, developmental delays, and motor deficits.

The virulence of each neurotropic arbovirus as measured by case fatality rates varies on the high end from 50-75% for EEEV and 20-50% for JEV (132). On the low end, La Crosse virus case fatality rates are about 0.5 %, and the majority of neurotropic arboviruses including WEEV, SLEV, and WNV have intermediate case fatality rates of 5-10% (132). Neurotropic arboviruses also have a wide range of case-to-infection ratios where the more prevalent West Nile, St. Louis, and La Crosse viruses have ratios of 1:100, 1:200, and 1:1000,

respectively, whereas the equine encephalitic alphaviruses have ratios ranging from 1:1 to 1:1000 (132). In the United States, there are about 5-10 cases of each of the equine encephalitis viruses and about 75 cases for LACV and SLEV annually; however, all of these viruses undergo sporadic epidemics in which the number of cases can soar into the thousands and historically reach as high as several hundred thousand (64, 132, 142). For example, prior to the introduction of WNV to North America in 1999, WNV was not endemic to the continent; now, approximately 1000-3000 cases and 100-300 deaths can be attributed to it each year (132, 142). However, neurotropic arbovirus epidemics do not necessarily involve geographical relocation to areas with immunologically naïve populations (64).

Predilection for clinically apparent disease of specific age groups varies among the neurotropic arboviruses. La Crosse encephalitis primarily infects children less than 15 years old whereas WNV typically causes disease in the elderly (132). SLEV causes a milder disease in the young and a more severe disease in those greater than 40 years of age (132). The equine encephalitic alphaviruses all have a predilection for children, which is most apparent for WEEV where the case to infection ratio is 1:1 for infants versus 1:1000 for adults (132). Interestingly, WEEV also has a slight predilection for causing disease in males over females, a feature of WEEV epidemiology that remains relatively understudied (64, 132). In summary, neurotropic arboviruses generally cause severe, sporadic epidemics, especially in vulnerable human populations including

the young and the old, and there are currently no broadly approved antiviral medications or vaccines to treat or prevent these infections.

Neurotropic Arbovirus Biology

Neurotropic arboviruses belong to one of three viral families: *Flaviviridae,* *Bunyaviridae,* and *Togaviridae*. Each of these families has a unique genomic structure, and that of the equine encephalitic alphaviruses will be thoroughly reviewed in a later section. The genomes of flaviviruses and togaviruses consist of a single positive-sense RNA that can be immediately transcribed upon entry into the cytosol (94, 106). Both togavirus and flavivirus genomes contain 5' cap structures analogous to that of cellular mRNAs, but only togavirus genomes are 3' polyadenylated (94, 106). Furthermore, the togavirus structural proteins are translated as a polyprotein from a transcript whose production is controlled by a viral subgenomic promoter on the viral negative-sense genomic strand. Due to this genomic architecture, expression of alphavirus structural proteins requires viral RNA replication (94). In contrast, flavivirus structural proteins are synthesized directly from genomic RNA (106). Unlike flavi- and togavirus genomes, bunyavirus genomes consist of three negative-sense RNA segments which lack 5' caps and polyadenylated tails, and some bunyaviruses also have ambisense segments (151). The negative orientation of the bunyavirus genomic segments necessitates the inclusion of at least one viral RNA-dependent RNA polymerase (RdRp) within each viral particle to initiate synthesis of positive-

sense strands to produce viral proteins and negative-sense genomic strands for packaging into viral progeny (151). Despite the obvious differences in genomic architecture and RNA replication strategies among the neurotropic arboviruses, important similarities among these viruses exist such as: a) they consist of an enveloped viral particle with an encapsidated RNA genome; b) they almost exclusively replicate in the cytoplasm of host cells; and c) they have the ability to directly infect and damage CNS neurons (64, 94, 106, 151). Due to these important similarities and differences, interaction of these viruses with neuronal innate immune pathways may also have both unique and common features.

The natural life cycle of neurotropic arboviruses involves an enzootic cycle generally between mosquitoes and birds or other small animals (64, 72, 132, 142, 151). Periodically, an epizootic cycle initiates resulting in the infection of larger mammals and humans; however, humans and large mammals are generally dead-end hosts and, except for VEEV epizootics and horses, do not sustain epizootic cycles (26, 64, 72, 132, 142, 151). The involvement of abundant non-human reservoirs in the natural life cycle of neurotropic arboviruses makes them an important source of re-emerging pathogens with potentially increased virulence (71). One example of a re-emerging arboviral pathogen is that of Chickungunya virus, a close relative to the equine encephalitic arboviruses. From 2004-2009, this virus caused millions of cases of Chickungunya fever in south eastern Asia and the Indian subcontinent, which is characterized by fever, rash, and arthritis (157). It is hypothesized that mutations

in its receptor binding protein allowed Chickungunya virus to infect more anthropophilic mosquito vectors, thereby contributing to a massive outbreak of what was a relatively uncommon human pathogen (157).

Neurotropic arboviruses infect humans when an infected arthropod takes a blood meal from a human host. Depending on the virus, it may infect tissues at the site of infection and undergo local replication and subsequent viremia, or it may infect cells of the reticuloendothelial system and secondary lymphoid organs followed by replication in these secondary tissues and viremia (47, 64, 72, 108, 112, 130, 151). Viremia leads to CNS invasion, which for most neurotropic arboviruses is not completely understood but may involve infection of the olfactory neuroepithelium with passage through the cribiform plate and/or infection of cerebral endovascular cells and subsequent multifocal entry into the CNS (47, 64, 72, 130, 132, 151). Within the CNS, most neurotropic arboviruses primarily infect neurons with little infection of supporting neuronal cell types such as oligodendrocytes, astrocytes, and microglia (26, 47, 64, 72, 130, 132, 151). The areas of the CNS targeted by each neurotropic arbovirus varies slightly, but in general, the cortex, basal ganglia, and brainstem are most often affected (26, 47, 64, 72, 130, 132, 151). The histopathology of infected CNS tissue reveals wide-spread neuron destruction, perivascular cuffing with polymorphonuclear cells and mononuclear leukocytes, and vasculitis with vessel occlusion (26, 47, 64, 72, 130, 132, 151). Apoptotic glia and inflammatory cells are also often found near affected neurons, and the meninges can also become inflamed and/or

infected (26, 47, 64, 72, 130, 132, 151). Important for this body of work, the clinical symptoms of encephalitis and subsequent sequelae arise directly from viral-induced damage of neurons and partly from indirect damage of neurons due to edema and inflammation, suggesting that discovering ways of preventing neuron damage may lead to novel treatments for these devastating infections.

Immune Response to Neurotropic Arboviruses

The immune response to neurotropic arbovirus infection is complex and ultimately pathogen-specific, but a couple of important parallels can be discerned among these viruses. First, innate immune signaling is important for the response to many neurotropic arbovirus infections, as demonstrated by increased mortality, neurovirulence, viral load, and extraneural viral dissemination in the absence of an intact type-I IFN signaling pathway (18, 64, 110, 146, 179). Second, disease resolution and immune-mediated clearance of many neurotropic arboviruses requires adaptive B and T-cells (46, 64, 65). These observations indicate that a highly orchestrated immune response, involving both innate and adaptive branches of the immune system, is needed for successful resolution of neurotropic arboviral infections.

It is not particularly surprising that, like most viral infections, both the innate and adaptive immune systems are required for efficient resolution of neurotropic arbovirus infections, but immune-mediated clearance of virus from the CNS is likely more regulated than clearance from other sites of infection

because the brain is thought to be an immuno-privileged organ (65). For instance, cerebral capillary endothelial cells are relatively unreactive and contribute to a blood-brain barrier, which is a physiologic barrier that normally ensures low levels of leukocytes and lymphocytes within the CNS (30, 65, 87). The blood-brain barrier is not an absolute barrier because a systemic immune response to a peripheral infection can increase its permeability, resulting in increased CNS immune surveillance (79, 105). In addition to limiting immune system access to the CNS via the blood-brain barrier, the CNS also tightly regulates the adaptive immune response through limited MHC expression and active suppression of cytotoxic T-cell responses (65). These data suggest that the immune response within the CNS is highly regulated, a finding that may reflect the need of the CNS to preserve vital CNS neurons, which have a very limited self-renewal capacity, from immune-mediated damage.

Most cell-types in the CNS play an active role in the regulated immune response to neurotropic viral infections, including neurons, astrocytes, and microglia (46, 65, 72, 100, 131, 151). For instance, neurons may participate in the innate response by generating antiviral type-I and II interferons (44, 65, 125, 131), but these same cytokines can also be neurotoxic when produced in excess (5, 65, 131). Like neurons, glial cells (astrocytes, oligodendrocytes, and microglia) are capable of producing an innate response, and microglia, which are the myeloid-derived resident cell-type in the CNS, contain highly active TLR-mediated pathways (103, 140). Importantly, glial cell PRR signaling may mediate

the neuropathology of several diseases, including viral encephalomyelitis (103, 140). These observations further demonstrate the intricacy and the participation of multiple CNS resident cell types in immune responses within the CNS.

Neurons are relatively resistant to both viral-induced death and T-cell killing, which is consistent with their limited capacity for self-renewal, and suggests that immune-mediated clearance of virus from the CNS is neuron sparing (65). Furthermore, clearance of virus from neurons is generally heavily dependent on antibody and cytokine responses, whereas cytotoxic T-cell responses may not be required for all neurotropic pathogens (46, 65). Due to the general neuron-sparing nature of the immune response in the CNS, symptom resolution may be due to an immune response that checks viral replication and spread and may not completely eliminate all viral RNA (65). Consistent with this, viral RNA can be detected in the CNS throughout the life of recovered animals along with antiviral antibody, which suggests that low-level, non-cytolytic, immune-mediated control may be required for long-term resolution of viral-induced disease (64, 65, 127). In summary, all arms of the immune system are involved in neurotropic arbovirus resolution, including innate responses from neurons, and the clearance of virus from the CNS is highly regulated and neuron-sparing.

Neurotropic Alphavirus Basic Biology and Replication Cycle

Alphaviruses have long been used as model neurotropic arbovirus pathogens and are generally subdivided into new and old world viruses based on their location primarily in the western or eastern hemispheres, respectively (150). The commonly studied old world alphaviruses, Sindbis (SIN) and Semliki Forest (SFV) viruses, cause a febrile illness associated with rash and polyarthropathy, whereas the more virulent new world alphaviruses WEEV, EEEV, and VEEV typically cause CNS infections (26, 45, 51). The new world alphaviruses naturally infect the CNS (26, 32, 75). Thus, we chose WEEV as our model alphavirus to study the interaction of neurotropic arboviruses with neuronal innate immune pathways. However, most of the knowledge regarding alphavirus biology and neuropathogenesis was gained by studying old world pathogens such as SFV and neuro-adapted SINV, suggesting that our knowledge of encephalitic alphavirus pathogenesis may be incomplete.

The alphavirus genome is roughly 11-12 kb in length and encodes the non-structural proteins, which are required for RNA replication, on the 5' two-thirds, and the viral structural genes on the 3' one-third (**Fig 1.1**) (94). Non-structural protein-1 (nsP1) is a methyl-transferase involved in 5'-capping (118). Non-structural protein-2 (nsP2) contains both helicase and protease activity. The nsP2 helicase is required for efficient replication, and the protease activity is required for polyprotein processing (62, 171). Non-structural protein-3 (nsP3) is a phosphoprotein with no known function, although it appears to play a role in

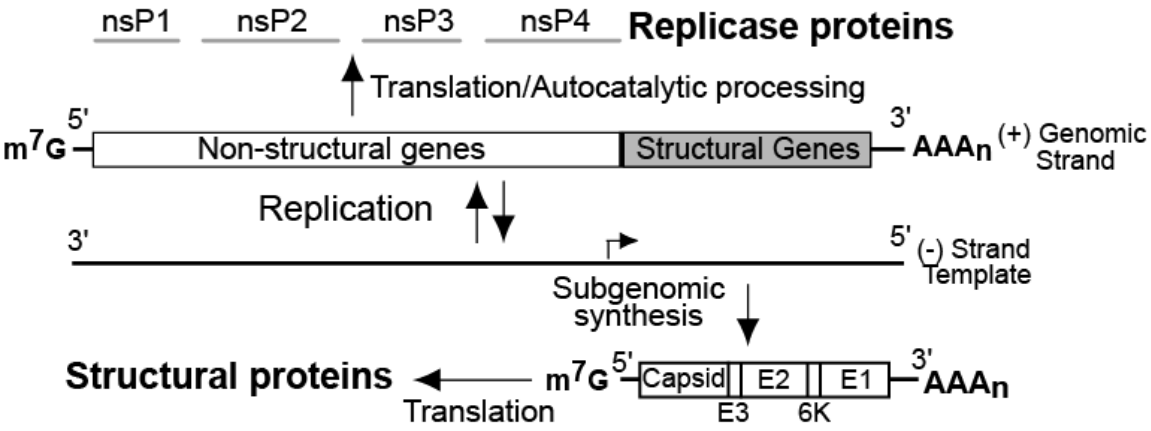

Figure 1.1. Alphavirus genome architecture and replication. Upon entry into the cytosol, the non-structural proteins are translated, autocatalytically processed, and mediate production of negative-sense templates and subsequent positive-sense genomic strands. Viral replicase proteins also produce subgenomic templates, which encode the structural proteins, via a subgenomic promoter encoded on the negative-sense genomic template. For further details see text.

replication and may mediate neurovirulence in old world alphaviruses (98, 167, 177). The viral RdRp and core of the alphavirus replication complex is encoded by nsP4 (135). The structural components include the capsid, which encapsidates the RNA genome, and the envelope glycoproteins, which mediate viral attachment and entry (94, 158).

Alphavirus entry into host cells requires clathrin-mediated endocytosis and is highly pH-dependent (94, 158). A specific cellular receptor has not been identified, and it is proposed that several may be sufficient given the broad tissue tropism and species host range of alphaviruses (94, 158). Due to the complex and incomplete understanding of host receptors required for alphavirus attachment and entry, the neurotropism of the new world alphaviruses remains poorly understood but may be dependent on increased heparin sulfate binding relative to old world alphaviruses (143). Consistent with this, serially passaged old world alphaviruses develop mutations in envelope protein-2 which enhances heparin sulfate binding and correlates with increased neurovirulence (143). Furthermore, old world viruses, versus naturally encephalitic new-world alphaviruses, poorly bind heparin sulfate (143). These observations indicate that alphavirus attachment to and entry into host cells requires clathrin-mediated endocytosis, but host and viral factors mediating attachment and neurotropism remain poorly defined and may be complex and multifactorial.

The alphavirus glycoproteins E1 and E2, which span the viral envelope, mediate the entry process, where cell binding is largely attributed to E2 (94, 158).

Upon acidification, E1, which is a type-II fusion protein, exposes its fusion peptide and, through large conformational changes, mediates the fusion of the viral envelope with the endosomal membrane resulting in the release of the nucleocapsid core into the cytosol (94, 158). After entering the cytosol, the RNA genome is immediately translated by host machinery (**Fig 1.1**) (64, 158). This generates the predominant polyprotein, nsP123, and the minor polyprotein, nsP1234, via read-through of an opal codon (94, 158). These polyproteins are autocatalytically processed via the protease activity of nsP2 (94, 158). The sequential processing of these polyproteins into their constituent parts forms distinct replication complexes which preferentially produce negative-sense RNA strands followed by positive-sense genomic RNA strands and finally sub-genomic RNA strands (94, 158). The viral replication complexes recognize and bind promoter-like elements termed conserved sequence elements (CSE) located at the 5' and 3' ends of the viral RNA and at the sub-genomic promoter near the junction of the nsP4 and capsid genes (94, 158). Within host cells, the viral replication complexes are located on the cytosolic surface of cellular membranes. These membranes are thought to be derived from endosomes or lysosomes but are often ambiguously termed cytopathic vacuoles (94, 158). Following subgenomic RNA synthesis, the structural genes are translated via host machinery into a poly-protein with capsid on the N-terminus and E1 on the C-terminus (**Fig 1.1**) (94, 158). Immediately following translation, capsid is released via autoproteolytic activity of a protease domain located in the C-

terminus of capsid (94, 158), a fact that, along with polyprotein processing of the nsPs, will be important for understanding the design of constructs used in chapter III. Release of capsid exposes a signal peptide on the N-terminus of the new polyprotein containing the envelope proteins (94, 158). This signal sequence directs the envelope proteins to the ER-Golgi network for further post-translational processing, including glycosolation and modification by host proteases, before being translocated to the cellular membrane (94, 158). Meanwhile, capsid associates with viral RNA genomes via packaging sequences on its N-terminus and forms neucleocapsid cores that then interact with envelope proteins near the cell membrane (94, 158). Finally, viral particles bud from the cell surface (94, 158).

Alphavirus Phylogeny

Alphaviruses are believed to be derived from an unknown protoalphavirus that originated in the Americas and gave rise to the new and old world alphaviruses in existence today (64). Alphavirus phylogeny is based on both sequence analysis and envelope protein antigenic complexes. Generally these two methods produce similar phylogenetic trees except for where on these trees each method places WEEV. The reason for this is that WEEV is a recombinant alphavirus in which the non-structural proteins and capsid are derived from an EEEV-like common relative, and the envelope glycoproteins are derived from a Sindbis virus-like relative (74). This will be important for this body of work

because the old and new world alphaviruses utilize either nsP2 or capsid, respectively, to mediate important virulence mechanisms described below.

Immune Response to Neurotropic Alphaviruses

Neurotropic alphavirus pathogenesis and the immune response mounted against alphaviruses are generally similar to the description given above regarding all neurotropic arboviruses; however, some aspects of neuropathogenesis are far better characterized for alphaviruses than other neurotropic arboviruses. For instance, the humoral immune response is incredibly important for alphavirus encephalitis resolution, and passive administration of protective antibodies can be therapeutic for established infections (73). These protective antibodies don't have to be neutralizing, are independent of complement, are generally directed against viral E1 or E2, can decrease intracellular replication, are non-lytic, and are synergistic with type-I IFNs (64, 65, 85, 116, 156). Furthermore, WEEV patients lacking an antibody response at the time of presentation are more likely to die (64, 65). Another particularly well-studied area of alphavirus neuropathogenesis is that type-II IFN, namely IFNγ, can clear virus from certain neuronal populations in the absence of a B-cell response (27). Finally, increased neuronal maturation is inversely proportional to alphavirus virulence and cytopathic effect (17). This phenomenon is independent of developmental changes in the adaptive immune system and the induction of type-I IFN (32, 67, 70). In fact, younger animals, and possibly

immature neurons, actually produce more inflammatory cytokines and type-I IFNs than older animals, which may contribute to the increased severity of neurotropic alphaviruses in younger animals (68). While seemingly unrelated to developmental changes in the adaptive immune system and induction of type-I IFNs, the resistance of mature neurons to neurotropic alphavirus infections has been attributed to neuronal resistance to virus-induced apoptosis (164-166) and may be augmented by increased IFN responsiveness of mature neurons relative to immature neurons (66, 67, 69, 70, 101, 102). These observations outline many of the similarities of the immune response to diverse alphaviruses and suggest that significant amounts of alphavirus biology can be learned by studying model alphaviruses.

As described above, there are important similarities in the immune response to most alphaviruses. However, the majority of alphavirus pathogenesis studies examined old world alphaviruses, which in humans are not naturally encephalitic, and recently, important differences in pathogenic mechanisms between new and old world alphaviruses have emerged. For instance, the ability of alphaviruses to induce a cytopathic effect and shut down host macromolecular synthesis has long been a proposed virulence mechanism. For the old world alphaviruses, nsP2 mediates neurovirulence, cytopathic effect (CPE), shut off of host macromolecular synthesis, and interference with type-I IFN induction (32, 96). In contrast, the capsid protein of new world alphaviruses mediates CPE, shut off of host macromolecular synthesis, and may mediate

interference with type-I IFN induction (22, 25, 60, 63). This difference is important because shut down of host macromolecular synthesis may inhibit the induction of an innate antiviral response. In support of this, attenuated strains of new world alphaviruses contain mutations in critical residues of capsid responsible for inhibition of host macromolecular synthesis (2, 3, 59, 60); and chimeric viruses containing new world non-structural proteins and old world structural proteins were cleared from IFNα/β competent cells but replicated similar to their wild-type counterparts in IFNα/β deficient cells (10). The capsid protein from the new world virus VEEV also blocks nuclear import (60); however, it is unclear whether capsid-mediated inhibition of nuclear import blocks nuclear translocation of innate antiviral transcription factors. In contrast, old world nsP2 does not appear to affect virus-induced nuclear translocation of innate antiviral transcription factors (10, 11). Furthermore, it is unclear whether new world capsid-mediated CPE, shut off of host macromolecular synthesis, and interference with type-I IFN induction are the result of one common mechanism or are all independent functions of capsid. In the case of old world nsP2, these functions may be distinct given that nsP2 mutants have been identified that no longer inhibit either type-I IFN induction, host transcription, or host translation (22, 25). In addition to nsP2, virulence determinants mapped to the cleavage site between nsp1 and 2 also influence inhibition of type-I IFN induction independent of shut off of host macromolecular synthesis (22, 63). These studies highlight the fact that while much can be learned about alphavirus pathogenesis by studying

model old world viruses, important differences between the encephalitic new world and non-encephalitic old world alphaviruses exist, especially with regard to how each group of viruses shuts down host gene expression and interferes with innate immune responses.

Just as old and new world alphaviruses have distinct pathogenic mechanisms, there are also important pathogenic differences among the encephalitic new world alphaviruses. For instance, VEEV pathogenesis has a prominent lymphoid component, whereas EEEV largely spares the lymphatic system and appears to avoid replication in myeloid lineage cells altogether (38). In addition, VEEV robustly increases serum type-I IFNs as do old world alphaviruses (57), whereas EEEV fails to do so (154, 164-166). In fact, attenuated strains of EEEV correlated with increased induction of type-I IFNs in vivo (57). Altogether, these alphavirus pathogenesis studies demonstrate that parallels among alphaviruses exist in terms of pathogenic mechanisms and immune responses mounted against them, but, as with many closely related viruses, important differences are also present. In this body of work, I chose WEEV as a model neurotropic arbovirus for two main reasons. First, it is the least studied of the new world encephalitic alphaviruses and may be particularly illuminating for alphavirus pathogenesis because it is a recombinant virus between new and old world alphaviruses. Second, while WEEV requires BSL3 containment, it is safer than other new world encephalitic alphaviruses for healthy lab personnel to manipulate due to its lower case to infection ratio for adults.

Ultimately, all observations presented in this body of work will need to be verified for the other new world encephalitic alphaviruses and, more generally, neurotropic arboviruses, but I reasoned that studying the lesser characterized and recombinant alphavirus, WEEV, would reveal novel insight about alphavirus and potentially neurotropic arbovirus biology.

Innate Antiviral Pattern Recognition Receptor Pathways

Gerneral Characteristics

Innate immune pathways are early responses important for pathogen control, and are activated by pattern recognition receptors that bind ligands containing pathogen- or danger-associated molecular patterns, such as modified carbohydrate or nucleic acid structures (58). For antiviral innate immune responses, ligation of these receptors induces a signal transduction cascade that results in the production of type-I IFNs, other proinflammatory cytokines, and cell-intrinsic factors important for the generation of an antiviral cellular microenvironment (99, 133). In addition, antiviral PRR signaling is important for activating an appropriate adaptive immune response (133), which is required for the eventual clearance of most viral infections (7). Thus, PRR-mediated innate immune signaling serves a pivotal role in stimulating rapid yet nonspecific antiviral activity while also providing activation signals for more specialized adaptive immune responses.

There are three general steps in innate antiviral immune responses: recognition, amplification, and effector production (**Fig 1.2**). Activation is achieved by receptors that activate several transcription factors via phosphorylation events or degradation of transcription factor inhibitors. These activation events often result in transcription factor dimerization and nuclear translocation. Once in the nucleus, activated transcription factors then induce the expression of many genes important for mounting a cellular antiviral response including the type-I IFNs (24). Type-I IFNs then signal in either a paracrine or autocrine manner through the type-I IFN receptor (IFNAR). The interferon receptor signals in a JAK/STAT-dependent manner and activates the transcription factor complex interferon-stimulated gene factor-3 (ISGF3) (95). ISGF3 binds interferon-stimulated response elements (ISREs) present in the promoters of interferon-stimulated genes (ISGs) and promotes their expression (143). There are several IFN-stimulated genes that act directly as antiviral effectors, but many are also components of antiviral PRR pathways, which provides a mechanism for positive feedback regulation and amplification (143). PRR pathway activation is initiated by four groups of antiviral PRR receptors: the cytosolic retinoic acid gene-I-like (RLR) receptors; the cytosolic nucleotide-binding oligomerization domain (NOD)-like receptors (NLR); the cytosolic DNA recognition receptors; and the transmembrane toll-like receptors (TLR) (95, 133). Due to differential expression, ligand specificity, and pathogen-

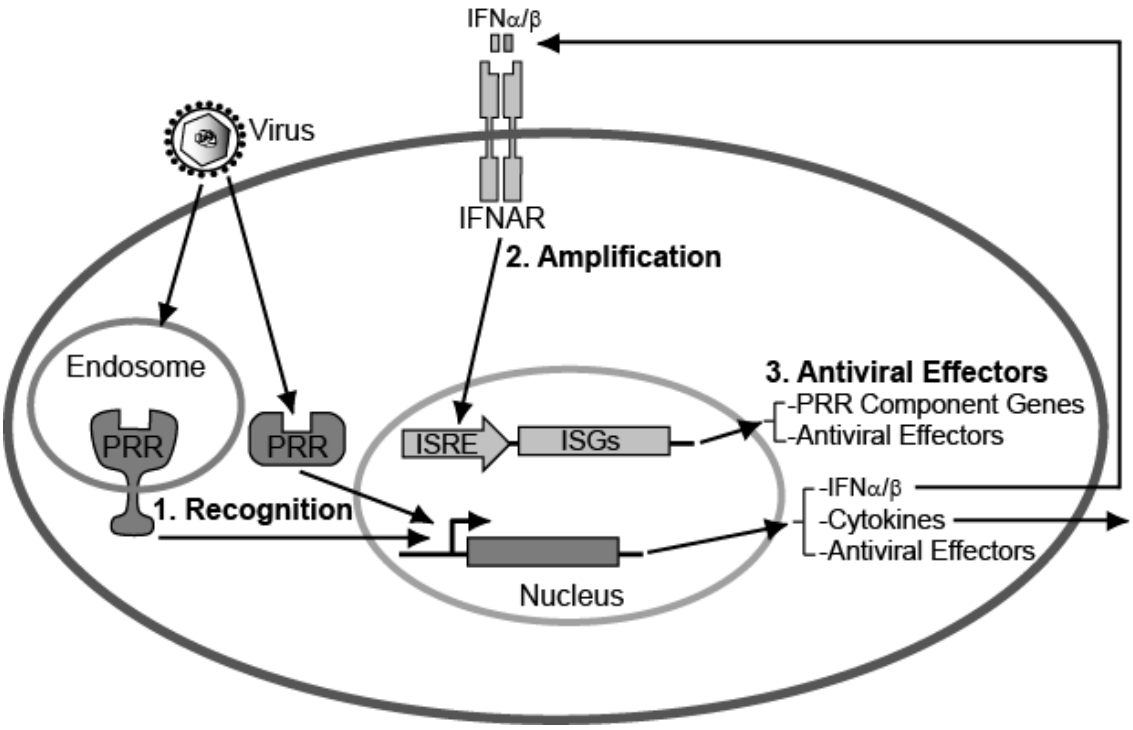

Figure 1.2. Innate antiviral signaling pathways. 1. Recognition. Innate antiviral signaling is initiated via ligation of pattern recognition receptors (PRR), which signal the induction of cytokines, antiviral effector genes, and type-I IFNs (IFNα/β). **2. Amplification.** Type-I IFNs are then secreted and undergo autocrine/paracrine signaling through the type-I IFN receptor (IFNAR) resulting in the induction of interferon-stimulated genes (ISGs) that contain interferon-stimulated response elements (ISRE) in their promoters. ISGs encode pattern recognition receptor pathway components, thereby providing amplification and positive feedback on pattern recognition receptor-mediated signaling. **3. Antiviral Effectors.** Many ISGs and genes directly induced by PRR signaling encode proteins with potent antiviral effects.

mediated interference, PRRs respond to viral infections in both a pathogen and cell type-specific manner (161, 184).

Cytosolic Antiviral PRR Pathways

The RLR pathways are initiated by the receptors RIG-I, melanoma differentiation-associated gene 5 (MDA5), and laboratory of genetics and physiology-2 (LGP2) (**Fig 1.3**) (95, 161, 184, 185). RLRs recognize non-self RNAs via a DexD/H-box RNA helicase domain and signal via two N-terminal caspase recruitment domains (CARDs) that mediate downstream protein-protein interactions required for antiviral signaling (95, 161, 184). However, LGP2 lacks CARD domains and, depending on the context, appears to function as either a positive or negative regulator of RLR signaling (185). RIG-I and LGP2 contain C-terminal regulatory domains that inhibit CARD-mediated signal transduction in the absence of ligand (184). In contrast, MDA5 lacks a regulatory domain (184), and overexpression of MDA5 robustly activates downstream signal transduction in the absence of ligand (184). Despite being highly similar, the RLRs appear to differentially recognize specific, non-self RNA moieties and viral pathogens (9). For instance, RIG-I recognizes 5' triphosphorylated double-stranded RNAs, homopolymeric RNA motifs, short dsRNAs (<2 kb), unanchored polyubiquitin chains, and many families of RNA viruses, whereas MDA5 recognizes picornaviruses and long dsRNAs (>2 kb) often mimicked by the synthetic dsRNA molecule polyinosinic-polycytidylic acid (poly(I-C)) (92, 93, 161, 184).

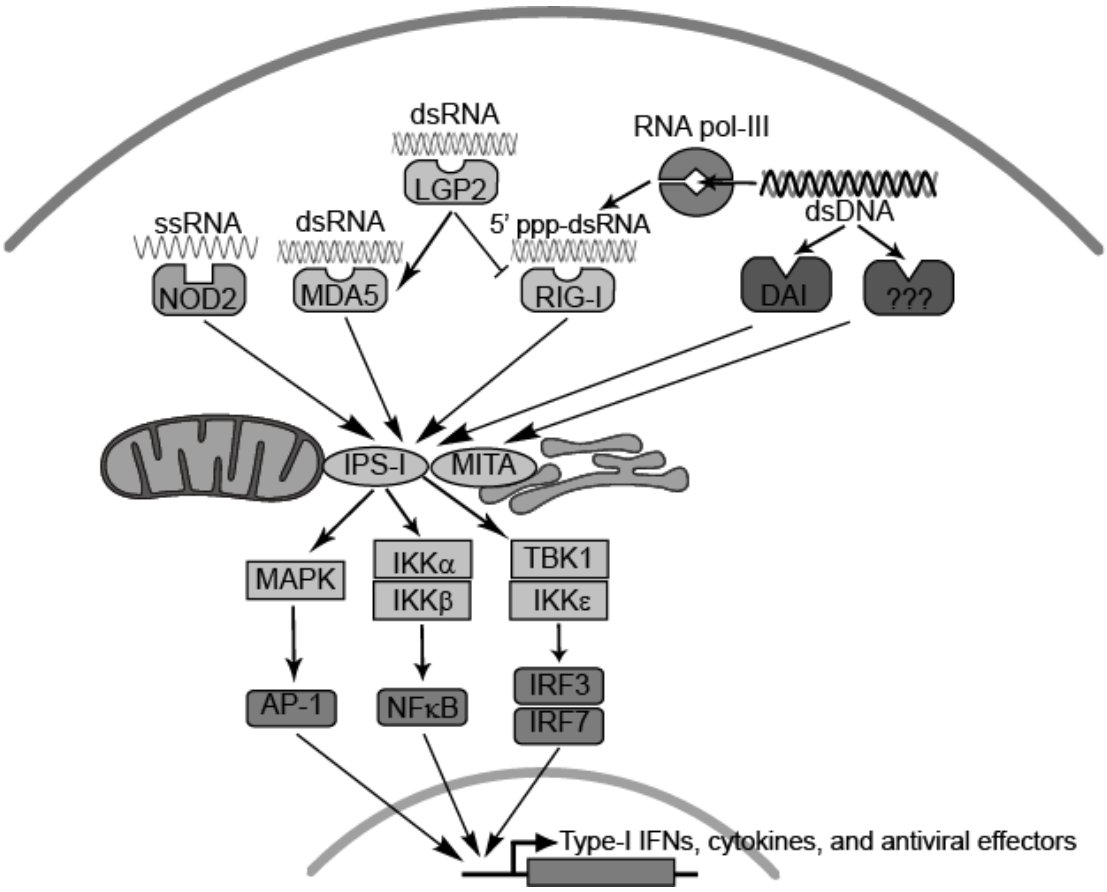

Figure 1.3. Cytosolic antiviral PRR signaling pathways. Receptor ligation results in the formation of signaling complexes dependent on the adaptors IPS-I and MITA, which mediate the activation of kinases. These kinases then activate antiviral transcription factors, which translocate into the nucleus and induce cytokines, antiviral effectors, and type-I IFNs. For further details see text.

RLR-mediated signal transduction requires the CARD-containing mitochondrial adaptor protein interferon-β promoter stimulator protein-1 (IPS-1) (also referred to as Cardif, MAVS, and VISA) (139, 161, 184, 185, 187). IPS-I, when localized to peroxisomes, can also mediate an antiviral signal transduction pathway that is independent of type-I IFNs (185). IPS-I serves as a scaffold for the formation of a large signaling complex that is formed when ligand-bound RLRs interact with IPS-1 via intermolecular CARD interactions (49). This large signaling complex mediates the assembly of several important signaling molecules, including TRAF3, TRAF6, and FADD, resulting in the activation of numerous kinases including MAPKs, IKKα, IKKβ, IKKε, and TBK1 (161, 184). These kinases then activate the transcription factors NF-κB, IRF3, IRF7, and AP1, which induce the expression of antiviral genes, inflammatory cytokines, and type-I IFNs (161, 184).

In addition to antiviral signaling, RLRs also activate inflammatory pathways which classically involve NFκB-dependent induction of the prototypic inflammatory cytokine, pro-IL-1β, and formation of an inflammasome that activates Caspase-1 which cleaves pro-IL-1β to form mature, bioactive IL-1β (161, 184, 185). RLRs induce inflammatory NFκB-dependent cytokines IL-6 and IL-1β in a manner dependent on IPS-I and CARD9, whereas type-I IFN induction is independent of CARD9 (186). Interestingly, RIG-I and MDA5-mediated IL-1β maturation is independent of IPS-1, and each receptor induces a

slightly different inflammasome (136). For instance, RIG-I-mediated maturation of pro-IL-1β requires the inflammasome adaptor ASC and activates Caspase-1, but the process is independent of the well characterized but relatively non-specific NLRP3-containing inflammasome (136). In contrast, MDA5-mediated maturation of pro-IL-1β induces an inflammasome containing NLRP3 (136). Unlike canonical IPS-I-dependent RLR signaling, it is unclear if inflammatory RLR signaling pathways mediate a direct antiviral effect, but an indirect antiviral effect may be important given the long standing link between inflammatory responses and induction of adaptive immunity (136).

RLR pathways are highly regulated, and several negative and positive regulators have been identified. Mediator of IRF3 activation (MITA) (also known as stimulator of interferon genes (STING)), a transmembrane protein potentially located on ER and mitochondria, positively regulates RLR signaling (6, 86, 162). Another mitochondrial protein and member of the NLR family, NLRX1, negatively regulates RLR signaling (161, 184). Ubiquitination mediated via several enzymes has both negative and positive effects on RLR signaling. The ring-finger protein, RNF125, ubiquitinates MITA, and potentially other molecules in the RLR pathway, resulting in decreased signal transduction (120). In contrast, the E3 ubiquitinase, tripartite motif protein-25 (TRIM25), specifically ubiquitinates RIG-I, which is required for RIG-I and IPS-I interaction and subsequent signal transduction (161, 184). In addition, Riplet (also termed RNF135 and REUL) ubiquitinates and positively regulates RIG-I independent of TRIM25 (161, 184).

Finally, the ubiquitin ligase A20 and the ubiquitin modifying enzymes CYLD and DUBA negatively regulate RLR signaling (161, 184). The autophagy-related complex, Atg5-Atg12, also negatively regulates RLR signaling despite having a positive regulatory role for TLR-mediated signaling (161, 184). Specific negative regulation of MDA5 is achieved by dihydroacetone kinase (DAK) (161, 184). Interestingly, small self RNAs generated by the antiviral effector genes OAS and RnaseL amplify RLR signal transduction (48). These studies highlight the intricate and complex nature of these pathways and demonstrate the many mechanisms the host employs to fine-tune and appropriately regulate RLR pathways.

In additon to RLRs, the NLR NOD2 also recognizes viral RNA in the cytoplasm and induces an antiviral signal transduction pathway requiring IPS-I and IRF3 (**Fig 1.3**) (113). NOD2 recognizes ssRNA and protects mice from respiratory syncytial virus pathogenesis, but the role this receptor plays in other viral infections needs further investigation (144).

The induction of an innate antiviral response by cytosolic DNA requires the classic PRR pathway transcription factors IRF3 and NFκB as well as the kinases TBK1 and IKKε (**Fig 1.3**) (144). Just as cytoplasmic recognition of RNA is achieved by a variety of receptors, the recognition of cytoplasmic DNA is complex, redundant, cell type-, and species-specific (84, 161, 184). One mechanism involves the transcription of 5' triphosphorylated dsRNA from cytoplasmic dsDNA by RNA polymerase III (84, 161, 184). These transcribed

RNAs then serve as ligands for RIG-I (1, 35, 84, 161, 184). RNA polymerase III templates include the mimetic of B-form DNA, poly(dA-dT), and the viruses adenovirus, herpes virus, and Epstein-Barr virus (1, 35). Another candidate cytoplasmic DNA sensor is DNA-dependent activator of IFN-regulatory factors (DAI; also known as ZBP1), which activates IRF3 and NFκB in response to poly(dA-dT) (35); however, deletion of DAI in mice had no effect on DNA-induced interferon production, suggesting redundant mechanisms for cytoplasmic DNA detection (160). Recent reports also indicate that an AIM2-containing inflammasome recognizes dsDNA and requires ASC for the activation of caspase-1 and subsequent release of the inflammatory cytokine IL-1β (84, 88, 160, 161, 184). However, this pathway does not induce type-I interferons, and it is unclear if it produces a direct antiviral effect.

Several signaling molecules, in addition to STING and downstream kinases and transcription factors, mediate antiviral signal transduction in response to both cytoplasmic dsDNA and dsRNA. High mobility group box-1 (HMGB1) is regarded as an universal sentinel for nucleic acid-mediated innate immune responses (53, 83, 84, 161, 184). HMGB1 appears to mediate the early capture and delivery of nucleic acids to their appropriate receptors for induction of antiviral signaling (182). In addition to HMGB1, a coactivator pathway responsive to both dsDNA and dsRNA increases type-I IFN induction (161, 182). This pathway is mediated by the nucleic acid receptor LRRFIP1, which upon ligation leads to the activation of β-catenin (183). Activated β-catenin then

interacts with IRF3 and the IRF3 coactivator p300 resulting in enhanced transcription of IRF3 antiviral target genes (183). However, the requirement of LRRFIP1 for antiviral responses in vivo remains to be tested. These studies further demonstrate the intricate mechanisms cells employ to detect and respond to cytosolic viral pathogen associated molecular patterns, and this intricacy generates a plethora of unanswered questions suggesting that much remains to be learned about these pathways.

TLR-mediated Antiviral PRR Pathways

The transmembrane toll-like receptors mediate antiviral signaling by detecting pathogen-associated molecular patterns at the cell membrane or within endosomes (**Fig 1.4**) (183). At the cell membrane, TLR4 recognizes viral glycoproteins (95), whereas the ligand for the antiviral activity of cell-surface localized TLR2 remains to be determined (95). While TLR4 and 2 likely recognize their ligands at the cell surface, induction of an antiviral response following ligation of these receptors requires internalization (13). In contrast to TLR 4 and 2, TLR3, TLR7/8, and TLR9 are localized to endosomes where they recognize dsRNA, ssRNA, and hypomethylated CpG DNA motifs, respectively (13, 19, 95). Generation of signaling-competent TLR9, and possibly TLR7, requires proteolytic cleavage of the ectodomain within endosomes (19, 137), but no cleavage of TLR3 has been observed (19, 52, 129). Trafficking of TLR3, TLR7/8, and TLR9 to endosomes requires the ER protein UNC93B1

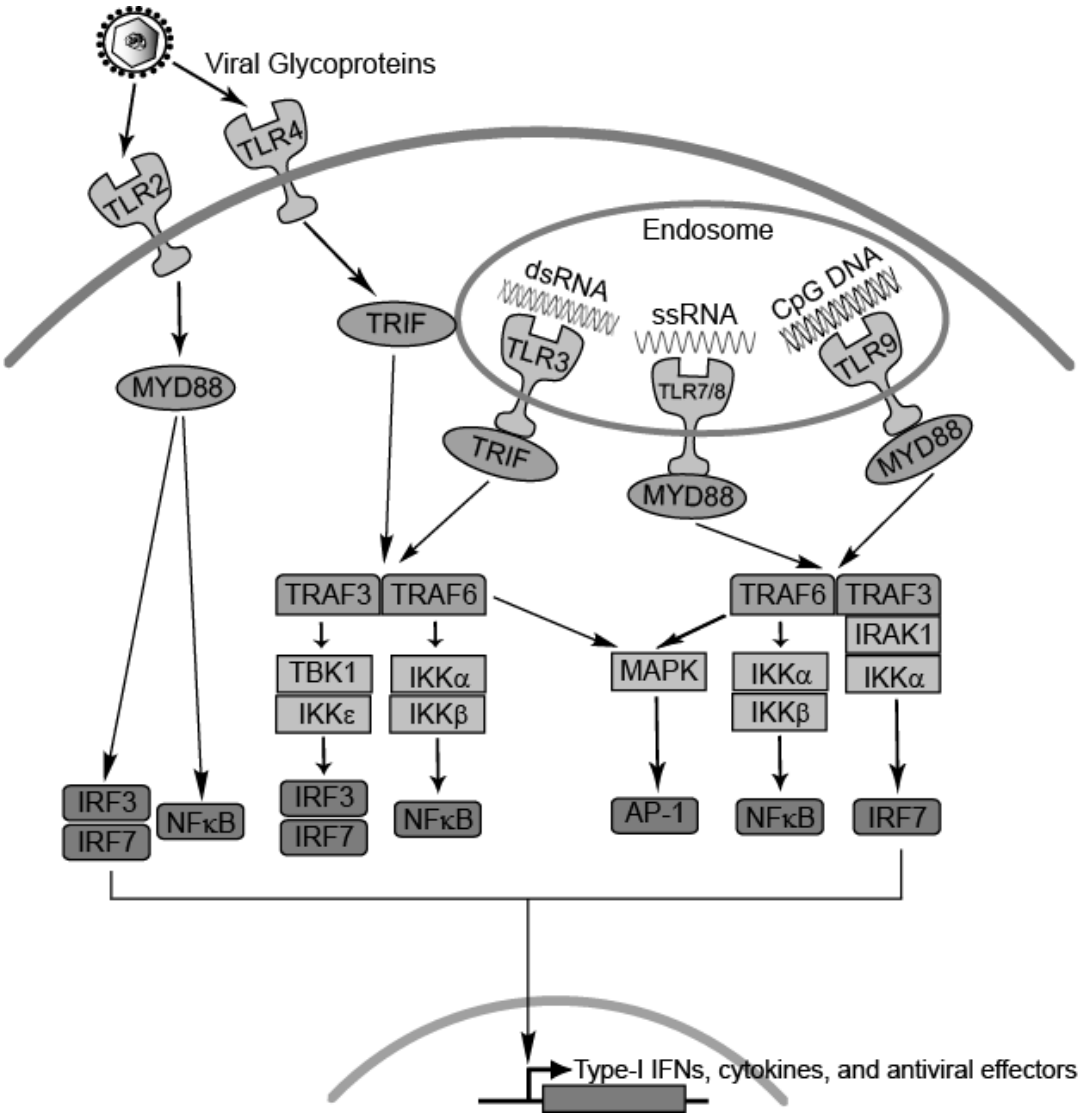

Figure 1.4. Toll-like receptor-mediated antiviral PRR signaling pathways. Receptor ligation results in the formation of signaling complexes dependent on the adaptors MYD88 and TRIF, which mediate the activation of kinases. These kinases then activate antiviral transcription factors, which translocate into the nucleus and induce cytokines, antiviral effectors, and type-I IFNs. For further details see text.

(19, 95, 161), and mutations in UNC93B1 increase human susceptibility to viral pathogens including HSV encephalitis (19, 95, 161). TLR3 has also been observed on the surface of certain cell types including neuronal cells (31), but it is unclear if this population of TLR3 mediates antiviral signal transduction.

Like the RLRs, the TLRs require specific adaptor proteins for efficient antiviral signal transduction. TLRs 2, 7, 8, and 9 all require the adaptor molecule myeloid differentiation primary response gene 88 (MYD88) for antiviral signal transduction (19). In contrast, TLR3 requires the adaptor TIR-domain-containing adapter-inducing interferon-β (TRIF) (13, 95). Both TIR-domain-containing adaptors interact with the cytoplasmic TIR domains of ligand-bound TLRs (95). Most antiviral TLRs utilize TRAF3 and TRAF6 for signal transduction and activate the kinases MAPK's, IKKα, IKKβ, IKKε, and TBK1 (95). In addition, phophatidylinositol-3 kinases (PI3K) are positive signal transducers for TLR7 (19, 95, 161, 184), may be negative signal transducers for TLR4 (29), and are reported to be both positive and negative regulators of TLR3 (4). As with RLR-mediated antiviral signaling, these kinases activate the transcription factors AP1, NFκB, IRF3, and IRF7; however, TLR7/8 and 9 largely depend on IKKα and IRAK1 for activation of primarily IRF7 and not IRF3 (4, 50, 147). In contrast, TLR3 and 4 activate both IRF3 and IRF7 via the kinases TBK1/IKKε (19, 95, 161, 184).

Similar to the RLR pathways, the TLR pathways are highly regulated, a topic that has been extensively reviewed (19, 95, 161, 184). Of note, there are

parallels between the regulation of antiviral RLR and TLR signal transduction pathways, suggesting that some communication and integration of signals between the cytosolic and TLR pathways takes place. This is best exemplified by the negative regulation of TLRs and RLRs by the ubiquitin modifying enzymes DUBA and A20 (19, 95, 161, 184). In addition to common regulatory mechanisms between RLR and TLR pathways, regulatory mechanisms favoring distinct TLR-mediated signals have also been described. For instance, the E3 ubiquitin ligase NRDP1 promotes the activation of TRIF-dependent activation of IRF3 while inhibiting MYD88-dependent activation of NFκB (19, 95, 161, 184), suggesting that NRDP1 promotes antiviral TLR signaling and blocks inflammatory TLR signaling. Just as with the cytosolic PRRs, regulation of the TLR pathways is also complex and suggests that further study is likely to reveal novel biology underlying these important antiviral pathways.

Ligands and Viruses Recognized by PRRs

Due in part to ligand specificity, differential expression, and pathogen-mediated interference, PRRs differentially recognize and respond to distinct viral infections, but some pathogens are recognized by several receptors (**Table 1.2**) (173). Limited information is available regarding what receptors recognize neurotropic arboviruses in neurons, but WNV is recognized by both RIG-I and MDA5 in non-neuronal cell types (19, 95, 161, 184, 185) and TLR3 in neurons (55, 56). Japanese encephalitis virus is recognized by RIG-I (40), but it is unclear if

Table 1.2. Antiviral PRRs.

PRR	Location	Ligand	Virus Family
RLR			
LGP2	Cytoplasm	dsRNA	+ Picornaviruses and paramyxoviruses - Rhabdoviruses
MDA5	Cytoplasm	dsRNA	Picornaviruses Caliciviruses Coronaviruses Reoviruses Flaviviruses Togaviruses
RIG-I	Cytoplasm	Short, 5'-triphosphorylated dsRNA and poly-ubiquitin chains	Orthomyxoviruses Rhabdoviruses Paramyxoviruses Flaviviruses Reoviruses Togaviruses
NLR			
NOD2	Cytoplasm	ssRNA	Paramyxoviruses
Cytosolic DNA			
DAI	Cytoplasm	B-form DNA	Herpesviruses
RNApol III/RIG-I	Cytoplasm	B-form DNA	Herpesviruses Adenoviruses
TLR			
TLR2	Plasma membrane/ intracellular		Herpeseviruses Poxviruses
TLR3	Endosome	dsRNA	Reoviruses Flaviviruses Picornaviruses Paramyxoviruses Rhabdoviruses Herpesviruses Arenaviruses
TLR4	Plasma membrane/intracellular	Viral glycoproteins	Paramyxoviruses Retroviruses
TLR7/8	Endosome	ssRNA	Rhabdoviruses Orthomyxoviruses
TLR9	Endosome	CpG DNA	Herpesviruses

"+/-" indicates positive/negative regulation of signal transduction.

neurons have this capability. To date, it is unknown what PRRs recognize new world encephalitic alphaviruses, but evidence exists for the recognition of old world alphaviruses, which are not naturally encephalitic, via RIG-I or MDA5 depending on the cell type and virus (93). The non-arboviral encephalitic rabies and herpes viruses are recognized by RIG-I and TLR9, respectively (25, 134), and TLR3 may recognize rabies virus in neuronal cells (95, 185). Further work will need to clarify what receptors recognize neurotropic arboviruses and if they do so in neurons.

Antiviral Mechanisms of PRR Pathways

The ability of PRR pathways to induce an antiviral effect is partly due to the direct or indirect induction of antiviral effector genes. There are a multitude of these genes, many of which have uncharacterized mechanisms of action. However, one well-characterized antiviral effector system involves the oligoadenylate synthetase (OAS) genes and RNaseL. OAS, upon ligation of viral RNA, synthesizes 2'-5'-linked oligoadenylate which then binds and activates RNaseL resulting in the degradation of host and viral RNA and the subsequent inhibition of viral propagation (137). The antiviral activity of PRR pathways can also be attributed to altruistic induction of apoptosis in virally infected cells, thereby limiting viral replication and spread (20, 145). Direct PRR pathway-mediated induction of apoptosis is achieved by activation of IRF3 triggering the interaction of IRF3 with the pro-apoptotic protein Bax (16, 78, 81, 153). IRF3 and Bax then

translocate to the mitochondria and activate the mitochondrial apoptosis pathway (34). Interestingly, IRF3-dependent induction of apoptosis in conjuction with Bax does not require IRF3's DNA binding domain, suggesting that this process is independent of an IRF3-mediated transcriptional response (34). In addition to direct PRR pathway-mediated induction of altruistic apoptosis, there are multiple indirect mechanisms for viral activation of apoptosis including damage of host cell machinery by OAS-RNaseL (34). Paradoxically, PRR pathway activation can be both cell sparing and cell death promoting when activated by viral pathogens. Presumably cells are spared when antiviral effectors are sufficient to control viral replication, but when antiviral effectors are insufficient to control viral replication, cells undergo altruistic apoptosis. In the end, the effectiveness of either antiviral effectors or altruistic apoptosis to produce a net antiviral effect may depend on the pathogen, the pathogen load, and the responding cell type.

In addition to immediate local antiviral effects, PRR pathway activation has profound effects on the entire immune response (20). These effects are largely due to type-IFNs, but other inflammatory cytokines induced by PRR signaling may also play a role. Early after infection, chemokines, cytokines, and type-I IFNs induced by PRR signaling mediate the upregulation of adhesion molecules and promote the migration of inflammatory cells (7). PRR-mediated induction of type-I IFN alerts and helps activate natural killer cells and local antigen presenting cells, such as dendritic cells, which are important for activating adaptive responses (7). In addition, type-I IFNs directly influence adaptive

responses by regulating T-cell activation and memory and influencing B cell functions such as antibody secretion and isotype switching (7). The influence of PRR pathways on adaptive responses to neurotropic arboviruses has been studied for WNV: virus-infected IPS-$1^{-/-}$ mice mount an altered inflammatory response and ultimately ineffective humoral and T-cell responses (7). These studies indicate that early PRR pathway responses are crucial for producing not only early, non-specific antiviral responses, but also for mediating highly effective and specific adaptive responses and eventual disease resolution.

Cell Type-Specific PRR Signaling

The molecular mechanisms of antiviral PRR signaling have been defined primarily using a limited number of cell lines and primary cell types, many of which are derived from small rodent models; and these include professional immune cells such as dendritic cells or macrophages. These studies have revealed important cell type-specific differences in antiviral PRR pathways. For example, dendritic cells express relatively high basal levels of TLR7 and TLR9, and as a result vigorously respond to ligands for these receptors (159). In contrast, “non-professional” immune cells, such as fibroblasts, use primarily cytoplasmic RLRs for innate antiviral pathway activation (36), although some cell types such as keratinocytes (92) and respiratory epithelial cells (175) can also mount vigorous TLR-mediated antiviral responses. Plasmacytoid dendritic cells also constitutively express the transcription factor IRF7, which is thought to

contribute to their ability to produce IFNα rapidly after PRR-mediated stimulation (91), whereas IFNα production in other cell types occurs later if at all, and is linked to IFNβ-mediated induction of IRF7 (14, 36, 82). Interestingly, TLR2 antiviral signaling is unique to an inflammatory monocyte population (115, 148, 149), and myeloid cells remain responsive to WNV virus even when the key transcription factors IRF3 and IRF7 are deleted, which is in contrast to both WNV-infected fibroblasts and cortical neurons (13). Additional examples of cell type-specific differences in innate antiviral immunity include a lower basal activity of PRR pathways in cardiac fibroblasts compared to cardiac myocytes (43), differential responses of specific human hepatocyte cell lines to poly(I-C) and Sendai virus (SeV) stimulation (190), and cell type-specific roles for IRF3 and IRF7 in response to West Nile virus infection (104). Furthermore, species-specific differences also exist with respect to DAI (107) and TLR expression, regulation, and function (39, 41). These observations suggest that caution should be exercised in extrapolating results on innate antiviral pathway activity between species and cell types.

Neuronal Antiviral PRR Pathways

Little is known regarding the PRR antiviral pathways that are active in CNS neurons or how these pathways may influence neurotropic arbovirus pathogenesis, but important observations have been made. For instance, several studies have examined the role of TLR3 in response to CNS viral

infections (76, 77, 138, 178). These studies demonstrated expression of TLR3 in human neurons (28, 40, 89, 117, 137) and enhanced West Nile virus replication in cortical neurons isolated from TLR3$^{-/-}$ mice (28, 89, 117, 137, 189). However, the potential antiviral role of TLR3-mediated pathways is controversial and may be pathogen-specific (40). For example, humans with a TLR3 deficiency have a genetic predisposition to herpes simplex virus encephalitis (172), but mice are protected from rabies virus encephalitis when TLR3 is deleted (188). Furthermore, TLR3$^{-/-}$ mice have been shown to have both increased (117) and decreased (176) susceptibility to West Nile virus (WNV) encephalitis. However, these studies cannot fully separate the neuron-specific activity of TLR3 from other cell types, including professional immune cells such as macrophages and dendritic cells. Although CNS neurons from TLR3$^{-/-}$ mice have a modest increase in WNV production, when infected in culture (40), suggesting that neuronal TLR3-mediated responses can have antiviral effects, further studies in mice with conditional cell-specific TLR3 deletions will be required to fully delineate the potential antiviral activity of TLR3-activated innate immune pathways in neurons and their role in viral pathogenesis. In addition to the neuronal TLR3 studies, many groups have demonstrated virus-mediated and, in some cases, neurotropic arbovirus-mediated induction of type-I IFNs in CNS neurons both in vitro (40) and in vivo (39-41, 137). The interaction between neurotropic arboviruses and RLR pathways is best characterized for West Nile virus encephalitis in which replication is enhanced and type-I IFN induction is

reduced in cortical neurons isolated from IPS-$1^{-/-}$, $IRF7^{-/-}$, and $IRF7/3^{-/-}$ mice (44). In addition to putative antiviral functions, PRR pathways have also been implicated in neuronal development (39-41, 43, 159), neuronal regeneration (141), and neuroinflammatory diseases (28, 111). Altogether, these reports suggest that CNS neurons possess active PRRs that may have multiple physiologic functions, but the full extent of their activity and influence on neurotropic arbovirus pathogenesis remain to be determined.

Viral Countermeasures to Antiviral PRR Pathways

Antiviral PRR pathways protect host cells and tissues against viral infections, yet many viruses, including neurotropic arboviruses, possess PRR pathway countermeasures allowing them to efficiently replicate, avoid immune detection, and cause disease (37, 119). Often, viruses encode more than one PRR pathway evasive or inhibitory protein, and many of these viral proteins mediate evasion or subversion of PRR signaling in multiple ways. Two of the best characterized mechanisms for viral interference of PRR pathways involve the NS1 protein of influenza virus and the NS3-4A protein of hepatitis C virus. Influenza NS1 sequesters viral dsRNA and binds RIG-I, thereby suppressing RIG-I signaling (21). Hepatitis C NS3-4A inhibits TLR3 signaling by degrading TRIF, disables RLR signaling by cleaving IPS-I from its mitochondrial tether, and decreases IRF3 phosphorylation by disrupting the TBK1-IRF3 interaction (170). Neurotropic arboviruses also interfere with antiviral PRR signaling. For instance,

the NS2A and NS1 proteins of WNV inhibit the activation of antiviral PRR pathways (170) resulting in higher viral replication and enhanced virulence in a manner that may be both viral strain- and cell type-dependent. The neurotropic arbovirus LACV also interferes with host antiviral signaling. The NSs protein of LACV mediates this effect by potently inhibiting type-I IFN induction, and mutant LACV lacking NSs robustly induces type-I IFNs resulting in reduced virulence (42, 46, 109, 180). These studies demonstrate that viruses are not just passive agents that activate PRR signaling, but that they likely co-evolved with their respective hosts and actively interact and modulate the antiviral effects of PRR pathways.

PRR Pathway Associated Diseases and Pathologies

PRR pathways mediate potent antiviral responses, and these pathways are checked by a large number of negative regulators. Unfortunately, misregulation of antiviral PRR pathways can also drive or influence a multitude of diseases including carcinogeneis and autoimmune diseases such as systemic lupus erythematosus, Crohn's disease, and antiphospholipid antibody syndrome (18). Furthermore, human variants in *MDA5* protect against type-I diabetes (161, 184), and within the CNS, unchecked or inappropriately activated antiviral PRR pathways may mediate neuroinflammatory diseases such as multiple sclerosis, amyotrophic lateral sclerosis, and Alzheimer's disease (124). Additionally, antiviral PRR pathways within CNS cells may play a role in chronic pain and

seizure development (15, 61, 97, 100, 114, 119, 126, 163). These observations highlight the importance of studying PRR pathways so that we can better understand the disease processes they mediate. Ultimately, the study of PRR pathways may lead to the development of therapies to treat viral infections by activating PRR pathways or inhibiting viral countermeasures to PRR pathways. Alternatively, therapies may be designed to inhibit the inappropriate activation of PRR signaling to treat autoimmune disorders and cancer.

Summary

Neurotropic arboviruses cause devastating CNS infections where the extent of virus-mediated destruction of neurons is often an important determinant in the severity and clinical outcome after infection. Early cellular innate immune responses are often vital for effective pathogen control, and I hypothesized that an effective neuronal innate immune response may be crucial to prevent the essentially irreversible loss of critical central nervous system neurons by neurotropic arboviruses. To begin testing this hypothesis, chapter II describes efforts to identify highly active neuronal innate antiviral pathways, and chapter III tests the impact these pathways have on neurotropic arbovirus infection of neurons and how these viruses counteract neuronal innate immune pathways. In chapter IV, I take a different approach to preventing neurotropic arbovirus-mediated neuronal death by identifying small molecules that inhibit neurotropic arbovirus replication and enhance cell viability, which may be useful for mono-therapy or in combination with potential therapeutics designed to enhance the neuronal innate immune response or inhibit viral countermeasures to the innate immune response. Chapter V discusses the overall relevance of these studies and potential future directions.

References

1. **Ablasser, A., F. Bauernfeind, G. Hartmann, E. Latz, K. A. Fitzgerald, and V. Hornung.** 2009. RIG-I-dependent sensing of poly(dA:dT) through the induction of an RNA polymerase III-transcribed RNA intermediate. Nat Immunol **10:**1065-72.
2. **Aguilar, P. V., L. W. Leung, E. Wang, S. C. Weaver, and C. F. Basler.** 2008. A five-amino-acid deletion of the eastern equine encephalitis virus capsid protein attenuates replication in mammalian systems but not in mosquito cells. J Virol **82:**6972-83.
3. **Aguilar, P. V., S. C. Weaver, and C. F. Basler.** 2007. Capsid protein of eastern equine encephalitis virus inhibits host cell gene expression. J Virol **81:**3866-76.
4. **Aksoy, E., W. Vanden Berghe, S. Detienne, Z. Amraoui, K. A. Fitzgerald, G. Haegeman, M. Goldman, and F. Willems.** 2005. Inhibition of phosphoinositide 3-kinase enhances TRIF-dependent NF-kappa B activation and IFN-beta synthesis downstream of Toll-like receptor 3 and 4. Eur J Immunol **35:**2200-9.
5. **Akwa, Y., D. E. Hassett, M. L. Eloranta, K. Sandberg, E. Masliah, H. Powell, J. L. Whitton, F. E. Bloom, and I. L. Campbell.** 1998. Transgenic expression of IFN-alpha in the central nervous system of mice protects against lethal neurotropic viral infection but induces inflammation and neurodegeneration. J Immunol **161:**5016-26.
6. **Allen, I. C., M. A. Scull, C. B. Moore, E. K. Holl, E. McElvania-TeKippe, D. J. Taxman, E. H. Guthrie, R. J. Pickles, and J. P. Ting.** 2009. The NLRP3 inflammasome mediates in vivo innate immunity to influenza A virus through recognition of viral RNA. Immunity **30:**556-65.
7. **Alsharifi, M., A. Mullbacher, and M. Regner.** 2008. Interferon type I responses in primary and secondary infections. Immunol Cell Biol **86:**239-45.
8. **Anderson, J. F., and J. J. Rahal.** 2002. Efficacy of interferon alpha-2b and ribavirin against West Nile virus in vitro. Emerg Infect Dis **8:**107-8.
9. **Andrejeva, J., K. S. Childs, D. F. Young, T. S. Carlos, N. Stock, S. Goodbourn, and R. E. Randall.** 2004. The V proteins of paramyxoviruses bind the IFN-inducible RNA helicase, mda-5, and inhibit its activation of the IFN-beta promoter. Proc Natl Acad Sci U S A **101:**17264-9.
10. **Atasheva, S., A. Fish, M. Fornerod, and E. I. Frolova.** 2010. Venezuelan equine Encephalitis virus capsid protein forms a tetrameric complex with CRM1 and importin alpha/beta that obstructs nuclear pore complex function. J Virol **84:**4158-71.
11. **Atasheva, S., N. Garmashova, I. Frolov, and E. Frolova.** 2008. Venezuelan equine encephalitis virus capsid protein inhibits nuclear import in Mammalian but not in mosquito cells. J Virol **82:**4028-41.

12. **Barabe, N. D., G. A. Rayner, M. E. Christopher, L. P. Nagata, and J. Q. Wu.** 2007. Single-dose, fast-acting vaccine candidate against western equine encephalitis virus completely protects mice from intranasal challenge with different strains of the virus. Vaccine **25:**6271-6.
13. **Barbalat, R., L. Lau, R. M. Locksley, and G. M. Barton.** 2009. Toll-like receptor 2 on inflammatory monocytes induces type I interferon in response to viral but not bacterial ligands. Nat Immunol **10:**1200-7.
14. **Barchet, W., M. Cella, B. Odermatt, C. Asselin-Paturel, M. Colonna, and U. Kalinke.** 2002. Virus-induced interferon alpha production by a dendritic cell subset in the absence of feedback signaling in vivo. J Exp Med **195:**507-16.
15. **Beg, A. A.** 2002. Endogenous ligands of Toll-like receptors: implications for regulating inflammatory and immune responses. Trends Immunol **23:**509-12.
16. **Besch, R., H. Poeck, T. Hohenauer, D. Senft, G. Hacker, C. Berking, V. Hornung, S. Endres, T. Ruzicka, S. Rothenfusser, and G. Hartmann.** 2009. Proapoptotic signaling induced by RIG-I and MDA-5 results in type I interferon-independent apoptosis in human melanoma cells. J Clin Invest **119:**2399-411.
17. **Binder, G. K., and D. E. Griffin.** 2001. Interferon-gamma-mediated site-specific clearance of alphavirus from CNS neurons. Science **293:**303-306.
18. **Blakqori, G., S. Delhaye, M. Habjan, C. D. Blair, I. Sanchez-Vargas, K. E. Olson, G. Attarzadeh-Yazdi, R. Fragkoudis, A. Kohl, U. Kalinke, S. Weiss, T. Michiels, P. Staeheli, and F. Weber.** 2007. La Crosse bunyavirus nonstructural protein NSs serves to suppress the type I interferon system of mammalian hosts. J Virol **81:**4991-9.
19. **Blasius, A. L., and B. Beutler.** 2010. Intracellular toll-like receptors. Immunity **32:**305-15.
20. **Borden, E. C., G. C. Sen, G. Uze, R. H. Silverman, R. M. Ransohoff, G. R. Foster, and G. R. Stark.** 2007. Interferons at age 50: past, current and future impact on biomedicine. Nat Rev Drug Discov **6:**975-90.
21. **Bowie, A. G., and L. Unterholzner.** 2008. Viral evasion and subversion of pattern-recognition receptor signalling. Nat Rev Immunol **8:**911-22.
22. **Breakwell, L., P. Dosenovic, G. B. Karlsson Hedestam, M. D'Amato, P. Liljestrom, J. Fazakerley, and G. M. McInerney.** 2007. Semliki Forest virus nonstructural protein 2 is involved in suppression of the type I interferon response. J Virol **81:**8677-84.
23. **Bronze, M. S., M. M. Huycke, L. J. Machado, G. W. Voskuhl, and R. A. Greenfield.** 2002. Viral agents as biological weapons and agents of bioterrorism. Am.J.Med.Sci. **323:**316-325.
24. **Burdeinick-Kerr, R., J. Wind, and D. E. Griffin.** 2007. Synergistic roles of antibody and interferon in noncytolytic clearance of Sindbis virus from different regions of the central nervous system. J Virol **81:**5628-36.

25. **Burke, C. W., C. L. Gardner, J. J. Steffan, K. D. Ryman, and W. B. Klimstra.** 2009. Characteristics of alpha/beta interferon induction after infection of murine fibroblasts with wild-type and mutant alphaviruses. Virology.
26. **Calisher, C. H.** 1994. Medically important arboviruses of the United States and Canada. Clin.Microbiol.Rev. **7:**89-116.
27. **Calisher, C. H., V. P. Berardi, D. J. Muth, and E. E. Buff.** 1986. Specificity of immunoglobulin M and G antibody responses in humans infected with eastern and western equine encephalitis viruses: application to rapid serodiagnosis. J.Clin.Microbiol. **23:**369-372.
28. **Cameron, J. S., L. Alexopoulou, J. A. Sloane, A. B. DiBernardo, Y. Ma, B. Kosaras, R. Flavell, S. M. Strittmatter, J. Volpe, R. Sidman, and T. Vartanian.** 2007. Toll-like receptor 3 is a potent negative regulator of axonal growth in mammals. J Neurosci **27:**13033-41.
29. **Cao, W., S. Manicassamy, H. Tang, S. P. Kasturi, A. Pirani, N. Murthy, and B. Pulendran.** 2008. Toll-like receptor-mediated induction of type I interferon in plasmacytoid dendritic cells requires the rapamycin-sensitive PI(3)K-mTOR-p70S6K pathway. Nat Immunol **9:**1157-64.
30. **Carrithers, M. D., I. Visintin, S. J. Kang, and C. A. Janeway, Jr.** 2000. Differential adhesion molecule requirements for immune surveillance and inflammatory recruitment. Brain **123 (Pt 6):**1092-101.
31. **Casrouge, A., S. Y. Zhang, C. Eidenschenk, E. Jouanguy, A. Puel, K. Yang, A. Alcais, C. Picard, N. Mahfoufi, N. Nicolas, L. Lorenzo, S. Plancoulaine, B. Senechal, F. Geissmann, K. Tabeta, K. Hoebe, X. Du, R. L. Miller, B. Heron, C. Mignot, T. B. de Villemeur, P. Lebon, O. Dulac, F. Rozenberg, B. Beutler, M. Tardieu, L. Abel, and J. L. Casanova.** 2006. Herpes simplex virus encephalitis in human UNC-93B deficiency. Science **314:**308-12.
32. **Castorena, K. M., D. C. Peltier, W. Peng, and D. J. Miller.** 2008. Maturation-dependent responses of human neuronal cells to western equine encephalitis virus infection and type I interferons. Virology **372:**208-20.
33. **CDC.** 2007. Biosafety in Microbiological and Biomedical Laboratories (BMBL) 5th ed.
34. **Chattopadhyay, S., J. T. Marques, M. Yamashita, K. L. Peters, K. Smith, A. Desai, B. R. Williams, and G. C. Sen.** 2010. Viral apoptosis is induced by IRF-3-mediated activation of Bax. Embo J **29:**1762-73.
35. **Chiu, Y. H., J. B. Macmillan, and Z. J. Chen.** 2009. RNA polymerase III detects cytosolic DNA and induces type I interferons through the RIG-I pathway. Cell **138:**576-91.
36. **Colonna, M., G. Trinchieri, and Y. J. Liu.** 2004. Plasmacytoid dendritic cells in immunity. Nat Immunol **5:**1219-26.
37. **Crack, P. J., and P. J. Bray.** 2007. Toll-like receptors in the brain and their potential roles in neuropathology. Immunol Cell Biol **85:**476-80.

38. **Cruz, C. C., M. S. Suthar, S. A. Montgomery, R. Shabman, J. Simmons, R. E. Johnston, T. E. Morrison, and M. T. Heise.** 2010. Modulation of type I IFN induction by a virulence determinant within the alphavirus nsP1 protein. Virology **399:**1-10.
39. **Daffis, S., M. A. Samuel, B. C. Keller, M. Gale, Jr., and M. S. Diamond.** 2007. Cell-specific IRF-3 responses protect against West Nile virus infection by interferon-dependent and -independent mechanisms. PLoS Pathog **3:**e106.
40. **Daffis, S., M. A. Samuel, M. S. Suthar, M. Gale, Jr., and M. S. Diamond.** 2008. Toll-like receptor 3 has a protective role against West Nile virus infection. J Virol **82:**10349-58.
41. **Daffis, S., M. A. Samuel, M. S. Suthar, B. C. Keller, M. Gale, Jr., and M. S. Diamond.** 2008. Interferon regulatory factor IRF-7 induces the antiviral alpha interferon response and protects against lethal West Nile virus infection. J Virol **82:**8465-75.
42. **Daffis, S., M. S. Suthar, M. Gale, Jr., and M. S. Diamond.** 2009. Measure and countermeasure: type I IFN (IFN-alpha/beta) antiviral response against West Nile virus. J Innate Immun **1:**435-45.
43. **Daffis, S., M. S. Suthar, K. J. Szretter, M. Gale, Jr., and M. S. Diamond.** 2009. Induction of IFN-beta and the innate antiviral response in myeloid cells occurs through an IPS-1-dependent signal that does not require IRF-3 and IRF-7. PLoS Pathog **5:**e1000607.
44. **Delhaye, S., S. Paul, G. Blakqori, M. Minet, F. Weber, P. Staeheli, and T. Michiels.** 2006. Neurons produce type I interferon during viral encephalitis. Proc Natl Acad Sci U S A **103:**7835-40.
45. **Deresiewicz, R. L., S. J. Thaler, L. Hsu, and A. A. Zamani.** 1997. Clinical and neuroradiographic manifestations of eastern equine encephalitis. N.Engl.J.Med. **336:**1867-1874.
46. **Diamond, M. S.** 2009. Virus and host determinants of West Nile virus pathogenesis. PLoS Pathog **5:**e1000452.
47. **Diamond, M. S., E. Mehlhop, T. Oliphant, and M. A. Samuel.** 2009. The host immunologic response to West Nile encephalitis virus. Front Biosci **14:**3024-34.
48. **Diao, F., S. Li, Y. Tian, M. Zhang, L. G. Xu, Y. Zhang, R. P. Wang, D. Chen, Z. Zhai, B. Zhong, P. Tien, and H. B. Shu.** 2007. Negative regulation of MDA5- but not RIG-I-mediated innate antiviral signaling by the dihydroxyacetone kinase. Proc Natl Acad Sci U S A **104:**11706-11.
49. **Dixit, E., S. Boulant, Y. Zhang, A. S. Lee, C. Odendall, B. Shum, N. Hacohen, Z. J. Chen, S. P. Whelan, M. Fransen, M. L. Nibert, G. Superti-Furga, and J. C. Kagan.** 2010. Peroxisomes are signaling platforms for antiviral innate immunity. Cell **141:**668-81.
50. **Dong, L. W., X. N. Kong, H. X. Yan, L. X. Yu, L. Chen, W. Yang, Q. Liu, D. D. Huang, M. C. Wu, and H. Y. Wang.** 2008. Signal regulatory protein

alpha negatively regulates both TLR3 and cytoplasmic pathways in type I interferon induction. Mol Immunol **45:**3025-35.

51. **Earnest, M. P., H. A. Goolishian, J. R. Calverley, R. O. Hayes, and H. R. Hill.** 1971. Neurologic, intellectual, and psychologic sequelae following western encephalitis. A follow-up study of 35 cases. Neurology **21:**969-974.
52. **Ewald, S. E., B. L. Lee, L. Lau, K. E. Wickliffe, G. P. Shi, H. A. Chapman, and G. M. Barton.** 2008. The ectodomain of Toll-like receptor 9 is cleaved to generate a functional receptor. Nature **456:**658-62.
53. **Fernandes-Alnemri, T., J. W. Yu, P. Datta, J. Wu, and E. S. Alnemri.** 2009. AIM2 activates the inflammasome and cell death in response to cytoplasmic DNA. Nature **458:**509-13.
54. **Fine, D. L., B. A. Roberts, S. J. Terpening, J. Mott, D. Vasconcelos, and R. V. House.** 2008. Neurovirulence evaluation of Venezuelan equine encephalitis (VEE) vaccine candidate V3526 in nonhuman primates. Vaccine **26:**3497-506.
55. **Fredericksen, B. L., and M. Gale, Jr.** 2006. West Nile virus evades activation of interferon regulatory factor 3 through RIG-I-dependent and -independent pathways without antagonizing host defense signaling. J Virol **80:**2913-23.
56. **Fredericksen, B. L., B. C. Keller, J. Fornek, M. G. Katze, and M. Gale, Jr.** 2008. Establishment and maintenance of the innate antiviral response to West Nile Virus involves both RIG-I and MDA5 signaling through IPS-1. J Virol **82:**609-16.
57. **Gardner, C. L., C. W. Burke, M. Z. Tesfay, P. J. Glass, W. B. Klimstra, and K. D. Ryman.** 2008. Eastern and Venezuelan equine encephalitis viruses differ in their ability to infect dendritic cells and macrophages: impact of altered cell tropism on pathogenesis. J Virol **82:**10634-46.
58. **Gardner, C. L., J. Yin, C. W. Burke, W. B. Klimstra, and K. D. Ryman.** 2009. Type I interferon induction is correlated with attenuation of a South American eastern equine encephalitis virus strain in mice. Virology **390:**338-47.
59. **Garmashova, N., S. Atasheva, W. Kang, S. C. Weaver, E. Frolova, and I. Frolov.** 2007. Analysis of Venezuelan equine encephalitis virus capsid protein function in the inhibition of cellular transcription. J Virol **81:**13552-65.
60. **Garmashova, N., R. Gorchakov, E. Volkova, S. Paessler, E. Frolova, and I. Frolov.** 2007. The Old World and New World alphaviruses use different virus-specific proteins for induction of transcriptional shutoff. J Virol **81:**2472-84.
61. **Ginsberg, S. D., J. E. Galvin, T. S. Chiu, V. M. Lee, E. Masliah, and J. Q. Trojanowski.** 1998. RNA sequestration to pathological lesions of neurodegenerative diseases. Acta Neuropathol **96:**487-94.

62. **Gomez de Cedron, M., N. Ehsani, M. L. Mikkola, J. A. Garcia, and L. Kaariainen.** 1999. RNA helicase activity of Semliki Forest virus replicase protein NSP2. FEBS Lett **448:**19-22.
63. **Gorchakov, R., E. Frolova, and I. Frolov.** 2005. Inhibition of transcription and translation in Sindbis virus-infected cells. J Virol **79:**9397-409.
64. **Griffin, D.** 2007. Alphaviruses. *In* D. Knipe, P. Howley, D. Griffin, R. Lamb, M. Martin, B. Roizman, and S. Straus (ed.), Field's Virology 5th ed. Lippincott Williams & Wilkins.
65. **Griffin, D. E.** 2003. Immune responses to RNA-virus infections of the CNS. Nat Rev Immunol **3:**493-502.
66. **Griffin, D. E.** 2005. Neuronal cell death in alphavirus encephalomyelitis. Curr Top Microbiol Immunol **289:**57-77.
67. **Griffin, D. E.** 1998. A review of alphavirus replication in neurons. Neurosci.Biobehav.Rev. **22:**721-723.
68. **Griffin, D. E.** 1976. Role of the immune response in age-dependent resistance of mice to encephalitis due to Sindbis virus. J.Infect.Dis. **133:**456-464.
69. **Griffin, D. E., B. Levine, W. R. Tyor, P. C. Tucker, and J. M. Hardwick.** 1994. Age-dependent susceptibility to fatal encephalitis: alphavirus infection of neurons. Arch.Virol.Suppl **9:**31-39.
70. **Griffin, D. E., B. Levine, S. Ubol, and J. M. Hardwick.** 1994. The effects of alphavirus infection on neurons. Ann.Neurol. **35 Suppl:**S23-S27.
71. **Gubler, D. J.** 2002. The global emergence/resurgence of arboviral diseases as public health problems. Arch Med Res **33:**330-42.
72. **Gubler, D. J., G. Kuno, and L. Markoff.** 2007. Flaviviruses. *In* D. Knipe, P. Howley, D. Griffin, R. Lamb, M. Martin, B. Roizman, and S. Straus (ed.), Field's Virology, 5 ed. Lippincott Williams & Wilkins.
73. **Hahn, C. S., S. Lustig, E. G. Strauss, and J. H. Strauss.** 1988. Western equine encephalitis virus is a recombinant virus. Proc Natl Acad Sci U S A **85:**5997-6001.
74. **Hahn, C. S., S. Lustig, E. G. Strauss, and J. H. Strauss.** 1988. Western equine encephalitis virus is a recombinant virus. Proc.Natl.Acad.Sci.U.S.A **85:**5997-6001.
75. **Hardy, J. L., S. B. Presser, R. E. Chiles, and W. C. Reeves.** 1997. Mouse and baby chicken virulence of enzootic strains of western equine encephalomyelitis virus from California. Am.J.Trop.Med.Hyg. **57:**240-244.
76. **Heil, F., H. Hemmi, H. Hochrein, F. Ampenberger, C. Kirschning, S. Akira, G. Lipford, H. Wagner, and S. Bauer.** 2004. Species-specific recognition of single-stranded RNA via toll-like receptor 7 and 8. Science **303:**1526-9.
77. **Heinz, S., V. Haehnel, M. Karaghiosoff, L. Schwarzfischer, M. Muller, S. W. Krause, and M. Rehli.** 2003. Species-specific regulation of Toll-like receptor 3 genes in men and mice. J Biol Chem **278:**21502-9.

78. **Heylbroeck, C., S. Balachandran, M. J. Servant, C. DeLuca, G. N. Barber, R. Lin, and J. Hiscott.** 2000. The IRF-3 transcription factor mediates Sendai virus-induced apoptosis. J Virol **74:**3781-92.
79. **Hickey, W. F.** 2001. Basic principles of immunological surveillance of the normal central nervous system. Glia **36:**118-24.
80. **Holbrook, M. R., and B. B. Gowen.** 2008. Animal models of highly pathogenic RNA viral infections: encephalitis viruses. Antiviral Res **78:**69-78.
81. **Holm, G. H., J. Zurney, V. Tumilasci, S. Leveille, P. Danthi, J. Hiscott, B. Sherry, and T. S. Dermody.** 2007. Retinoic acid-inducible gene-I and interferon-beta promoter stimulator-1 augment proapoptotic responses following mammalian reovirus infection via interferon regulatory factor-3. J Biol Chem **282:**21953-61.
82. **Honda, K., and T. Taniguchi.** 2006. IRFs: master regulators of signalling by Toll-like receptors and cytosolic pattern-recognition receptors. Nat Rev Immunol **6:**644-58.
83. **Hornung, V., A. Ablasser, M. Charrel-Dennis, F. Bauernfeind, G. Horvath, D. R. Caffrey, E. Latz, and K. A. Fitzgerald.** 2009. AIM2 recognizes cytosolic dsDNA and forms a caspase-1-activating inflammasome with ASC. Nature **458:**514-8.
84. **Hornung, V., and E. Latz.** 2010. Intracellular DNA recognition. Nat Rev Immunol **10:**123-30.
85. **Hunt, A. R., and J. T. Roehrig.** 1985. Biochemical and biological characteristics of epitopes on the E1 glycoprotein of western equine encephalitis virus. Virology **142:**334-46.
86. **Ichinohe, T., H. K. Lee, Y. Ogura, R. Flavell, and A. Iwasaki.** 2009. Inflammasome recognition of influenza virus is essential for adaptive immune responses. J Exp Med **206:**79-87.
87. **Irani, D. N., and D. E. Griffin.** 1996. Regulation of lymphocyte homing into the brain during viral encephalitis at various stages of infection. J.Immunol. **156:**3850-3857.
88. **Ishii, K. J., T. Kawagoe, S. Koyama, K. Matsui, H. Kumar, T. Kawai, S. Uematsu, O. Takeuchi, F. Takeshita, C. Coban, and S. Akira.** 2008. TANK-binding kinase-1 delineates innate and adaptive immune responses to DNA vaccines. Nature **451:**725-9.
89. **Jackson, A. C., J. P. Rossiter, and M. Lafon.** 2006. Expression of Toll-like receptor 3 in the human cerebellar cortex in rabies, herpes simplex encephalitis, and other neurological diseases. J Neurovirol **12:**229-34.
90. **Jordan, I., T. Briese, N. Fischer, J. Y. Lau, and W. I. Lipkin.** 2000. Ribavirin inhibits West Nile virus replication and cytopathic effect in neural cells. J Infect Dis **182:**1214-7.
91. **Kalali, B. N., G. Kollisch, J. Mages, T. Muller, S. Bauer, H. Wagner, J. Ring, R. Lang, M. Mempel, and M. Ollert.** 2008. Double-stranded RNA induces an antiviral defense status in epidermal keratinocytes through

TLR3-, PKR-, and MDA5/RIG-I-mediated differential signaling. J Immunol **181:**2694-704.

92. **Kato, H., S. Sato, M. Yoneyama, M. Yamamoto, S. Uematsu, K. Matsui, T. Tsujimura, K. Takeda, T. Fujita, O. Takeuchi, and S. Akira.** 2005. Cell type-specific involvement of RIG-I in antiviral response. Immunity **23:**19-28.
93. **Kato, H., O. Takeuchi, S. Sato, M. Yoneyama, M. Yamamoto, K. Matsui, S. Uematsu, A. Jung, T. Kawai, K. J. Ishii, O. Yamaguchi, K. Otsu, T. Tsujimura, C. S. Koh, C. Reis e Sousa, Y. Matsuura, T. Fujita, and S. Akira.** 2006. Differential roles of MDA5 and RIG-I helicases in the recognition of RNA viruses. Nature **441:**101-5.
94. **Kuhn, R. J.** 2007. *Togaviridae*: The Viruses and Their Replication. *In* D. Knipe, P. Howley, D. Griffin, R. Lamb, M. Martin, B. Roizman, and S. Straus (ed.), Field's Virology, 5 ed. Lippincott Williams & Wilkins.
95. **Kumar, H., T. Kawai, and S. Akira.** 2009. Pathogen recognition in the innate immune response. Biochem J **420:**1-16.
96. **Labrada, L., X. H. Liang, W. Zheng, C. Johnston, and B. Levine.** 2002. Age-dependent resistance to lethal alphavirus encephalitis in mice: analysis of gene expression in the central nervous system and identification of a novel interferon-inducible protective gene, mouse ISG12. J.Virol. **76:**11688-11703.
97. **Lafon, M., F. Megret, M. Lafage, and C. Prehaud.** 2006. The innate immune facet of brain: human neurons express TLR-3 and sense viral dsRNA. J Mol Neurosci **29:**185-94.
98. **Lastarza, M. W., J. A. Lemm, and C. M. Rice.** 1994. Genetic analysis of the nsP3 region of Sindbis virus: evidence for roles in minus-strand and subgenomic RNA synthesis. J.Virol. **68:**5781-5791.
99. **Lee, M. S., and Y. J. Kim.** 2007. Signaling pathways downstream of pattern-recognition receptors and their cross talk. Annu Rev Biochem **76:**447-80.
100. **Lehnardt, S.** 2010. Innate immunity and neuroinflammation in the CNS: the role of microglia in Toll-like receptor-mediated neuronal injury. Glia **58:**253-63.
101. **Levine, B., J. E. Goldman, H. H. Jiang, D. E. Griffin, and J. M. Hardwick.** 1996. Bc1-2 protects mice against fatal alphavirus encephalitis. Proc.Natl.Acad.Sci.U.S.A **93:**4810-4815.
102. **Levine, B., Q. Huang, J. T. Isaacs, J. C. Reed, D. E. Griffin, and J. M. Hardwick.** 1993. Conversion of lytic to persistent alphavirus infection by the bcl-2 cellular oncogene. Nature **361:**739-742.
103. **Li, J., Y. Liu, and X. Zhang.** 2010. Murine Coronavirus Induces Type I Interferon in Oligodendrocytes Through Recognition by RIG-I and MDA5. J Virol **84:**6472-82.

104. **Li, K., Z. Chen, N. Kato, M. Gale, Jr., and S. M. Lemon.** 2005. Distinct poly(I-C) and virus-activated signaling pathways leading to interferon-beta production in hepatocytes. J Biol Chem **280:**16739-47.
105. **Licinio, J., and M. L. Wong.** 1997. Pathways and mechanisms for cytokine signaling of the central nervous system. J Clin Invest **100:**2941-7.
106. **Lindebach, B. D., H.-J. Thiel, and C. M. Rice.** 2007. *Flaviviridae*: The Viruses and Their Replication. *In* D. Knipe, P. Howley, D. Griffin, R. Lamb, M. Martin, B. Roizman, and S. Straus (ed.), Field's Virology. Lippincott Williams & Wilkins.
107. **Lippmann, J., S. Rothenburg, N. Deigendesch, J. Eitel, K. Meixenberger, V. van Laak, H. Slevogt, D. N'Guessan P, S. Hippenstiel, T. Chakraborty, A. Flieger, N. Suttorp, and B. Opitz.** 2008. IFNbeta responses induced by intracellular bacteria or cytosolic DNA in different human cells do not require ZBP1 (DLM-1/DAI). Cell Microbiol **10:**2579-88.
108. **Liu, C., D. W. Voth, P. Rodina, L. R. Shauf, and G. Gonzalez.** 1970. A comparative study of the pathogenesis of western equine and eastern equine encephalomyelitis viral infections in mice by intracerebral and subcutaneous inoculations. J Infect Dis **122:**53-63.
109. **Liu, W. J., X. J. Wang, D. C. Clark, M. Lobigs, R. A. Hall, and A. A. Khromykh.** 2006. A single amino acid substitution in the West Nile virus nonstructural protein NS2A disables its ability to inhibit alpha/beta interferon induction and attenuates virus virulence in mice. J Virol **80:**2396-404.
110. **Lobigs, M., A. Mullbacher, Y. Wang, M. Pavy, and E. Lee.** 2003. Role of type I and type II interferon responses in recovery from infection with an encephalitic flavivirus. J Gen Virol **84:**567-72.
111. **Ma, Y., J. Li, I. Chiu, Y. Wang, J. A. Sloane, J. Lu, B. Kosaras, R. L. Sidman, J. J. Volpe, and T. Vartanian.** 2006. Toll-like receptor 8 functions as a negative regulator of neurite outgrowth and inducer of neuronal apoptosis. J Cell Biol **175:**209-15.
112. **MacDonald, G. H., and R. E. Johnston.** 2000. Role of dendritic cell targeting in Venezuelan equine encephalitis virus pathogenesis. J Virol **74:**914-22.
113. **Malathi, K., B. Dong, M. Gale, Jr., and R. H. Silverman.** 2007. Small self-RNA generated by RNase L amplifies antiviral innate immunity. Nature **448:**816-9.
114. **Marcinkiewicz, M.** 2002. BetaAPP and furin mRNA concentrates in immature senile plaques in the brain of Alzheimer patients. J Neuropathol Exp Neurol **61:**815-29.
115. **Marie, I., J. E. Durbin, and D. E. Levy.** 1998. Differential viral induction of distinct interferon-alpha genes by positive feedback through interferon regulatory factor-7. EMBO J **17:**6660-9.

116. **Mathews, J. H., and J. T. Roehrig.** 1982. Determination of the protective epitopes on the glycoproteins of Venezuelan equine encephalomyelitis virus by passive transfer of monoclonal antibodies. J.Immunol. **129:**2763-2767.
117. **Menager, P., P. Roux, F. Megret, J. P. Bourgeois, A. M. Le Sourd, A. Danckaert, M. Lafage, C. Prehaud, and M. Lafon.** 2009. Toll-like receptor 3 (TLR3) plays a major role in the formation of rabies virus Negri Bodies. PLoS Pathog **5:**e1000315.
118. **Mi, S., R. Durbin, H. V. Huang, C. M. Rice, and V. Stollar.** 1989. Association of the Sindbis virus RNA methyltransferase activity with the nonstructural protein nsP1. Virology **170:**385-91.
119. **Moisse, K., and M. J. Strong.** 2006. Innate immunity in amyotrophic lateral sclerosis. Biochim Biophys Acta **1762:**1083-93.
120. **Moore, C. B., D. T. Bergstralh, J. A. Duncan, Y. Lei, T. E. Morrison, A. G. Zimmermann, M. A. Accavitti-Loper, V. J. Madden, L. Sun, Z. Ye, J. D. Lich, M. T. Heise, Z. Chen, and J. P. Ting.** 2008. NLRX1 is a regulator of mitochondrial antiviral immunity. Nature **451:**573-7.
121. **Morrey, J. D., D. F. Smee, R. W. Sidwell, and C. Tseng.** 2002. Identification of active antiviral compounds against a New York isolate of West Nile virus. Antiviral Res **55:**107-16.
122. **Mueller, N. H., N. Pattabiraman, C. Ansarah-Sobrinho, P. Viswanathan, T. C. Pierson, and R. Padmanabhan.** 2008. Identification and biochemical characterization of small-molecule inhibitors of west nile virus serine protease by a high-throughput screen. Antimicrob Agents Chemother **52:**3385-93.
123. **Nagata, L. P., W. G. Hu, S. A. Masri, G. A. Rayner, F. L. Schmaltz, D. Das, J. Wu, M. C. Long, C. Chan, D. Proll, S. Jager, L. Jebailey, M. R. Suresh, and J. P. Wong.** 2005. Efficacy of DNA vaccination against western equine encephalitis virus infection. Vaccine **23:**2280-3.
124. **Nejentsev, S., N. Walker, D. Riches, M. Egholm, and J. A. Todd.** 2009. Rare variants of IFIH1, a gene implicated in antiviral responses, protect against type 1 diabetes. Science **324:**387-9.
125. **Neumann, H., H. Schmidt, E. Wilharm, L. Behrens, and H. Wekerle.** 1997. Interferon gamma gene expression in sensory neurons: evidence for autocrine gene regulation. J Exp Med **186:**2023-31.
126. **Nguyen, M. D., T. D'Aigle, G. Gowing, J. P. Julien, and S. Rivest.** 2004. Exacerbation of motor neuron disease by chronic stimulation of innate immunity in a mouse model of amyotrophic lateral sclerosis. J Neurosci **24:**1340-9.
127. **Noran, H. H.** 1944. Chronic Equine Encephalitis. Am J Pathol **20:**259-267.
128. **Noueiry, A. O., P. D. Olivo, U. Slomczynska, Y. Zhou, B. Buscher, B. Geiss, M. Engle, R. M. Roth, K. M. Chung, M. Samuel, and M. S. Diamond.** 2007. Identification of novel small-molecule inhibitors of West Nile virus infection. J Virol **81:**11992-2004.

129. **Park, B., M. M. Brinkmann, E. Spooner, C. C. Lee, Y. M. Kim, and H. L. Ploegh.** 2008. Proteolytic cleavage in an endolysosomal compartment is required for activation of Toll-like receptor 9. Nat Immunol **9:**1407-14.
130. **Parsonson, I. M., and D. A. McPhee.** 1985. Bunyavirus pathogenesis. Adv Virus Res **30:**279-316.
131. **Paul, S., C. Ricour, C. Sommereyns, F. Sorgeloos, and T. Michiels.** 2007. Type I interferon response in the central nervous system. Biochimie **89:**770-8.
132. **Peters, C. J.** 2008. Infections Caused by Arthropod- and Rodent-Borne Viruses. *In* B. E. Fauci AS, Kasper DL, Hauser SL, Longo DL, Jameson JL, Loscalzo J (ed.), Harrison's Principles of Internal Medicine, 17 ed.
133. **Pichlmair, A., and C. Reis e Sousa.** 2007. Innate recognition of viruses. Immunity **27:**370-83.
134. **Pichlmair, A., O. Schulz, C. P. Tan, J. Rehwinkel, H. Kato, O. Takeuchi, S. Akira, M. Way, G. Schiavo, and C. Reis e Sousa.** 2009. Activation of MDA5 requires higher-order RNA structures generated during virus infection. J Virol **83:**10761-9.
135. **Poch, O., I. Sauvaget, M. Delarue, and N. Tordo.** 1989. Identification of four conserved motifs among the RNA-dependent polymerase encoding elements. EMBO J. **8:**3867-3874.
136. **Poeck, H., M. Bscheider, O. Gross, K. Finger, S. Roth, M. Rebsamen, N. Hannesschlager, M. Schlee, S. Rothenfusser, W. Barchet, H. Kato, S. Akira, S. Inoue, S. Endres, C. Peschel, G. Hartmann, V. Hornung, and J. Ruland.** 2010. Recognition of RNA virus by RIG-I results in activation of CARD9 and inflammasome signaling for interleukin 1 beta production. Nat Immunol **11:**63-9.
137. **Prehaud, C., F. Megret, M. Lafage, and M. Lafon.** 2005. Virus infection switches TLR-3-positive human neurons to become strong producers of beta interferon. J Virol **79:**12893-904.
138. **Rehli, M.** 2002. Of mice and men: species variations of Toll-like receptor expression. Trends Immunol **23:**375-8.
139. **Rehwinkel, J., and C. Reis e Sousa.** 2010. RIGorous detection: exposing virus through RNA sensing. Science **327:**284-6.
140. **Rivest, S.** 2009. Regulation of innate immune responses in the brain. Nat Rev Immunol **9:**429-39.
141. **Rolls, A., R. Shechter, A. London, Y. Ziv, A. Ronen, R. Levy, and M. Schwartz.** 2007. Toll-like receptors modulate adult hippocampal neurogenesis. Nat Cell Biol **9:**1081-8.
142. **Ropper AH, S. M.** 2009. Viral Infections of the Nervous System, Chronic Meningitis, and Prion Diseases. *In* S. M. Ropper AH (ed.), Adams and Victor's Principles of Neurology
9ed. McGraw-Hill.
143. **Ryman, K. D., and W. B. Klimstra.** 2008. Host responses to alphavirus infection. Immunol Rev **225:**27-45.

144. **Sabbah, A., T. H. Chang, R. Harnack, V. Frohlich, K. Tominaga, P. H. Dube, Y. Xiang, and S. Bose.** 2009. Activation of innate immune antiviral responses by Nod2. Nat Immunol **10:**1073-80.
145. **Sadler, A. J., and B. R. Williams.** 2008. Interferon-inducible antiviral effectors. Nat Rev Immunol **8:**559-68.
146. **Samuel, M. A., and M. S. Diamond.** 2005. Alpha/beta interferon protects against lethal West Nile virus infection by restricting cellular tropism and enhancing neuronal survival. J Virol **79:**13350-61.
147. **Sarkar, S. N., K. L. Peters, C. P. Elco, S. Sakamoto, S. Pal, and G. C. Sen.** 2004. Novel roles of TLR3 tyrosine phosphorylation and PI3 kinase in double-stranded RNA signaling. Nat Struct Mol Biol **11:**1060-7.
148. **Sato, M., N. Hata, M. Asagiri, T. Nakaya, T. Taniguchi, and N. Tanaka.** 1998. Positive feedback regulation of type I IFN genes by the IFN-inducible transcription factor IRF-7. FEBS Lett **441:**106-10.
149. **Sato, M., H. Suemori, N. Hata, M. Asagiri, K. Ogasawara, K. Nakao, T. Nakaya, M. Katsuki, S. Noguchi, N. Tanaka, and T. Taniguchi.** 2000. Distinct and essential roles of transcription factors IRF-3 and IRF-7 in response to viruses for IFN-alpha/beta gene induction. Immunity **13:**539-48.
150. **Schlesinger, S., and M. J. Schlesinger.** 2001. Togaviridae: The Viruses and Their Replication, p. 895-916. *In* D. M. Knipe, P. M. Howley, D. E. Griffin, R. A. Lamb, M. A. Martin, B. Roizman, and S. S. Straus (ed.), Fields Virology, Fourth ed. Lippincott Williams & Wilkins, Philadelphia.
151. **Schmaljohn, C. S., and S. T. Nichol.** 2007. *Bunyaviridae*. *In* D. Knipe, P. Howley, D. Griffin, R. Lamb, M. Martin, B. Roizman, and S. Straus (ed.), Field's Virolgoy, 5 ed. Lippincott Williams & Wilkins.
152. **Schoepp, R. J., J. F. Smith, and M. D. Parker.** 2002. Recombinant chimeric western and eastern equine encephalitis viruses as potential vaccine candidates. Virology **302:**299-309.
153. **Sharif-Askari, E., P. Nakhaei, S. Oliere, V. Tumilasci, E. Hernandez, P. Wilkinson, R. Lin, J. Bell, and J. Hiscott.** 2007. Bax-dependent mitochondrial membrane permeabilization enhances IRF3-mediated innate immune response during VSV infection. Virology **365:**20-33.
154. **Sherman, L. A., and D. E. Griffin.** 1990. Pathogenesis of encephalitis induced in newborn mice by virulent and avirulent strains of Sindbis virus. J.Virol. **64:**2041-2046.
155. **Sidwell, R. W., and D. F. Smee.** 2003. Viruses of the Bunya- and Togaviridae families: potential as bioterrorism agents and means of control. Antiviral Res **57:**101-11.
156. **Stanley, J., S. J. Cooper, and D. E. Griffin.** 1986. Monoclonal antibody cure and prophylaxis of lethal Sindbis virus encephalitis in mice. J.Virol. **58:**107-115.

157. **Staples, J. E., R. F. Breiman, and A. M. Powers.** 2009. Chikungunya fever: an epidemiological review of a re-emerging infectious disease. Clin Infect Dis **49:**942-8.
158. **Strauss, J. H., and E. G. Strauss.** 1994. The alphaviruses: gene expression, replication, and evolution. Microbiol Rev **58:**491-562.
159. **Suthar, M. S., D. Y. Ma, S. Thomas, J. M. Lund, N. Zhang, S. Daffis, A. Y. Rudensky, M. J. Bevan, E. A. Clark, M. K. Kaja, M. S. Diamond, and M. Gale, Jr.** 2010. IPS-1 is essential for the control of West Nile virus infection and immunity. PLoS Pathog **6:**e1000757.
160. **Takaoka, A., Z. Wang, M. K. Choi, H. Yanai, H. Negishi, T. Ban, Y. Lu, M. Miyagishi, T. Kodama, K. Honda, Y. Ohba, and T. Taniguchi.** 2007. DAI (DLM-1/ZBP1) is a cytosolic DNA sensor and an activator of innate immune response. Nature **448:**501-5.
161. **Takeuchi, O., and S. Akira.** 2010. Pattern recognition receptors and inflammation. Cell **140:**805-20.
162. **Thomas, P. G., P. Dash, J. R. Aldridge, Jr., A. H. Ellebedy, C. Reynolds, A. J. Funk, W. J. Martin, M. Lamkanfi, R. J. Webby, K. L. Boyd, P. C. Doherty, and T. D. Kanneganti.** 2009. The intracellular sensor NLRP3 mediates key innate and healing responses to influenza A virus via the regulation of caspase-1. Immunity **30:**566-75.
163. **Town, T., D. Jeng, L. Alexopoulou, J. Tan, and R. A. Flavell.** 2006. Microglia recognize double-stranded RNA via TLR3. J Immunol **176:**3804-12.
164. **Trgovcich, J., J. F. Aronson, J. C. Eldridge, and R. E. Johnston.** 1999. TNFalpha, interferon, and stress response induction as a function of age-related susceptibility to fatal Sindbis virus infection of mice. Virology **263:**339-348.
165. **Trgovcich, J., J. F. Aronson, and R. E. Johnston.** 1996. Fatal Sindbis virus infection of neonatal mice in the absence of encephalitis. Virology **224:**73-83.
166. **Trgovcich, J., K. Ryman, P. Extrom, J. C. Eldridge, J. F. Aronson, and R. E. Johnston.** 1997. Sindbis virus infection of neonatal mice results in a severe stress response. Virology **227:**234-238.
167. **Tuittila, M., and A. E. Hinkkanen.** 2003. Amino acid mutations in the replicase protein nsP3 of Semliki Forest virus cumulatively affect neurovirulence. J Gen Virol **84:**1525-33.
168. **Turell, M. J., G. V. Ludwig, J. Kondig, and J. F. Smith.** 1999. Limited potential for mosquito transmission of genetically engineered, live-attenuated Venezuelan equine encephalitis virus vaccine candidates. Am.J.Trop.Med.Hyg. **60:**1041-1044.
169. **Turell, M. J., and M. D. Parker.** 2008. Protection of hamsters by Venezuelan equine encephalitis virus candidate vaccine V3526 against lethal challenge by mosquito bite and intraperitoneal injection. Am J Trop Med Hyg **78:**328-32.

170. **Unterholzner, L., and A. G. Bowie.** 2008. The interplay between viruses and innate immune signaling: recent insights and therapeutic opportunities. Biochem Pharmacol **75:**589-602.
171. **Vasiljeva, L., L. Valmu, L. Kaariainen, and A. Merits.** 2001. Site-specific protease activity of the carboxyl-terminal domain of Semliki Forest virus replicase protein nsP2. J Biol Chem **276:**30786-93.
172. **Vercammen, E., J. Staal, and R. Beyaert.** 2008. Sensing of viral infection and activation of innate immunity by toll-like receptor 3. Clin Microbiol Rev **21:**13-25.
173. **Wang, C., T. Chen, J. Zhang, M. Yang, N. Li, X. Xu, and X. Cao.** 2009. The E3 ubiquitin ligase Nrdp1 'preferentially' promotes TLR-mediated production of type I interferon. Nat Immunol **10:**744-52.
174. **Wang, E., O. Petrakova, A. P. Adams, P. V. Aguilar, W. Kang, S. Paessler, S. M. Volk, I. Frolov, and S. C. Weaver.** 2007. Chimeric Sindbis/eastern equine encephalitis vaccine candidates are highly attenuated and immunogenic in mice. Vaccine **25:**7573-81.
175. **Wang, Q., D. R. Nagarkar, E. R. Bowman, D. Schneider, B. Gosangi, J. Lei, Y. Zhao, C. L. McHenry, R. V. Burgens, D. J. Miller, U. Sajjan, and M. B. Hershenson.** 2009. Role of double-stranded RNA pattern recognition receptors in rhinovirus-induced airway epithelial cell responses. J Immunol **183:**6989-97.
176. **Wang, T., T. Town, L. Alexopoulou, J. F. Anderson, E. Fikrig, and R. A. Flavell.** 2004. Toll-like receptor 3 mediates West Nile virus entry into the brain causing lethal encephalitis. Nat Med **10:**1366-73.
177. **Wang, Y. F., S. G. Sawicki, and D. L. Sawicki.** 1994. Alphavirus nsP3 functions to form replication complexes transcribing negative-strand RNA. J.Virol. **68:**6466-6475.
178. **Werling, D., O. C. Jann, V. Offord, E. J. Glass, and T. J. Coffey.** 2009. Variation matters: TLR structure and species-specific pathogen recognition. Trends Immunol **30:**124-30.
179. **White, L. J., J. G. Wang, N. L. Davis, and R. E. Johnston.** 2001. Role of alpha/beta interferon in Venezuelan equine encephalitis virus pathogenesis: effect of an attenuating mutation in the 5' untranslated region. J Virol **75:**3706-18.
180. **Wilson, J. R., P. F. de Sessions, M. A. Leon, and F. Scholle.** 2008. West Nile virus nonstructural protein 1 inhibits TLR3 signal transduction. J Virol **82:**8262-71.
181. **Wu, J. Q., N. D. Barabe, D. Chau, C. Wong, G. R. Rayner, W. G. Hu, and L. P. Nagata.** 2007. Complete protection of mice against a lethal dose challenge of western equine encephalitis virus after immunization with an adenovirus-vectored vaccine. Vaccine **25:**4368-75.
182. **Yanai, H., T. Ban, Z. Wang, M. K. Choi, T. Kawamura, H. Negishi, M. Nakasato, Y. Lu, S. Hangai, R. Koshiba, D. Savitsky, L. Ronfani, S. Akira, M. E. Bianchi, K. Honda, T. Tamura, T. Kodama, and T.**

Taniguchi. 2009. HMGB proteins function as universal sentinels for nucleic-acid-mediated innate immune responses. Nature **462:**99-103.
183. **Yang, P., H. An, X. Liu, M. Wen, Y. Zheng, Y. Rui, and X. Cao.** 2010. The cytosolic nucleic acid sensor LRRFIP1 mediates the production of type I interferon via a beta-catenin-dependent pathway. Nat Immunol **11:**487-94.
184. **Yoneyama, M., and T. Fujita.** 2010. Recognition of viral nucleic acids in innate immunity. Rev Med Virol **20:**4-22.
185. **Yoneyama, M., and T. Fujita.** 2009. RNA recognition and signal transduction by RIG-I-like receptors. Immunol Rev **227:**54-65.
186. **Yu, H. B., and B. B. Finlay.** 2008. The caspase-1 inflammasome: a pilot of innate immune responses. Cell Host Microbe **4:**198-208.
187. **Zeng, W., L. Sun, X. Jiang, X. Chen, F. Hou, A. Adhikari, M. Xu, and Z. J. Chen.** 2010. Reconstitution of the RIG-I pathway reveals a signaling role of unanchored polyubiquitin chains in innate immunity. Cell **141:**315-30.
188. **Zhang, S. Y., E. Jouanguy, S. Ugolini, A. Smahi, G. Elain, P. Romero, D. Segal, V. Sancho-Shimizu, L. Lorenzo, A. Puel, C. Picard, A. Chapgier, S. Plancoulaine, M. Titeux, C. Cognet, H. von Bernuth, C. L. Ku, A. Casrouge, X. X. Zhang, L. Barreiro, J. Leonard, C. Hamilton, P. Lebon, B. Heron, L. Vallee, L. Quintana-Murci, A. Hovnanian, F. Rozenberg, E. Vivier, F. Geissmann, M. Tardieu, L. Abel, and J. L. Casanova.** 2007. TLR3 deficiency in patients with herpes simplex encephalitis. Science **317:**1522-7.
189. **Zhou, Y., L. Ye, Q. Wan, L. Zhou, X. Wang, J. Li, S. Hu, D. Zhou, and W. Ho.** 2009. Activation of Toll-like receptors inhibits herpes simplex virus-1 infection of human neuronal cells. J Neurosci Res **87:**2916-25.
190. **Zurney, J., K. E. Howard, and B. Sherry.** 2007. Basal expression levels of IFNAR and Jak-STAT components are determinants of cell-type-specific differences in cardiac antiviral responses. J Virol **81:**13668-80.

Chapter II

Human Neuronal Cells Possess Functional Cytoplasmic and Toll-Like Receptor-Mediated Innate Immune Pathways Influenced by Phosphatidylinositol-3 Kinase Signaling

Innate immune pathways are early defense responses important for the immediate control and eventual clearance of many pathogens, where signaling is initiated via pattern recognition receptor-mediated events that occur in a ligand- and cell-type specific manner. Within CNS neurons, innate immune pathways are likely crucial to control pathogens that target these essential yet virtually irreplaceable cells. However, relatively little is known about the induction and regulation of neuronal pattern recognition receptor signaling. In this report, we used human neuronal cell lines and primary rat neuronal cultures to examine pattern recognition receptor expression and function. We found that several innate immune receptor ligands, including Sendai virus, the dsRNA mimetic polyinosinic-polycytidylic acid, and LPS all activated differentiation-dependent neuronal innate immune pathways. Functional genetic analyses revealed that interferon regulatory factor 3-mediated pathways that resulted in IFNβ transcriptional upregulation were activated in cultured human neuronal cells by the pattern recognition receptors TLR3, melanoma differentiated-associated gene 5, or retinoic acid inducible gene I in a ligand-specific manner. Furthermore, genome-wide transcriptional array and targeted genetic and pharmacologic analyses identified PI3K signaling as crucial for the induction of

innate immune pathways in neurons. These results indicate that human neuronal cells possess specific and functional pattern recognition receptor pathways essential for the effective induction of innate immune responses, and suggest that neurons can play an active role in defense against neurotropic pathogens.

Introduction

Innate immune pathways are early responses important for pathogen control, and are activated by pattern recognition receptors (PRRs) that bind ligands containing pathogen- or danger-associated molecular patterns, such as modified carbohydrate or nucleic acid structures (39). For antiviral innate immune responses, ligation of these receptors induces a signal transduction cascade that results in the production of type-I IFNs, other proinflammatory cytokines, and cell-intrinsic factors important for the generation of an antiviral cellular microenvironment (51). In addition, antiviral PRR signaling is important for activating an appropriate adaptive immune response, which is required for the eventual clearance of many viral infections. Thus, PRR-mediated innate immune pathway signaling serves a pivotal role in stimulating rapid yet nonspecific antiviral activity while also providing activation signals for the production of more specialized adaptive immune responses.

There are three general steps in innate antiviral immune responses: activation, amplification, and effector production. Antiviral PRR signaling is initiated by a variety of receptors, including the transmembrane TLR proteins 2, 3, 4, 7/8, and 9, and the cytoplasmic retinoic acid inducible gene I (RIG-I)-like receptors (RLRs) RIG-I and melanoma differentiated-associated gene 5 (MDA5) (51). TLR3, TLR7/8, and TLR9 recognize the non-self nucleic acid moieties dsRNA, ssRNA, and hypomethylated CpG DNA, respectively, whereas TLR4 recognizes viral glycoproteins and the viral ligand for TLR2 remains to be identified. In the cytoplasm, RIG-I binds double-stranded 5’ triphosphorylated

RNAs, homopolymeric RNA motifs, and short dsRNAs less than 2 kb in length (63, 64), whereas MDA5 recognizes complex dsRNAs greater than 2 kb in length (52) that can be mimicked by the synthetic dsRNA molecule polyinosinic-polycytidylic acid (poly(I-C)) (74). Due in part to this ligand specificity, PRRs differentially recognize and respond to distinct viral infections (39). After PRR ligation, signal transduction is mediated by several distinct adaptor proteins, including MyD88, TIR-domain-containing adapter-inducing IFN-β (TRIF), and IFN-β promoter stimulator protein 1 (IPS-1; also referred to as Cardif, MAVS, and VISA) (39, 51). These adaptor protein complexes activate the transcription factors NFκB and IFN regulatory factor 3 (IRF3) via multiple downstream kinases. Activated NFκB and IRF3 subsequently upregulate the expression of many genes important for mounting a robust antiviral response, including type-I IFNs (56), which function in either a paracrine or autocrine manner to induce IFN-stimulated genes that contain IFN-stimulated response elements (ISREs) within their promoters. There are several IFN-stimulated genes that act directly as antiviral effectors, but many are also components of antiviral PRR pathways, which provides a mechanism for positive feedback regulation and amplification (39, 51).

The molecular mechanisms of antiviral PRR signaling have been defined primarily using a limited number of cell lines and primary cell types, many of which are derived from small rodent models and are professional immune cells such as dendritic cells or macrophages. These studies have revealed important cell type-specific differences in antiviral PRR pathways. For example, dendritic

cells express relatively high basal levels of TLR7 and TLR9, and as a result vigorously respond to ligands for these receptors (8). In contrast, "non-professional" immune cells such as fibroblasts use primarily cytoplasmic RLRs for innate antiviral pathway activation (34), although some cell types such as keratinocytes (32) and respiratory epithelial cells (70) can also mount vigorous TLR-mediated antiviral responses. Plasmacytoid dendritic cells also constitutively express the transcription factor IRF7, which is thought to contribute to their ability to produce IFNα rapidly after PRR-mediated stimulation (2, 8, 27), whereas IFNα production in other cell types occurs later, if at all, and is linked to IFNβ-mediated induction of IRF7 (44, 61, 62). Additional examples of cell type-specific differences in innate antiviral immunity include a lower basal activity of PRR pathways in cardiac fibroblasts compared cardiac myocytes (80), differential responses of specific human hepatocyte cell lines to poly(I-C) and Sendai virus (SeV) stimulation (42), and cell type-specific roles for IRF3 and IRF7 in response to West Nile virus infection (13, 15). Furthermore, species-specific differences also exist with respect to TLR expression, regulation, and function (25, 26, 57, 72). These observations suggest that caution should be exercised in extrapolating results on innate antiviral pathway activity between species and cell types.

Viruses from several families preferentially infect CNS neurons, and the extent of neurotropic virus-mediated cell death can be an important determinant in the severity and clinical outcome of infection (22). Thus, an effective neuronal innate antiviral response that controls virus replication until an adaptive immune

response can be generated may be crucial to prevent the essentially irreversible loss of these critical cells. However, we have limited knowledge regarding the PRR antiviral pathways that are active in CNS neurons. TLR3 expression has been reported in human neurons (3, 30, 45, 54, 79), West Nile virus replication is enhanced in cortical neurons isolated from TLR3$^{-/-}$ mice (14), and neural progenitor cells respond to poly(I-C) stimulation by reducing proliferation and neurosphere formation in a TLR3-dependent manner (41). Furthermore, studies have demonstrated virus-mediated induction of type-I IFNs in CNS neurons both in vitro (13-15, 54) and in vivo (16). In addition to putative antiviral functions, PRR pathways have been implicated in neuronal development (58), neuronal regeneration (3, 43), and neuroinflammatory diseases (12, 46). Altogether, these reports suggest that CNS neurons possess active PRRs that may have multiple physiologic functions, but the full extent of their activity and the downstream components that mediate their activation remain to be determined.

In this report, we use both global and targeted approaches to examine PRR expression and pathway activity in response to RLR and TLR ligands. We found that human neuronal cells show differentiation-dependent selective responses to TLR3-, TLR4-, MDA5-, and RIG-I-mediated stimulation. Furthermore, detailed genetic and pharmacologic studies revealed that select neuronal innate immune pathways were dependent on PI3K activity. These results demonstrate that human neuronal cells are immunologically active and possess specific and non-redundant functional PRR pathways that may play a protective role in neurotropic virus pathogenesis.

Materials and Methods

Plasmids

We purchased the reporter plasmids pISRE-SEAP and pNFκB-SEAP, the wild type expression plasmid pTLR3, the dominant negative-expression plasmids pDN-TLR3(ΔTIR), pDN-TRIF(TIR), and pDN-RIG-I(ΔN), and the short-hairpin RNA expression plasmid pshRNA-MDA5 from InvivoGen (San Diego, CA). The dominant negative expression plasmid pDN-IRF3(ΔN) was generously provided by Rongtuan Lin (McGill University, Montreal). We purchased the lentivirus short-hairpin RNA expression plasmids pGIPZ-shCD14 and pGIPZ-shPI3K110α from Open Biosystems (Huntsville, AL). The lentivirus helper plasmids pCMV-VSV/G and pCMV-Gag/Pol were generously provided by David Markovitz (University of Michigan, Ann Arbor, MI).

Virus

Recombinant SeV that contains a GFP tag between the viral P and M genes was generously provided by Valery Grdzelishvilli (University of North Carolina at Charlotte, Charlotte, NC) and was expanded twice through Vero cells at a low multiplicity of infection to generate viral stocks. SeV growth curves were analyzed by monitoring GFP accumulation in infected cells using a FLUOstar Omega plate reader (BMG Labtech, Durham, NC) and black-walled, translucent-bottomed 96-well tissue culture plates.

Lentivirus production for shRNA knockdown was done as previously described (33). Briefly, HEK293FT cells at 90% confluence were incubated with

25 μg/ml chloroquine and transfected either pGIPZ-shCD14 or pGIPZ-shPI3K110α and the packaging plasmids pCMV-VSV/G and pCMV-Gag/Pol using calcium chloride. Virus was harvested from clarified supernatants at 24 and 48 h after transfection and stored at 4°C in the dark prior to cell infections.

Antibodies, Cytokines, PRR Ligands, and Kinase Inhibitors

Antibodies against GAPDH and IRF3 were purchased from Santa Cruz Biotechnology (Santa Cruz, CA), antibodies against synaptophysin, neurofilament 200, and glial fibrillary acidic protein were purchased from Sigma (St. Louis, MO), antibodies against TLR3 were purchased from either Santa Cruz Biotechnology (clone TLR3.7, catalog no. sc-32232) or Imigenex (San Diego, CA; clone 40C1285.6, catalog no. IMG-315A), antibodies against PI3K p110α were purchased from Cell Signaling Technology (Danvers, MA), and antibodies against RIG-I were purchased from Alexis Biochemical (San Diego, CA). Antibodies against MDA5 were generously provided by Paul Fisher (Columbia University, New York, NY). Neutralizing antisera against type I IFNs and the corresponding control sera were obtained from the Biodefense and Emerging Infections (BEI) Research Resources Repository (Manassas, VA). All secondary antibodies for immunoblotting and immunofluorescence staining were purchased from Jackson Immunoresearch (West Grove, PA).

Recombinant human IFNα-A/D and rat IFNα were purchased from PBL Biomedical Laboratories (Piscataway, NJ), recombinant human TNFα was purchased from R&D Systems (Minneapolis, MN), and human leukocyte IFNα

and fibroblast IFNβ were obtained from the BEI Repository. All cytokines were stored in single use aliquots at -80°C. Ultrapure *E. coli* K12 LPS, the imidazoquinoline derivative CLO97, and the CpG-containing synthetic oligonucleotide ODN2006 were purchased from InvivoGen. Poly(I-C) was purchased from either Sigma or InvivoGen and stored as a 5-10 mg/ml solution in sterile water at -20°C. We transfected poly(I-C) using Lipofectamine 2000 (Invitrogen) at a ratio of 200 μg poly(I-C) per 60 μl of Lipofectamine 2000 in a total volume of 150 μl Opti-MEM I (Gibco) media.

The kinase inhibitor library was provided by the University of Michigan Center for Chemical Genomics and was originally purchased from TimTec (Newark, DE). The kinase inhibitors LY294002 and TGX-221 were purchased from Calbiochem (San Diego, CA) and the kinase inhibitors AS-252424 and p110α inhibitor 2 were purchased from Cayman Chemical (Ann Arbor, MI).

Cell Culture

BE(2)-C, SHSY-5Y, HCN-1A, U937, and Vero cells were all obtained from the American Type Culture Collection (Manassas, VA). We differentiated BE(2)-C cells with all-*trans* retinoic acid as previously described (5), the non-malignant human cortical neuronal cell line HCN-1A with nerve growth factor, 1-isobutyl-3-methylxanthine, and dibutyryl cAMP as previously described (59), and human monocytic U937 cells with 15 nM PMA for 48 h. To avoid potential confounding effects of cell differentiation on transfection or transduction efficiency, we generated stable cell lines prior to differentiation. BE(2)-C and SH-SY5Y cells

were transfected with reporter gene-, dominant negative-, or shRNA-expressing plasmids using Lipofectamine 2000 according to the manufacturer's instruction (Invitrogen, Carlsbad, CA), whereas U937 cells were transfected by electroporation using a GenePulser Xcell according to the manufacturer's instructions (Bio-Rad, Hercules, CA). For lentiviral transduction, cells were infected with recombinant lentiviruses in the presence of 8 μg/ml polybrene. Cell lines were passed at least three times in the presence of selection antibiotic prior to use in experiments, and selection agents were removed for retinoic acid- or PMA-induced differentiation.

Primary rat neuronal cultures were prepared from embryonic day 18 Sprague-Dawley rat cortices according to the supplier's recommendations (BrainBits LLC, Springfield, IL). Briefly, cortices were digested with 2 mg/ml papain (Worthington, Lakewood, NJ) for 30 minutes at 30°C in HibernateE solution (BrainBits LLC) without calcium followed by gentle trituration. Cell suspensions were allowed to settle by gravity for 1 min to remove large debris, supernatants were collected and centrifuged at 500 x g for 5 min, cell pellets were gently resuspended in Neurobasal E media supplemented with 2% B27 (Gibco, Grand Island, NY), 500 μM L-glutamine, 10 units/ml penicillin, and 10 μg/ml streptomycin, dispensed into poly-D-lysine-coated plates at 1 x 10^5 cells/cm^2, and incubated at 37°C with 5% CO_2. Eighteen to twenty-four h after plating the media was completely replaced and on subsequent days half of the culture volume was replaced. Cells were routinely used at 12-14 days after plating, at which time immunofluorescence staining showed that ~95% of cells

expressed the transmembrane synaptic vesicle glycoprotein synaptophysin and neurofilament 200, which are both markers of mature neurons, but not the astrocyte marker glial fibrillary acid protein (**Supplemental Fig S2.1.A and B**). Furthermore, primary rat neuronal cultures were also highly sensitive to glutamate-mediated excitotoxicity (**Supplemental Fig S2.1.C**), which is a well described phenotype of mature cortical neurons in vitro (77).

Cell Viability and SEAP Assays

Cell viability was determined with either Alamar Blue according to the manufacturer's instructions (AbD Serotec, Oxford, UK) or an MTT assay as previously described (5). Secreted alkaline phosphatase (SEAP) assays were conducted using Quanti-Blue substrate according to manufacturer's instructions (InvivoGen). Fluorescence and absorbance endpoint values for viability and SEAP assays were obtained with a FLUOstar Omega plate reader.

Immunoblotting, Immunofluorescence, and RT-PCR Analysis

Immunoblotting, immunofluorescence staining of cultured cells, and RT-PCR were done as previously described (5, 49) with the following modifications. For TLR3 immunoblotting, membranes were blocked with PBS containing 1% BSA and 1% polyvinylpyrrolidone, and TLR3-specific bands were detected with the Imigenex monoclonal antibody, a biotinylated secondary antibody, and streptavidin-conjugated HRP. For TLR3 immunofluorescence staining, cells were permeabilized with 0.1% Triton X-100 after paraformaldehyde fixation,

immunostained with the Santa Cruz monoclonal antibody, a biotinylated secondary antibody, and streptavidin-conjugated PE. Primer sequences for PCR are available upon request.

Microarray, Pathway Analysis, and Validation

Total RNA was isolated from five independent sets of cultures containing similar numbers of immature BE(2)-C or differentiated BE(2)-C/m cells using TRIzol (Invitrogen), digested with RQ1 DNaseI (Promega), and repurified using an RNeasy kit (Qiagen, Valencia, CA) according to the manufacturer's instructions. RNA integrity and quantity were assessed using a microfluidics-based Agilent 2100 Bioanalyzer (Foster City, CA). RNA labeling, hybridization, and array scanning was done by either SeqWright DNA Technology Services (Houston, TX) or the University of Michigan Microarray core facility using biotinylated amplified cRNAs and Affymetrix Human U133 Plus 2.0 microarray chips. Complete original data files for all microarray experiments have been deposited in the Gene Expression Omnibus (GEO) database (http://www.ncbi.nlm.nih.gov/geo/) under the accession number GSE16452.

The Genomatix ChipInspector software package (Genomatix Software Inc., Ann Arbor, MI; www.genomatix.de) was used for primary microarray data analysis. This program uses a single probe method with an enhanced statistics package based on the original SAM algorithm (67) that incorporates a *t*-test with a permuted artificial background to reduce false-positives. The following parameters were chosen to identify sets of differentially regulated transcripts: (i)

false-discovery rate of 1%; (ii) three probe minimum coverage; and (iii) expression level $\log_2$ change ≥ 0.5 (~1.4-fold) compared to control. Similar results were obtained when microarray data were analyzed with the Affymetrix package of Bioconductor (29). The list of genes preferentially upregulated in differentiated BE(2)-C/m cells were analyzed using Ingenuity Pathway Analysis software (Ingenuity Systems, Redwood, CA; www.ingenuity.com). This analysis used the Ingenuity Pathway Analysis library of 103 signaling and 80 metabolic canonical pathways to identify those that were most significant to the data set. This significance was measured by determining the ratio of the number of genes from the data set that map to a particular canonical pathway to the total number of genes for that pathway, and calculating a subsequent *p*-value using a Fischer's exact test. The association with a particular canonical pathway was considered significant if the *p*-value < 0.05.

To validate microarray results, PI3K-AKT pathway real-time RT-PCR arrays (SABiosciences, Frederick, MD) were used to analyze transcript expression level differences between two independent sets of immature BE(2)-C and differentiated BE(2)-C/m cultures. Total RNA was isolated as described above and RNA integrity and quantity was assessed using non-denaturing agarose gel electrophoresis and spectrophotometry, respectively. cDNA synthesis and real time PCR were conducted using the manufacturer's recommended reagents and protocols for the BioRad iCycler iQ thermocycler, and fluorescence threshold cycle (C_t) values were calculated using SDS 700 system software (Bio-Rad). Results were normalized to the average C_t for 5

housekeeping genes contained on the RT-PCR array and $\Delta\Delta C_t$ values were calculated to determine expression changes. Genes that reached the C_t maximum of 35 in either trial were excluded from the analysis.

Statistical Analysis

Microarray and pathway statistical analyses are described above. For comparative analyses we used a two-tailed Student's *t*-test assuming unequal variances where a p-value of < 0.05 was considered significant. Quantitative EC_{50} and IC_{50} values were calculated using Prism GraphPad 3.0 software. Unless otherwise indicated, presented results are representative of at least three independent experiments, where quantitative data represent the mean ± SEM.

Results

Poly(I-C) Induces PRR Pathway Activation and IFNβ Production in Differentiated Human Neuronal Cells

To initially study neuronal PRR pathway activity, we used the previously characterized human BE(2)-C neuronal culture model (50). This neuroblastoma cell line can be differentiated in the presence of retinoic acid to form cells with morphological, biochemical, and physiological characteristics of mature human neurons, and it has been used to demonstrate differentiation-dependent responses of human neuronal cells to type-I IFN stimulation and neurotropic virus infection (5). We generated stable cell lines that expressed either an NFκB promoter-driven or IRSE promoter-driven SEAP reporter gene, induced differentiation with retinoic acid, and examined reporter gene activity in tissue culture supernatants of cells stimulated with poly(I-C), which is a dsRNA mimetic and potent inducer of PRR pathway activation (74). We used increasing concentrations of poly(I-C) delivered either extracellularly for cell surface or endosomal TLR activation or complexed with Lipofectamine and transfected for intracellular RLR stimulation, and examined responses in both undifferentiated and differentiated BE(2)-C cell lines (**Fig 2.1**). Both NFκB (**Fig 2.1.A**) and ISRE (**Fig 2.1.B**) promoter-driven reporters showed dose responsive expression in differentiated BE(2)-C/m cells with both extracellular and transfected poly(I-C), whereas essentially no responses were seen in undifferentiated cells. Calculated poly(I-C) concentrations that produced 50% maximal responses (EC_{50} values) in differentiated BE(2)-C/m cells were between ~10 ng/ml and 10 μg/ml (**Table 2.1**).

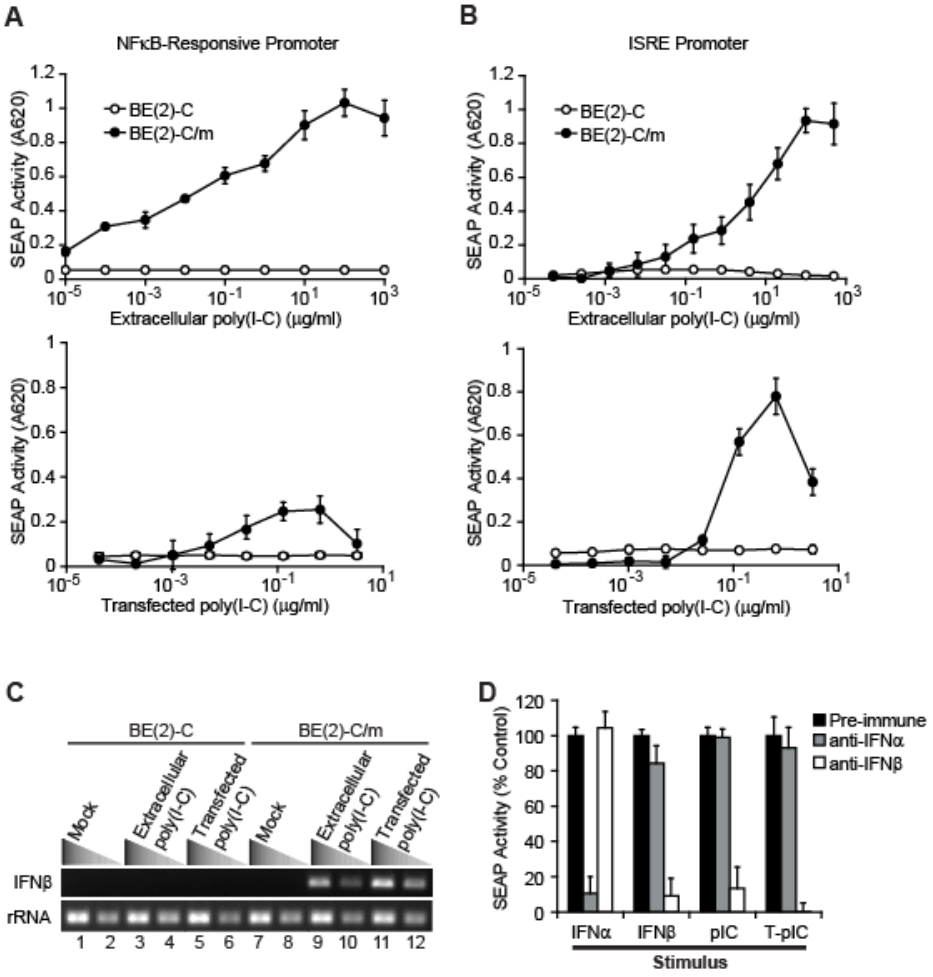

Figure 2.1. Poly(I-C) activates NFκB and ISRE promoters and induces IFNβ production in human neuronal cells. A and B. Similar numbers of NFκB (A) or ISRE (B) promoter-reporter cells were stimulated with increasing amounts of extracellular poly(I-C) (upper graphs) or transfected poly(I-C) (lower graphs), and SEAP reporter activity in culture supernatants was measured 20 h after stimulation. **C.** BE(2)-C (lanes 1-6) or BE(2)-C/m (lanes 7-12) cells were stimulated with 100 μg/ml extracellular poly(I-C) (lanes 3, 4, 9, and 10) or 700 ng/ml transfected poly(I-C) (lanes 5, 6, 11, and 12) for 10 h, and IFNβ and rRNA transcript levels were assessed via RT-PCR. Adjacent lanes for individual samples represent results using 10-fold dilutions of cDNA. **D.** BE(2)-C/m ISRE reporter cells were stimulated with either 20 IU/ml human leukocyte IFNα, 20 IU/ml human fibroblast IFNβ, 100 μg/ml extracellular poly(I-C) (pIC), or 600 ng/ml transfected poly(I-C) (T-pIC) in the presence of neutralizing IFNα or IFNβ antisera at concentrations capable of neutralizing 4000 IU/ml of IFNα or IFNβ, respectively. Results are expressed as the percent SEAP activity compared to control samples incubated with pre-immune serum.

The inability of undifferentiated BE(2)-C cells to respond to poly(I-C) was not due to inactive ISRE or NFκB promoters, as universal type I IFNα-A/D stimulated ISRE-SEAP activity, albeit with a 4-fold higher IFNα-A/D EC_{50} compared to differentiated BE(2)-C/m cells (5). Furthermore, TNFα, a potent NFκB inducer, stimulated NFκB-SEAP activity in undifferentiated BE(2)-C cells, although EC_{50} values were approximately 30-fold higher in undifferentiated compared to differentiated cells (850 vs 25 pg/ml, respectively). We obtained similar results using reporter cell lines generated from SH-SY5Y cells, another human neuronal cell line unrelated to BE(2)-C cells (19) (**Supplemental Fig S2.2.A**).

The poly(I-C) stimulated ISRE promoter-driven SEAP expression seen in differentiated BE(2)-C/m cells could have been due to type-I IFN production and autocrine activity or IFN-independent ISRE activation (48). To initially examine endogenous IFNβ transcription in response to poly(I-C) stimulation we used semi-quantitative RT-PCR (**Fig 2.1.C**). Poly(I-C) delivered both extracellularly and by transfection stimulated IFNβ mRNA upregulation in differentiated BE(2)-C/m cells, whereas undifferentiated cells showed no responses, consistent with the reporter gene expression results (**Figs 2.1.A and B**). We also observed poly(I-C)-stimulated IFNβ mRNA induction with differentiated HCN-1A cells (**Supplemental Fig S2.2.C**), a non-malignant human cortical neuronal cell line (59). Furthermore, we observed ~10- and 100-fold increases in IFNβ mRNA up regulation in differentiated primary rat cortical neurons stimulated with extracellular or transfected poly(I-C), respectively (see Fig 2.5.B below). These results suggested that transcriptional upregulation of type-I IFNs in response to

PRR stimulation in differentiated BE(2)-C/m cells was not due to their derivation from neuroblastoma cells.

To further examine the potential for autocrine type I IFN activity in human neuronal cells we conducted antibody neutralization experiments (**Fig 2.1.D**). We simultaneously incubated cells with poly(I-C) and control pre-immune serum or antisera specific for human IFNα or IFNβ, and measured SEAP activity in tissue culture supernatants. To determine antibody specificity and neutralization efficiency, we stimulated control wells with either human leukocyte IFNα or fibroblast IFNβ instead of poly(I-C). The ISRE-SEAP responses of differentiated BE(2)-C/m cells to both extracellular and transfected poly(I-C) were significantly reduced by IFNβ- but not IFNα-specific antisera (**Fig 2.1.D**). We obtained similar results with differentiated SH-SY5Y cells (**Supplemental Fig S2.2.B**). These results indicated that differentiated human neuronal cells activated NFκB and ISRE promoters in response to poly(I-C) stimulation, and that ISRE promoter activation was due to IFNβ production and autocrine activity.

SeV Infection Activates PRR Pathways in Human Neuronal Cells

To determine if neuronal PRR pathways are also activated in the context of a virus infection we used SeV, which has been shown to potently induce innate immune responses in other cell types (42). We infected undifferentiated and differentiated BE(2)-C cells expressing an NFκB promoter-driven reporter gene with increasing doses of recombinant GFP-tagged SeV and measured SEAP activity in tissue culture supernatants 30 h post-infection (hpi). We observed

dose-dependent NFκB responses only in differentiated BE(2)-C/m cells (**Fig 2.2.A**), which was not due to differences in SeV replication kinetics (**Fig 2.2.B**). Furthermore, SeV infection also induced endogenous IFNβ mRNA upregulation in both differentiated BE(2)-C/m cells (**Fig 2.2.C**) and primary rat cortical neurons (**Supplemental Fig S2.1.F**). However, the response in BE(2)-C/m cells was delayed until 20 hpi (**Fig 2.2.C**, compare lanes 3 and 6), whereas the transcriptional response to poly(I-C) stimulation was much more rapid (**Fig 2.2.C**, lane 2). The delayed IFNβ transcriptional response until 20 hpi corresponded with early logarithmic replication of SeV (**Fig 2.2.B**), suggesting that active viral replication was required for IFNβ mRNA induction. In support of this conclusion, UV inactivation of SeV abrogated IFNβ mRNA transcriptional responses (**Supplemental Fig S2.3**). Thus, both synthetic and natural PRR ligands were capable of activating innate immune pathways and IFNβ transcriptional upregulation in differentiated human neuronal cells.

Human Neuronal Cells Show Restricted Responses to PRR Ligands

Poly(I-C) and SeV are stimuli that are frequently used to activate innate immune pathways via TLR3, MDA5, or RIG-I. To determine whether the differentiation-dependent responses of BE(2)-C cells to poly(I-C) and SeV extended to other stimuli, we examined several additional PRR ligands (**Table 2.1**). We stimulated NFκB or ISRE promoter-driven reporter cell lines with increasing concentrations of LPS, the imidazoquinoline compound derivative CLO97, or the CpG-containing oligonucleotide ODN2006, which are ligands for TLR4, TLR7/8, or TLR9,

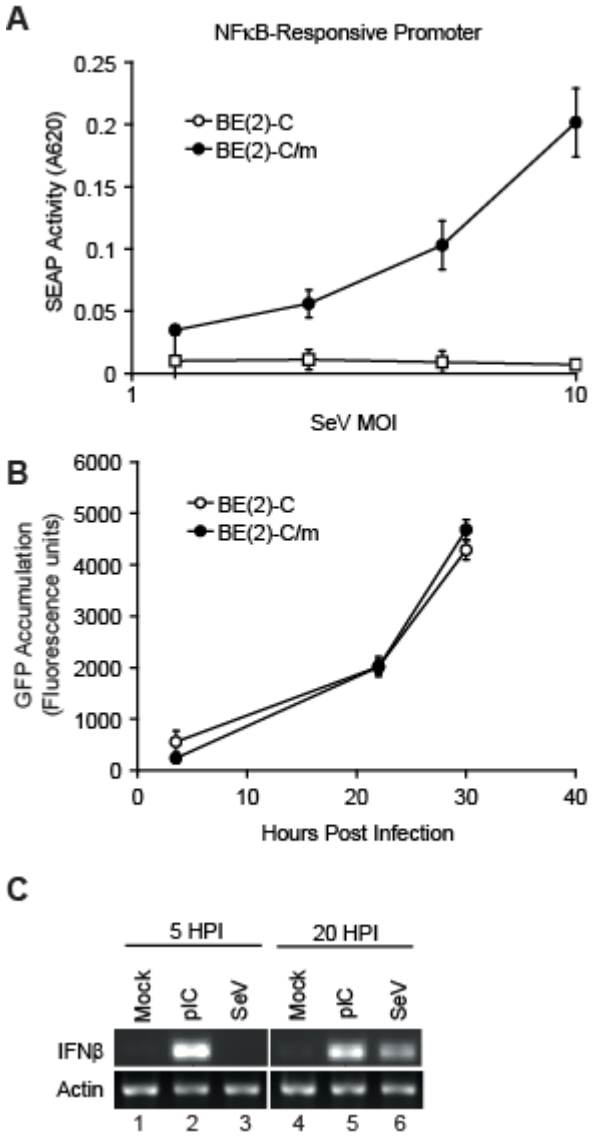

Figure 2.2. SeV infection induces a neuronal PRR response. A. NFκB reporter cells were infected with GFP-tagged SeV using an increasing multiplicity of infection (MOI), and SEAP reporter activity was assessed at 30 hpi. **B.** Cells were infected as in *A* and SeV replication, assessed by GFP fluorescence, was measured. **C.** BE(2)-C/m cells were stimulated with 100 μg/ml extracellular poly(I-C) (pIC, lanes 2 and 5) or infected with SeV at an MOI of 10 (lanes 3 and 6), and IFNβ mRNA or rRNA accumulation was assessed via RT-PCR 5 h (lanes 1-3) or 20 h (lanes 4-6) later.

Table 2.1. Human neuronal responses to PRR ligands.

Stimulus	NFκB promoter		ISRE promoter	
	BE(2)-C	BE(2)-C/m	BE(2)-C	BE(2)-C/m
Extracellular poly(I-C)	> 1000 μg/ml*	0.093 ± 0.036 μg/ml	> 1000 μg/ml	8.0 ± 3.5 μg/ml
Transfected poly(I-C)	> 400 μg/ml	0.015 ± 0.007 μg/ml	> 400 μg/ml	0.043 ± 0.003 μg/ml
LPS	> 100 μg/ml	0.012 ± 0.004 μg/ml	> 100 μg/ml	> 100 μg/ml
Imidazoquinoline	> 25 μg/ml	> 25 μg/ml	> 25 μg/ml	> 25 μg/ml
CpG DNA	> 25 μM	> 25 μM	> 25 μM	> 25 μM

*Results represent EC_{50} values for the indicated stimulus, promoter reporter, and cell line combination. Where appropriate, values are presented as the mean ± SEM.

respectively (39). BE(2)-C cells showed a differentiation-dependent response to LPS using an NFκB promoter-driven reporter, whereas the ISRE promoter-driven reporter was not stimulated by LPS regardless of cell differentiation. This observation was consistent with the differentiation-dependent expression of TLR4 and its co-receptor CD14 identified by microarray analyses (see below, **Supplemental Tables S2.1 and S2.2** available online with publication doi/10.4049/jimmunol.0904133), and published studies demonstrating TLR4 expression in primary CNS neurons and neuronal cell lines (66, 79). Neither CLO97 nor ODN2006 stimulated reporter gene activity in BE(2)-C cells regardless of differentiation (**Table 2.1**), even though these TLR ligands were able to activate an NFκB promoter-driven reporter in differentiated U937 cells, a human macrophage cell line (21) (**Supplemental Fig S2.4**). We did not specifically examine TLR7/8 or TLR9 expression, and therefore cannot exclude the possibility that the inability of BE(2)-C cells to respond to CLO97 or ODN2006 was secondary to the absence of these TLRs. However, published data suggest that mRNAs for TLR7, 8, and 9 are present in some primary neurons and neuronal cell lines (79). Nevertheless, these results suggested that human neuronal cells possess restricted PRR-mediated responses, and ligands that stimulated predominantly antiviral innate immune pathways via TLR3- , MDA5-, or RIG-I-mediated responses were particularly active. Thus, we specifically focused subsequent studies on these pathways.

Differentiated Neurons Express TLR3, MDA5, and RIG-I

We initially examined the expression of TLR3, MDA5, and RIG-I in neuronal cells by immunoblotting and immunofluorescence microscopy (**Fig 2.3**). Previously published studies have demonstrated TLR3 expression in both cultured human and rodent neurons and CNS tissue sections (3, 30, 45, 54, 66), and we also observed TLR3 expression in lysates from undifferentiated BE(2)-C cells (**Fig 2.3.A**, lane 1), differentiated BE(2)-C/m cells (**Fig 2.3.A**, lanes 2-4), and primary rat neurons (**Fig 2.3.A**, lane 5). To validate the specificity of TLR3 immunoblotting, we used lysates from BE(2)-C/m cells transfected with plasmids overexpressing either wild-type TLR3 (**Fig 2.3.A**, lane 3) or a dominant-negative mutant that contains a deletion of the TIR domain (**Fig 2.3.A**, lane 4). We also examined TLR3 expression in BE(2)-C/m cells by immunofluorescence microscopy, and observed a punctate cytoplasmic distribution (**Fig 2.3.B**,upper right image), that was particularly evident at higher magnification (**Fig 2.3.B**, lower left image). We observed a similar distribution pattern but increased TLR3 immunofluorescent signal intensity in cells transfected with a plasmid overexpressing wild-type TLR3 (**Fig 2.3.B**, lower right image). These immunofluorescence results were consistent with the previously described endosomal localization of TLR3 in cultured human neuronal cells (45). Furthermore, immunoblot analysis revealed that both MDA5 and RIG-I were expressed in human BE(2)-C cells (**Fig 2.3.C**, lanes 1-4) and primary rat neurons

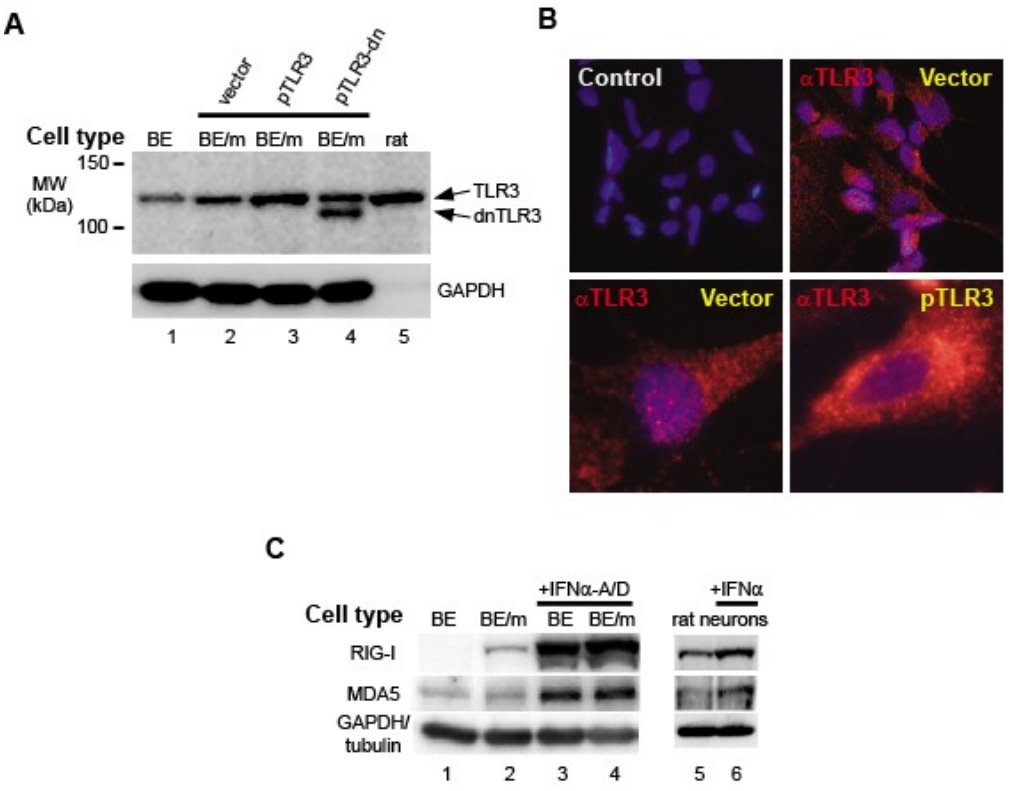

Figure 2.3. Human neuronal cells and differentiated rodent neurons express antiviral PRRs. A. Lysates from BE(2)-C cells (lane 1), differentiated BE(2)-C/m cells (lanes 2-4), or primary rat neurons (lane 5) were immunoblotted for TLR3 levels. To validate antibody specificity, BE(2)-C/m cells were transfected with either empty vector (lane 2) or plasmids expressing wild-type TLR3 (lane 3) or a dominant-negative (dn) TLR3 (lane 4) that contains a TIR domain deletion. The human TLR3 gene encodes a 904 amino acid protein with a predicted MW of 103 kDa, although it is heavily glycosylated. The TLR3 ΔTIR mutant contains a 162 amino acid deletion that reduces the predicted MW by approximately 18 kDa. The GAPDH-specific monoclonal antibody used for immunoblotting cross-reacted poorly with the rat lysate (lane 5), but total protein staining showed that the rat lysate sample contained approximately 2- to 3-fold more total protein than the other lanes (data not shown). **B.** Immunofluorescent staining of TLR3 expression in BE(2)-C/m cells. The primary TLR3-specific antibody was excluded during incubation in control cells (upper left image). Nuclei were stained with DAPI (blue), whereas the punctate PE-staining (red) indicates TLR3 expression. Cells in the upper right and lower left images were transfected with empty vector, whereas cells in the lower right image were transfected with a plasmid expressing wild-type TLR3. We also saw a similar punctuate pattern but increased TLR3 signal intensity in cells transfected with the dnTLR3 expression plasmid (data not shown). **C.** Lysates from BE(2)-C cells (lanes 1 and 3), differentiated BE(2)-C/m cells (lanes 2 and 4), or primary rat neurons (lanes 5 and 6), were immunoblotted for RIG-I, MDA5, and GAPDH (human) or tubulin (rat) levels. Lysates from cells treated with 100 IU/ml human IFNα-A/D for 6 h (lanes 3 and 4) or 50 IU/ml rat IFNα for 24 h (lane 6) were used as controls to validate the identity of RIG-I and MDA5 as IFN-stimulated genes.

(**Fig 2.3.C**, lanes 5 and 6). Interestingly, although RIG-I expression increased with BE(2)-C differentiation, probably due to the use of retinoic acid to induce neuronal maturation, MDA5 expression levels were independent of differentiation (**Fig 2.3.C**, lanes 1 and 2). However, the expression of both PRRs increased in response to type-I IFN stimulation in both human BE(2)-C neuronal cells (**Fig 2.3.C**, lanes 3 and 4) and primary rat neurons (**Fig 2.3.C**, lane 6). These results suggested that the three PRRs associated with potent antiviral innate immune responses, TLR3, MDA5, and RIG-I, are expressed in human neuronal cells and differentiated neurons.

Specific PRRs are Required for Poly(I-C)- and SeV-Mediated Activation of Innate Immune Pathways in Human Neuronal Cells

We next examined the functional impact of PRR expression on neuronal innate immune responses using genetic disruption of receptor function (**Fig 2.4**). To disrupt TLR3- or RIG-I-mediated pathway activation in BE(2)-C/m cells, we used stable cell lines expressing specific dominant-negative mutants. Initial experiments using transient transfection with the TLR3 ΔTIR mutant described above showed an approximate 50% reduction in extracellular poly(I-C)-stimulated ISRE-SEAP activity (**Supplemental Fig S2.5.A**). However, we were unable to generate stable cell lines constitutively expressing this construct, and therefore we subsequently targeted a downstream signaling molecule. Since TLR3 is the only known dsRNA-sensing PRR to use the adaptor protein TRIF for

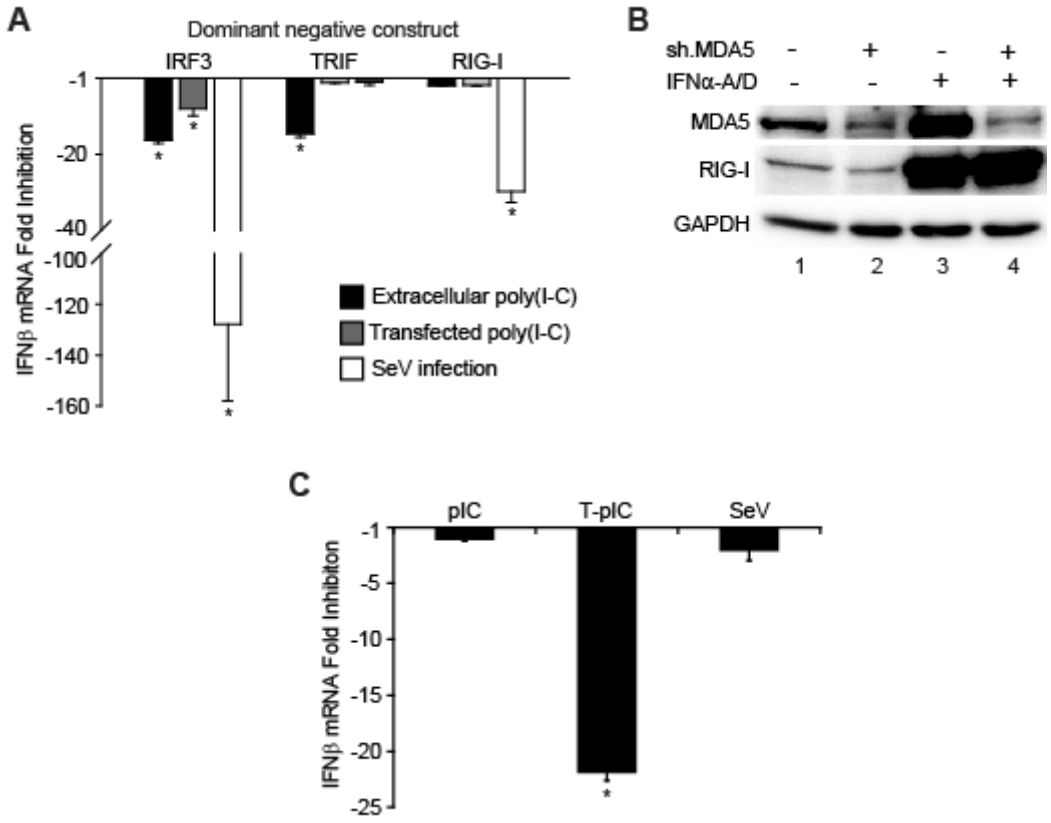

Figure 2.4. Human neuronal cells possess functional PRR-mediated innate immune pathways. A. BE(2)-C/m cells stably overexpressing dominant negative forms of IRF3, TRIF, or RIG-I were stimulated with 100 μg/ml extracellular poly(I-C) or 700 ng/ml transfected poly(I-C) for 10 h, or infected with SeV for 30 h, and IFNβ mRNA levels were measured by quantitative RT-PCR using rRNA transcript levels as the loading control. Results are expressed as the fold-change compared to similarly stimulated cells stably transfected with an empty vector. **B.** Lysates from BE(2)-C/m cells stably transfected with plasmids expressing shRNAs targeted against either a control protein (lanes 1 and 3) or MDA5 (lanes 2 and 4) were immunoblotted for MDA5, RIG-I, and GAPDH expression levels. The level of MDA5 suppression in cells expressing an MDA5-specific shRNA was 44.5 ± 7.4% compared to control cells. Live-cell imaging of differentiated cells also demonstrated that greater than 95% of cells expressed the control GFP reporter gene encoded on the shRNA expression plasmid (data not shown). Lysates from cells treated with 1000 IU/ml IFNα-A/D for 12 h (lanes 3 and 4) served as positive controls to validate the specificity of shRNA-mediated knockdown of MDA5 under enhanced expression levels. **C.** IFNβ mRNA levels in BE(2)-C/m cells stably expressing an MDA5-targeted shRNA after stimulation with extracellular poly(I-C) (pIC), transfected poly(I-C) (T-pIC), or infected with SeV as described above. Transcript levels were determined by quantitative RT-PCR and results are expressed as the fold-change compared to similarly stimulated cells stably transfected with an shRNA-encoding vector targeting an irrelevant control protein. *p-value < 0.05.

signal transduction (51), we used a TRIF mutant that contains only the TIR domain (73) to disrupt TLR3 function. In contrast, both RIG-I and MDA5 use the adaptor protein IPS-1 (51). We therefore used an N-terminal RIG-I deletion mutant (75) to disrupt RIG-I function. As a positive control we used a dominant negative IRF3 mutant (6), since this transcription factor is a central regulator of innate antiviral responses (51). We generated BE(2)-C cell lines stably transfected with individual constitutive expression plasmids encoding the dominant negative mutants described above, differentiated cells with retinoic acid, stimulated with either extracellular or transfected poly(I-C) or infected with recombinant SeV, and measured IFNβ mRNA induction by quantitative RT-PCR (**Fig 2.4.A**). Dominant negative IRF3 expression inhibited the IFNβ transcriptional responses to all three stimuli, where the largest decrease (~130-fold) was seen with SeV infection. In contrast, dominant negative TRIF expression specifically inhibited extracellular poly(I-C)-stimulated responses, whereas dominant-negative RIG-I expression specifically inhibited SeV-stimulated responses.

To disrupt MDA5-mediated pathway activation in BE(2)-C/m cells, we depleted receptor levels through stable expression of a plasmid encoding a short hairpin RNA (shRNA) specifically targeting MDA5 (**Fig 2.4.B and C**). We initially optimized conditions and obtained a 40-50% reduction in MDA5 expression levels in BE(2)-C/m cells without significantly altering expression levels of the related RLR, RIG-I (**Fig 2.4.B**, compare lanes 1 and 2). Depletion of MDA5 inhibited the IFNβ transcriptional response to stimulation with transfected poly(I-

C) but not with extracellular poly(I-C) or SeV infection (**Fig 2.4.C**). These results indicated that human neuronal cells possess functional TLR3-, MDA5-, and RIG-I-activated pathways that respond to specific stimuli.

Neuronal Cell Differentiation Modulates Innate Immune Signaling Pathway Component Expression

There are multiple signal transduction events that occur between PRR interaction with its ligand and downstream antiviral effector production. To identify potential neuronal components involved in these events, we used genome-wide transcriptional microarray results combined with pathway analyses and compared BE(2)-C cells before and after retinoic acid-mediated differentiation. This approach was feasible since BE(2)-C cells showed minimal responsiveness to select PRR ligand stimulation (**Figs 2.1 and 2.2, Table 2.1**) prior to differentiation. We identified 1,002 upregulated and 863 downregulated genes in differentiated BE(2)-C/m cells. The complete list of differentially regulated genes is provided in Supplemental Table A.1.

We subsequently conducted an in silico analysis with upregulated genes that were assigned to known cellular pathways using Ingenuity Pathway software to identify potential innate immune networks active in neuronal PRR signaling. We identified 29 canonical signaling pathways preferentially upregulated in differentiated BE(2)-C/m cells, 9 of which have been linked with innate immunity (**Table 2.2**). We were particularly interested in the identification of the PI3K/AKT signaling pathway, as PI3Ks have been implicated as positive and negative

Table 2.2. Signaling pathways preferentially upregulated in differentiated human BE(2)-C/m neuronal cells.

SIGNALING PATHWAY*	NO. OF GENES	*P*-VALUE
14-3-3-mediated signaling	21	0.0016
α-Adrenergic signaling	13	0.0089
Axonal guidance signaling	38	0.0044
cAMP-mediated signaling†	18	0.0162
Cardiac β-adrenergic signaling	15	0.0129
Caveolar-mediated endocytosis	11	0.0155
Ephrin receptor signaling	23	0.0010
ERK/MAPK signaling†	20	0.0158
Fcγ receptor-mediated phagocytosis in macrophages and monocytes	12	0.0269
G-protein coupled receptor signaling†	24	0.0025
Hepatic fibrosis/stellate cell activation	21	0.0001
IGF-1 signaling	17	0.0001
IL-8 signaling†	20	0.0098
Insulin receptor signaling	15	0.0209
Integrin signaling†	24	0.0029
Leukocyte extravasation signaling	19	0.0457
Neuregulin signaling	15	0.0006
Neurotrophin/TRK signaling†	10	0.0112
Notch signaling	8	0.0037
p53 signaling†	11	0.0355
PI3K/AKT signaling†	15	0.0102
PTEN signaling	15	0.0008
PXR/RXR activation	9	0.0417
RAR activation	25	0.0002
Synaptic long term potentiation	14	0.0115
TGF-β signaling†	14	0.0007
Tight junction signaling	18	0.0174
VDR/RXR activation	13	0.0021
Wnt/β-catenin signaling	22	0.0011

*The listed pathways were identified as significantly associated with BE(2)-C differentiation using Ingenuity Pathway Analysis software and datasets derived from both Genomatix and Affymetrix Bioconductor analyses of microarray data. Only those pathways identified with both datasets are shown, where the number of genes and *p*-values listed are from the Genomatix dataset analysis.

†Signaling pathways associated with innate immunity in the literature are shown in bold. These pathways were identified by the presence of at least 10 Medline co-references with the keywords “innate” and “immunity”.

regulators of TLR3-mediated signaling events (1, 18, 23, 60, 65, 78), TLR3 expression and function have been implicated in neuronal antiviral responses (3, 14, 30, 45, 54), and the extracellular poly(I-C) stimulation experiments implicated an active TLR3-mediated pathway in differentiated BE(2)-C/m cells (**Figs 2.1 and 2.4**). To validate the microarray results with a particular focus on the PI3K/AKT pathway, we used a microplate-based quantitative RT-PCR array that included 71 genes associated with this pathway. Using this targeted array we validated the transcriptional upregulation of 19 genes in differentiated BE(2)-C/m cells that are associated with PIK3 signaling, including *AKT3, APC, CD14, CTNNB1, FOXO1, FOXO3, FRAP, GSK3B, ITGB1, JUN, MAPK8, PAK1, PDPK1, PI3KCA, PI3KR1, RASA1, TLR4, TSC2*, and *YWHAH* (**Supplemental Table S2.2**). Furthermore, we validated increased protein expression levels of the PI3K regulatory subunit isoform p85α encoded by the *PI3KR1* gene in differentiated BE(2)-C/m cells by immunoblotting (**Supplemental Fig S2.6**). These results suggested that canonical PI3K/AKT pathway components were involved in neuronal innate immune responses.

PI3K Inhibition Blocks Poly(I-C)-Mediated Innate Immune System Activation in Neuronal Cells

To examine the potential functional role of PI3K in neuronal PRR pathway signaling we initially used the universal PI3K inhibitor LY294002 (11). We incubated differentiated BE(2)-C/m cells expressing ISRE or NFκB promoter-driven reporter genes with increasing concentrations of LY294002, stimulated

with extracellular or transfected poly(I-C), LPS, IFNα-A/D, or TNFα, and measured SEAP activity in tissue culture supernatants after 20 h (**Fig 2.5.A**). Initial viability studies showed minimal cytotoxicity with up to 25 μM LY294002 in BE(2)-C/m cells (**Supplemental Fig S2.7**). LY294002 potently inhibited both extracellular and transfected poly(I-C) stimulation in ISRE reporter cells with an IC_{50} of approximately 7 μM (**Fig 2.5.A**, top graph), but had no effect on NFκB promoter activation in response to poly(I-C), LPS, or TNFα (**Fig 2.5.A**, bottom graph). The inhibition of LY294002 on the IRSE promoter-driven reporter gene was due to disruption of autocrine IFNβ production rather than feedback signaling and amplification, as LY294002 had no effect on exogenous IFNα-A/D stimulation of ISRE promoter reporter cells (**Fig 2.5.A**, top graph) but did suppress poly(I-C)-stimulated IFNβ mRNA transcriptional upregulation (see below, **Fig 2.6.B**). Furthermore, LY294002 suppressed poly(I-C)-stimulated IFNβ mRNA transcriptional upregulation in primary rat cortical neurons (**Fig 2.5.B**). These results suggested that PI3K is involved in NFκB-independent neuronal PRR pathways stimulated by poly(I-C) and mediated through TLR3 and MDA5.

To gain further insight into the signaling molecules involved in neuronal PRR pathway activation, we used a defined library of kinase inhibitors and examined their effects on poly(I-C)-mediated activation of differentiated BE(2)-C/m cells expressing an ISRE promoter-driven reporter. This library contains 99 inhibitors targeting 48 different kinases, including several involved in canonical PI3K/AKT signaling networks (**Supplemental Table S2.3**).

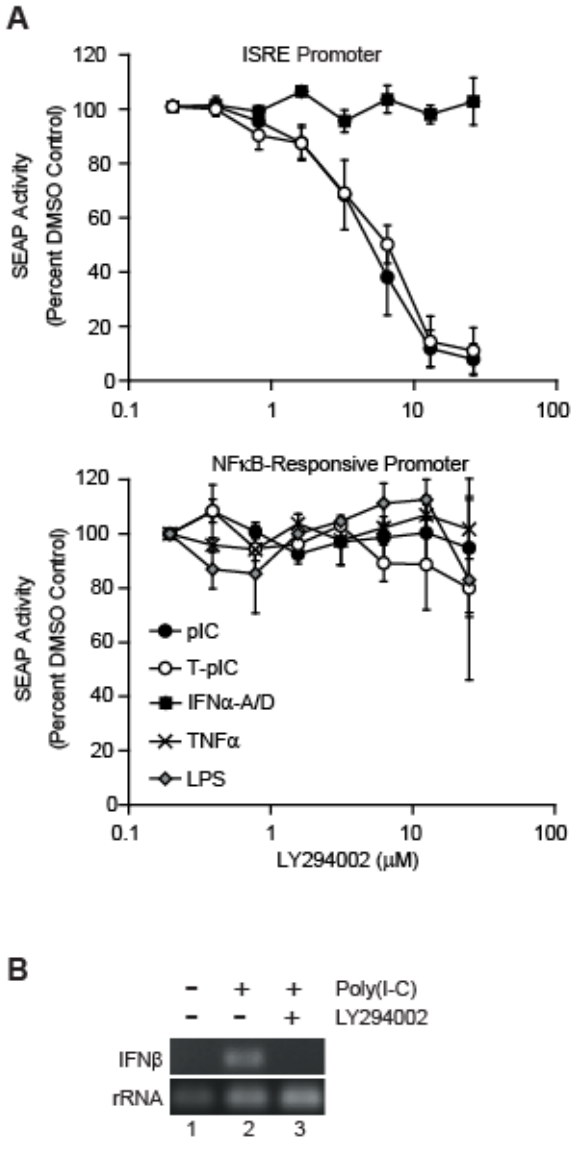

Figure 2.5. Neuronal response to poly(I-C) is mediated by PI3K. A. BE(2)-C/m ISRE (upper graph) and NFκB (lower graph) promoter-driven reporter cells were treated with an increasing concentration of LY294002, stimulated with 100 μg/ml extracellular poly(I-C) (pIC), 700 ng/ml transfected poly(I-C) (T-pIC), 100 IU/ml IFNα-A/D, 50 ng/ml TNFα, or 500 ng/ml LPS, and SEAP reporter activity was measured 24 h later. Results are expressed as the percentage of SEAP activity compared to DMSO-treated controls. TNFα and LPS were used as controls only with NFκB promoter-driven reporter cells as the ISRE reporter cells did not respond to either stimuli even in the absence of LY294002 (see Table 2.1 and data not shown). **B.** Primary rat cortical neurons were treated with either DMSO (lanes 1 and 2) or 10 μM LY294002 (lane 3), stimulated with 50 μg/ml of extracellular poly(I-C) for 8 h (lanes 2 and 3), and IFNβ mRNA levels were assessed by RT-PCR.

Each inhibitor was serially diluted in duplicate from 100 to 0.8 μM, incubated with reporter cells stimulated with extracellular or transfected poly(I-C), and SEAP activity was measured after 20 h. To control for non-specific cytotoxicity, we conducted parallel viability assays. We identified 23 kinase inhibitors that blocked either extracellular or transfected poly(I-C)-mediated activation of an ISRE promoter-driven reporter gene in differentiated BE(2)-C/m cells (**Table 2.3**). Interestingly, there was not a complete overlap between the lists of inhibitors that disrupted extracellular vs. transfected poly(I-C) stimulation. For example, inhibitors of epidermal growth factor receptor kinase were more active against transfected poly(I-C) (**Supplemental Table S2.3**), suggesting that further studies using these pharmacologic probes may provide additional information regarding potential divergences in neuronal PRR signaling pathways.

One noteworthy observation from the kinase inhibitor library studies in the context of our previous results was the identified activity of several PI3K inhibitors (**Table 2.3**). However, these active compounds were either general PI3K inhibitors or targeted to the PI3K p110α subunit, where compounds targeted to the PI3K p110β or p110γ subunits were not active in this medium throughput assay. The PI3K complex consists of a receptor subunit that binds activated membrane-associated receptors and recruits a p110 catalytic subunit (α, β, or γ) that mediates the conversion of phosphatidylinositol (4,5)-bisphosphate to phosphatidylinositol (3,4,5)-trisphosphate, which is generally required for downstream signaling (68). To validate the kinase inhibitor library

Table 2.3. Kinase inhibitors that suppressed poly(I-C)-mediated ISRE promoter stimulation in human neuronal cells.

INHIBITOR*	TARGET(S)†
BML-257	AKT
Triciribine	AKT
Terreic acid	BTK
Flavopiridiol	CDK 1,2,4
Apigenin	CK-II
PI-103	DNA-PL, PI3K p110α, mTOR
Tyrphostin 25	EGFRK
Tyrphostin 51	EGFRK
BML-265	EGFRK
5-Iodotubercidin	ERK2, Adenosine kinase, CK1, CK2
PK412	FTL3, Src, ABL
GSK3 Inhibitor XIII	GSK3
Purvalanol A	GSK3-α/β, CDKs
ZM 449829	JAK-3
Rapamycin	mTOR
2-Aminopurine	P58 PITSLRE-β1
LY294002	PI3K
Quercetin dehydrate	PI3K
PI3Kα Inhibitor 2	PI3K p110α
H8	PKA, PKG
Palmitoyl-DL-carnitine Cl	PKC
HBDDE (2,2',3,3',4,4'-Hexahydroxy-1,1'-biphenyl-6,6'-dimethanol dimethyl ether)	PKCα, PKCγ
Rottlerin	PKCδ
Tyrphostin AG 1288	Tyrosine kinases

*The listed inhibitors suppressed ISRE promoter-driven reporter gene activity in BE(2)-C/m cells with IC_{50} values < 20 μM for either extracellular or transfected poly(I-C) and had CC_{50} values > 20 μM. Inhibitors with activity against PI3K are shown in bold italics type.

†Kinase abbreviations: AKT, protein kinase B; BTK, Bruton's tyrosine kinase; CDK, cyclin-dependent kinase; CK, creatine kinase; EGFRK, epidermal growth factor receptor kinase; ERK, extracellular signal-regulated kinase; FLT3, FMS-like tyrosine kinase 3; GSK3, glycogen synthase kinase 3; JAK, Janus kinase; mTOR, mammalian target of rapamycin; PKA/PKC/PKG, protein kinase A/C/G.

results, we purchased new inhibitors specifically targeting p110α (PI3K p110α Inhibitor 2), p110β (TGX-221), or p110γ (AS-252424), and used these compounds in detailed dose-titration studies with the same reporter cell line used for the kinase inhibitor library medium throughput assays (**Fig 2.6.A**). The PI3K p110α-specific inhibitor blocked both extracellular and transfected poly(I-C)-activated ISRE reporter activity with IC_{50} values of 0.5 and 1.6 μM, respectively (**Fig 2.6.A**, upper graph). In contrast, neither the p110β-specific (**Fig 2.6.A**, middle graph) nor p110γ-specific (**Fig 2.6.A**, lower graph) inhibitor significantly suppressed poly(I-C)-stimulated reporter gene activity until reaching concentrations greater than 10 μM, at which point their subunit specificity decreases significantly (31, 53). To verify the ability of PI3K subunit-specific inhibitors to block the induction of endogenous IFNβ mRNA, we examined the effects of LY294002, p110α Inhibitor 2, and AS-2552424 on IFNβ mRNA transcription after poly(I-C) stimulation in BE(2)-C/m cells (**Fig 2.6.B**). We found that both LY294002 and the PI3K p110α-selective inhibitor significantly suppressed IFNβ mRNA transcriptional activation when stimulated with either extracellular or transfected poly(I-C), whereas the p110γ-selective inhibitor had no effect.

Finally, to provide genetic validation for the inhibitor studies, we depleted protein levels through stable shRNA expression targeted against the PI3K p110α subunit (**Fig 2.7**). We obtained an approximate 60% reduction in PI3K p110α levels in differentiated BE(2)-C/m cells (**Fig 2.7.A**), which resulted in

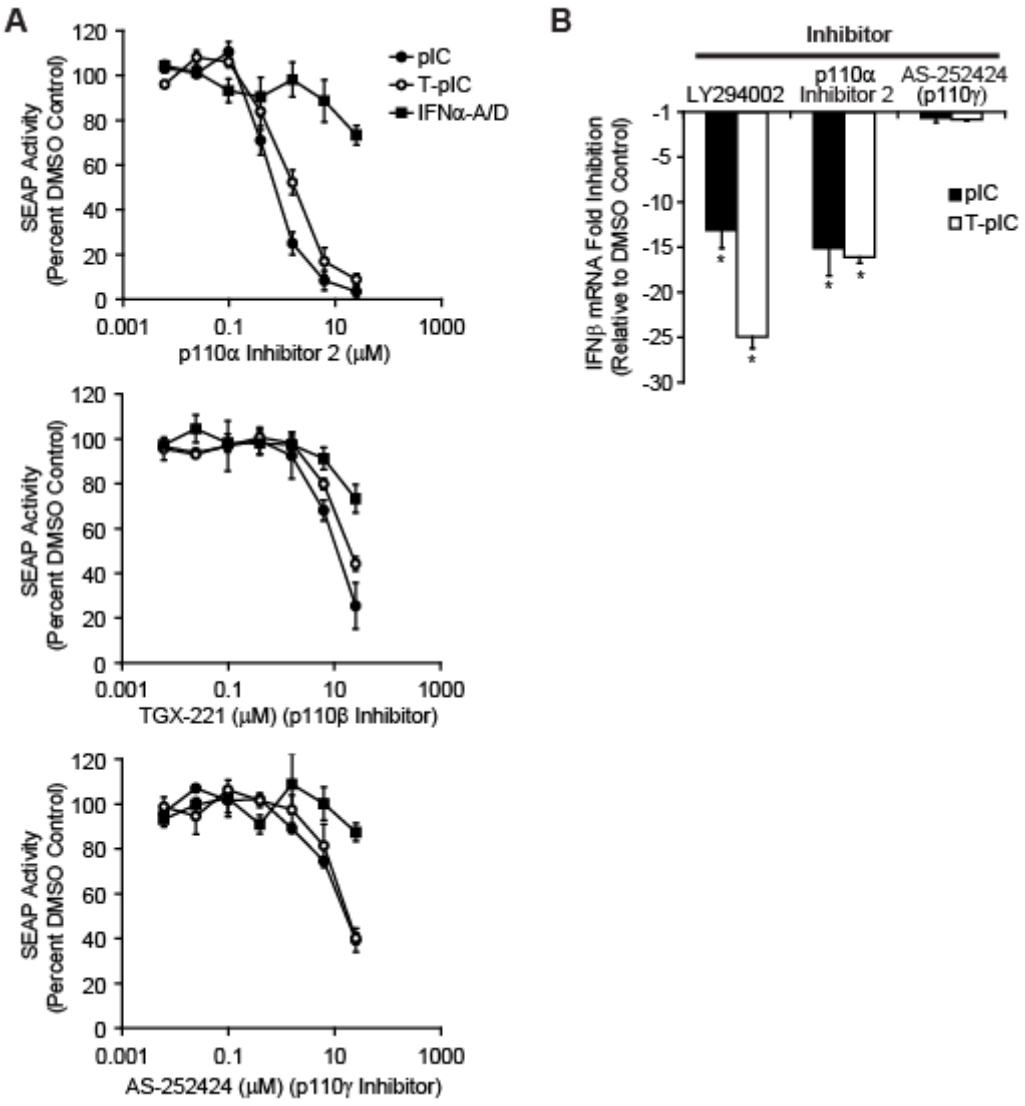

Figure 2.6. PI3K catalytic subunit p110α mediates human neuronal cell responses to poly(I-C). A. BE(2)-C/m ISRE reporter cells were treated with increasing concentrations of a selective PI3K p110α (p110a Inhibitor 2), p110β (TGX-221), or p110γ (AS-252424) catalytic subunit inhibitor, stimulated with 100 μg/ml extracellular poly(I-C) (pIC), 700 ng/ml transfected poly(I-C) (T-pIC), or 100 IU/ml IFNα-A/D, and SEAP reporter activity was measured 20 h later. Results are presented as the percent reporter gene activity compared to DMSO-treated controls. **B.** BE(2)-C/m cells were treated with 10 μM LY294002, 5 μM p110α Inhibitor 2, or 5 μM AS-252424, stimulated with poly(I-C) as described above, and IFNβ mRNA levels were measured 4 h later by quantitative RT-PCR. **p*-values < 0.05.

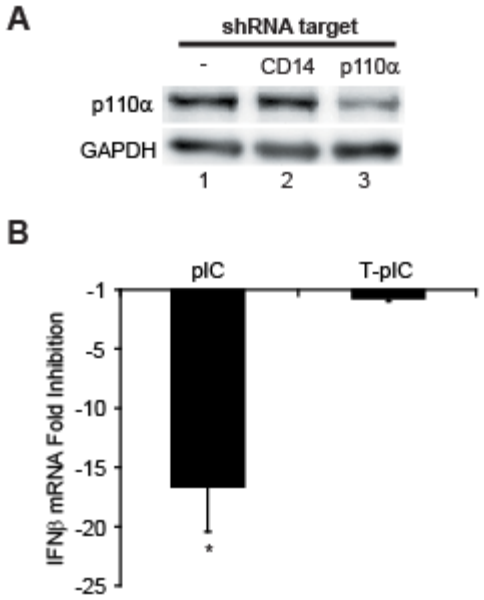

Figure 2.7. The PI3K p110α catalytic subunit mediates a TLR3-dependent response in neuronal cells. A. Lysates from BE(2)-C/m cells stably transduced with lentiviruses expressing an empty vector (lane 1) or shRNAs targeted against either a control protein (CD14, lane 2) or PI3K p110α (lane 3) were immunoblotted for p110α and GAPDH expression levels. The level of suppression in cells expressing a p110α-specific shRNA was 60.4 ± 4.9% compared to control cells. Live-cell imaging of differentiated cells also demonstrated that greater than 95% of cells expressed the control GFP reporter gene encoded on the shRNA expression plasmid (data not shown). **B.** IFNβ mRNA levels in BE(2)-C/m cells stably expressing a p110α-targeted shRNA after stimulation with extracellular poly(I-C) (pIC) or transfected poly(I-C) (T-pIC) as described in Fig 2.6. Transcript levels were determined by quantitative RT-PCR and results are expressed as the fold-change compared to similarly stimulated cells stably transfected with an shRNA-encoding vector targeting an irrelevant control protein. **p*-value < 0.05.

significant inhibition of extracellular poly(I-C)-mediated stimulation of IFNβ mRNA transcription (**Fig 2.7.B**). However, in contrast to results with p110α-specific inhibitors (**Fig 2.6**), shRNA-mediated knockdown of p110α protein levels did not suppress the ability of transfected poly(I-C) to stimulate IFNβ mRNA transcription (**Fig 2.7.B**). The ability of the p110α-depleted neuronal cells to remain responsive to transfected poly(I-C) may have been due to an insufficient depletion of p110α levels, which is consistent with a reproducible three-fold higher IC_{50} of the p110α-specific inhibitor for transfected versus extracellular poly(I-C) mediated neuronal responses (**Fig 2.6.A**). Nevertheless, these results indicated that PI3K, and in particular the p110α subunit, modulates TLR3- and possibly MDA5-dependent innate immune pathway activation in human neuronal cells.

Discussion

The innate immune system plays a critical role in both the initial response to an invading pathogen, which frequently limits or contains pathogen replication and dissemination, and the induction of an effective adaptive immune response, which is most often the primary mechanism for pathogen clearance. The characteristics of the innate immune response are determined in part by the pathogen initiating the response but can also be influenced by the type of cell in which the response is generated. In this report we examined the functional PRR-mediated pathways present in human neuronal cells and differentiated primary rat neurons, with a particular focus on those pathways previously identified as being important for antiviral innate immune responses in other cell types. We drew four main conclusions. First, human neuronal cells possess functional TLR3-, TLR4-, RIG-I-, and MDA5-mediated PRR pathways whose activity was maturation-dependent. Second, both extracellular and transfected poly(I-C) induced potent IFNβ induction in neurons that resulted in autocrine ISRE activation. Third, the neuronal antiviral innate immune pathways mediated by TLR3, RIG-I, and MDA5 are non-redundant and preferentially respond to distinct ligands. Fourth, TLR3- and possibly MDA5-mediated neuronal responses are positively regulated by the PI3K pathway, and in particular the PI3K p110α subunit. These results indicate that human neuronal cells possess a relatively broad complement of PRR-mediated innate immune pathways, and that those pathways typically stimulated by viral pathogens via nucleic acid recognition are particularly active.

Previous studies on PRR pathways in CNS neurons have focused predominantly on TLR-mediated pathways and have examined their impact on multiple aspects of brain physiology, including development and regeneration (40). Several studies have examined the role of TLR3 in response to CNS viral infections (3, 14, 30, 45, 54), although the potential antiviral role of TLR3-mediated pathways is controversial and may be pathogen-specific (69). For example, humans with a TLR3 deficiency have a genetic predisposition to herpes simplex virus encephalitis (76), but $TLR3^{-/-}$ mice have decreased susceptibility to rabies virus encephalitis (45). Furthermore, $TLR3^{-/-}$ mice have been shown to have both increased (71) and decreased (14) susceptibility to West Nile virus (WNV) encephalitis. However, these studies cannot fully separate the neuron-specific activity of TLR3 from other cell types, including professional immune cells such as macrophages and dendritic cells. Although CNS neurons from $TLR3^{-/-}$ mice have a modest increase in WNV production when infected in culture (14), suggesting that neuronal TLR3-mediated responses can have antiviral effects, further studies in mice with conditional cell-specific TLR3 deletions will be required to fully delineate the potential antiviral activity of TLR3-activated innate immune pathways in neurons and their role in viral pathogenesis.

In contrast to TLR3, neuronal innate immune responses mediated by the cytosolic PRRs RIG-I and MDA5 have been less well studied. The expression of both RIG-I or MDA5 could be induced by IFNβ or WNV infection in cultured mouse cortical neurons, but basal expression was not detected by immunoblotting (13). Although we also found that both RLRs were upregulated

with type-I IFN treatment of human neuronal cells, we did detect basal expression, especially in differentiated cells. Furthermore, we found that both RIG-I- and MDA5-mediated pathways were active in human neuronal cells. The presence of functional cytosolic PRR-activated innate immune pathways in neurons is not surprising, as the innate antiviral responses to several neurotropic viruses has been shown to involve RIG-I- and/or MDA5-mediated pathways in non-neuronal cells (20, 35). However, the outcome of these responses may differ significantly between neuronal and non-neuronal cells, where mature CNS neurons are essentially irreplaceable and therefore initiation of an altruistic apoptotic cascade may result in irreversible damage to the host, despite simultaneously preventing virus spread. One intriguing hypothesis is that neuronal PRR responses, potentially augmented or modulated by PRR-initiated responses in other CNS-resident cells such as astrocytes or microglia, control virus replication *and* promote neuronal survival through either previously unrecognized or uncharacterized pathways. Consistent with this hypothesis, results presented in chapter III suggest that the neurotropic alphavirus western equine encephalitis virus activates an IRF3-dependent pro-survival pathway in human neuronal cells. Detailed studies in chapter III will describe efforts to examine the roles of TLR3-, RIG-I, and MDA5-activated pathways in human neurons in response to a variety of neurotropic viruses in an attempt to more fully explore this hypothesis.

The signal transduction pathways that mediate PRR-activated immune responses are complex and interconnected at multiple levels. Several steps in

these pathways are mediated by cellular kinases, and we found that the PI3K pathway was important for optimal TLR3- and possibly MDA5-activated responses in human neuronal cells. The PI3K pathway has previously been implicated in innate immune pathway regulation, and in particular TLR3-mediated signaling (24). However, both stimulatory (18, 60) and inhibitory (1) effects on TLR3-mediated signaling have been observed, which may be explained in part by cell type differences. Our results suggest that the PI3K pathway plays a stimulatory role in neuronal TLR3-mediated responses, and is necessary for full IFNβ mRNA induction. Furthermore, both pharmacologic and genetic approaches identified a potential role for PI3K, and in particular the PI3K p110α subunit, in neuronal MDA5-mediated signaling. Although the PI3K pathway has been tentatively implicated in cytoplasmic RLR-initiated signaling (50), the majority of work thus far has focused on its effects during TLR-initiated signaling (24). Cellular PI3K/AKT pathways are essential for neuronal development and survival (9, 10, 28), suggesting a potential link between antiviral PRR pathway activation and the ability of neurons to overcome an infection until an adaptive immune response can be fully established. Additional studies will be required to further delineate the precise PI3K pathway components involved in neuronal antiviral PRR activation, but our kinase inhibitor library studies suggest that protein kinase B (AKT), mammalian target of rapamycin (mTOR), and glycogen synthase kinase 3 may be involved. All of these kinases participate in PI3K signaling and have been implicated in innate immunity in non-neuronal model systems (4, 7, 36-38, 47).

Innate immune pathway stimulation via TLRs or RLRs eventually results in the activation of multiple genes involved in immune responses (39, 51). For antiviral pathway stimulation via TLR3, RIG-I, or MDA5, one important group of upregulated genes are type-I IFNs, and in particular IFNβ in non-professional immune cells (56). Indeed, IFNβ mRNA upregulation is a convenient marker of innate antiviral pathway activation, which we used to monitor responses to TLR3, RIG-I, and MDA5 ligands. Furthermore, we found that BE(2)-C/m human neuronal cells are capable of synthesizing and excreting IFNβ in response to specific PRR stimulation, consistent with previously published studies in other cultured human neuronal cell lines (54) and rodent neurons both in vitro (13-15) and in vivo (16). However, whether neuronal IFNβ production in vivo in response to neurotropic pathogens or other CNS inflammatory conditions plays an important role in either the amelioration or augmentation of disease is controversial. Studies in conditional knockout mice that have disrupted type-I IFN receptor expression in neuroectodermal cells, which includes neurons, indicate that responses to type-I IFNs are important to control virus spread within the CNS (17) but not in the progression of experimental autoimmune inflammatory disease (55). Similar studies with mice containing conditional disruption of IFNβ production in CNS-resident cells will be needed to definitively examine the potential importance of neuronal type-I IFN production in vivo.

References

1. **Aksoy, E., W. Vanden Berghe, S. Detienne, Z. Amraoui, K. A. Fitzgerald, G. Haegeman, M. Goldman, and F. Willems.** 2005. Inhibition of phosphoinositide 3-kinase enhances TRIF-dependent NF-kappa B activation and IFN-beta synthesis downstream of Toll-like receptor 3 and 4. Eur J Immunol **35:**2200-9.
2. **Barchet, W., M. Cella, B. Odermatt, C. Asselin-Paturel, M. Colonna, and U. Kalinke.** 2002. Virus-induced interferon alpha production by a dendritic cell subset in the absence of feedback signaling in vivo. J Exp Med **195:**507-16.
3. **Cameron, J. S., L. Alexopoulou, J. A. Sloane, A. B. DiBernardo, Y. Ma, B. Kosaras, R. Flavell, S. M. Strittmatter, J. Volpe, R. Sidman, and T. Vartanian.** 2007. Toll-like receptor 3 is a potent negative regulator of axonal growth in mammals. J Neurosci **27:**13033-41.
4. **Cao, W., S. Manicassamy, H. Tang, S. P. Kasturi, A. Pirani, N. Murthy, and B. Pulendran.** 2008. Toll-like receptor-mediated induction of type I interferon in plasmacytoid dendritic cells requires the rapamycin-sensitive PI(3)K-mTOR-p70S6K pathway. Nat Immunol **9:**1157-64.
5. **Castorena, K. M., D. C. Peltier, W. Peng, and D. J. Miller.** 2008. Maturation-dependent responses of human neuronal cells to western equine encephalitis virus infection and type I interferons. Virology **372:**208-20.
6. **Clement, J. F., A. Bibeau-Poirier, S. P. Gravel, N. Grandvaux, E. Bonneil, P. Thibault, S. Meloche, and M. J. Servant.** 2008. Phosphorylation of IRF-3 on Ser 339 generates a hyperactive form of IRF-3 through regulation of dimerization and CBP association. J Virol **82:**3984-96.
7. **Colina, R., M. Costa-Mattioli, R. J. Dowling, M. Jaramillo, L. H. Tai, C. J. Breitbach, Y. Martineau, O. Larsson, L. Rong, Y. V. Svitkin, A. P. Makrigiannis, J. C. Bell, and N. Sonenberg.** 2008. Translational control of the innate immune response through IRF-7. Nature **452:**323-8.
8. **Colonna, M., G. Trinchieri, and Y. J. Liu.** 2004. Plasmacytoid dendritic cells in immunity. Nat Immunol **5:**1219-26.
9. **Cosker, K. E., and B. J. Eickholt.** 2007. Phosphoinositide 3-kinase signalling events controlling axonal morphogenesis. Biochem Soc Trans **35:**207-10.
10. **Cosker, K. E., S. Shadan, M. van Diepen, C. Morgan, M. Li, V. Allen-Baume, C. Hobbs, P. Doherty, S. Cockcroft, and B. J. Eickholt.** 2008. Regulation of PI3K signalling by the phosphatidylinositol transfer protein PITPalpha during axonal extension in hippocampal neurons. J Cell Sci **121:**796-803.
11. **Crabbe, T., M. J. Welham, and S. G. Ward.** 2007. The PI3K inhibitor arsenal: choose your weapon! Trends Biochem Sci **32:**450-6.
12. **Crack, P. J., and P. J. Bray.** 2007. Toll-like receptors in the brain and their potential roles in neuropathology. Immunol Cell Biol **85:**476-80.

13. **Daffis, S., M. A. Samuel, B. C. Keller, M. Gale, and M. S. Diamond.** 2007. Cell-Specific IRF-3 Responses Protect against West Nile Virus Infection by Interferon-Dependent and -Independent Mechanisms. PLoS Pathog **3:**e106.
14. **Daffis, S., M. A. Samuel, M. S. Suthar, M. Gale, Jr., and M. S. Diamond.** 2008. Toll-like receptor 3 has a protective role against West Nile virus infection. J Virol **82:**10349-58.
15. **Daffis, S., M. A. Samuel, M. S. Suthar, B. C. Keller, M. Gale, Jr., and M. S. Diamond.** 2008. Interferon regulatory factor IRF-7 induces the antiviral alpha interferon response and protects against lethal West Nile virus infection. J Virol **82:**8465-75.
16. **Delhaye, S., S. Paul, G. Blakqori, M. Minet, F. Weber, P. Staeheli, and T. Michiels.** 2006. Neurons produce type I interferon during viral encephalitis. Proc Natl Acad Sci U S A **103:**7835-40.
17. **Detje, C. N., T. Meyer, H. Schmidt, D. Kreuz, J. K. Rose, I. Bechmann, M. Prinz, and U. Kalinke.** 2009. Local type I IFN receptor signaling protects against virus spread within the central nervous system. J Immunol **182:**2297-304.
18. **Dong, L. W., X. N. Kong, H. X. Yan, L. X. Yu, L. Chen, W. Yang, Q. Liu, D. D. Huang, M. C. Wu, and H. Y. Wang.** 2008. Signal regulatory protein alpha negatively regulates both TLR3 and cytoplasmic pathways in type I interferon induction. Mol Immunol **45:**3025-35.
19. **Encinas, M., M. Iglesias, Y. Liu, H. Wang, A. Muhaisen, V. Cena, C. Gallego, and J. X. Comella.** 2000. Sequential treatment of SH-SY5Y cells with retinoic acid and brain-derived neurotrophic factor gives rise to fully differentiated, neurotrophic factor-dependent, human neuron-like cells. J Neurochem **75:**991-1003.
20. **Fredericksen, B. L., B. C. Keller, J. Fornek, M. G. Katze, and M. Gale, Jr.** 2008. Establishment and maintenance of the innate antiviral response to West Nile Virus involves both RIG-I and MDA5 signaling through IPS-1. J Virol **82:**609-16.
21. **Greene, C. M., N. G. McElvaney, S. J. O'Neill, and C. C. Taggart.** 2004. Secretory leucoprotease inhibitor impairs Toll-like receptor 2- and 4-mediated responses in monocytic cells. Infect Immun **72:**3684-7.
22. **Griffin, D. E.** 2003. Immune responses to RNA-virus infections of the CNS. Nat Rev Immunol **3:**493-502.
23. **Hazeki, K., S. Kinoshita, T. Matsumura, K. Nigorikawa, H. Kubo, and O. Hazeki.** 2006. Opposite effects of wortmannin and 2-(4-morpholinyl)-8-phenyl-1(4H)-benzopyran-4-one hydrochloride on toll-like receptor-mediated nitric oxide production: negative regulation of nuclear factor-{kappa}B by phosphoinositide 3-kinase. Mol Pharmacol **69:**1717-24.
24. **Hazeki, K., K. Nigorikawa, and O. Hazeki.** 2007. Role of phosphoinositide 3-kinase in innate immunity. Biol Pharm Bull **30:**1617-23.
25. **Heil, F., H. Hemmi, H. Hochrein, F. Ampenberger, C. Kirschning, S. Akira, G. Lipford, H. Wagner, and S. Bauer.** 2004. Species-specific

recognition of single-stranded RNA via toll-like receptor 7 and 8. Science **303:**1526-9.

26. **Heinz, S., V. Haehnel, M. Karaghiosoff, L. Schwarzfischer, M. Muller, S. W. Krause, and M. Rehli.** 2003. Species-specific regulation of Toll-like receptor 3 genes in men and mice. J Biol Chem **278:**21502-9.
27. **Honda, K., and T. Taniguchi.** 2006. IRFs: master regulators of signalling by Toll-like receptors and cytosolic pattern-recognition receptors. Nat Rev Immunol **6:**644-58.
28. **Hu, J. Y., Y. Chen, and S. Schacher.** 2007. Protein kinase C regulates local synthesis and secretion of a neuropeptide required for activity-dependent long-term synaptic plasticity. J Neurosci **27:**8927-39.
29. **Irizarry, R. A., B. Hobbs, F. Collin, Y. D. Beazer-Barclay, K. J. Antonellis, U. Scherf, and T. P. Speed.** 2003. Exploration, normalization, and summaries of high density oligonucleotide array probe level data. Biostatistics **4:**249-64.
30. **Jackson, A. C., J. P. Rossiter, and M. Lafon.** 2006. Expression of Toll-like receptor 3 in the human cerebellar cortex in rabies, herpes simplex encephalitis, and other neurological diseases. J Neurovirol **12:**229-34.
31. **Jackson, S. P., S. M. Schoenwaelder, I. Goncalves, W. S. Nesbitt, C. L. Yap, C. E. Wright, V. Kenche, K. E. Anderson, S. M. Dopheide, Y. Yuan, S. A. Sturgeon, H. Prabaharan, P. E. Thompson, G. D. Smith, P. R. Shepherd, N. Daniele, S. Kulkarni, B. Abbott, D. Saylik, C. Jones, L. Lu, S. Giuliano, S. C. Hughan, J. A. Angus, A. D. Robertson, and H. H. Salem.** 2005. PI 3-kinase p110beta: a new target for antithrombotic therapy. Nat Med **11:**507-14.
32. **Kalali, B. N., G. Kollisch, J. Mages, T. Muller, S. Bauer, H. Wagner, J. Ring, R. Lang, M. Mempel, and M. Ollert.** 2008. Double-stranded RNA induces an antiviral defense status in epidermal keratinocytes through TLR3-, PKR-, and MDA5/RIG-I-mediated differential signaling. J Immunol **181:**2694-704.
33. **Kappes, F., J. Fahrer, M. S. Khodadoust, A. Tabbert, C. Strasser, N. Mor-Vaknin, M. Moreno-Villanueva, A. Burkle, D. M. Markovitz, and E. Ferrando-May.** 2008. DEK is a poly(ADP-ribose) acceptor in apoptosis and mediates resistance to genotoxic stress. Mol Cell Biol **28:**3245-57.
34. **Kato, H., S. Sato, M. Yoneyama, M. Yamamoto, S. Uematsu, K. Matsui, T. Tsujimura, K. Takeda, T. Fujita, O. Takeuchi, and S. Akira.** 2005. Cell type-specific involvement of RIG-I in antiviral response. Immunity **23:**19-28.
35. **Kato, H., O. Takeuchi, S. Sato, M. Yoneyama, M. Yamamoto, K. Matsui, S. Uematsu, A. Jung, T. Kawai, K. J. Ishii, O. Yamaguchi, K. Otsu, T. Tsujimura, C. S. Koh, C. Reis e Sousa, Y. Matsuura, T. Fujita, and S. Akira.** 2006. Differential roles of MDA5 and RIG-I helicases in the recognition of RNA viruses. Nature **441:**101-5.
36. **Kaur, S., A. Sassano, B. Dolniak, S. Joshi, B. Majchrzak-Kita, D. P. Baker, N. Hay, E. N. Fish, and L. C. Platanias.** 2008. Role of the Akt

pathway in mRNA translation of interferon-stimulated genes. Proc Natl Acad Sci U S A **105:**4808-13.

37. **Kaur, S., A. Sassano, A. M. Joseph, B. Majchrzak-Kita, E. A. Eklund, A. Verma, S. M. Brachmann, E. N. Fish, and L. C. Platanias.** 2008. Dual regulatory roles of phosphatidylinositol 3-kinase in IFN signaling. J Immunol **181:**7316-23.
38. **Kroczynska, B., S. Kaur, E. Katsoulidis, B. Majchrzak-Kita, A. Sassano, S. C. Kozma, E. N. Fish, and L. C. Platanias.** 2009. Interferon-dependent engagement of eukaryotic initiation factor 4B via S6 kinase (S6K)- and ribosomal protein S6K-mediated signals. Mol Cell Biol **29:**2865-75.
39. **Kumar, H., T. Kawai, and S. Akira.** 2009. Pathogen recognition in the innate immune response. Biochem J **420:**1-16.
40. **Larsen, P. H., T. H. Holm, and T. Owens.** 2007. Toll-like receptors in brain development and homeostasis. Sci STKE **2007:**pe47.
41. **Lathia, J. D., E. Okun, S. C. Tang, K. Griffioen, A. Cheng, M. R. Mughal, G. Laryea, P. K. Selvaraj, C. ffrench-Constant, T. Magnus, T. V. Arumugam, and M. P. Mattson.** 2008. Toll-like receptor 3 is a negative regulator of embryonic neural progenitor cell proliferation. J Neurosci **28:**13978-84.
42. **Li, K., Z. Chen, N. Kato, M. Gale, Jr., and S. M. Lemon.** 2005. Distinct poly(I-C) and virus-activated signaling pathways leading to interferon-beta production in hepatocytes. J Biol Chem **280:**16739-47.
43. **Ma, Y., J. Li, I. Chiu, Y. Wang, J. A. Sloane, J. Lu, B. Kosaras, R. L. Sidman, J. J. Volpe, and T. Vartanian.** 2006. Toll-like receptor 8 functions as a negative regulator of neurite outgrowth and inducer of neuronal apoptosis. J Cell Biol **175:**209-15.
44. **Marie, I., J. E. Durbin, and D. E. Levy.** 1998. Differential viral induction of distinct interferon-alpha genes by positive feedback through interferon regulatory factor-7. EMBO J **17:**6660-9.
45. **Menager, P., P. Roux, F. Megret, J. P. Bourgeois, A. M. Le Sourd, A. Danckaert, M. Lafage, C. Prehaud, and M. Lafon.** 2009. Toll-like receptor 3 (TLR3) plays a major role in the formation of rabies virus Negri Bodies. PLoS Pathog **5:**e1000315.
46. **Moisse, K., and M. J. Strong.** 2006. Innate immunity in amyotrophic lateral sclerosis. Biochim Biophys Acta **1762:**1083-93.
47. **Ohtani, M., S. Nagai, S. Kondo, S. Mizuno, K. Nakamura, M. Tanabe, T. Takeuchi, S. Matsuda, and S. Koyasu.** 2008. Mammalian target of rapamycin and glycogen synthase kinase 3 differentially regulate lipopolysaccharide-induced interleukin-12 production in dendritic cells. Blood **112:**635-43.
48. **Paladino, P., D. T. Cummings, R. S. Noyce, and K. L. Mossman.** 2006. The IFN-independent response to virus particle entry provides a first line of antiviral defense that is independent of TLRs and retinoic acid-inducible gene I. J Immunol **177:**8008-16.

49. **Peng, W., D. C. Peltier, M. J. Larsen, P. D. Kirchhoff, S. D. Larsen, R. R. Neubig, and D. J. Miller.** 2009. Identification of thieno[3,2-b]pyrrole derivatives as novel small molecule inhibitors of neurotropic alphaviruses. J Infect Dis **199:**950-7.
50. **Peverali, F. A., D. Orioli, L. Tonon, P. Ciana, G. Bunone, M. Negri, and G. Della-Valle.** 1996. Retinoic acid-induced growth arrest and differentiation of neuroblastoma cells are counteracted by N-myc and enhanced by max overexpressions. Oncogene **12:**457-62.
51. **Pichlmair, A., and C. Reis e Sousa.** 2007. Innate recognition of viruses. Immunity **27:**370-83.
52. **Pichlmair, A., O. Schulz, C. P. Tan, J. Rehwinkel, H. Kato, O. Takeuchi, S. Akira, M. Way, G. Schiavo, and C. Reis e Sousa.** 2009. Activation of MDA5 requires higher-order RNA structures generated during virus infection. J Virol **83:**10761-9.
53. **Pomel, V., J. Klicic, D. Covini, D. D. Church, J. P. Shaw, K. Roulin, F. Burgat-Charvillon, D. Valognes, M. Camps, C. Chabert, C. Gillieron, B. Francon, D. Perrin, D. Leroy, D. Gretener, A. Nichols, P. A. Vitte, S. Carboni, C. Rommel, M. K. Schwarz, and T. Ruckle.** 2006. Furan-2-ylmethylene thiazolidinediones as novel, potent, and selective inhibitors of phosphoinositide 3-kinase gamma. J Med Chem **49:**3857-71.
54. **Prehaud, C., F. Megret, M. Lafage, and M. Lafon.** 2005. Virus infection switches TLR-3-positive human neurons to become strong producers of beta interferon. J Virol **79:**12893-904.
55. **Prinz, M., H. Schmidt, A. Mildner, K. P. Knobeloch, U. K. Hanisch, J. Raasch, D. Merkler, C. Detje, I. Gutcher, J. Mages, R. Lang, R. Martin, R. Gold, B. Becher, W. Bruck, and U. Kalinke.** 2008. Distinct and nonredundant in vivo functions of IFNAR on myeloid cells limit autoimmunity in the central nervous system. Immunity **28:**675-86.
56. **Randall, R. E., and S. Goodbourn.** 2008. Interferons and viruses: an interplay between induction, signalling, antiviral responses and virus countermeasures. J Gen Virol **89:**1-47.
57. **Rehli, M.** 2002. Of mice and men: species variations of Toll-like receptor expression. Trends Immunol **23:**375-8.
58. **Rolls, A., R. Shechter, A. London, Y. Ziv, A. Ronen, R. Levy, and M. Schwartz.** 2007. Toll-like receptors modulate adult hippocampal neurogenesis. Nat Cell Biol **9:**1081-8.
59. **Ronnett, G. V., L. D. Hester, J. S. Nye, K. Connors, and S. H. Snyder.** 1990. Human cortical neuronal cell line: establishment from a patient with unilateral megalencephaly. Science **248:**603-605.
60. **Sarkar, S. N., K. L. Peters, C. P. Elco, S. Sakamoto, S. Pal, and G. C. Sen.** 2004. Novel roles of TLR3 tyrosine phosphorylation and PI3 kinase in double-stranded RNA signaling. Nat Struct Mol Biol **11:**1060-7.
61. **Sato, M., N. Hata, M. Asagiri, T. Nakaya, T. Taniguchi, and N. Tanaka.** 1998. Positive feedback regulation of type I IFN genes by the IFN-inducible transcription factor IRF-7. FEBS Lett **441:**106-10.

62. **Sato, M., H. Suemori, N. Hata, M. Asagiri, K. Ogasawara, K. Nakao, T. Nakaya, M. Katsuki, S. Noguchi, N. Tanaka, and T. Taniguchi.** 2000. Distinct and essential roles of transcription factors IRF-3 and IRF-7 in response to viruses for IFN-alpha/beta gene induction. Immunity **13:**539-48.
63. **Schlee, M., A. Roth, V. Hornung, C. A. Hagmann, V. Wimmenauer, W. Barchet, C. Coch, M. Janke, A. Mihailovic, G. Wardle, S. Juranek, H. Kato, T. Kawai, H. Poeck, K. A. Fitzgerald, O. Takeuchi, S. Akira, T. Tuschl, E. Latz, J. Ludwig, and G. Hartmann.** 2009. Recognition of 5' triphosphate by RIG-I helicase requires short blunt double-stranded RNA as contained in panhandle of negative-strand virus. Immunity **31:**25-34.
64. **Schmidt, A., T. Schwerd, W. Hamm, J. C. Hellmuth, S. Cui, M. Wenzel, F. S. Hoffmann, M. C. Michallet, R. Besch, K. P. Hopfner, S. Endres, and S. Rothenfusser.** 2009. 5'-triphosphate RNA requires base-paired structures to activate antiviral signaling via RIG-I. Proc Natl Acad Sci U S A **106:**12067-72.
65. **Sly, L. M., M. J. Hamilton, E. Kuroda, V. W. Ho, F. L. Antignano, S. L. Omeis, C. J. van Netten-Thomas, D. Wong, H. K. Brugger, O. Williams, M. E. Feldman, B. T. Houseman, D. Fiedler, K. M. Shokat, and G. Krystal.** 2009. SHIP prevents lipopolysaccharide from triggering an antiviral response in mice. Blood **113:**2945-54.
66. **Tang, S. C., T. V. Arumugam, X. Xu, A. Cheng, M. R. Mughal, D. G. Jo, J. D. Lathia, D. A. Siler, S. Chigurupati, X. Ouyang, T. Magnus, S. Camandola, and M. P. Mattson.** 2007. Pivotal role for neuronal Toll-like receptors in ischemic brain injury and functional deficits. Proc Natl Acad Sci U S A **104:**13798-803.
67. **Tusher, V. G., R. Tibshirani, and G. Chu.** 2001. Significance analysis of microarrays applied to the ionizing radiation response. Proc Natl Acad Sci U S A **98:**5116-21.
68. **Vanhaesebroeck, B., K. Ali, A. Bilancio, B. Geering, and L. C. Foukas.** 2005. Signalling by PI3K isoforms: insights from gene-targeted mice. Trends Biochem Sci **30:**194-204.
69. **Vercammen, E., J. Staal, and R. Beyaert.** 2008. Sensing of viral infection and activation of innate immunity by toll-like receptor 3. Clin Microbiol Rev **21:**13-25.
70. **Wang, Q., D. R. Nagarkar, E. R. Bowman, D. Schneider, B. Gosangi, J. Lei, Y. Zhao, C. L. McHenry, R. V. Burgens, D. J. Miller, U. Sajjan, and M. B. Hershenson.** 2009. Role of double-stranded RNA pattern recognition receptors in rhinovirus-induced airway epithelial cell responses. J Immunol **183:**6989-97.
71. **Wang, T., T. Town, L. Alexopoulou, J. F. Anderson, E. Fikrig, and R. A. Flavell.** 2004. Toll-like receptor 3 mediates West Nile virus entry into the brain causing lethal encephalitis. Nat Med **10:**1366-73.
72. **Werling, D., O. C. Jann, V. Offord, E. J. Glass, and T. J. Coffey.** 2009. Variation matters: TLR structure and species-specific pathogen recognition. Trends Immunol **30:**124-30.

73. **Yamamoto, M., S. Sato, K. Mori, K. Hoshino, O. Takeuchi, K. Takeda, and S. Akira.** 2002. Cutting edge: a novel Toll/IL-1 receptor domain-containing adapter that preferentially activates the IFN-beta promoter in the Toll-like receptor signaling. J Immunol **169:**6668-72.
74. **Yoneyama, M., and T. Fujita.** 2009. RNA recognition and signal transduction by RIG-I-like receptors. Immunol Rev **227:**54-65.
75. **Yoneyama, M., M. Kikuchi, K. Matsumoto, T. Imaizumi, M. Miyagishi, K. Taira, E. Foy, Y. M. Loo, M. Gale, Jr., S. Akira, S. Yonehara, A. Kato, and T. Fujita.** 2005. Shared and unique functions of the DExD/H-box helicases RIG-I, MDA5, and LGP2 in antiviral innate immunity. J Immunol **175:**2851-8.
76. **Zhang, S. Y., E. Jouanguy, S. Ugolini, A. Smahi, G. Elain, P. Romero, D. Segal, V. Sancho-Shimizu, L. Lorenzo, A. Puel, C. Picard, A. Chapgier, S. Plancoulaine, M. Titeux, C. Cognet, H. von Bernuth, C. L. Ku, A. Casrouge, X. X. Zhang, L. Barreiro, J. Leonard, C. Hamilton, P. Lebon, B. Heron, L. Vallee, L. Quintana-Murci, A. Hovnanian, F. Rozenberg, E. Vivier, F. Geissmann, M. Tardieu, L. Abel, and J. L. Casanova.** 2007. TLR3 deficiency in patients with herpes simplex encephalitis. Science **317:**1522-7.
77. **Zhang, Y., and B. R. Bhavnani.** 2006. Glutamate-induced apoptosis in neuronal cells is mediated via caspase-dependent and independent mechanisms involving calpain and caspase-3 proteases as well as apoptosis inducing factor (AIF) and this process is inhibited by equine estrogens. BMC Neurosci **7:**49.
78. **Zhao, Y., M. A. Rivieccio, S. Lutz, E. Scemes, and C. F. Brosnan.** 2006. The TLR3 ligand polyI: C downregulates connexin 43 expression and function in astrocytes by a mechanism involving the NF-kappaB and PI3 kinase pathways. Glia **54:**775-85.
79. **Zhou, Y., L. Ye, Q. Wan, L. Zhou, X. Wang, J. Li, S. Hu, D. Zhou, and W. Ho.** 2009. Activation of Toll-like receptors inhibits herpes simplex virus-1 infection of human neuronal cells. J Neurosci Res **87:**2916-25.
80. **Zurney, J., K. E. Howard, and B. Sherry.** 2007. Basal expression levels of IFNAR and Jak-STAT components are determinants of cell-type-specific differences in cardiac antiviral responses. J Virol **81:**13668-80.

Appendix to Chapter II: Supplemental Data

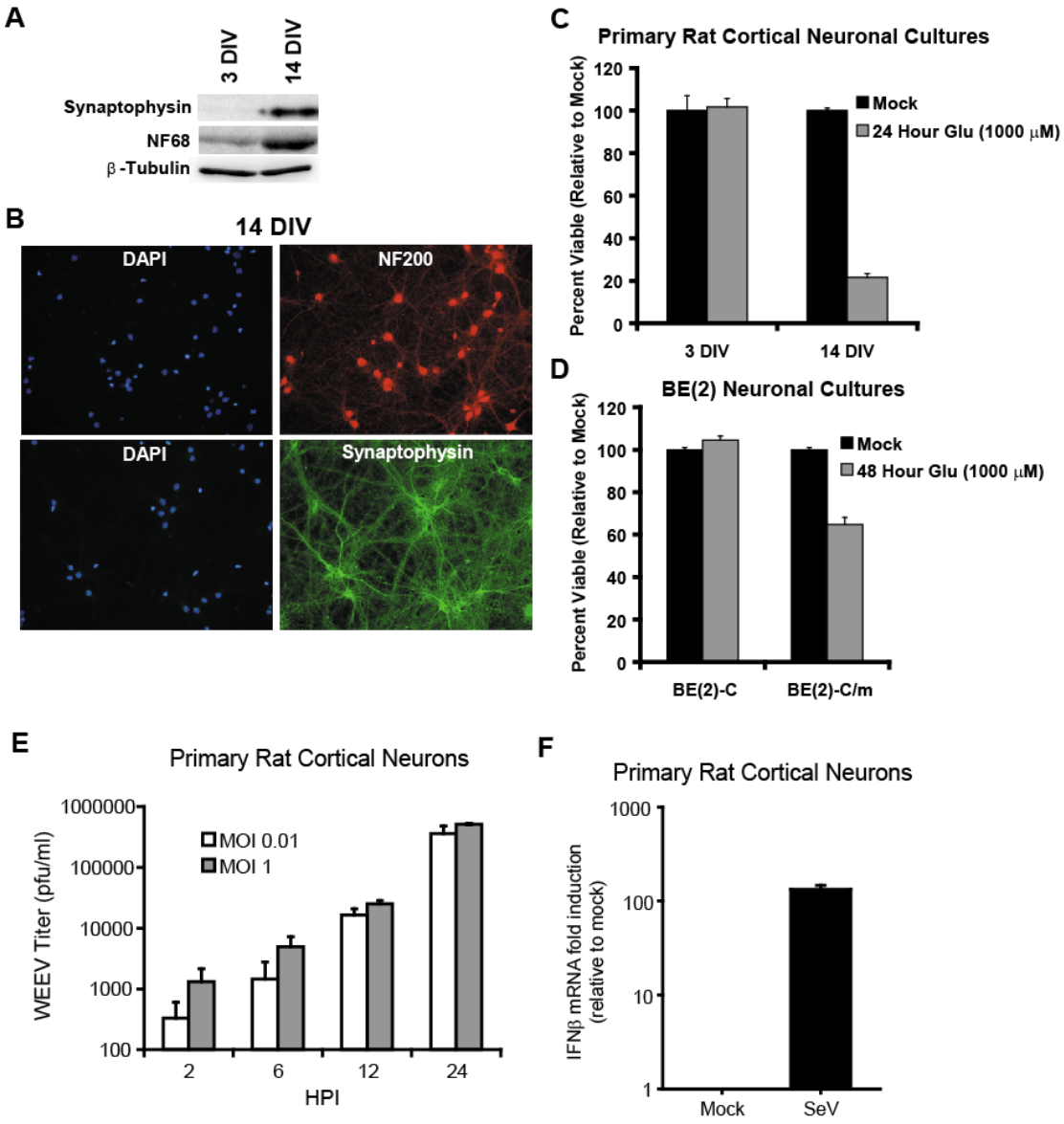

Supplemental Figure S2.1. Validation of primary cortical neuronal cultures. **A.** 3 or 14 day in vitro (DIV) rat primary cortical neuron lysates were immunoblotted for synaptophysin, NF68, or β-tubulin. **B.** Immunofluorescence images of 14 DIV rat neurons were stained with DAPI, NF200, or synaptophysin. 400X images are shown. **C and D.** Primary (C) or BE(2)-C-derived (D) neuronal cultures were treated with glutamate (Glu) as indicated, and viability was measured 24 hours later via a luminescent ATP (C) or MTT (D) assay. **E.** 14 DIV primary neurons were infected with WEEV, and supernatants were titered via plaque assay. **F.** 14 DIV cortical neurons were infected with SeV MOI 0.1, RNA was harvested 72 hours later, and IFNβ mRNA was analyzed via quantitative RT-PCR. Data are representative of 3 independent trials for A, B, and C and 2 trials for D, E, and F.

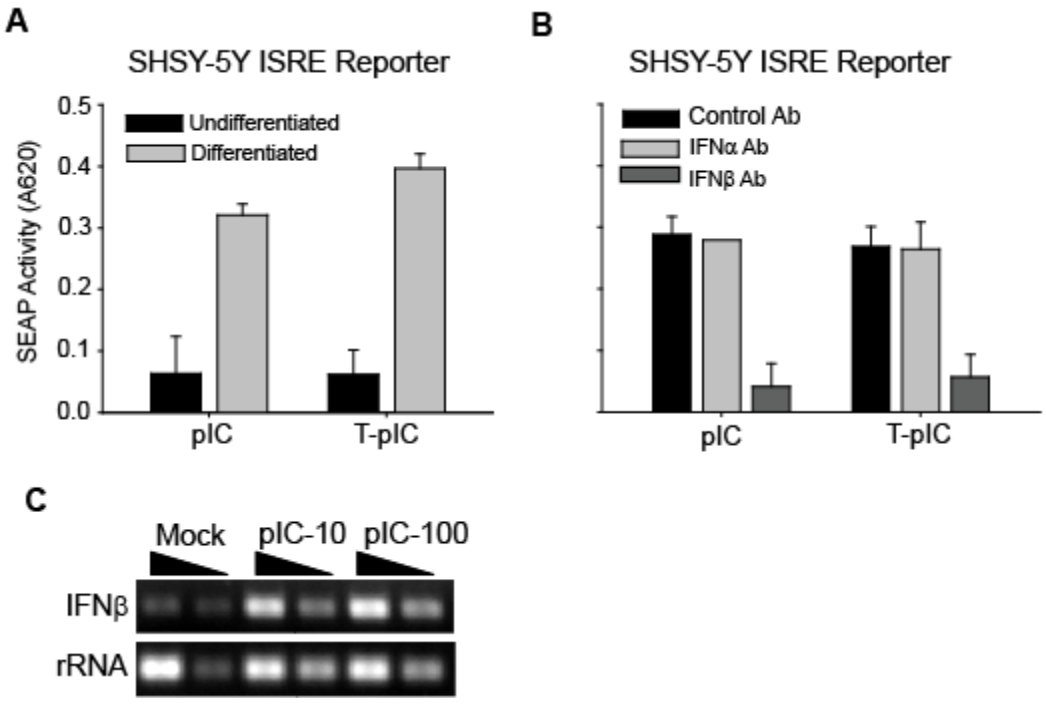

Supplemental Figure S2.2. PRR signaling in SYSY-5Y and HCN-1A neuronal cells. A. Undifferentiated and differentiated SHSY-5Y human neuroblastoma cells stably expressing an ISRE-SEAP reporter were stimulated with pIC (1.5 μg/ml) or T-pIC (0.015 μg/ml), and SEAP was measured 24 hours later. **B.** Differentiated SHSY-5Y ISRE reporter cells were stimulated with pIC or T-pIC along with either a control, IFNα (10,000 neutralizing units), or IFNβ (2000 neutralizing units) neutralizing antibody. SEAP activity was measured 24 hours later. **C.** Differentiated HCN-1A neuronal cells were mock-treated or treated with 10 or 100 μg/ml pIC. 20 hours later RNA was harvested, and IFNβ and rRNA transcripts were assessed via RT-PCR. Adjacent lanes represent ten-fold dilutions of cDNA. Data are representative of 2 independent trials for A and B and one trial for C. Error bars represent standard deviations of duplicate wells.

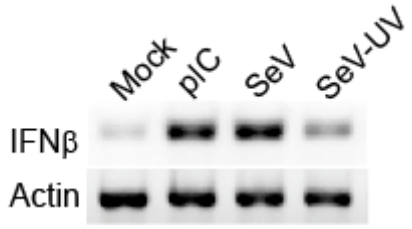

Supplemental Figure S2.3. UV-treated SeV fails to robustly induce IFNβ mRNA in neuronal cells. BE(2)-C/m cells were mock treated, treated with pIC, infected with SeV (MOI 5), or UV-treated SeV. RNA was harvested 20 hours later, and IFNβ and actin transcripts were measured via RT-PCR. Data are representative of 2 independent trials.

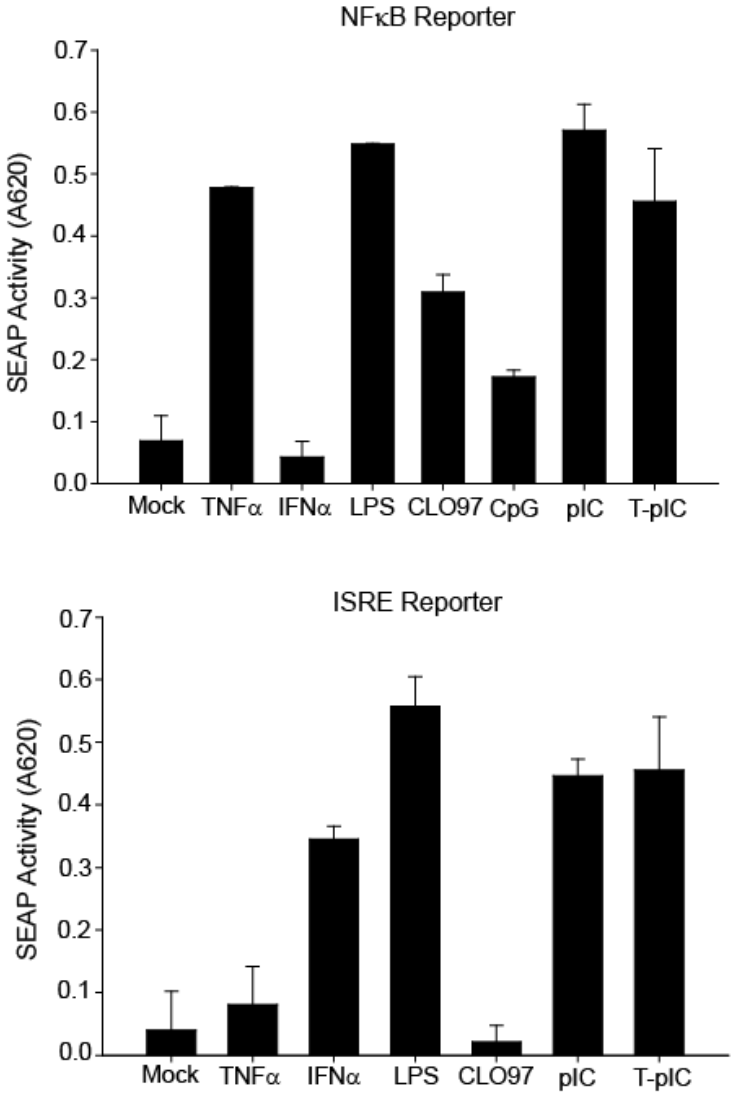

Supplemental Figure S2.4. PRR responses in U937 human monocyte-derived macrophages. U937 monocytes stably expressing an NFκB- or ISRE-SEAP reporter were differentiated and stimulated with a panel of PRR ligands. All ligands were tested at starting concentrations at least 5 times the manufacturer's suggested concentration and at dilutions covering at least 3 orders of magnitude. Stimuli were delivered for 24 hours followed by assessment of SEAP activity. Representative concentrations are shown. **A.** NFκB reporter cells were stimulated with TNFα (100 ng/ml), IFNα-A/D (10 U/ml), LPS (10 ng/ml), CLO97 (5 μg/ml), CpG (10 μM), pIC (5 μg/ml), or T-pIC (5 ug/ml). **B.** ISRE reporter cells were stimulated as in A except 1 μg/ml of LPS, 50 μg/ml of T-pIC, or 100 μg/ml of pIC was used. Data are representative of 3 independent trials. Error bars represent standard deviations of duplicate wells.

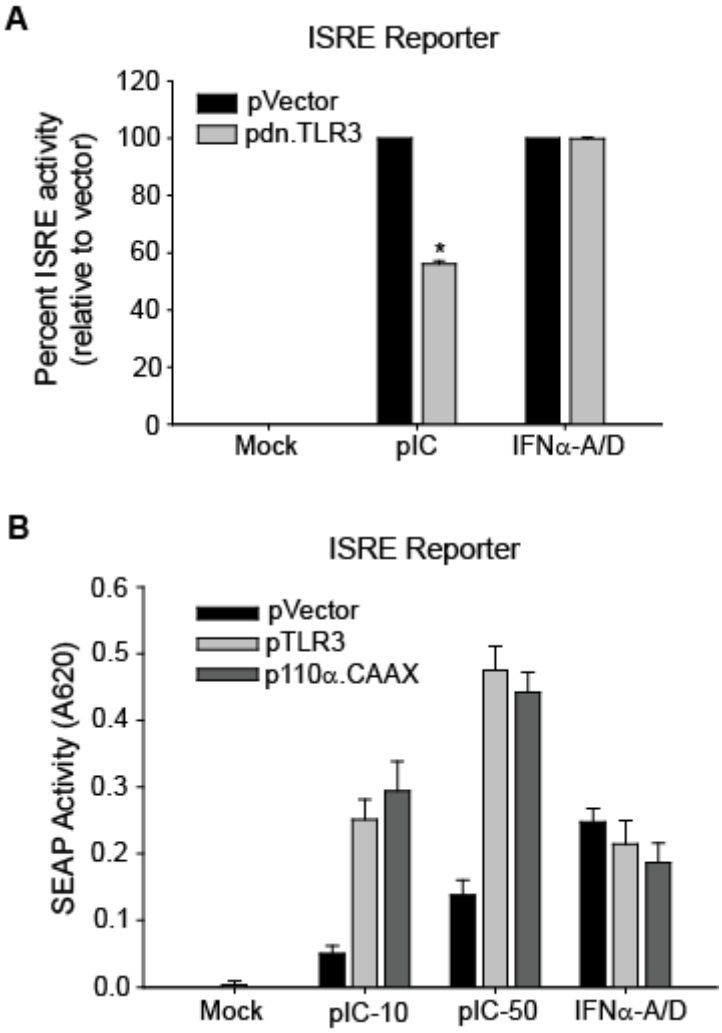

Supplemental Figure S2.5. TLR3- and PI3K p110α-dependent responses in neuronal cells. A. ISRE reporter BE(2)-C/m cells were transfected with a vector control or a dominant negative TLR3 (pdn.TLR3) for 48 hours. Cells were then stimulated for 24 hours with pIC (50 μg/ml) or IFNα-A/D (100 U/ml) for 24 hours. **B.** Cells were treated as in A except a wild-type TLR3 (pTLR3) or constitutively active PI3K p110α (p110α.CAAX) were transiently expressed, and cells were stimulated with pIC at either 10 (pIC-10) or 50 (pIC-50) μg/ml. In A, averages and SEMs are displayed from 2 trials. Data are representative of 1 trial for B where error bars represent standard deviations of duplicate wells. *$p <$ 0.05.

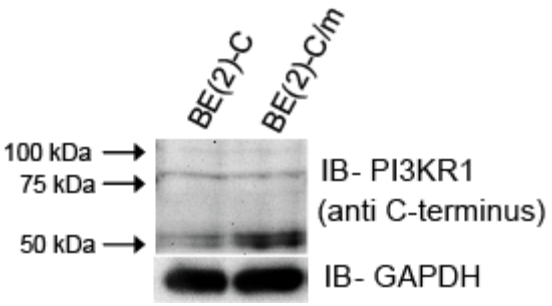

Supplemental Figure S2.6. PI3KR1 protein expression increases upon neuronal differentiation. BE(2)-C or BE(2)-C/m lysates were analyzed by Western blot for PI3KR1 or GAPDH expression. Data are representative of 2 trials.

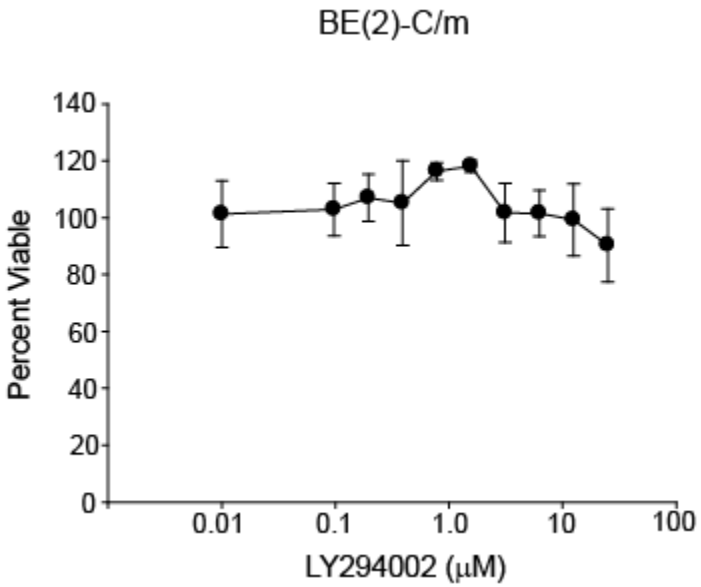

Supplemental Figure S2.7. LY294002 cytotoxicity in BE(2)-C/m cells. BE(2)-C/m cells were treated with the indicated concentrations of LY294002 for 24 hours. Percent viability relative to DMSO treated controls was measured via an AlamarBlue assay. Averages and SEMs are displayed from 2 trials.

Supplemental Table S2.1. BE(2)-C Genomatix Microarray Analysis.

Differentiated BE(2)-C/m vs. Undifferentiated BE(2)-C cells

Parameters: 5 independent experiments (biological replicates)
Genomatix ChipInspector program with exhaustive pairwise analysis
FDR 1%, minimum 3 probe coverage, $\log_2$ fold change >= 0.5 (approx 1.4-fold)

Genes Increased with Neuronal Differentiation

Gene Symbol	Gene Name	Fold Change
A1BG	alpha-1-B glycoprotein	1.5
AAK1	AP2 associated kinase 1	1.4
AATK	apoptosis-associated tyrosine kinase	1.6
ABAT	4-aminobutyrate aminotransferase	1.6
ABCA1	ATP-binding cassette, sub-family A (ABC1), member 1	1.8
ABCB1	ATP-binding cassette, sub-family B (MDR/TAP), member 1	1.8
ABCG1	ATP-binding cassette, sub-family G (WHITE), member 1	1.5
ABHD14A	abhydrolase domain containing 14A	1.5
ABI3BP	ABI gene family, member 3 (NESH) binding protein	2.7
ACADVL	acyl-Coenzyme A dehydrogenase, very long chain	1.4
ACCN4	amiloride-sensitive cation channel 4, pituitary	2.1
ACP6	acid phosphatase 6, lysophosphatidic	1.7
ACTA2	actin, alpha 2, smooth muscle, aorta	4.6
ACTG2	actin, gamma 2, smooth muscle, enteric	1.5
ADAM19	ADAM metallopeptidase domain 19 (meltrin beta)	1.7
ADAMTS5	ADAM metallopeptidase with thrombospondin type 1 motif, 5 (aggrecanase-2)	1.5
ADAMTS9	ADAM metallopeptidase with thrombospondin type 1 motif, 9	1.6
ADCY1	adenylate cyclase 1 (brain)	1.8
ADD3	adducin 3 (gamma)	2.5
ADH5	alcohol dehydrogenase 5 (class III), chi polypeptide	1.6
ADM	adrenomedullin	1.7
AK3L1	adenylate kinase 3-like 1	1.7
AKAP9	A kinase (PRKA) anchor protein (yotiao) 9	1.4
AKR1C1	aldo-keto reductase family 1, member C1 (dihydrodiol dehydrogenase 1; 20-alpha (3-alpha)-hydroxysteroid dehydrogenase)	1.5
AKR1C2	aldo-keto reductase family 1, member C2 (dihydrodiol dehydrogenase 2; bile acid binding protein; 3-alpha hydroxysteroid dehydrogenase, type III)	1.8
AKTIP	AKT interacting protein	1.5
ALCAM	activated leukocyte cell adhesion molecule	1.5
ALS2	amyotrophic lateral sclerosis 2 (juvenile)	1.5
AMHR2	anti-Mullerian hormone receptor, type II	1.6
ANGPT1	angiopoietin 1	1.5
ANGPTL6	angiopoietin-like 6	1.4
ANK2	ankyrin 2, neuronal	1.9
ANKRA2	ankyrin repeat, family A (RFXANK-like), 2	1.6
ANKRD1	ankyrin repeat domain 1 (cardiac muscle)	1.9
ANKRD6	ankyrin repeat domain 6	1.5
ANTXR2	anthrax toxin receptor 2	2.1
ANXA1	annexin A1	2.9
ANXA3	annexin A3	1.7
ANXA6	annexin A6	1.5
AP1G2	adaptor-related protein complex 1, gamma 2 subunit	1.5

AP1S2	adaptor-related protein complex 1, sigma 2 subunit	1.7
AP2B1	adaptor-related protein complex 2, beta 1 subunit	1.5
APBA1	amyloid beta (A4) precursor protein-binding, family A, member 1 (X11)	1.6
APC	adenomatous polyposis coli	1.5
APC2	adenomatosis polyposis coli 2	1.6
APLP2	amyloid beta (A4) precursor-like protein 2	1.7
AQP1	aquaporin 1 (Colton blood group)	1.5
AQP3	aquaporin 3 (Gill blood group)	2.0
AQP6	aquaporin 6, kidney specific	1.4
ARG2	arginase, type II	1.5
ARHGAP17	Rho GTPase activating protein 17	1.4
ARHGAP26	Rho GTPase activating protein 26	2.1
ARHGAP29	Rho GTPase activating protein 29	2.1
ARHGDIB	Rho GDP dissociation inhibitor (GDI) beta	1.6
ARHGEF17	Rho guanine nucleotide exchange factor (GEF) 17	1.4
ARHGEF3	Rho guanine nucleotide exchange factor (GEF) 3	3.1
ARHGEF7	Rho guanine nucleotide exchange factor (GEF) 7	1.4
ARL15	ADP-ribosylation factor-like 15	1.4
ARL6	ADP-ribosylation factor-like 6	1.7
ARL6IP5	ADP-ribosylation-like factor 6 interacting protein 5	1.5
ARMC9	armadillo repeat containing 9	1.5
ARMCX1	armadillo repeat containing, X-linked 1	1.5
ARMCX3	armadillo repeat containing, X-linked 3	1.5
ARNT2	aryl-hydrocarbon receptor nuclear translocator 2	2.0
ARNTL	aryl hydrocarbon receptor nuclear translocator-like	1.5
ASAH1	N-acylsphingosine amidohydrolase (acid ceramidase) 1	2.0
ASL	argininosuccinate lyase	1.6
ASTN1	astrotactin 1	2.0
ATAD1	ATPase family, AAA domain containing 1	1.4
ATCAY	ataxia, cerebellar, Cayman type (caytaxin)	1.7
ATP1A3	ATPase, Na+/K+ transporting, alpha 3 polypeptide	1.8
ATP1B1	ATPase, Na+/K+ transporting, beta 1 polypeptide	1.5
ATP2B1	ATPase, Ca++ transporting, plasma membrane 1	1.8
ATP2B3	ATPase, Ca++ transporting, plasma membrane 3	1.4
ATP2B4	ATPase, Ca++ transporting, plasma membrane 4	1.5
ATP6V0A1	ATPase, H+ transporting, lysosomal V0 subunit a1	1.5
ATP6V1A	ATPase, H+ transporting, lysosomal 70kDa, V1 subunit A	1.7
ATP6V1G2	ATPase, H+ transporting, lysosomal 13kDa, V1 subunit G2	1.6
ATP6V1H	ATPase, H+ transporting, lysosomal 50/57kDa, V1 subunit H	1.4
ATP7A	ATPase, Cu++ transporting, alpha polypeptide (Menkes syndrome)	3.4
AUTS2	autism susceptibility candidate 2	1.7
AXL	AXL receptor tyrosine kinase	1.6
B4GALNT1	beta-1,4-N-acetyl-galactosaminyl transferase 1	1.8
BACH2	BTB and CNC homology 1, basic leucine zipper transcription factor 2	1.9
BAI3	brain-specific angiogenesis inhibitor 3	1.5
BASP1	brain abundant, membrane attached signal protein 1	1.7
BCAS3	breast carcinoma amplified sequence 3	1.7
BCL2	B-cell CLL/lymphoma 2	1.6
BDKRB2	bradykinin receptor B2	1.5
BEX2	brain expressed X-linked 2	1.8
BEX4	BEX family member 4	1.7
BEX5	BEX family member 5	2.0

BLCAP	bladder cancer associated protein	1.5
BMP6	bone morphogenetic protein 6	1.6
BMP7	bone morphogenetic protein 7 (osteogenic protein 1)	2.1
BMPR1B	bone morphogenetic protein receptor, type IB	1.4
BMPR2	bone morphogenetic protein receptor, type II (serine/threonine kinase)	1.8
BNIP3L	BCL2/adenovirus E1B 19kDa interacting protein 3-like	1.7
BOK	BCL2-related ovarian killer	1.8
BRSK1	BR serine/threonine kinase 1	1.4
BSCL2	Bernardinelli-Seip congenital lipodystrophy 2 (seipin)	1.4
BTG2	BTG family, member 2	1.6
BVES	blood vessel epicardial substance	1.8
C16orf5	chromosome 16 open reading frame 5	1.4
C17orf28	chromosome 17 open reading frame 28	1.5
C19orf63	chromosome 19 open reading frame 63	1.6
C1orf76	chromosome 1 open reading frame 76	1.5
C4orf6	chromosome 4 open reading frame 6	15.0
C5orf13	chromosome 5 open reading frame 13	2.6
C5orf5	chromosome 5 open reading frame 5	1.4
C6orf134	chromosome 6 open reading frame 134	1.7
C7	complement component 7	1.6
C8orf4	chromosome 8 open reading frame 4	1.4
C8orf70	chromosome 8 open reading frame 70	1.5
C9orf127	chromosome 9 open reading frame 127	1.5
C9orf19	chromosome 9 open reading frame 19	1.6
C9orf95	chromosome 9 open reading frame 95	1.8
CA11	carbonic anhydrase XI	2.0
CACNA1B	calcium channel, voltage-dependent, N type, alpha 1B subunit	1.8
CACNB1	calcium channel, voltage-dependent, beta 1 subunit	1.4
CACNB3	calcium channel, voltage-dependent, beta 3 subunit	1.8
CACNG2	calcium channel, voltage-dependent, gamma subunit 2	1.5
CADM1	cell adhesion molecule 1	1.7
CADM3	cell adhesion molecule 3	1.6
CADM4	cell adhesion molecule 4	1.5
CADPS	Ca2+-dependent secretion activator	2.2
CALCA	calcitonin-related polypeptide alpha	1.5
CALCB	calcitonin-related polypeptide beta	25.7
CALCOCO1	calcium binding and coiled-coil domain 1	1.5
CALM1	calmodulin 1 (phosphorylase kinase, delta)	1.6
CAMK2B	calcium/calmodulin-dependent protein kinase (CaM kinase) II beta	1.7
CAMTA1	calmodulin binding transcription activator 1	1.7
CAP2	CAP, adenylate cyclase-associated protein, 2 (yeast)	1.5
CASD1	CAS1 domain containing 1	1.5
CASP6	caspase 6, apoptosis-related cysteine peptidase	1.4
CASZ1	castor zinc finger 1	1.6
CBL	Cas-Br-M (murine) ecotropic retroviral transforming sequence	1.5
CCDC80	coiled-coil domain containing 80	1.5
CCL2	chemokine (C-C motif) ligand 2	3.6
CCNA1	cyclin A1	1.7
CCNDBP1	cyclin D-type binding-protein 1	1.9
CCNG2	cyclin G2	2.2
CD14	CD14 molecule	1.9
CD151	CD151 molecule (Raph blood group)	1.6
CD177	CD177 molecule	3.4

CD200	CD200 molecule	1.9
CD24	CD24 molecule	3.8
CD276	CD276 molecule	1.5
CD44	CD44 molecule (Indian blood group)	2.1
CD59	CD59 molecule, complement regulatory protein	2.1
CDC14B	CDC14 cell division cycle 14 homolog B (S. cerevisiae)	1.4
CDC42	cell division cycle 42 (GTP binding protein, 25kDa)	1.5
CDH11	cadherin 11, type 2, OB-cadherin (osteoblast)	1.9
CDH12	cadherin 12, type 2 (N-cadherin 2)	1.7
CDK5R1	cyclin-dependent kinase 5, regulatory subunit 1 (p35)	1.5
CDK5R2	cyclin-dependent kinase 5, regulatory subunit 2 (p39)	1.6
CDK6	cyclin-dependent kinase 6	1.5
CDKN1A	cyclin-dependent kinase inhibitor 1A (p21, Cip1)	1.6
CDKN2B	cyclin-dependent kinase inhibitor 2B (p15, inhibits CDK4)	2.1
CDKN2D	cyclin-dependent kinase inhibitor 2D (p19, inhibits CDK4)	1.6
CEBPD	CCAAT/enhancer binding protein (C/EBP), delta	2.2
CFI	complement factor I	2.1
CHAC1	ChaC, cation transport regulator homolog 1 (E. coli)	1.5
CHRM1	cholinergic receptor, muscarinic 1	1.6
CHRM3	cholinergic receptor, muscarinic 3	2.0
CHST11	carbohydrate (chondroitin 4) sulfotransferase 11	2.1
CLASP2	cytoplasmic linker associated protein 2	1.8
CLCN5	chloride channel 5 (nephrolithiasis 2, X-linked, Dent disease)	2.5
CLCN6	chloride channel 6	1.5
CLIP1	CAP-GLY domain containing linker protein 1	1.5
CLIP2	CAP-GLY domain containing linker protein 2	1.7
CLIP3	CAP-GLY domain containing linker protein 3	2.3
CLSTN2	calsyntenin 2	1.6
CLSTN3	calsyntenin 3	1.6
CMAH	cytidine monophosphate-N-acetylneuraminic acid hydroxylase (CMP-N-acetylneuraminate monooxygenase) pseudogene	1.7
CMIP	c-Maf-inducing protein	1.5
CNN1	calponin 1, basic, smooth muscle	1.6
CNN2	calponin 2	1.7
CNTN1	contactin 1	1.5
COL12A1	collagen, type XII, alpha 1	1.5
COL13A1	collagen, type XIII, alpha 1	2.0
COL1A1	collagen, type I, alpha 1	3.6
COL3A1	collagen, type III, alpha 1 (Ehlers-Danlos syndrome type IV, autosomal dominant)	3.5
COL4A1	collagen, type IV, alpha 1	1.9
COL4A2	collagen, type IV, alpha 2	2.0
COL5A1	collagen, type V, alpha 1	1.8
COL6A3	collagen, type VI, alpha 3	1.4
COLQ	collagen-like tail subunit (single strand of homotrimer) of asymmetric acetylcholinesterase	1.8
CORO1A	coronin, actin binding protein, 1A	1.7
COTL1	coactosin-like 1 (Dictyostelium)	1.8
CPA4	carboxypeptidase A4	4.6
CPE	carboxypeptidase E	2.9
CPEB4	cytoplasmic polyadenylation element binding protein 4	1.9
CPNE3	copine III	1.5
CPT1C	carnitine palmitoyltransferase 1C	1.5
CPVL	carboxypeptidase, vitellogenic-like	1.6

CRABP2	cellular retinoic acid binding protein 2	8.6
CRB1	crumbs homolog 1 (Drosophila)	1.8
CREB5	cAMP responsive element binding protein 5	1.4
CRH	corticotropin releasing hormone	2.2
CRIM1	cysteine rich transmembrane BMP regulator 1 (chordin-like)	4.8
CRMP1	collapsin response mediator protein 1	1.4
CRYGC	crystallin, gamma C	4.7
CRYM	crystallin, mu	1.7
CSRP1	cysteine and glycine-rich protein 1	1.4
CSRP2	cysteine and glycine-rich protein 2	1.5
CTGF	connective tissue growth factor	7.0
CTNNA1	catenin (cadherin-associated protein), alpha 1, 102kDa	1.5
CTNNA2	catenin (cadherin-associated protein), alpha 2	1.5
CTSB	cathepsin B	3.1
CTSC	cathepsin C	1.4
CTSH	cathepsin H	3.2
CXADR	coxsackie virus and adenovirus receptor	1.8
CXCL12	chemokine (C-X-C motif) ligand 12 (stromal cell-derived factor 1)	1.4
CYB5R3	cytochrome b5 reductase 3	1.5
CYFIP2	cytoplasmic FMR1 interacting protein 2	2.1
CYP1A1	cytochrome P450, family 1, subfamily A, polypeptide 1	1.7
CYP26A1	cytochrome P450, family 26, subfamily A, polypeptide 1	37.5
CYP26B1	cytochrome P450, family 26, subfamily B, polypeptide 1	4.2
CYP3A5	cytochrome P450, family 3, subfamily A, polypeptide 5	1.7
CYR61	cysteine-rich, angiogenic inducer, 61	1.6
CYTL1	cytokine-like 1	2.3
DAAM1	dishevelled associated activator of morphogenesis 1	2.0
DACH1	dachshund homolog 1 (Drosophila)	2.0
DACT3	dapper, antagonist of beta-catenin, homolog 3 (Xenopus laevis)	1.7
DCHS1	dachsous 1 (Drosophila)	1.8
DCLK1	doublecortin-like kinase 1	6.8
DCLK2	doublecortin-like kinase 2	2.0
DCTN4	dynactin 4 (p62)	1.5
DCX	doublecortex; lissencephaly, X-linked (doublecortin)	5.4
DDAH2	dimethylarginine dimethylaminohydrolase 2	1.7
DDEF1	development and differentiation enhancing factor 1	1.6
DDEF2	development and differentiation enhancing factor 2	2.5
DDIT3	DNA-damage-inducible transcript 3	1.4
DDX17	DEAD (Asp-Glu-Ala-Asp) box polypeptide 17	1.5
DFNA5	deafness, autosomal dominant 5	1.6
DHRS3	dehydrogenase/reductase (SDR family) member 3	2.2
DIRAS3	DIRAS family, GTP-binding RAS-like 3	2.1
DKK2	dickkopf homolog 2 (Xenopus laevis)	2.5
DLG2	discs, large homolog 2, chapsyn-110 (Drosophila)	5.8
DLL3	delta-like 3 (Drosophila)	1.7
DOCK11	dedicator of cytokinesis 11	1.4
DOCK4	dedicator of cytokinesis 4	1.8
DPP6	dipeptidyl-peptidase 6	3.1
DPYSL3	dihydropyrimidinase-like 3	2.0
DPYSL4	dihydropyrimidinase-like 4	2.8
DRAM	damage-regulated autophagy modulator	1.7
DST	dystonin	1.6
DUSP1	dual specificity phosphatase 1	1.5

DUSP6	dual specificity phosphatase 6	5.3
DUSP8	dual specificity phosphatase 8	1.6
DYNC1I1	dynein, cytoplasmic 1, intermediate chain 1	2.0
DYRK1B	dual-specificity tyrosine-(Y)-phosphorylation regulated kinase 1B	1.5
DYSF	dysferlin, limb girdle muscular dystrophy 2B (autosomal recessive)	1.5
E2F7	E2F transcription factor 7	1.4
EDG1	endothelial differentiation, sphingolipid G-protein-coupled receptor, 1	1.6
EDG2	endothelial differentiation, lysophosphatidic acid G-protein-coupled receptor, 2	1.5
EDN1	endothelin 1	1.8
EDNRA	endothelin receptor type A	1.7
EFHA2	EF-hand domain family, member A2	1.6
EGR1	early growth response 1	1.9
EGR3	early growth response 3	2.8
EHD3	EH-domain containing 3	1.6
EIF4E3	eukaryotic translation initiation factor 4E family member 3	1.7
ELAVL1	ELAV (embryonic lethal, abnormal vision, Drosophila)-like 1 (Hu antigen R)	1.6
ELAVL2	ELAV (embryonic lethal, abnormal vision, Drosophila)-like 2 (Hu antigen B)	1.4
ELAVL3	ELAV (embryonic lethal, abnormal vision, Drosophila)-like 3 (Hu antigen C)	1.6
ELAVL4	ELAV (embryonic lethal, abnormal vision, Drosophila)-like 4 (Hu antigen D)	2.3
ELMO2	engulfment and cell motility 2	1.4
ELMOD1	ELMO/CED-12 domain containing 1	1.7
EMCN	endomucin	1.6
ENO2	enolase 2 (gamma, neuronal)	1.5
ENO3	enolase 3 (beta, muscle)	1.6
ENPP2	ectonucleotide pyrophosphatase/phosphodiesterase 2 (autotaxin)	1.4
ENPP4	ectonucleotide pyrophosphatase/phosphodiesterase 4 (putative function)	1.6
ENSA	endosulfine alpha	1.5
EPAS1	endothelial PAS domain protein 1	1.9
EPB41L1	erythrocyte membrane protein band 4.1-like 1	1.4
EPB49	erythrocyte membrane protein band 4.9 (dematin)	1.7
EPS15	epidermal growth factor receptor pathway substrate 15	1.4
ETHE1	ethylmalonic encephalopathy 1	5.6
EXOC1	exocyst complex component 1	1.5
EXOC6B	exocyst complex component 6B	3.3
EXPH5	exophilin 5	1.5
FAM127A	family with sequence similarity 127, member A	1.7
FAM13A1	family with sequence similarity 13, member A1	1.7
FAM38A	family with sequence similarity 38, member A	1.6
FAM84B	family with sequence similarity 84, member B	1.4
FAT	FAT tumor suppressor homolog 1 (Drosophila)	1.5
FAT4	FAT tumor suppressor homolog 4 (Drosophila)	1.6
FBLIM1	filamin binding LIM protein 1	1.6
FBXL2	F-box and leucine-rich repeat protein 2	1.7
FCHO2	FCH domain only 2	1.6
FDFT1	farnesyl-diphosphate farnesyltransferase 1	1.4
FER1L3	fer-1-like 3, myoferlin (C. elegans)	1.5
FEZ2	fasciculation and elongation protein zeta 2 (zygin II)	1.5

FGF1	fibroblast growth factor 1 (acidic)	1.5
FGF13	fibroblast growth factor 13	2.3
FGL1	fibrinogen-like 1	1.4
FHL1	four and a half LIM domains 1	1.4
FHOD3	formin homology 2 domain containing 3	1.5
FIBIN	fin bud initiation factor	1.5
FIG4	FIG4 homolog (S. cerevisiae)	1.6
FILIP1L	filamin A interacting protein 1-like	1.9
FKBP1B	FK506 binding protein 1B, 12.6 kDa	1.8
FLJ22536	hypothetical locus LOC401237	2.4
FLNB	filamin B, beta (actin binding protein 278)	2.9
FLOT1	flotillin 1	1.5
FMNL2	formin-like 2	1.7
FN1	fibronectin 1	7.7
FNBP1L	formin binding protein 1-like	1.9
FNDC4	fibronectin type III domain containing 4	1.6
FNDC5	fibronectin type III domain containing 5	2.6
FOXC1	forkhead box C1	2.0
FOXN3	forkhead box N3	1.4
FOXO1	forkhead box O1	1.8
FOXO3	forkhead box O3	2.0
FREM1	FRAS1 related extracellular matrix 1	2.2
FRS3	fibroblast growth factor receptor substrate 3	1.4
FSTL1	follistatin-like 1	8.8
FSTL3	follistatin-like 3 (secreted glycoprotein)	1.4
FUCA1	fucosidase, alpha-L- 1, tissue	1.6
FZD5	frizzled homolog 5 (Drosophila)	1.5
G0S2	G0/G1switch 2	1.6
GAB2	GRB2-associated binding protein 2	2.3
GABARAPL1	GABA(A) receptor-associated protein like 1	1.5
GABBR1	gamma-aminobutyric acid (GABA) B receptor, 1	1.9
GAL	galanin prepropeptide	2.9
GALNT7	UDP-N-acetyl-alpha-D-galactosamine:polypeptide N-acetylgalactosaminyltransferase 7 (GalNAc-T7)	1.4
GALR1	galanin receptor 1	2.2
GAS2	growth arrest-specific 2	1.8
GATS	opposite strand transcription unit to STAG3	1.8
GBP1	guanylate binding protein 1, interferon-inducible, 67kDa	1.4
GDAP1	ganglioside-induced differentiation-associated protein 1	1.5
GDAP1L1	ganglioside-induced differentiation-associated protein 1-like 1	1.7
GDF1	growth differentiation factor 1	2.1
GDF10	growth differentiation factor 10	1.8
GDF15	growth differentiation factor 15	2.9
GDI1	GDP dissociation inhibitor 1	1.5
GFRA2	GDNF family receptor alpha 2	1.6
GJA5	gap junction protein, alpha 5, 40kDa	1.7
GKAP1	G kinase anchoring protein 1	1.6
GLIPR1	GLI pathogenesis-related 1 (glioma)	1.6
GLIS2	GLIS family zinc finger 2	1.5
GLS	glutaminase	1.6
GNAO1	guanine nucleotide binding protein (G protein), alpha activating activity polypeptide O	2.4
GNAQ	guanine nucleotide binding protein (G protein), q polypeptide	1.5
GNB5	guanine nucleotide binding protein (G protein), beta 5	1.5

GNG2	guanine nucleotide binding protein (G protein), gamma 2	2.3
GNG3	guanine nucleotide binding protein (G protein), gamma 3	3.3
GNG4	guanine nucleotide binding protein (G protein), gamma 4	1.5
GNPTAB	N-acetylglucosamine-1-phosphate transferase, alpha and beta subunits	1.4
GNS	glucosamine (N-acetyl)-6-sulfatase (Sanfilippo disease IIID)	1.4
GPC2	glypican 2	2.0
GPM6B	glycoprotein M6B	1.9
GPNMB	glycoprotein (transmembrane) nmb	2.0
GPR124	G protein-coupled receptor 124	1.5
GPR137B	G protein-coupled receptor 137B	2.0
GPR160	G protein-coupled receptor 160	1.4
GPR161	G protein-coupled receptor 161	1.5
GPR176	G protein-coupled receptor 176	1.5
GPR22	G protein-coupled receptor 22	1.8
GPR56	G protein-coupled receptor 56	1.5
GPR64	G protein-coupled receptor 64	1.9
GPR68	G protein-coupled receptor 68	1.5
GPR83	G protein-coupled receptor 83	1.6
GPR85	G protein-coupled receptor 85	1.6
GPRC5A	G protein-coupled receptor, family C, group 5, member A	1.5
GRB10	growth factor receptor-bound protein 10	1.5
GREM1	gremlin 1, cysteine knot superfamily, homolog (Xenopus laevis)	1.7
GRIA1	glutamate receptor, ionotropic, AMPA 1	1.5
GRIA2	glutamate receptor, ionotropic, AMPA 2	2.0
GRK4	G protein-coupled receptor kinase 4	1.5
GRK5	G protein-coupled receptor kinase 5	1.9
H2AFY2	H2A histone family, member Y2	1.5
HBEGF	heparin-binding EGF-like growth factor	1.9
HBP1	HMG-box transcription factor 1	1.5
HEBP2	heme binding protein 2	3.4
HECW2	HECT, C2 and WW domain containing E3 ubiquitin protein ligase 2	1.4
HERV-FRD	HERV-FRD provirus ancestral Env polyprotein	1.8
HEY1	hairy/enhancer-of-split related with YRPW motif 1	1.5
HIC1	hypermethylated in cancer 1	1.7
HIST2H2BE	histone cluster 2, H2be	1.7
HIVEP2	human immunodeficiency virus type I enhancer binding protein 2	1.4
HLA-DPB1	major histocompatibility complex, class II, DP beta 1	1.7
HLA-DRB1	major histocompatibility complex, class II, DR beta 1	2.2
HMGCL	3-hydroxymethyl-3-methylglutaryl-Coenzyme A lyase (hydroxymethylglutaricaciduria)	1.4
HOMER3	homer homolog 3 (Drosophila)	1.5
HOXA5	homeobox A5	2.0
HOXC4	homeobox C4	1.5
HOXD1	homeobox D1	1.9
HOXD10	homeobox D10	2.5
HOXD11	homeobox D11	1.5
HOXD4	homeobox D4	1.8
HOXD9	homeobox D9	1.8
HPCAL1	hippocalcin-like 1	1.6
HRASLS3	HRAS-like suppressor 3	1.7
HRH1	histamine receptor H1	1.6
HS6ST3	heparan sulfate 6-O-sulfotransferase 3	1.7
HSD17B2	hydroxysteroid (17-beta) dehydrogenase 2	2.4

HSPB8	heat shock 22kDa protein 8	1.4
HTN1	histatin 1	2.0
HTN3	histatin 3	1.8
HTR2B	5-hydroxytryptamine (serotonin) receptor 2B	3.2
IDH1	isocitrate dehydrogenase 1 (NADP+), soluble	2.0
IDS	iduronate 2-sulfatase (Hunter syndrome)	1.5
IER3	immediate early response 3	1.7
IFI16	interferon, gamma-inducible protein 16	1.7
IFNAR2	interferon (alpha, beta and omega) receptor 2	1.5
IGF2	insulin-like growth factor 2 (somatomedin A)	2.0
IGF2R	insulin-like growth factor 2 receptor	1.4
IGFBP3	insulin-like growth factor binding protein 3	2.6
IGFBP5	insulin-like growth factor binding protein 5	1.9
IGFBP6	insulin-like growth factor binding protein 6	1.9
IGH	immunoglobulin heavy locus	2.1
IGSF11	immunoglobulin superfamily, member 11	1.8
IL13RA1	interleukin 13 receptor, alpha 1	1.5
IL17D	interleukin 17D	1.8
INHBA	inhibin, beta A	2.5
INSC	inscuteable homolog (Drosophila)	1.5
INSM1	insulinoma-associated 1	1.6
IRF9	interferon regulatory factor 9	1.7
ISYNA1	myo-inositol 1-phosphate synthase A1	1.6
ITGA1	integrin, alpha 1	5.7
ITGA2	integrin, alpha 2 (CD49B, alpha 2 subunit of VLA-2 receptor)	1.5
ITGA3	integrin, alpha 3 (antigen CD49C, alpha 3 subunit of VLA-3 receptor)	2.2
JAG1	jagged 1 (Alagille syndrome)	1.5
JARID1B	jumonji, AT rich interactive domain 1B	2.9
JARID2	jumonji, AT rich interactive domain 2	1.8
JMJD1A	jumonji domain containing 1A	1.6
JMJD2B	jumonji domain containing 2B	1.5
JMJD2C	jumonji domain containing 2C	1.5
JMJD3	jumonji domain containing 3, histone lysine demethylase	1.5
JPH3	junctophilin 3	1.8
JUB	jub, ajuba homolog (Xenopus laevis)	1.7
JUND	jun D proto-oncogene	1.4
JUP	junction plakoglobin	1.7
KALRN	kalirin, RhoGEF kinase	1.6
KBTBD11	kelch repeat and BTB (POZ) domain containing 11	1.4
KCNA3	potassium voltage-gated channel, shaker-related subfamily, member 3	1.7
KCNAB1	potassium voltage-gated channel, shaker-related subfamily, beta member 1	3.0
KCNIP4	Kv channel interacting protein 4	1.6
KCNJ2	potassium inwardly-rectifying channel, subfamily J, member 2	2.2
KCNMA1	potassium large conductance calcium-activated channel, subfamily M, alpha member 1	1.9
KCNMB4	potassium large conductance calcium-activated channel, subfamily M, beta member 4	1.7
KCNQ2	potassium voltage-gated channel, KQT-like subfamily, member 2	1.5
KCNT2	potassium channel, subfamily T, member 2	1.5
KCTD13	potassium channel tetramerisation domain containing 13	1.7
KDELR3	KDEL (Lys-Asp-Glu-Leu) endoplasmic reticulum protein retention	1.7

	receptor 3	
KIAA0513	KIAA0513	1.5
KIAA0746	KIAA0746 protein	1.7
KIAA1109	KIAA1109	1.4
KIAA1199	KIAA1199	1.5
KIDINS220	kinase D-interacting substrate of 220 kDa	1.6
KIF13B	kinesin family member 13B	1.5
KIF1A	kinesin family member 1A	1.5
KIF1B	kinesin family member 1B	2.2
KIF3A	kinesin family member 3A	1.5
KIF3C	kinesin family member 3C	1.9
KIF5A	kinesin family member 5A	1.7
KIF5C	kinesin family member 5C	2.2
KIFAP3	kinesin-associated protein 3	2.1
KIRREL	kin of IRRE like (Drosophila)	1.4
KLC1	kinesin light chain 1	2.2
KLF5	Kruppel-like factor 5 (intestinal)	1.5
KLF7	Kruppel-like factor 7 (ubiquitous)	1.5
KLHDC9	kelch domain containing 9	1.5
KLHL13	kelch-like 13 (Drosophila)	1.6
KLHL24	kelch-like 24 (Drosophila)	1.4
KLHL7	kelch-like 7 (Drosophila)	2.0
KRT18	keratin 18	6.5
KRT7	keratin 7	1.6
KRT86	keratin 86	1.5
LAMP2	lysosomal-associated membrane protein 2	1.4
LAPTM4A	lysosomal-associated protein transmembrane 4 alpha	1.4
LARP6	La ribonucleoprotein domain family, member 6	1.9
LASP1	LIM and SH3 protein 1	1.8
LASS5	LAG1 homolog, ceramide synthase 5	1.5
LATS2	LATS, large tumor suppressor, homolog 2 (Drosophila)	1.6
LBH	limb bud and heart development homolog (mouse)	2.5
LCOR	ligand dependent nuclear receptor corepressor	1.7
LCP1	lymphocyte cytosolic protein 1 (L-plastin)	1.9
LEF1	lymphoid enhancer-binding factor 1	1.6
LGALS3	lectin, galactoside-binding, soluble, 3	2.0
LHFPL2	lipoma HMGIC fusion partner-like 2	2.2
LIN7B	lin-7 homolog B (C. elegans)	1.4
LMBRD1	LMBR1 domain containing 1	1.9
LMO3	LIM domain only 3 (rhombotin-like 2)	2.1
LOC57228	small trans-membrane and glycosylated protein	1.8
LONRF2	LON peptidase N-terminal domain and ring finger 2	2.2
LOXL2	lysyl oxidase-like 2	1.6
LPHN1	latrophilin 1	1.4
LRP12	low density lipoprotein-related protein 12	1.5
LRRC15	leucine rich repeat containing 15	1.4
LRRFIP1	leucine rich repeat (in FLII) interacting protein 1	1.9
LRRN3	leucine rich repeat neuronal 3	1.6
LTB4DH	leukotriene B4 12-hydroxydehydrogenase	1.7
LTBP1	latent transforming growth factor beta binding protein 1	2.2
LTBP3	latent transforming growth factor beta binding protein 3	2.1
LTK	leukocyte receptor tyrosine kinase	1.4
LYST	lysosomal trafficking regulator	1.7

MAB21L1	mab-21-like 1 (C. elegans)	1.4
MAFB	v-maf musculoaponeurotic fibrosarcoma oncogene homolog B (avian)	1.4
MAFF	v-maf musculoaponeurotic fibrosarcoma oncogene homolog F (avian)	1.5
MAFK	v-maf musculoaponeurotic fibrosarcoma oncogene homolog K (avian)	2.6
MAGED2	melanoma antigen family D, 2	1.7
MAGEH1	melanoma antigen family H, 1	1.4
MAML3	mastermind-like 3 (Drosophila)	1.5
MAOA	monoamine oxidase A	1.8
MAP1B	microtubule-associated protein 1B	1.8
MAP1LC3A	microtubule-associated protein 1 light chain 3 alpha	1.4
MAP1LC3B	microtubule-associated protein 1 light chain 3 beta	2.4
MAP3K13	mitogen-activated protein kinase kinase kinase 13	1.7
MAP3K5	mitogen-activated protein kinase kinase kinase 5	1.6
MAP3K9	mitogen-activated protein kinase kinase kinase 9	2.0
MAP4	microtubule-associated protein 4	2.1
MAP4K4	mitogen-activated protein kinase kinase kinase kinase 4	1.4
MAP6	microtubule-associated protein 6	1.5
MAPK10	mitogen-activated protein kinase 10	1.5
MAPK8	mitogen-activated protein kinase 8	1.6
MAPKAPK3	mitogen-activated protein kinase-activated protein kinase 3	1.8
MAPRE2	microtubule-associated protein, RP/EB family, member 2	1.4
MAPRE3	microtubule-associated protein, RP/EB family, member 3	1.5
MAPT	microtubule-associated protein tau	2.3
MARCH6	membrane-associated ring finger (C3HC4) 6	1.4
MARCKSL1	MARCKS-like 1	1.6
MAST1	microtubule associated serine/threonine kinase 1	1.5
MAST4	microtubule associated serine/threonine kinase family member 4	1.8
MATN2	matrilin 2	1.5
MBNL3	muscleblind-like 3 (Drosophila)	1.7
MCC	mutated in colorectal cancers	1.8
MCF2L	MCF.2 cell line derived transforming sequence-like	1.8
MDK	midkine (neurite growth-promoting factor 2)	2.3
MEIS1	Meis homeobox 1	2.3
MEIS3	Meis homeobox 3	2.0
MEST	mesoderm specific transcript homolog (mouse)	14.2
MGAT3	mannosyl (beta-1,4-)-glycoprotein beta-1,4-N-acetylglucosaminyltransferase	1.5
MGAT4B	mannosyl (alpha-1,3-)-glycoprotein beta-1,4-N-acetylglucosaminyltransferase, isozyme B	1.6
MGP	matrix Gla protein	7.8
MGST3	microsomal glutathione S-transferase 3	1.9
MID1IP1	MID1 interacting protein 1 (gastrulation specific G12 homolog (zebrafish))	1.4
MLLT11	myeloid/lymphoid or mixed-lineage leukemia (trithorax homolog, Drosophila); translocated to, 11	1.8
MLLT4	myeloid/lymphoid or mixed-lineage leukemia (trithorax homolog, Drosophila); translocated to, 4	1.4
MMP1	matrix metallopeptidase 1 (interstitial collagenase)	2.0
MMP11	matrix metallopeptidase 11 (stromelysin 3)	1.5
MMP15	matrix metallopeptidase 15 (membrane-inserted)	1.5
MOAP1	modulator of apoptosis 1	1.5

MOXD1	monooxygenase, DBH-like 1	2.2
MRAS	muscle RAS oncogene homolog	1.4
MSRB3	methionine sulfoxide reductase B3	1.4
MTA3	metastasis associated 1 family, member 3	1.6
MUC12	mucin 12, cell surface associated	1.7
MYADM	myeloid-associated differentiation marker	2.4
MYC	v-myc myelocytomatosis viral oncogene homolog (avian)	2.3
MYLK	myosin light chain kinase	1.9
MYO5A	myosin VA (heavy chain 12, myoxin)	2.1
MYO6	myosin VI	1.6
MYPN	myopalladin	1.7
MYRIP	myosin VIIA and Rab interacting protein	1.9
MYST4	MYST histone acetyltransferase (monocytic leukemia) 4	1.5
N4BP2L2	NEDD4 binding protein 2-like 2	1.4
NAB2	NGFI-A binding protein 2 (EGR1 binding protein 2)	1.6
NANOS1	nanos homolog 1 (Drosophila)	1.6
NAP1L2	nucleosome assembly protein 1-like 2	2.0
NAP1L5	nucleosome assembly protein 1-like 5	1.4
NAV2	neuron navigator 2	1.4
NBEA	neurobeachin	1.8
NCAM1	neural cell adhesion molecule 1	1.6
NCAM2	neural cell adhesion molecule 2	2.4
NCOA3	nuclear receptor coactivator 3	1.5
NCOA7	nuclear receptor coactivator 7	1.6
NDN	necdin homolog (mouse)	1.7
NDRG4	NDRG family member 4	2.2
NEBL	nebulette	1.6
NEDD9	neural precursor cell expressed, developmentally down-regulated 9	1.6
NEIL2	nei like 2 (E. coli)	1.5
NELL2	NEL-like 2 (chicken)	3.5
NEO1	neogenin homolog 1 (chicken)	1.4
NEURL2	neuralized homolog 2 (Drosophila)	1.4
NFASC	neurofascin homolog (chicken)	1.5
NFIB	nuclear factor I/B	1.5
NFIL3	nuclear factor, interleukin 3 regulated	2.2
NGB	neuroglobin	1.5
NGFR	nerve growth factor receptor (TNFR superfamily, member 16)	2.0
NID1	nidogen 1	1.9
NIPSNAP3A	nipsnap homolog 3A (C. elegans)	1.5
NLRP1	NLR family, pyrin domain containing 1	2.1
NNMT	nicotinamide N-methyltransferase	1.9
NOTCH2	Notch homolog 2 (Drosophila)	2.3
NOVA1	neuro-oncological ventral antigen 1	1.6
NPC2	Niemann-Pick disease, type C2	3.2
NPPA	natriuretic peptide precursor A	1.5
NPPB	natriuretic peptide precursor B	3.5
NPR1	natriuretic peptide receptor A/guanylate cyclase A (atrionatriuretic peptide receptor A)	1.5
NPTX1	neuronal pentraxin I	1.4
NPTX2	neuronal pentraxin II	2.5
NR0B1	nuclear receptor subfamily 0, group B, member 1	5.5
NR0B2	nuclear receptor subfamily 0, group B, member 2	1.4
NR3C1	nuclear receptor subfamily 3, group C, member 1 (glucocorticoid receptor)	1.5

NRG1	neuregulin 1	1.5
NRG3	neuregulin 3	1.9
NRXN2	neurexin 2	1.4
NT5E	5'-nucleotidase, ecto (CD73)	2.2
NTNG2	netrin G2	1.5
NTRK2	neurotrophic tyrosine kinase, receptor, type 2	1.4
NUAK1	NUAK family, SNF1-like kinase, 1	3.0
OLFM3	olfactomedin 3	1.6
OLFML3	olfactomedin-like 3	2.0
ONECUT2	one cut homeobox 2	1.5
OPTN	optineurin	1.8
OSBPL8	oxysterol binding protein-like 8	1.4
OSTF1	osteoclast stimulating factor 1	2.9
P4HA2	procollagen-proline, 2-oxoglutarate 4-dioxygenase (proline 4-hydroxylase), alpha polypeptide II	1.4
PACSIN2	protein kinase C and casein kinase substrate in neurons 2	1.5
PAK3	p21 (CDKN1A)-activated kinase 3	1.5
PAK7	p21(CDKN1A)-activated kinase 7	1.5
PALM	paralemmin	1.9
PANX1	pannexin 1	1.5
PAPSS1	3'-phosphoadenosine 5'-phosphosulfate synthase 1	1.6
PAPSS2	3'-phosphoadenosine 5'-phosphosulfate synthase 2	1.5
PART1	prostate androgen-regulated transcript 1	1.5
PBX3	pre-B-cell leukemia homeobox 3	1.9
PBXIP1	pre-B-cell leukemia homeobox interacting protein 1	1.4
PCBP4	poly(rC) binding protein 4	1.7
PCDH7	protocadherin 7	1.7
PCDHA9	protocadherin alpha 9	1.8
PCDHB9	protocadherin beta 9	1.5
PCNXL2	pecanex-like 2 (Drosophila)	1.4
PCSK1N	proprotein convertase subtilisin/kexin type 1 inhibitor	2.8
PCSK5	proprotein convertase subtilisin/kexin type 5	1.5
PDE11A	phosphodiesterase 11A	1.5
PDE4DIP	phosphodiesterase 4D interacting protein (myomegalin)	1.5
PDE5A	phosphodiesterase 5A, cGMP-specific	1.4
PDLIM5	PDZ and LIM domain 5	1.8
PDLIM7	PDZ and LIM domain 7 (enigma)	1.5
PDZD2	PDZ domain containing 2	1.7
PDZK1	PDZ domain containing 1	2.4
PECI	peroxisomal D3,D2-enoyl-CoA isomerase	1.6
PELI1	pellino homolog 1 (Drosophila)	1.5
PGAM2	phosphoglycerate mutase 2 (muscle)	1.9
PGM2L1	phosphoglucomutase 2-like 1	2.5
PGPEP1	pyroglutamyl-peptidase I	1.5
PHLDA2	pleckstrin homology-like domain, family A, member 2	1.9
PHLDB2	pleckstrin homology-like domain, family B, member 2	1.7
PHOX2A	paired-like homeobox 2a	1.6
PHOX2B	paired-like homeobox 2b	1.7
PI15	peptidase inhibitor 15	2.5
PID1	phosphotyrosine interaction domain containing 1	1.4
PIK3R1	phosphoinositide-3-kinase, regulatory subunit 1 (alpha)	2.3
PIPOX	pipecolic acid oxidase	1.7
PITPNC1	phosphatidylinositol transfer protein, cytoplasmic 1	1.8
PITPNM1	phosphatidylinositol transfer protein, membrane-associated 1	1.5

PKIA	protein kinase (cAMP-dependent, catalytic) inhibitor alpha	1.6
PKIG	protein kinase (cAMP-dependent, catalytic) inhibitor gamma	1.5
PLAT	plasminogen activator, tissue	3.3
PLAUR	plasminogen activator, urokinase receptor	1.4
PLB1	phospholipase B1	1.4
PLD3	phospholipase D family, member 3	2.1
PLEKHA5	pleckstrin homology domain containing, family A member 5	1.4
PLEKHA6	pleckstrin homology domain containing, family A member 6	4.2
PLK2	polo-like kinase 2 (Drosophila)	8.3
PLSCR3	phospholipid scramblase 3	1.6
PLXNA2	plexin A2	3.0
PLXNA3	plexin A3	1.5
PLXNB1	plexin B1	1.5
PNMAL1	PNMA-like 1	1.5
PNOC	prepronociceptin	1.5
PNRC1	proline-rich nuclear receptor coactivator 1	1.7
PPAP2A	phosphatidic acid phosphatase type 2A	1.6
PPAP2B	phosphatidic acid phosphatase type 2B	1.6
PPAPDC1A	phosphatidic acid phosphatase type 2 domain containing 1A	3.3
PPARG	peroxisome proliferator-activated receptor gamma	1.8
PPFIBP2	PTPRF interacting protein, binding protein 2 (liprin beta 2)	1.4
PPIC	peptidylprolyl isomerase C (cyclophilin C)	1.6
PPM2C	protein phosphatase 2C, magnesium-dependent, catalytic subunit	1.6
PPP1R14A	protein phosphatase 1, regulatory (inhibitor) subunit 14A	1.4
PPP1R15A	protein phosphatase 1, regulatory (inhibitor) subunit 15A	1.4
PPP2R2B	protein phosphatase 2 (formerly 2A), regulatory subunit B, beta isoform	1.5
PPP2R2C	protein phosphatase 2 (formerly 2A), regulatory subunit B, gamma isoform	1.7
PPP2R5B	protein phosphatase 2, regulatory subunit B', beta isoform	1.6
PRAF2	PRA1 domain family, member 2	1.6
PRCP	prolylcarboxypeptidase (angiotensinase C)	1.6
PRDM1	PR domain containing 1, with ZNF domain	2.1
PREP	prolyl endopeptidase	1.6
PRG2	plasticity-related gene 2	1.7
PRICKLE1	prickle homolog 1 (Drosophila)	2.6
PRKACB	protein kinase, cAMP-dependent, catalytic, beta	1.4
PRKAR2B	protein kinase, cAMP-dependent, regulatory, type II, beta	2.2
PRKCE	protein kinase C, epsilon	1.6
PRKCH	protein kinase C, eta	3.3
PRKCZ	protein kinase C, zeta	2.0
PRNP	prion protein (p27-30) (Creutzfeldt-Jakob disease, Gerstmann-Strausler-Scheinker syndrome, fatal familial insomnia)	1.5
PROK2	prokineticin 2	1.5
PROM1	prominin 1	1.4
PRSS12	protease, serine, 12 (neurotrypsin, motopsin)	2.2
PRSS23	protease, serine, 23	3.6
PSAP	prosaposin (variant Gaucher disease and variant metachromatic leukodystrophy)	1.5
PSCD3	pleckstrin homology, Sec7 and coiled-coil domains 3	1.5
PSEN1	presenilin 1 (Alzheimer disease 3)	1.5
PSEN2	presenilin 2 (Alzheimer disease 4)	1.5
PTGIR	prostaglandin I2 (prostacyclin) receptor (IP)	1.9
PTPN18	protein tyrosine phosphatase, non-receptor type 18 (brain-derived)	1.5

PTPN21	protein tyrosine phosphatase, non-receptor type 21	1.5
PTPRE	protein tyrosine phosphatase, receptor type, E	1.8
PTPRF	protein tyrosine phosphatase, receptor type, F	1.5
PTPRH	protein tyrosine phosphatase, receptor type, H	3.1
PTPRM	protein tyrosine phosphatase, receptor type, M	1.6
PTPRN2	protein tyrosine phosphatase, receptor type, N polypeptide 2	1.8
PTPRR	protein tyrosine phosphatase, receptor type, R	1.6
PTRF	polymerase I and transcript release factor	1.5
PTTG1IP	pituitary tumor-transforming 1 interacting protein	1.5
PTX3	pentraxin-related gene, rapidly induced by IL-1 beta	9.0
PURG	purine-rich element binding protein G	1.8
PVRL2	poliovirus receptor-related 2 (herpesvirus entry mediator B)	1.5
QPCT	glutaminyl-peptide cyclotransferase (glutaminyl cyclase)	1.4
QPRT	quinolinate phosphoribosyltransferase (nicotinate-nucleotide pyrophosphorylase (carboxylating))	1.6
QSOX1	quiescin Q6 sulfhydryl oxidase 1	1.4
RAB20	RAB20, member RAS oncogene family	3.5
RAB27B	RAB27B, member RAS oncogene family	1.5
RAB2B	RAB2B, member RAS oncogene family	2.0
RAB38	RAB38, member RAS oncogene family	12.1
RAB39B	RAB39B, member RAS oncogene family	1.7
RAB3A	RAB3A, member RAS oncogene family	1.8
RAB4B	RAB4B, member RAS oncogene family	1.4
RAB5B	RAB5B, member RAS oncogene family	1.5
RAB6B	RAB6B, member RAS oncogene family	2.2
RABAC1	Rab acceptor 1 (prenylated)	1.4
RAI14	retinoic acid induced 14	2.5
RALB	v-ral simian leukemia viral oncogene homolog B (ras related; GTP binding protein)	1.6
RAMP1	receptor (G protein-coupled) activity modifying protein 1	1.7
RARA	retinoic acid receptor, alpha	1.6
RARB	retinoic acid receptor, beta	2.4
RASA1	RAS p21 protein activator (GTPase activating protein) 1	2.7
RASGRF1	Ras protein-specific guanine nucleotide-releasing factor 1	1.7
RBM9	RNA binding motif protein 9	1.6
RBP1	retinol binding protein 1, cellular	3.4
RBPMS	RNA binding protein with multiple splicing	1.4
RCAN2	regulator of calcineurin 2	2.0
RDH10	retinol dehydrogenase 10 (all-trans)	1.7
REC8	REC8 homolog (yeast)	1.8
REEP1	receptor accessory protein 1	3.2
REEP2	receptor accessory protein 2	1.5
REG3G	regenerating islet-derived 3 gamma	2.5
RET	ret proto-oncogene	2.4
RFTN1	raftlin, lipid raft linker 1	1.5
RGS16	regulator of G-protein signaling 16	1.6
RGS4	regulator of G-protein signaling 4	2.5
RHBDD2	rhomboid domain containing 2	1.4
RHOBTB3	Rho-related BTB domain containing 3	1.4
RHOC	ras homolog gene family, member C	1.7
RIT2	Ras-like without CAAX 2	1.8
RNASEL	ribonuclease L (2',5'-oligoisoadenylate synthetase-dependent)	1.5
RND3	Rho family GTPase 3	2.7
RNF103	ring finger protein 103	1.4

RNF11	ring finger protein 11	1.7
RNF146	ring finger protein 146	1.5
RNF19A	ring finger protein 19A	1.5
RNF24	ring finger protein 24	1.5
ROR1	receptor tyrosine kinase-like orphan receptor 1	1.5
RP1-21O18.1	kazrin	1.5
RP4-691N24.1	ninein-like	1.7
RSL1D1	ribosomal L1 domain containing 1	1.5
RTN1	reticulon 1	2.1
RTN2	reticulon 2	1.5
RUFY2	RUN and FYVE domain containing 2	1.5
RUFY3	RUN and FYVE domain containing 3	2.3
RUSC2	RUN and SH3 domain containing 2	1.5
RYBP	RING1 and YY1 binding protein	1.6
S100A10	S100 calcium binding protein A10	2.0
S100A13	S100 calcium binding protein A13	1.8
S100A16	S100 calcium binding protein A16	2.0
SALL2	sal-like 2 (Drosophila)	1.4
SAMD9	sterile alpha motif domain containing 9	1.5
SAMD9L	sterile alpha motif domain containing 9-like	1.7
SBK1	SH3-binding domain kinase 1	2.4
SCARB2	scavenger receptor class B, member 2	1.6
SCG2	secretogranin II (chromogranin C)	1.7
SCG5	secretogranin V (7B2 protein)	3.6
SCN2A	sodium channel, voltage-gated, type II, alpha subunit	1.6
SCN3A	sodium channel, voltage-gated, type III, alpha subunit	2.6
SCOC	short coiled-coil protein	1.7
SCRG1	scrapie responsive protein 1	2.4
SDC3	syndecan 3	1.4
SDC4	syndecan 4	1.7
SDCBP	syndecan binding protein (syntenin)	1.8
SEMA3C	sema domain, immunoglobulin domain (Ig), short basic domain, secreted, (semaphorin) 3C	1.5
SEMA4F	sema domain, immunoglobulin domain (Ig), transmembrane domain (TM) and short cytoplasmic domain, (semaphorin) 4F	1.5
SEPT3	septin 3	2.3
SEPT6	septin 6	1.7
SEPT8	septin 8	1.8
SERINC1	serine incorporator 1	1.9
SERINC3	serine incorporator 3	1.7
SERP2	stress-associated endoplasmic reticulum protein family member 2	1.8
SERPINB9	serpin peptidase inhibitor, clade B (ovalbumin), member 9	1.6
SERPINE1	serpin peptidase inhibitor, clade E (nexin, plasminogen activator inhibitor type 1), member 1	1.9
SERPINE2	serpin peptidase inhibitor, clade E (nexin, plasminogen activator inhibitor type 1), member 2	1.4
SERPINI1	serpin peptidase inhibitor, clade I (neuroserpin), member 1	1.6
SFXN3	sideroflexin 3	1.5
SGCB	sarcoglycan, beta (43kDa dystrophin-associated glycoprotein)	1.4
SGIP1	SH3-domain GRB2-like (endophilin) interacting protein 1	2.2
SH2D3C	SH2 domain containing 3C	1.5
SH3BGRL	SH3 domain binding glutamic acid-rich protein like	1.9
SH3BGRL2	SH3 domain binding glutamic acid-rich protein like 2	1.6
SH3BP5	SH3-domain binding protein 5 (BTK-associated)	2.3

SH3D19	SH3 domain containing 19	1.4
SH3KBP1	SH3-domain kinase binding protein 1	1.5
SH3PXD2A	SH3 and PX domains 2A	1.5
SHANK3	SH3 and multiple ankyrin repeat domains 3	1.9
SHC1	SHC (Src homology 2 domain containing) transforming protein 1	1.6
SHC2	SHC (Src homology 2 domain containing) transforming protein 2	1.9
SIGIRR	single immunoglobulin and toll-interleukin 1 receptor (TIR) domain	2.1
SKAP2	src kinase associated phosphoprotein 2	1.4
SLC12A6	solute carrier family 12 (potassium/chloride transporters), member 6	1.4
SLC16A2	solute carrier family 16, member 2 (monocarboxylic acid transporter 8)	1.4
SLC17A5	solute carrier family 17 (anion/sugar transporter), member 5	1.6
SLC18A3	solute carrier family 18 (vesicular acetylcholine), member 3	1.5
SLC22A17	solute carrier family 22, member 17	1.7
SLC23A2	solute carrier family 23 (nucleobase transporters), member 2	1.4
SLC25A24	solute carrier family 25 (mitochondrial carrier; phosphate carrier), member 24	1.6
SLC27A6	solute carrier family 27 (fatty acid transporter), member 6	1.6
SLC30A3	solute carrier family 30 (zinc transporter), member 3	1.5
SLC35D2	solute carrier family 35, member D2	1.4
SLC40A1	solute carrier family 40 (iron-regulated transporter), member 1	1.7
SLC44A2	solute carrier family 44, member 2	1.4
SLC47A1	solute carrier family 47, member 1	1.5
SLC6A17	solute carrier family 6, member 17	2.0
SLIT2	slit homolog 2 (Drosophila)	4.2
SLITRK6	SLIT and NTRK-like family, member 6	1.6
SMAD1	SMAD family member 1	1.6
SMAD3	SMAD family member 3	1.5
SMARCA1	SWI/SNF related, matrix associated, actin dependent regulator of chromatin, subfamily a, member 1	1.4
SMARCD3	SWI/SNF related, matrix associated, actin dependent regulator of chromatin, subfamily d, member 3	1.5
SMOX	spermine oxidase	1.4
SMPD3	sphingomyelin phosphodiesterase 3, neutral membrane (neutral sphingomyelinase II)	1.5
SMURF2	SMAD specific E3 ubiquitin protein ligase 2	1.5
SMYD3	SET and MYND domain containing 3	1.5
SNAI2	snail homolog 2 (Drosophila)	1.4
SNAP25	synaptosomal-associated protein, 25kDa	2.1
SNCG	synuclein, gamma (breast cancer-specific protein 1)	1.4
SNIP	SNAP25-interacting protein	1.5
SNN	stannin	1.8
SNRPN	small nuclear ribonucleoprotein polypeptide N	1.4
SOCS2	suppressor of cytokine signaling 2	2.9
SOCS5	suppressor of cytokine signaling 5	1.5
SOCS6	suppressor of cytokine signaling 6	1.8
SOHLH2	spermatogenesis and oogenesis specific basic helix-loop-helix 2	1.4
SORCS2	sortilin-related VPS10 domain containing receptor 2	2.6
SORL1	sortilin-related receptor, L(DLR class) A repeats-containing	2.7
SOX11	SRY (sex determining region Y)-box 11	1.6
SOX4	SRY (sex determining region Y)-box 4	1.8
SOX9	SRY (sex determining region Y)-box 9 (campomelic dysplasia, autosomal sex-reversal)	1.4

SPARC	secreted protein, acidic, cysteine-rich (osteonectin)	2.5
SPARCL1	SPARC-like 1 (mast9, hevin)	1.4
SPG3A	spastic paraplegia 3A (autosomal dominant)	1.5
SPIN1	spindlin 1	1.5
SPINK5	serine peptidase inhibitor, Kazal type 5	1.5
SPOCK1	sparc/osteonectin, cwcv and kazal-like domains proteoglycan (testican) 1	1.7
SPOCK2	sparc/osteonectin, cwcv and kazal-like domains proteoglycan (testican) 2	1.6
SPP1	secreted phosphoprotein 1 (osteopontin, bone sialoprotein I, early T-lymphocyte activation 1)	1.7
SPRY1	sprouty homolog 1, antagonist of FGF signaling (Drosophila)	1.6
SPTAN1	spectrin, alpha, non-erythrocytic 1 (alpha-fodrin)	1.6
SRA1	steroid receptor RNA activator 1	1.6
SRC	v-src sarcoma (Schmidt-Ruppin A-2) viral oncogene homolog (avian)	1.4
SRGAP1	SLIT-ROBO Rho GTPase activating protein 1	1.4
SRPX	sushi-repeat-containing protein, X-linked	1.5
SRrp35	serine-arginine repressor protein (35 kDa)	1.6
SST	somatostatin	6.0
SSTR2	somatostatin receptor 2	1.5
ST6GALNAC3	ST6 (alpha-N-acetyl-neuraminyl-2,3-beta-galactosyl-1,3)-N-acetylgalactosaminide alpha-2,6-sialyltransferase 3	1.8
ST8SIA4	ST8 alpha-N-acetyl-neuraminide alpha-2,8-sialyltransferase 4	1.9
STAU2	staufen, RNA binding protein, homolog 2 (Drosophila)	1.6
STC1	stanniocalcin 1	1.7
STK17A	serine/threonine kinase 17a	1.6
STK32B	serine/threonine kinase 32B	2.5
STMN2	stathmin-like 2	1.8
STMN4	stathmin-like 4	5.5
STX12	syntaxin 12	1.7
STX7	syntaxin 7	1.5
STX8	syntaxin 8	1.5
STXBP1	syntaxin binding protein 1	1.6
SUCNR1	succinate receptor 1	5.0
SULT1E1	sulfotransferase family 1E, estrogen-preferring, member 1	1.9
SULT4A1	sulfotransferase family 4A, member 1	1.9
SYN1	synapsin I	1.5
SYNGR1	synaptogyrin 1	1.7
SYNGR3	synaptogyrin 3	3.1
SYNJ2	synaptojanin 2	1.5
SYNPO	synaptopodin	1.4
SYNPO2	synaptopodin 2	1.9
SYT1	synaptotagmin I	1.6
SYT11	synaptotagmin XI	2.4
SYT4	synaptotagmin IV	2.2
SYT5	synaptotagmin V	1.7
TAGLN	transgelin	7.3
TAGLN3	transgelin 3	5.0
TBC1D9	TBC1 domain family, member 9 (with GRAM domain)	1.7
TBX2	T-box 2	1.4
TBX3	T-box 3 (ulnar mammary syndrome)	1.7
TCEA2	transcription elongation factor A (SII), 2	1.5
TCEAL7	transcription elongation factor A (SII)-like 7	1.9

TDRD7	tudor domain containing 7	1.6
TFAP2B	transcription factor AP-2 beta (activating enhancer binding protein 2 beta)	1.4
TFDP2	transcription factor Dp-2 (E2F dimerization partner 2)	1.7
TGFB1	transforming growth factor, beta 1	2.5
TGFB1I1	transforming growth factor beta 1 induced transcript 1	1.8
TGFBR1	transforming growth factor, beta receptor I (activin A receptor type II-like kinase, 53kDa)	1.5
TGIF1	TGFB-induced factor homeobox 1	1.6
TGM2	transglutaminase 2 (C polypeptide, protein-glutamine-gamma-glutamyltransferase)	2.5
THBS1	thrombospondin 1	2.2
THBS2	thrombospondin 2	2.3
TIMP2	TIMP metallopeptidase inhibitor 2	1.7
TLE3	transducin-like enhancer of split 3 (E(sp1) homolog, Drosophila)	1.5
TLR4	toll-like receptor 4	1.4
TM4SF1	transmembrane 4 L six family member 1	1.7
TM4SF4	transmembrane 4 L six family member 4	1.8
TM7SF2	transmembrane 7 superfamily member 2	1.8
TMEFF1	transmembrane protein with EGF-like and two follistatin-like domains 1	1.6
TMEM130	transmembrane protein 130	1.7
TMEM2	transmembrane protein 2	1.9
TMEM35	transmembrane protein 35	2.6
TMEM45A	transmembrane protein 45A	1.6
TMEM59L	transmembrane protein 59-like	1.6
TMEPAI	transmembrane, prostate androgen induced RNA	1.6
TMSB10	thymosin beta 10	1.9
TMSB4Y	thymosin beta 4, Y-linked	1.6
TMSL8	thymosin-like 8	3.3
TNFRSF10B	tumor necrosis factor receptor superfamily, member 10b	1.5
TNFRSF12A	tumor necrosis factor receptor superfamily, member 12A	1.9
TNIK	TRAF2 and NCK interacting kinase	1.7
TNRC4	trinucleotide repeat containing 4	1.8
TNS3	tensin 3	12.4
TOM1L2	target of myb1-like 2 (chicken)	1.5
TOX2	TOX high mobility group box family member 2	2.4
TP53BP1	tumor protein p53 binding protein 1	1.4
TP53I3	tumor protein p53 inducible protein 3	1.6
TP53INP1	tumor protein p53 inducible nuclear protein 1	2.6
TP53INP2	tumor protein p53 inducible nuclear protein 2	3.0
TPPP3	tubulin polymerization-promoting protein family member 3	2.1
TPST1	tyrosylprotein sulfotransferase 1	2.0
TRAF3IP2	TRAF3 interacting protein 2	1.5
TRAK1	trafficking protein, kinesin binding 1	1.5
TRIB2	tribbles homolog 2 (Drosophila)	1.7
TRIM2	tripartite motif-containing 2	1.4
TRIM36	tripartite motif-containing 36	1.7
TRIM5	tripartite motif-containing 5	1.4
TSC22D3	TSC22 domain family, member 3	1.5
TSHZ1	teashirt zinc finger homeobox 1	1.6
TSPAN13	tetraspanin 13	2.2
TSPAN18	tetraspanin 18	1.4
TSPAN31	tetraspanin 31	1.6

TSPAN5	tetraspanin 5	1.8
TSPAN7	tetraspanin 7	1.5
TSPAN8	tetraspanin 8	1.6
TSPYL2	TSPY-like 2	1.8
TTC3	tetratricopeptide repeat domain 3	1.5
TTC8	tetratricopeptide repeat domain 8	1.6
TUBB2B	tubulin, beta 2B	1.7
TUBB3	tubulin, beta 3	1.8
TUSC3	tumor suppressor candidate 3	1.4
UBE2H	ubiquitin-conjugating enzyme E2H (UBC8 homolog, yeast)	1.5
UBE2L6	ubiquitin-conjugating enzyme E2L 6	1.5
UCHL1	ubiquitin carboxyl-terminal esterase L1 (ubiquitin thiolesterase)	1.5
UGCG	UDP-glucose ceramide glucosyltransferase	1.4
USP11	ubiquitin specific peptidase 11	1.6
USP20	ubiquitin specific peptidase 20	1.4
VAMP2	vesicle-associated membrane protein 2 (synaptobrevin 2)	1.5
VANGL2	vang-like 2 (van gogh, Drosophila)	1.6
VASH1	vasohibin 1	1.4
VAT1	vesicle amine transport protein 1 homolog (T. californica)	2.2
VCAN	versican	1.6
VEZT	vezatin, adherens junctions transmembrane protein	1.5
VIM	vimentin	1.6
VLDLR	very low density lipoprotein receptor	2.1
VTN	vitronectin	1.6
WARS	tryptophanyl-tRNA synthetase	1.7
WDR44	WD repeat domain 44	1.4
WSB1	WD repeat and SOCS box-containing 1	1.5
WSCD2	WSC domain containing 2	1.5
WWTR1	WW domain containing transcription regulator 1	1.6
XPNPEP1	X-prolyl aminopeptidase (aminopeptidase P) 1, soluble	1.5
XYLT1	xylosyltransferase I	2.1
YAP1	Yes-associated protein 1, 65kDa	1.5
YIPF5	Yip1 domain family, member 5	1.5
YPEL1	yippee-like 1 (Drosophila)	1.5
YPEL5	yippee-like 5 (Drosophila)	2.2
ZBTB20	zinc finger and BTB domain containing 20	1.8
ZBTB38	zinc finger and BTB domain containing 38	1.5
ZDHHC2	zinc finger, DHHC-type containing 2	1.5
ZFHX3	zinc finger homeobox 3	1.5
ZFP90	zinc finger protein 90 homolog (mouse)	1.5
ZFPM1	zinc finger protein, multitype 1	2.0
ZKSCAN1	zinc finger with KRAB and SCAN domains 1	1.4
ZNF10	zinc finger protein 10	1.4
ZNF135	zinc finger protein 135	1.8
ZNF177	zinc finger protein 177	1.4
ZNF193	zinc finger protein 193	1.5
ZNF238	zinc finger protein 238	1.7
ZNF25	zinc finger protein 25	1.5
ZNF587	zinc finger protein 587	1.4
ZNF627	zinc finger protein 627	1.7
ZNF711	zinc finger protein 711	1.5
ZYX	zyxin	1.4

Genes Decreased with Neuronal Differentiation		
Gene Symbol	**Gene Name**	**Fold Change**
AATF	apoptosis antagonizing transcription factor	-1.6
ABCB10	ATP-binding cassette, sub-family B (MDR/TAP), member 10	-1.9
ABCB6	ATP-binding cassette, sub-family B (MDR/TAP), member 6	-1.5
ABCB9	ATP-binding cassette, sub-family B (MDR/TAP), member 9	-1.4
ABCE1	ATP-binding cassette, sub-family E (OABP), member 1	-1.5
ABCF1	ATP-binding cassette, sub-family F (GCN20), member 1	-1.5
ACE	angiotensin I converting enzyme (peptidyl-dipeptidase A) 1	-1.5
ADAMTS17	ADAM metallopeptidase with thrombospondin type 1 motif, 17	-1.6
ADAMTS3	ADAM metallopeptidase with thrombospondin type 1 motif, 3	-1.8
ADAT2	adenosine deaminase, tRNA-specific 2, TAD2 homolog (S. cerevisiae)	-1.4
ADRA2C	adrenergic, alpha-2C-, receptor	-2.0
AEBP2	AE binding protein 2	-1.5
AGPAT2	1-acylglycerol-3-phosphate O-acyltransferase 2 (lysophosphatidic acid acyltransferase, beta)	-1.6
AGPAT5	1-acylglycerol-3-phosphate O-acyltransferase 5 (lysophosphatidic acid acyltransferase, epsilon)	-1.4
AHCTF1	AT hook containing transcription factor 1	-1.5
AK1	adenylate kinase 1	-1.4
AK2	adenylate kinase 2	-1.5
ALDH18A1	aldehyde dehydrogenase 18 family, member A1	-1.4
AMD1	adenosylmethionine decarboxylase 1	-1.4
ANLN	anillin, actin binding protein	-1.7
ANP32B	acidic (leucine-rich) nuclear phosphoprotein 32 family, member B	-1.6
ANP32E	acidic (leucine-rich) nuclear phosphoprotein 32 family, member E	-1.5
ARF6	ADP-ribosylation factor 6	-1.4
ARHGAP10	Rho GTPase activating protein 10	-1.8
ARL5A	ADP-ribosylation factor-like 5A	-1.4
ARS2	arsenate resistance protein 2	-1.5
ASAM	adipocyte-specific adhesion molecule	-1.7
ASPH	aspartate beta-hydroxylase	-1.5
ASPM	asp (abnormal spindle) homolog, microcephaly associated (Drosophila)	-1.7
ASXL1	additional sex combs like 1 (Drosophila)	-1.6
ATAD2	ATPase family, AAA domain containing 2	-1.8
ATAD3A	ATPase family, AAA domain containing 3A	-1.6
ATAD5	ATPase family, AAA domain containing 5	-1.6
ATF1	activating transcription factor 1	-1.5
ATG3	ATG3 autophagy related 3 homolog (S. cerevisiae)	-1.6
ATIC	5-aminoimidazole-4-carboxamide ribonucleotide formyltransferase/IMP cyclohydrolase	-1.7
ATP5D	ATP synthase, H+ transporting, mitochondrial F1 complex, delta subunit	-1.4
ATP5G1	ATP synthase, H+ transporting, mitochondrial F0 complex, subunit C1 (subunit 9)	-1.5
ATPBD4	ATP binding domain 4	-1.8
ATR	ataxia telangiectasia and Rad3 related	-1.5
ATXN7	ataxin 7	-1.4
AURKA	aurora kinase A	-1.8
AURKAIP1	aurora kinase A interacting protein 1	-1.5
AURKB	aurora kinase B	-1.9

B3GNT2	UDP-GlcNAc:betaGal beta-1,3-N-acetylglucosaminyltransferase 2	-1.5
BAALC	brain and acute leukemia, cytoplasmic	-1.6
BAG3	BCL2-associated athanogene 3	-1.5
BARD1	BRCA1 associated RING domain 1	-1.7
BAZ1A	bromodomain adjacent to zinc finger domain, 1A	-1.5
BCCIP	BRCA2 and CDKN1A interacting protein	-1.5
BCL11A	B-cell CLL/lymphoma 11A (zinc finger protein)	-1.6
BDH1	3-hydroxybutyrate dehydrogenase, type 1	-1.5
BIRC5	baculoviral IAP repeat-containing 5 (survivin)	-1.7
BLM	Bloom syndrome	-1.4
BRCA1	breast cancer 1, early onset	-1.6
BRCA2	breast cancer 2, early onset	-1.5
BRMS1	breast cancer metastasis suppressor 1	-1.5
BRP44L	brain protein 44-like	-1.5
BUB1B	BUB1 budding uninhibited by benzimidazoles 1 homolog beta (yeast)	-1.6
BXDC2	brix domain containing 2	-1.5
BZW2	basic leucine zipper and W2 domains 2	-1.5
C10orf119	chromosome 10 open reading frame 119	-1.5
C10orf2	chromosome 10 open reading frame 2	-1.4
C13orf34	chromosome 13 open reading frame 34	-1.6
C17orf79	chromosome 17 open reading frame 79	-1.5
C17orf81	chromosome 17 open reading frame 81	-1.8
C19orf48	chromosome 19 open reading frame 48	-1.5
C1orf107	chromosome 1 open reading frame 107	-1.4
C1orf43	chromosome 1 open reading frame 43	-1.9
C1QBP	complement component 1, q subcomponent binding protein	-1.7
C20orf20	chromosome 20 open reading frame 20	-1.6
C21orf45	chromosome 21 open reading frame 45	-1.6
C6orf153	chromosome 6 open reading frame 153	-1.4
C6orf159	chromosome 6 open reading frame 159	-1.6
C6orf173	chromosome 6 open reading frame 173	-1.8
C6orf66	chromosome 6 open reading frame 66	-1.7
C7orf23	chromosome 7 open reading frame 23	-1.5
CABC1	chaperone, ABC1 activity of bc1 complex homolog (S. pombe)	-1.6
CABLES1	Cdk5 and Abl enzyme substrate 1	-1.5
CACNA2D2	calcium channel, voltage-dependent, alpha 2/delta subunit 2	-1.8
CACNG4	calcium channel, voltage-dependent, gamma subunit 4	-1.6
CACYBP	calcyclin binding protein	-1.5
CAD	carbamoyl-phosphate synthetase 2, aspartate transcarbamylase, and dihydroorotase	-1.6
CALML4	calmodulin-like 4	-1.6
CAMK4	calcium/calmodulin-dependent protein kinase IV	-1.5
CAMKK1	calcium/calmodulin-dependent protein kinase kinase 1, alpha	-1.5
CARD9	caspase recruitment domain family, member 9	-1.6
CASC5	cancer susceptibility candidate 5	-1.5
CASP3	caspase 3, apoptosis-related cysteine peptidase	-1.7
CASP7	caspase 7, apoptosis-related cysteine peptidase	-1.5
CBLB	Cas-Br-M (murine) ecotropic retroviral transforming sequence b	-1.4
CBX3	chromobox homolog 3 (HP1 gamma homolog, Drosophila)	-1.4
CBX5	chromobox homolog 5 (HP1 alpha homolog, Drosophila)	-1.4
CCDC59	coiled-coil domain containing 59	-1.5
CCDC85B	coiled-coil domain containing 85B	-1.5
CCNA2	cyclin A2	-1.5

CCNB1	cyclin B1	-1.7
CCNB2	cyclin B2	-1.6
CCNC	cyclin C	-1.6
CCNE2	cyclin E2	-1.7
CCT6A	chaperonin containing TCP1, subunit 6A (zeta 1)	-1.5
CD320	CD320 molecule	-1.4
CD3EAP	CD3e molecule, epsilon associated protein	-1.7
CDC14A	CDC14 cell division cycle 14 homolog A (S. cerevisiae)	-1.5
CDC2	cell division cycle 2, G1 to S and G2 to M	-1.5
CDC20	cell division cycle 20 homolog (S. cerevisiae)	-1.9
CDC25A	cell division cycle 25 homolog A (S. pombe)	-1.6
CDC45L	CDC45 cell division cycle 45-like (S. cerevisiae)	-1.5
CDC6	cell division cycle 6 homolog (S. cerevisiae)	-1.7
CDC7	cell division cycle 7 homolog (S. cerevisiae)	-1.4
CDCA2	cell division cycle associated 2	-1.5
CDCA3	cell division cycle associated 3	-1.6
CDCA4	cell division cycle associated 4	-1.5
CDCA7	cell division cycle associated 7	-1.8
CDCA7L	cell division cycle associated 7-like	-2.3
CDCA8	cell division cycle associated 8	-1.5
CDH2	cadherin 2, type 1, N-cadherin (neuronal)	-1.5
CDK2	cyclin-dependent kinase 2	-1.4
CDKAL1	CDK5 regulatory subunit associated protein 1-like 1	-1.6
CDKN3	cyclin-dependent kinase inhibitor 3 (CDK2-associated dual specificity phosphatase)	-1.7
CDON	Cdon homolog (mouse)	-1.8
CDT1	chromatin licensing and DNA replication factor 1	-1.6
CENPA	centromere protein A	-1.6
CENPB	centromere protein B, 80kDa	-1.4
CENPE	centromere protein E, 312kDa	-1.6
CENPF	centromere protein F, 350/400ka (mitosin)	-1.5
CENPK	centromere protein K	-1.8
CENPM	centromere protein M	-1.9
CENPN	centromere protein N	-1.6
CEP55	centrosomal protein 55kDa	-1.5
CHAF1A	chromatin assembly factor 1, subunit A (p150)	-1.4
CHAF1B	chromatin assembly factor 1, subunit B (p60)	-1.5
CHCHD3	coiled-coil-helix-coiled-coil-helix domain containing 3	-1.6
CHCHD4	coiled-coil-helix-coiled-coil-helix domain containing 4	-1.4
CHD1L	chromodomain helicase DNA binding protein 1-like	-1.4
CHEK1	CHK1 checkpoint homolog (S. pombe)	-1.4
CHEK2	CHK2 checkpoint homolog (S. pombe)	-1.6
CHERP	calcium homeostasis endoplasmic reticulum protein	-1.4
CHORDC1	cysteine and histidine-rich domain (CHORD)-containing 1	-1.6
CHPT1	choline phosphotransferase 1	-1.5
CHRAC1	chromatin accessibility complex 1	-1.5
CHTF18	CTF18, chromosome transmission fidelity factor 18 homolog (S. cerevisiae)	-1.6
CINP	cyclin-dependent kinase 2-interacting protein	-1.5
CKS2	CDC28 protein kinase regulatory subunit 2	-1.7
CLN6	ceroid-lipofuscinosis, neuronal 6, late infantile, variant	-1.8
CMPK1	cytidine monophosphate (UMP-CMP) kinase 1, cytosolic	-1.5
CMTM7	CKLF-like MARVEL transmembrane domain containing 7	-1.8
CNBP	CCHC-type zinc finger, nucleic acid binding protein	-1.5

CNDP2	CNDP dipeptidase 2 (metallopeptidase M20 family)	-1.4
CNTNAP2	contactin associated protein-like 2	-1.4
COASY	Coenzyme A synthase	-1.6
COQ2	coenzyme Q2 homolog, prenyltransferase (yeast)	-1.5
COQ3	coenzyme Q3 homolog, methyltransferase (S. cerevisiae)	-1.6
CPLX2	complexin 2	-1.7
CPNE2	copine II	-1.4
CPNE8	copine VIII	-1.8
CPOX	coproporphyrinogen oxidase	-1.5
CREB3L2	cAMP responsive element binding protein 3-like 2	-1.5
CRIP1	cysteine-rich protein 1 (intestinal)	-2.5
CRTAP	cartilage associated protein	-1.5
CRY1	cryptochrome 1 (photolyase-like)	-1.4
CSE1L	CSE1 chromosome segregation 1-like (yeast)	-1.5
CTDSPL	CTD (carboxy-terminal domain, RNA polymerase II, polypeptide A) small phosphatase-like	-1.5
CTNNAL1	catenin (cadherin-associated protein), alpha-like 1	-2.0
CTNNBL1	catenin, beta like 1	-1.5
CTPS	CTP synthase	-1.5
CWF19L2	CWF19-like 2, cell cycle control (S. pombe)	-1.4
CYC1	cytochrome c-1	-1.6
CYGB	cytoglobin	-2.1
DARS	aspartyl-tRNA synthetase	-1.4
DAXX	death-associated protein 6	-1.4
DAZAP1	DAZ associated protein 1	-1.5
DBF4	DBF4 homolog (S. cerevisiae)	-1.5
DBR1	debranching enzyme homolog 1 (S. cerevisiae)	-1.5
DDN	dendrin	-1.6
DDT	D-dopachrome tautomerase	-1.5
DDX11	DEAD/H (Asp-Glu-Ala-Asp/His) box polypeptide 11 (CHL1-like helicase homolog, S. cerevisiae)	-1.7
DDX18	DEAD (Asp-Glu-Ala-Asp) box polypeptide 18	-1.5
DDX21	DEAD (Asp-Glu-Ala-Asp) box polypeptide 21	-1.5
DDX46	DEAD (Asp-Glu-Ala-Asp) box polypeptide 46	-1.6
DEK	DEK oncogene (DNA binding)	-1.6
DEPDC1	DEP domain containing 1	-1.5
DEPDC1B	DEP domain containing 1B	-1.5
DIAPH3	diaphanous homolog 3 (Drosophila)	-1.4
DKC1	dyskeratosis congenita 1, dyskerin	-1.5
DLEU1	deleted in lymphocytic leukemia, 1	-1.4
DLG7	discs, large homolog 7 (Drosophila)	-1.6
DLK1	delta-like 1 homolog (Drosophila)	-2.2
DNA2	DNA replication helicase 2 homolog (yeast)	-1.5
DNPEP	aspartyl aminopeptidase	-1.5
DOK4	docking protein 4	-1.9
DPP9	dipeptidyl-peptidase 9	-1.5
DRD2	dopamine receptor D2	-1.5
DSCC1	defective in sister chromatid cohesion 1 homolog (S. cerevisiae)	-1.7
DSN1	DSN1, MIND kinetochore complex component, homolog (S. cerevisiae)	-1.4
DTL	denticleless homolog (Drosophila)	-1.5
DTYMK	deoxythymidylate kinase (thymidylate kinase)	-1.7
DUSP7	dual specificity phosphatase 7	-1.5
DUT	deoxyuridine triphosphatase	-1.5

E2F1	E2F transcription factor 1	-1.5
E2F2	E2F transcription factor 2	-1.4
E2F8	E2F transcription factor 8	-1.7
EBF3	early B-cell factor 3	-2.5
EBNA1BP2	EBNA1 binding protein 2	-1.6
ECE2	endothelin converting enzyme 2	-1.5
ECSIT	ECSIT homolog (Drosophila)	-1.4
ECT2	epithelial cell transforming sequence 2 oncogene	-1.6
EDIL3	EGF-like repeats and discoidin I-like domains 3	-2.1
EED	embryonic ectoderm development	-1.4
EEF1E1	eukaryotic translation elongation factor 1 epsilon 1	-1.5
EFNB1	ephrin-B1	-1.4
EGFR	epidermal growth factor receptor (erythroblastic leukemia viral (v-erb-b) oncogene homolog, avian)	-1.4
EI24	etoposide induced 2.4 mRNA	-1.4
EIF2B5	eukaryotic translation initiation factor 2B, subunit 5 epsilon, 82kDa	-1.4
EIF2S1	eukaryotic translation initiation factor 2, subunit 1 alpha, 35kDa	-1.5
EIF3B	eukaryotic translation initiation factor 3, subunit B	-1.5
EIF3J	eukaryotic translation initiation factor 3, subunit J	-1.4
EIF3M	eukaryotic translation initiation factor 3, subunit M	-1.6
EIF4EBP1	eukaryotic translation initiation factor 4E binding protein 1	-1.4
EIF5B	eukaryotic translation initiation factor 5B	-1.5
ELMO1	engulfment and cell motility 1	-1.4
EMG1	EMG1 nucleolar protein homolog (S. cerevisiae)	-1.7
EMILIN1	elastin microfibril interfacer 1	-1.7
ENDOD1	endonuclease domain containing 1	-1.5
ENDOG	endonuclease G	-2.0
ENOSF1	enolase superfamily member 1	-1.5
ERCC6L	excision repair cross-complementing rodent repair deficiency, complementation group 6-like	-1.5
ERLIN1	ER lipid raft associated 1	-1.6
ERO1L	ERO1-like (S. cerevisiae)	-1.4
ESCO2	establishment of cohesion 1 homolog 2 (S. cerevisiae)	-1.4
ESF1	ESF1, nucleolar pre-rRNA processing protein, homolog (S. cerevisiae)	-1.6
ESPL1	extra spindle pole bodies homolog 1 (S. cerevisiae)	-1.4
ETF1	eukaryotic translation termination factor 1	-1.4
ETFA	electron-transfer-flavoprotein, alpha polypeptide (glutaric aciduria II)	-1.5
ETFB	electron-transfer-flavoprotein, beta polypeptide	-1.5
EXO1	exonuclease 1	-1.8
EXOSC2	exosome component 2	-1.6
EXOSC3	exosome component 3	-1.4
EXOSC5	exosome component 5	-1.7
EXOSC8	exosome component 8	-1.6
EXOSC9	exosome component 9	-1.5
EZH2	enhancer of zeste homolog 2 (Drosophila)	-1.4
FAIM	Fas apoptotic inhibitory molecule	-1.7
FAM105A	family with sequence similarity 105, member A	-1.5
FAM120A	family with sequence similarity 120A	-1.5
FAM26B	family with sequence similarity 26, member B	-1.4
FAM82C	family with sequence similarity 82, member C	-1.5
FAM83D	family with sequence similarity 83, member D	-1.8
FANCG	Fanconi anemia, complementation group G	-1.4

FANCI	Fanconi anemia, complementation group I	-1.6
FBL	fibrillarin	-1.7
FBXO5	F-box protein 5	-1.6
FDX1	ferredoxin 1	-1.4
FEN1	flap structure-specific endonuclease 1	-1.7
FGFR1OP2	FGFR1 oncogene partner 2	-1.4
FHL2	four and a half LIM domains 2	-1.4
FIGNL1	fidgetin-like 1	-1.6
FKBP4	FK506 binding protein 4, 59kDa	-1.5
FKBP5	FK506 binding protein 5	-1.5
FLJ45983	FLJ45983 protein	-1.7
FOXM1	forkhead box M1	-1.9
FOXP4	forkhead box P4	-1.5
FRAS1	Fraser syndrome 1	-1.7
FRMD3	FERM domain containing 3	-1.7
FRMD4B	FERM domain containing 4B	-1.5
FTSJ2	FtsJ homolog 2 (E. coli)	-1.5
FUBP3	far upstream element (FUSE) binding protein 3	-1.5
FUSIP1	FUS interacting protein (serine/arginine-rich) 1	-1.4
FUT9	fucosyltransferase 9 (alpha (1,3) fucosyltransferase)	-1.5
GABRA1	gamma-aminobutyric acid (GABA) A receptor, alpha 1	-1.4
GABRA4	gamma-aminobutyric acid (GABA) A receptor, alpha 4	-1.5
GABRB1	gamma-aminobutyric acid (GABA) A receptor, beta 1	-1.5
GALM	galactose mutarotase (aldose 1-epimerase)	-1.5
GALNAC4S-6ST	B cell RAG associated protein	-2.5
GALNT14	UDP-N-acetyl-alpha-D-galactosamine:polypeptide N-acetylgalactosaminyltransferase 14 (GalNAc-T14)	-2.3
GART	phosphoribosylglycinamide formyltransferase, phosphoribosylglycinamide synthetase, phosphoribosylaminoimidazole synthetase	-1.6
GATA3	GATA binding protein 3	-5.3
GEMIN5	gem (nuclear organelle) associated protein 5	-1.7
GEMIN6	gem (nuclear organelle) associated protein 6	-1.4
GINS1	GINS complex subunit 1 (Psf1 homolog)	-1.9
GLE1	GLE1 RNA export mediator homolog (yeast)	-1.5
GLO1	glyoxalase I	-1.8
GLRX2	glutaredoxin 2	-1.5
GLRX5	glutaredoxin 5	-1.6
GMNN	geminin, DNA replication inhibitor	-1.9
GNB4	guanine nucleotide binding protein (G protein), beta polypeptide 4	-1.7
GNL2	guanine nucleotide binding protein-like 2 (nucleolar)	-1.5
GPAM	glycerol-3-phosphate acyltransferase, mitochondrial	-1.5
GPATCH4	G patch domain containing 4	-1.8
GPBAR1	G protein-coupled bile acid receptor 1	-1.5
GPD2	glycerol-3-phosphate dehydrogenase 2 (mitochondrial)	-1.5
GPR107	G protein-coupled receptor 107	-1.4
GPR125	G protein-coupled receptor 125	-1.4
GRIA4	glutamate receptor, ionotrophic, AMPA 4	-2.1
GRID1	glutamate receptor, ionotropic, delta 1	-1.8
GRM5	glutamate receptor, metabotropic 5	-1.5
GSPT1	G1 to S phase transition 1	-1.4
GTF3C4	general transcription factor IIIC, polypeptide 4, 90kDa	-1.5
GTPBP4	GTP binding protein 4	-1.4

GTSE1	G-2 and S-phase expressed 1	-1.5
GUCY1B3	guanylate cyclase 1, soluble, beta 3	-1.4
GULP1	GULP, engulfment adaptor PTB domain containing 1	-1.5
GYG1	glycogenin 1	-1.5
H2AFX	H2A histone family, member X	-1.7
HAND1	heart and neural crest derivatives expressed 1	-1.7
HAT1	histone acetyltransferase 1	-1.6
HDAC1	histone deacetylase 1	-1.6
HDAC9	histone deacetylase 9	-1.9
HDGF	hepatoma-derived growth factor (high-mobility group protein 1-like)	-1.4
HELLS	helicase, lymphoid-specific	-1.7
HES1	hairy and enhancer of split 1, (Drosophila)	-1.4
HHEX	hematopoietically expressed homeobox	-1.5
HK2	hexokinase 2	-2.0
HMGN3	high mobility group nucleosomal binding domain 3	-1.5
HMMR	hyaluronan-mediated motility receptor (RHAMM)	-1.7
HNRPD	heterogeneous nuclear ribonucleoprotein D (AU-rich element RNA binding protein 1, 37kDa)	-1.5
HRSP12	heat-responsive protein 12	-1.7
HS3ST5	heparan sulfate (glucosamine) 3-O-sulfotransferase 5	-1.9
HS6ST2	heparan sulfate 6-O-sulfotransferase 2	-1.6
HSCB	HscB iron-sulfur cluster co-chaperone homolog (E. coli)	-1.5
HSPA14	heat shock 70kDa protein 14	-1.6
HSPA9	heat shock 70kDa protein 9 (mortalin)	-1.4
HSPC111	hypothetical protein HSPC111	-1.7
HSPE1	heat shock 10kDa protein 1 (chaperonin 10)	-1.5
ICAM3	intercellular adhesion molecule 3	-1.5
ID2	inhibitor of DNA binding 2, dominant negative helix-loop-helix protein	-1.4
ID3	inhibitor of DNA binding 3, dominant negative helix-loop-helix protein	-1.4
IFRD2	interferon-related developmental regulator 2	-1.6
IGFBP2	insulin-like growth factor binding protein 2, 36kDa	-1.8
IGFBP4	insulin-like growth factor binding protein 4	-3.0
IL11RA	interleukin 11 receptor, alpha	-1.8
ILKAP	integrin-linked kinase-associated serine/threonine phosphatase 2C	-1.5
IMPDH1	IMP (inosine monophosphate) dehydrogenase 1	-2.4
IMPDH2	IMP (inosine monophosphate) dehydrogenase 2	-1.5
INF2	inverted formin, FH2 and WH2 domain containing	-1.6
INSM2	insulinoma-associated 2	-1.9
IPO4	importin 4	-1.5
IRAK1	interleukin-1 receptor-associated kinase 1	-1.5
ISG20L1	interferon stimulated exonuclease gene 20kDa-like 1	-1.6
ITGA9	integrin, alpha 9	-2.4
ITGAV	integrin, alpha V (vitronectin receptor, alpha polypeptide, antigen CD51)	-1.4
ITGB1BP1	integrin beta 1 binding protein 1	-1.4
ITGB3BP	integrin beta 3 binding protein (beta3-endonexin)	-1.7
ITGB5	integrin, beta 5	-1.6
ITM2C	integral membrane protein 2C	-1.4
ITPA	inosine triphosphatase (nucleoside triphosphate pyrophosphatase)	-1.4
JOSD3	Josephin domain containing 3	-1.4
JUNDM2	Jun dimerization protein 2	-1.5
KANK2	KN motif and ankyrin repeat domains 2	-1.4

KAZALD1	Kazal-type serine peptidase inhibitor domain 1	-1.4
KCNG1	potassium voltage-gated channel, subfamily G, member 1	-1.5
KCNJ14	potassium inwardly-rectifying channel, subfamily J, member 14	-1.5
KCNK3	potassium channel, subfamily K, member 3	-1.5
KCTD3	potassium channel tetramerisation domain containing 3	-1.5
KHDRBS3	KH domain containing, RNA binding, signal transduction associated 3	-1.6
KHSRP	KH-type splicing regulatory protein	-1.4
KIAA0020	KIAA0020	-1.5
KIAA0101	KIAA0101	-1.7
KIAA0586	KIAA0586	-1.4
KIF11	kinesin family member 11	-1.8
KIF14	kinesin family member 14	-1.8
KIF15	kinesin family member 15	-1.4
KIF20A	kinesin family member 20A	-1.4
KIF22	kinesin family member 22	-1.5
KIF23	kinesin family member 23	-1.6
KIF2C	kinesin family member 2C	-1.4
KIF4A	kinesin family member 4A	-1.5
KLF15	Kruppel-like factor 15	-1.9
KPNB1	karyopherin (importin) beta 1	-1.5
KRIT1	KRIT1, ankyrin repeat containing	-1.5
KRR1	KRR1, small subunit (SSU) processome component, homolog (yeast)	-1.4
LARP7	La ribonucleoprotein domain family, member 7	-1.5
LBR	lamin B receptor	-1.5
LDB2	LIM domain binding 2	-1.9
LGR5	leucine-rich repeat-containing G protein-coupled receptor 5	-2.0
LHX9	LIM homeobox 9	-2.3
LIMD1	LIM domains containing 1	-1.8
LMNA	lamin A/C	-1.6
LMNB1	lamin B1	-1.6
LMNB2	lamin B2	-1.4
LMO4	LIM domain only 4	-1.7
LPGAT1	lysophosphatidylglycerol acyltransferase 1	-1.5
LPHN2	latrophilin 2	-1.5
LPPR4	plasticity related gene 1	-3.7
LRRC4C	leucine rich repeat containing 4C	-1.5
LSM2	LSM2 homolog, U6 small nuclear RNA associated (S. cerevisiae)	-1.5
LSM3	LSM3 homolog, U6 small nuclear RNA associated (S. cerevisiae)	-1.5
LSM5	LSM5 homolog, U6 small nuclear RNA associated (S. cerevisiae)	-1.6
LSM8	LSM8 homolog, U6 small nuclear RNA associated (S. cerevisiae)	-1.4
LUM	lumican	-2.3
LYAR	Ly1 antibody reactive homolog (mouse)	-1.7
LYPLA1	lysophospholipase I	-1.5
MAD2L1	MAD2 mitotic arrest deficient-like 1 (yeast)	-1.6
MAGOH	mago-nashi homolog, proliferation-associated (Drosophila)	-1.5
MAGOHB	mago-nashi homolog B (Drosophila)	-1.5
MAP3K3	mitogen-activated protein kinase kinase kinase 3	-1.5
MAP3K4	mitogen-activated protein kinase kinase kinase 4	-1.5
MAP7	microtubule-associated protein 7	-1.6
MASTL	microtubule associated serine/threonine kinase-like	-1.4
MAT2A	methionine adenosyltransferase II, alpha	-1.4
MBD2	methyl-CpG binding domain protein 2	-1.8

MBNL1	muscleblind-like (Drosophila)	-1.5
MCM10	minichromosome maintenance complex component 10	-1.8
MCM2	minichromosome maintenance complex component 2	-1.6
MCM3	minichromosome maintenance complex component 3	-1.7
MCM4	minichromosome maintenance complex component 4	-1.4
MCM5	minichromosome maintenance complex component 5	-1.6
MCM6	minichromosome maintenance complex component 6	-1.6
MCM7	minichromosome maintenance complex component 7	-1.6
MCM8	minichromosome maintenance complex component 8	-1.7
MDGA1	MAM domain containing glycosylphosphatidylinositol anchor 1	-1.5
MEG3	maternally expressed 3	-1.7
MELK	maternal embryonic leucine zipper kinase	-1.7
MEPCE	methylphosphate capping enzyme	-1.5
METTL7A	methyltransferase like 7A	-1.5
MFHAS1	malignant fibrous histiocytoma amplified sequence 1	-1.4
MGAT5B	mannosyl (alpha-1,6-)-glycoprotein beta-1,6-N-acetyl-glucosaminyltransferase, isozyme B	-1.8
MID1	midline 1 (Opitz/BBB syndrome)	-1.6
MIHG1	microRNA host gene (non-protein coding) 1	-1.5
MINA	MYC induced nuclear antigen	-1.5
MITF	microphthalmia-associated transcription factor	-1.5
MKI67	antigen identified by monoclonal antibody Ki-67	-1.6
MLF1IP	MLF1 interacting protein	-1.5
MND1	meiotic nuclear divisions 1 homolog (S. cerevisiae)	-1.5
MPHOSPH1	M-phase phosphoprotein 1	-1.7
MPHOSPH9	M-phase phosphoprotein 9	-1.5
MRE11A	MRE11 meiotic recombination 11 homolog A (S. cerevisiae)	-1.6
MRPL11	mitochondrial ribosomal protein L11	-1.8
MRPL12	mitochondrial ribosomal protein L12	-1.7
MRPL13	mitochondrial ribosomal protein L13	-1.6
MRPL23	mitochondrial ribosomal protein L23	-1.6
MRPL39	mitochondrial ribosomal protein L39	-1.5
MRPL43	mitochondrial ribosomal protein L43	-1.4
MRPS12	mitochondrial ribosomal protein S12	-1.4
MRPS18B	mitochondrial ribosomal protein S18B	-1.6
MRPS24	mitochondrial ribosomal protein S24	-1.5
MRPS7	mitochondrial ribosomal protein S7	-1.4
MSX2	msh homeobox 2	-1.5
MT2A	metallothionein 2A	-1.8
MTDH	metadherin	-1.5
MTHFD1	methylenetetrahydrofolate dehydrogenase (NADP+ dependent) 1, methenyltetrahydrofolate cyclohydrolase, formyltetrahydrofolate synthetase	-1.8
MTHFD1L	methylenetetrahydrofolate dehydrogenase (NADP+ dependent) 1-like	-1.6
MTHFD2	methylenetetrahydrofolate dehydrogenase (NADP+ dependent) 2, methenyltetrahydrofolate cyclohydrolase	-1.4
MTHFS	5,10-methenyltetrahydrofolate synthetase (5-formyltetrahydrofolate cyclo-ligase)	-1.5
MTIF2	mitochondrial translational initiation factor 2	-1.4
MTR	5-methyltetrahydrofolate-homocysteine methyltransferase	-1.5
MYBBP1A	MYB binding protein (P160) 1a	-1.5
MYBL2	v-myb myeloblastosis viral oncogene homolog (avian)-like 2	-1.6
MYCBP	c-myc binding protein	-1.4

NAF1	nuclear assembly factor 1 homolog (S. cerevisiae)	-1.5
NASP	nuclear autoantigenic sperm protein (histone-binding)	-1.4
NAT13	N-acetyltransferase 13	-1.5
NBN	nibrin	-1.4
NCAPD2	non-SMC condensin I complex, subunit D2	-1.8
NCAPD3	non-SMC condensin II complex, subunit D3	-1.6
NCAPG	non-SMC condensin I complex, subunit G	-1.8
NCAPG2	non-SMC condensin II complex, subunit G2	-1.5
NCAPH	non-SMC condensin I complex, subunit H	-1.6
NCL	nucleolin	-1.5
NDC80	NDC80 homolog, kinetochore complex component (S. cerevisiae)	-1.5
NDUFV1	NADH dehydrogenase (ubiquinone) flavoprotein 1, 51kDa	-1.4
NEFH	neurofilament, heavy polypeptide 200kDa	-3.6
NEIL3	nei endonuclease VIII-like 3 (E. coli)	-1.6
NEK2	NIMA (never in mitosis gene a)-related kinase 2	-1.6
NELL1	NEL-like 1 (chicken)	-1.9
NF2	neurofibromin 2 (merlin)	-1.4
NFATC3	nuclear factor of activated T-cells, cytoplasmic, calcineurin-dependent 3	-1.4
NFATC4	nuclear factor of activated T-cells, cytoplasmic, calcineurin-dependent 4	-1.5
NHS	Nance-Horan syndrome (congenital cataracts and dental anomalies)	-1.4
NID2	nidogen 2 (osteonidogen)	-2.2
NIP7	nuclear import 7 homolog (S. cerevisiae)	-1.6
NLE1	notchless homolog 1 (Drosophila)	-1.6
NMB	neuromedin B	-1.4
NMT1	N-myristoyltransferase 1	-1.4
NOC2L	nucleolar complex associated 2 homolog (S. cerevisiae)	-1.4
NOC3L	nucleolar complex associated 3 homolog (S. cerevisiae)	-1.8
NOL1	nucleolar protein 1, 120kDa	-1.5
NOL14	nucleolar protein 14	-1.5
NOL5A	nucleolar protein 5A (56kDa with KKE/D repeat)	-1.5
NOL7	nucleolar protein 7, 27kDa	-1.4
NOL8	nucleolar protein 8	-1.4
NOLA1	nucleolar protein family A, member 1 (H/ACA small nucleolar RNPs)	-1.4
NOLC1	nucleolar and coiled-body phosphoprotein 1	-1.4
NOX3	NADPH oxidase 3	-1.4
NP	nucleoside phosphorylase	-2.7
NPM1	nucleophosmin (nucleolar phosphoprotein B23, numatrin)	-1.9
NPM3	nucleophosmin/nucleoplasmin, 3	-1.7
NR2C2AP	nuclear receptor 2C2-associated protein	-1.4
NR2F2	nuclear receptor subfamily 2, group F, member 2	-1.6
NRCAM	neuronal cell adhesion molecule	-1.8
NRM	nurim (nuclear envelope membrane protein)	-1.5
NRP1	neuropilin 1	-1.8
NSBP1	nucleosomal binding protein 1	-1.8
NSMAF	neutral sphingomyelinase (N-SMase) activation associated factor	-1.5
NTHL1	nth endonuclease III-like 1 (E. coli)	-1.6
NTRK1	neurotrophic tyrosine kinase, receptor, type 1	-1.7
NUDT1	nudix (nucleoside diphosphate linked moiety X)-type motif 1	-1.5
NUF2	NUF2, NDC80 kinetochore complex component, homolog (S. cerevisiae)	-1.8

NUP107	nucleoporin 107kDa	-1.4
NUP153	nucleoporin 153kDa	-1.5
NUP155	nucleoporin 155kDa	-1.5
NUP205	nucleoporin 205kDa	-1.5
NUP37	nucleoporin 37kDa	-1.7
NUP43	nucleoporin 43kDa	-1.7
NUP85	nucleoporin 85kDa	-1.5
NUP88	nucleoporin 88kDa	-1.5
NUSAP1	nucleolar and spindle associated protein 1	-1.6
OAF	OAF homolog (Drosophila)	-1.8
OAS3	2'-5'-oligoadenylate synthetase 3, 100kDa	-1.5
ODC1	ornithine decarboxylase 1	-1.4
OIP5	Opa interacting protein 5	-1.7
OLFM1	olfactomedin 1	-3.4
OPRM1	opioid receptor, mu 1	-1.5
OPRS1	opioid receptor, sigma 1	-1.6
ORAI1	ORAI calcium release-activated calcium modulator 1	-1.6
ORC6L	origin recognition complex, subunit 6 like (yeast)	-1.5
P2RY11	purinergic receptor P2Y, G-protein coupled, 11	-1.5
PA2G4	proliferation-associated 2G4, 38kDa	-1.6
PAICS	phosphoribosylaminoimidazole carboxylase, phosphoribosylaminoimidazole succinocarboxamide synthetase	-1.4
PAK1IP1	PAK1 interacting protein 1	-1.5
PAP2D	phosphatidic acid phosphatase type 2	-1.8
PAPD5	PAP associated domain containing 5	-1.5
PARVA	parvin, alpha	-1.5
PAXIP1	PAX interacting (with transcription-activation domain) protein 1	-2.0
PBK	PDZ binding kinase	-1.8
PC	pyruvate carboxylase	-1.5
PCDH9	protocadherin 9	-1.9
PCNA	proliferating cell nuclear antigen	-1.5
PCOLCE	procollagen C-endopeptidase enhancer	-1.7
PCOLCE2	procollagen C-endopeptidase enhancer 2	-1.9
PDCD2	programmed cell death 2	-1.6
PDE2A	phosphodiesterase 2A, cGMP-stimulated	-1.9
PDE4D	phosphodiesterase 4D, cAMP-specific (phosphodiesterase E3 dunce homolog, Drosophila)	-1.4
PDE9A	phosphodiesterase 9A	-1.5
PDGFRB	platelet-derived growth factor receptor, beta polypeptide	-1.5
PEG10	paternally expressed 10	-1.6
PER2	period homolog 2 (Drosophila)	-1.4
PES1	pescadillo homolog 1, containing BRCT domain (zebrafish)	-1.5
PEX3	peroxisomal biogenesis factor 3	-1.4
PFAS	phosphoribosylformylglycinamidine synthase (FGAR amidotransferase)	-1.6
PGM2	phosphoglucomutase 2	-1.6
PHB	prohibitin	-1.5
PHF17	PHD finger protein 17	-1.5
PHF5A	PHD finger protein 5A	-1.5
PHIP	pleckstrin homology domain interacting protein	-1.5
PIF1	PIF1 5'-to-3' DNA helicase homolog (S. cerevisiae)	-1.4
PINX1	PIN2-interacting protein 1	-1.5
PLK1	polo-like kinase 1 (Drosophila)	-1.6
PLK4	polo-like kinase 4 (Drosophila)	-1.5

PLXND1	plexin D1	-1.9
PMM2	phosphomannomutase 2	-1.5
PMP22	peripheral myelin protein 22	-1.5
PMPCA	peptidase (mitochondrial processing) alpha	-1.5
PNPT1	polyribonucleotide nucleotidyltransferase 1	-1.5
POLA1	polymerase (DNA directed), alpha 1	-1.6
POLA2	polymerase (DNA directed), alpha 2 (70kD subunit)	-1.6
POLD2	polymerase (DNA directed), delta 2, regulatory subunit 50kDa	-1.5
POLD3	polymerase (DNA-directed), delta 3, accessory subunit	-1.5
POLE2	polymerase (DNA directed), epsilon 2 (p59 subunit)	-1.8
POLE3	polymerase (DNA directed), epsilon 3 (p17 subunit)	-1.8
POLQ	polymerase (DNA directed), theta	-1.6
POLR2C	polymerase (RNA) II (DNA directed) polypeptide C, 33kDa	-1.5
POLR2H	polymerase (RNA) II (DNA directed) polypeptide H	-1.5
POLR3C	polymerase (RNA) III (DNA directed) polypeptide C (62kD)	-1.4
POLR3G	polymerase (RNA) III (DNA directed) polypeptide G (32kD)	-1.6
POLR3K	polymerase (RNA) III (DNA directed) polypeptide K, 12.3 kDa	-1.5
POLRMT	polymerase (RNA) mitochondrial (DNA directed)	-1.4
POP5	processing of precursor 5, ribonuclease P/MRP subunit (S. cerevisiae)	-1.4
POP7	processing of precursor 7, ribonuclease P/MRP subunit (S. cerevisiae)	-1.5
PPARGC1B	peroxisome proliferator-activated receptor gamma, coactivator 1 beta	-1.5
PPFIBP1	PTPRF interacting protein, binding protein 1 (liprin beta 1)	-1.5
PPIF	peptidylprolyl isomerase F (cyclophilin F)	-1.7
PPIH	peptidylprolyl isomerase H (cyclophilin H)	-1.6
PPIL1	peptidylprolyl isomerase (cyclophilin)-like 1	-1.6
PPIL5	peptidylprolyl isomerase (cyclophilin)-like 5	-1.6
PPP1CA	protein phosphatase 1, catalytic subunit, alpha isoform	-1.4
PPP2R1B	protein phosphatase 2 (formerly 2A), regulatory subunit A, beta isoform	-1.6
PPRC1	peroxisome proliferator-activated receptor gamma, coactivator-related 1	-1.6
PRC1	protein regulator of cytokinesis 1	-1.5
PRELID1	PRELI domain containing 1	-1.5
PRICKLE4	prickle homolog 4 (Drosophila)	-1.5
PRIM1	primase, DNA, polypeptide 1 (49kDa)	-1.4
PRIM2	primase, DNA, polypeptide 2 (58kDa)	-1.5
PRKCA	protein kinase C, alpha	-2.3
PRKD3	protein kinase D3	-1.5
PRMT3	protein arginine methyltransferase 3	-1.5
PRPF3	PRP3 pre-mRNA processing factor 3 homolog (S. cerevisiae)	-1.5
PRPF4	PRP4 pre-mRNA processing factor 4 homolog (yeast)	-1.4
PRPH	peripherin	-2.0
PSAT1	phosphoserine aminotransferase 1	-1.6
PSD3	pleckstrin and Sec7 domain containing 3	-1.5
PSMC3IP	PSMC3 interacting protein	-1.5
PSMG1	proteasome (prosome, macropain) assembly chaperone 1	-1.7
PSMG3	proteasome (prosome, macropain) assembly chaperone 3	-1.4
PSMG4	proteasome (prosome, macropain) assembly chaperone 4	-1.6
PSRC1	proline/serine-rich coiled-coil 1	-1.7
PTBP1	polypyrimidine tract binding protein 1	-1.4
PTDSS1	phosphatidylserine synthase 1	-1.6

PTGER3	prostaglandin E receptor 3 (subtype EP3)	-1.5
PTGES2	prostaglandin E synthase 2	-1.4
PTN	pleiotrophin (heparin binding growth factor 8, neurite growth-promoting factor 1)	-1.8
PTPLA	protein tyrosine phosphatase-like (proline instead of catalytic arginine), member A	-1.4
PTPLB	protein tyrosine phosphatase-like (proline instead of catalytic arginine), member b	-1.4
PTPN13	protein tyrosine phosphatase, non-receptor type 13 (APO-1/CD95 (Fas)-associated phosphatase)	-1.5
PTPRK	protein tyrosine phosphatase, receptor type, K	-1.6
PTPRU	protein tyrosine phosphatase, receptor type, U	-1.7
PTTG1	pituitary tumor-transforming 1	-1.5
PUNC	putative neuronal cell adhesion molecule	-1.6
PUS1	pseudouridylate synthase 1	-1.7
PVRL1	poliovirus receptor-related 1 (herpesvirus entry mediator C)	-1.6
PWP2	PWP2 periodic tryptophan protein homolog (yeast)	-1.4
PXMP2	peroxisomal membrane protein 2, 22kDa	-1.4
QKI	quaking homolog, KH domain RNA binding (mouse)	-1.5
RAB27A	RAB27A, member RAS oncogene family	-1.7
RABGGTB	Rab geranylgeranyltransferase, beta subunit	-1.5
RAD18	RAD18 homolog (S. cerevisiae)	-1.4
RAD51	RAD51 homolog (RecA homolog, E. coli) (S. cerevisiae)	-1.5
RAD51AP1	RAD51 associated protein 1	-1.6
RAD54L	RAD54-like (S. cerevisiae)	-1.4
RANBP1	RAN binding protein 1	-1.6
RANBP5	RAN binding protein 5	-1.5
RASA3	RAS p21 protein activator 3	-1.5
RASEF	RAS and EF-hand domain containing	-2.2
RASL11B	RAS-like, family 11, member B	-1.4
RBBP8	retinoblastoma binding protein 8	-1.5
RBL1	retinoblastoma-like 1 (p107)	-1.6
RBM14	RNA binding motif protein 14	-1.4
RCC1	regulator of chromosome condensation 1	-1.6
RCOR1	REST corepressor 1	-1.5
RDX	radixin	-2.0
RELN	reelin	-3.7
RERG	RAS-like, estrogen-regulated, growth inhibitor	-2.1
REXO4	REX4, RNA exonuclease 4 homolog (S. cerevisiae)	-1.5
RFC2	replication factor C (activator 1) 2, 40kDa	-1.5
RFC3	replication factor C (activator 1) 3, 38kDa	-1.5
RFC4	replication factor C (activator 1) 4, 37kDa	-1.5
RFC5	replication factor C (activator 1) 5, 36.5kDa	-1.5
RFXAP	regulatory factor X-associated protein	-1.5
RGS10	regulator of G-protein signaling 10	-1.5
RGS19	regulator of G-protein signaling 19	-1.8
RHOB	ras homolog gene family, member B	-1.4
RHOU	ras homolog gene family, member U	-1.6
RIMS2	regulating synaptic membrane exocytosis 2	-2.2
RIN2	Ras and Rab interactor 2	-1.5
RIOK1	RIO kinase 1 (yeast)	-1.6
RMI1	RMI1, RecQ mediated genome instability 1, homolog (S. cerevisiae)	-1.5
RNASEH2A	ribonuclease H2, subunit A	-1.5

RNF138	ring finger protein 138	-1.5
RPA1	replication protein A1, 70kDa	-1.5
RPA3	replication protein A3, 14kDa	-1.5
RPL39L	ribosomal protein L39-like	-1.7
RPP25	ribonuclease P/MRP 25kDa subunit	-2.4
RPS19BP1	ribosomal protein S19 binding protein 1	-1.4
RPS24	ribosomal protein S24	-1.7
RRM1	ribonucleotide reductase M1	-1.6
RRM2	ribonucleotide reductase M2 polypeptide	-1.6
RRP1	ribosomal RNA processing 1 homolog (S. cerevisiae)	-1.4
RRP1B	ribosomal RNA processing 1 homolog B (S. cerevisiae)	-1.5
RRP9	ribosomal RNA processing 9, small subunit (SSU) processome component, homolog (yeast)	-1.6
RRS1	RRS1 ribosome biogenesis regulator homolog (S. cerevisiae)	-1.5
RUVBL1	RuvB-like 1 (E. coli)	-1.7
RWDD1	RWD domain containing 1	-1.5
RXRA	retinoid X receptor, alpha	-1.5
S100A4	S100 calcium binding protein A4	-2.0
SAC3D1	SAC3 domain containing 1	-1.5
SACM1L	SAC1 suppressor of actin mutations 1-like (yeast)	-1.5
SAP30	Sin3A-associated protein, 30kDa	-1.4
SASS6	spindle assembly 6 homolog (C. elegans)	-1.4
SC65	synaptonemal complex protein SC65	-1.5
SCARB1	scavenger receptor class B, member 1	-1.8
SCLY	selenocysteine lyase	-1.9
SCYE1	small inducible cytokine subfamily E, member 1 (endothelial monocyte-activating)	-1.4
SDC1	syndecan 1	-1.7
SDHD	succinate dehydrogenase complex, subunit D, integral membrane protein	-1.5
SEMA6A	sema domain, transmembrane domain (TM), and cytoplasmic domain, (semaphorin) 6A	-2.0
SEP15	15 kDa selenoprotein	-1.4
SEPT10	septin 10	-1.7
SERBP1	SERPINE1 mRNA binding protein 1	-1.4
SERPINF1	serpin peptidase inhibitor, clade F (alpha-2 antiplasmin, pigment epithelium derived factor), member 1	-1.5
SERTAD4	SERTA domain containing 4	-1.6
SF3A1	splicing factor 3a, subunit 1, 120kDa	-1.4
SF3A3	splicing factor 3a, subunit 3, 60kDa	-1.5
SF3B3	splicing factor 3b, subunit 3, 130kDa	-1.4
SFRS1	splicing factor, arginine/serine-rich 1 (splicing factor 2, alternate splicing factor)	-1.5
SFRS2	splicing factor, arginine/serine-rich 2	-1.4
SFXN2	sideroflexin 2	-1.5
SGOL2	shugoshin-like 2 (S. pombe)	-1.7
SHCBP1	SHC SH2-domain binding protein 1	-2.0
SHF	Src homology 2 domain containing F	-1.6
SHOX2	short stature homeobox 2	-2.6
SIVA1	SIVA1, apoptosis-inducing factor	-1.6
SIX3	SIX homeobox 3	-1.6
SLC10A4	solute carrier family 10 (sodium/bile acid cotransporter family), member 4	-1.9
SLC12A7	solute carrier family 12 (potassium/chloride transporters), member	-1.6

	7	
SLC12A8	solute carrier family 12 (potassium/chloride transporters), member 8	-1.6
SLC16A1	solute carrier family 16, member 1 (monocarboxylic acid transporter 1)	-1.4
SLC16A7	solute carrier family 16, member 7 (monocarboxylic acid transporter 2)	-1.5
SLC18A1	solute carrier family 18 (vesicular monoamine), member 1	-1.4
SLC1A5	solute carrier family 1 (neutral amino acid transporter), member 5	-1.5
SLC25A33	solute carrier family 25, member 33	-1.6
SLC25A37	solute carrier family 25, member 37	-1.4
SLC25A39	solute carrier family 25, member 39	-1.6
SLC29A1	solute carrier family 29 (nucleoside transporters), member 1	-1.5
SLC2A4RG	SLC2A4 regulator	-1.4
SLC30A5	solute carrier family 30 (zinc transporter), member 5	-1.5
SLC31A1	solute carrier family 31 (copper transporters), member 1	-1.6
SLC35A3	solute carrier family 35 (UDP-N-acetylglucosamine (UDP-GlcNAc) transporter), member A3	-1.4
SLC35F2	solute carrier family 35, member F2	-1.8
SLC39A14	solute carrier family 39 (zinc transporter), member 14	-1.6
SLC39A8	solute carrier family 39 (zinc transporter), member 8	-1.5
SLC5A6	solute carrier family 5 (sodium-dependent vitamin transporter), member 6	-1.6
SLCO4A1	solute carrier organic anion transporter family, member 4A1	-2.0
SLITRK5	SLIT and NTRK-like family, member 5	-1.5
SMAD6	SMAD family member 6	-1.7
SMARCD2	SWI/SNF related, matrix associated, actin dependent regulator of chromatin, subfamily d, member 2	-1.6
SMC2	structural maintenance of chromosomes 2	-1.7
SMC4	structural maintenance of chromosomes 4	-1.5
SNF1LK2	SNF1-like kinase 2	-1.5
SNHG5	small nucleolar RNA host gene (non-protein coding) 5	-1.5
SNRPA	small nuclear ribonucleoprotein polypeptide A	-1.5
SNRPB	small nuclear ribonucleoprotein polypeptides B and B1	-1.5
SNRPD1	small nuclear ribonucleoprotein D1 polypeptide 16kDa	-1.4
SNRPD3	small nuclear ribonucleoprotein D3 polypeptide 18kDa	-1.4
SNX3	sorting nexin 3	-1.4
SNX5	sorting nexin 5	-1.5
SOAT1	sterol O-acyltransferase (acyl-Coenzyme A: cholesterol acyltransferase) 1	-1.4
SOLH	small optic lobes homolog (Drosophila)	-1.5
SORBS2	sorbin and SH3 domain containing 2	-2.6
SOX2	SRY (sex determining region Y)-box 2	-1.5
SOX7	SRY (sex determining region Y)-box 7	-1.5
SPAG5	sperm associated antigen 5	-1.7
SPC24	SPC24, NDC80 kinetochore complex component, homolog (S. cerevisiae)	-1.5
SPC25	SPC25, NDC80 kinetochore complex component, homolog (S. cerevisiae)	-1.7
SPOCK3	sparc/osteonectin, cwcv and kazal-like domains proteoglycan (testican) 3	-2.6
SPTBN1	spectrin, beta, non-erythrocytic 1	-1.5
SRFBP1	serum response factor binding protein 1	-1.4
SRGAP2	SLIT-ROBO Rho GTPase activating protein 2	-1.5

SRM	spermidine synthase	-1.4
SS18L2	synovial sarcoma translocation gene on chromosome 18-like 2	-1.4
SSB	Sjogren syndrome antigen B (autoantigen La)	-1.5
SSFA2	sperm specific antigen 2	-1.6
SSRP1	structure specific recognition protein 1	-1.5
SSU72	SSU72 RNA polymerase II CTD phosphatase homolog (S. cerevisiae)	-1.5
ST3GAL4	ST3 beta-galactoside alpha-2,3-sialyltransferase 4	-1.4
STC2	stanniocalcin 2	-1.6
STEAP3	STEAP family member 3	-1.7
STIL	SCL/TAL1 interrupting locus	-1.6
STOM	stomatin	-1.5
STOML2	stomatin (EPB72)-like 2	-1.5
SUCLG2	succinate-CoA ligase, GDP-forming, beta subunit	-1.5
SULF2	sulfatase 2	-3.4
SUV39H1	suppressor of variegation 3-9 homolog 1 (Drosophila)	-1.5
SUV39H2	suppressor of variegation 3-9 homolog 2 (Drosophila)	-1.5
SUZ12	suppressor of zeste 12 homolog (Drosophila)	-1.5
SVIL	supervillin	-1.8
SYCP3	synaptonemal complex protein 3	-1.4
SYNCRIP	synaptotagmin binding, cytoplasmic RNA interacting protein	-1.6
SYPL1	synaptophysin-like 1	-1.4
TACC3	transforming, acidic coiled-coil containing protein 3	-1.6
TAF4B	TAF4b RNA polymerase II, TATA box binding protein (TBP)-associated factor, 105kDa	-1.6
TAF5	TAF5 RNA polymerase II, TATA box binding protein (TBP)-associated factor, 100kDa	-1.5
TARBP2	TAR (HIV-1) RNA binding protein 2	-1.5
TATDN2	TatD DNase domain containing 2	-1.4
TBC1D2B	TBC1 domain family, member 2B	-1.6
TBC1D4	TBC1 domain family, member 4	-1.6
TBRG4	transforming growth factor beta regulator 4	-1.5
TCF12	transcription factor 12 (HTF4, helix-loop-helix transcription factors 4)	-1.5
TCF19	transcription factor 19 (SC1)	-1.6
TCF7L2	transcription factor 7-like 2 (T-cell specific, HMG-box)	-1.8
TCHP	trichoplein, keratin filament binding	-1.5
TFAM	transcription factor A, mitochondrial	-1.6
TFB2M	transcription factor B2, mitochondrial	-1.5
TFEB	transcription factor EB	-1.5
TGS1	trimethylguanosine synthase homolog (S. cerevisiae)	-1.5
THAP11	THAP domain containing 11	-1.4
THOC4	THO complex 4	-1.4
THOC7	THO complex 7 homolog (Drosophila)	-1.5
THOP1	thimet oligopeptidase 1	-1.6
THRAP3	thyroid hormone receptor associated protein 3	-1.5
TIAM1	T-cell lymphoma invasion and metastasis 1	-1.5
TIFA	TRAF-interacting protein with forkhead-associated domain	-1.5
TIMELESS	timeless homolog (Drosophila)	-1.6
TIMM10	translocase of inner mitochondrial membrane 10 homolog (yeast)	-1.4
TIMM13	translocase of inner mitochondrial membrane 13 homolog (yeast)	-1.9
TIMM8A	translocase of inner mitochondrial membrane 8 homolog A (yeast)	-1.4
TIPIN	TIMELESS interacting protein	-1.8
TJAP1	tight junction associated protein 1 (peripheral)	-1.4

TLE1	transducin-like enhancer of split 1 (E(sp1) homolog, Drosophila)	-2.9
TLE2	transducin-like enhancer of split 2 (E(sp1) homolog, Drosophila)	-1.5
TMEM106C	transmembrane protein 106C	-1.4
TMEM115	transmembrane protein 115	-1.5
TMEM48	transmembrane protein 48	-1.6
TMEM97	transmembrane protein 97	-1.5
TMTC1	transmembrane and tetratricopeptide repeat containing 1	-1.9
TNFAIP2	tumor necrosis factor, alpha-induced protein 2	-1.5
TOB1	transducer of ERBB2, 1	-1.6
TOM1L1	target of myb1 (chicken)-like 1	-1.6
TOMM22	translocase of outer mitochondrial membrane 22 homolog (yeast)	-1.4
TOMM40	translocase of outer mitochondrial membrane 40 homolog (yeast)	-1.5
TOP1MT	topoisomerase (DNA) I, mitochondrial	-1.8
TOP2A	topoisomerase (DNA) II alpha 170kDa	-1.6
TOPBP1	topoisomerase (DNA) II binding protein 1	-1.5
TP53	tumor protein p53	-1.5
TPCN1	two pore segment channel 1	-1.5
TPD52	tumor protein D52	-1.5
TPST2	tyrosylprotein sulfotransferase 2	-2.4
TPX2	TPX2, microtubule-associated, homolog (Xenopus laevis)	-1.6
TRA	T cell receptor alpha locus	-1.7
TRAF5	TNF receptor-associated factor 5	-1.8
TRIM14	tripartite motif-containing 14	-1.5
TRIM24	tripartite motif-containing 24	-1.5
TRIM25	tripartite motif-containing 25	-1.5
TRIM59	tripartite motif-containing 59	-1.4
TRIM9	tripartite motif-containing 9	-2.0
TRIP13	thyroid hormone receptor interactor 13	-1.7
TROAP	trophinin associated protein (tastin)	-1.6
TRPA1	transient receptor potential cation channel, subfamily A, member 1	-3.2
TRPM7	transient receptor potential cation channel, subfamily M, member 7	-1.5
TSPO	translocator protein (18kDa)	-1.9
TSR1	TSR1, 20S rRNA accumulation, homolog (S. cerevisiae)	-1.6
TTF2	transcription termination factor, RNA polymerase II	-1.6
TTK	TTK protein kinase	-1.8
TUBD1	tubulin, delta 1	-1.4
TUBGCP3	tubulin, gamma complex associated protein 3	-1.5
TUSC4	tumor suppressor candidate 4	-1.5
TXN2	thioredoxin 2	-1.5
TXNDC1	thioredoxin domain containing 1	-1.8
TYMS	thymidylate synthetase	-1.7
UBAP2L	ubiquitin associated protein 2-like	-1.5
UBE2C	ubiquitin-conjugating enzyme E2C	-1.4
UBE2CBP	ubiquitin-conjugating enzyme E2C binding protein	-1.6
UBE2G2	ubiquitin-conjugating enzyme E2G 2 (UBC7 homolog, yeast)	-1.5
UCHL5	ubiquitin carboxyl-terminal hydrolase L5	-1.5
UCHL5IP	UCHL5 interacting protein	-2.0
UMPS	uridine monophosphate synthetase	-1.6
UNG	uracil-DNA glycosylase	-1.9
USP1	ubiquitin specific peptidase 1	-1.6
UTRN	utrophin	-2.0
VRK1	vaccinia related kinase 1	-1.5
WASF3	WAS protein family, member 3	-1.5

WDR4	WD repeat domain 4	-1.6
WDR5	WD repeat domain 5	-1.4
WDR61	WD repeat domain 61	-1.4
WDR77	WD repeat domain 77	-1.5
WDSOF1	WD repeats and SOF1 domain containing	-1.5
WFS1	Wolfram syndrome 1 (wolframin)	-1.4
WHSC1	Wolf-Hirschhorn syndrome candidate 1	-1.4
WIPF1	WAS/WASL interacting protein family, member 1	-1.8
WT1	Wilms tumor 1	-2.0
XPO1	exportin 1 (CRM1 homolog, yeast)	-1.4
XTP3TPA	XTP3-transactivated protein A	-1.7
ZAK	sterile alpha motif and leucine zipper containing kinase AZK	-1.4
ZBTB24	zinc finger and BTB domain containing 24	-1.5
ZFPM2	zinc finger protein, multitype 2	-3.3
ZFYVE16	zinc finger, FYVE domain containing 16	-1.6
ZMYND19	zinc finger, MYND-type containing 19	-1.4
ZNF367	zinc finger protein 367	-1.9
ZNF423	zinc finger protein 423	-1.5
ZNF503	zinc finger protein 503	-1.6
ZNF536	zinc finger protein 536	-1.6
ZNF804A	zinc finger protein 804A	-1.4
ZRF1	zuotin related factor 1	-1.8
ZWINT	ZW10 interactor	-1.5

Supplemental Table S2.2. Quantitative RT-PCR Validation of Microarray Results.

Superarray PI3K-Akt qRT-PCR Array

-Data normalized to average Ct for 5 control housekeeping genes; genes with maximal Ct = 35 in either trial not analyzed (italics)
-Averages calculated from two individual experiments, fold-change calculated from log2 transformed data
-Statistical analysis: two-tailed Student's t-test assuming unequal variance, significant upregulated genes in bold
-Microarray results using both Genomatix and Bioconductor software are shown for comparison; "-", not significant)

pRT-PCR array validation results				Microarray results (fold-change)	
Gene	**Fold change**	***p*-value**		**Genomatix**	**Bioconductor**
AKT1	3.3	0.232		-	-
AKT2	1.4	0.488		-	-
AKT3	**2.3**	**0.007**		-	-
APC	**7.1**	**0.006**		1.6	1.9
BAD	1.9	0.091		-	-
CASP9	3.7	0.087		-	-
CCND1	3.7	0.114		-	-
CD14	**27.9**	**0.000**		1.9	4.6
CDC42	2.6	0.113		1.5	2.1
CHUK	1.0	0.873		-	-
CSNK2A1	1.8	0.070		-	-
CTNNB1	**1.8**	**0.017**		-	-
EIF2AK2	1.5	0.430		-	-
EIF4B	1.7	0.165		-	-
EIF4E	1.3	0.513		1.7	2.0
EIF4EBP1	1.2	0.549		-1.4	-
EIF4G1	2.9	0.088		-	-
ELK1	1.5	0.143		-	-
FKBP1A	5.1	0.095		-	-
FOXO1	**86.3**	**0.011**		1.8	8.3
FOXO3	**4.6**	**0.004**		2.0	2.0
FRAP1	**1.3**	**0.020**		-	-
GRB10	*NA*	*NA*		-	4.1
GRB2	2.5	0.076		-	-
GSK3B	**3.0**	**0.036**		-	-
HRAS	1.6	0.505		-	-
HSPB1	1.6	0.364		-	-
IGF1R	3.7	0.071		-	-
IRAK1	2.2	0.166		-1.5	-
IRS1	1.2	0.095		-	-
ITGB1	**2.6**	**0.001**		-	2.1
JUN	**1.7**	**0.037**		-	-
MAP2K1	2.4	0.085		-	-
MAPK1	1.9	0.072		-	-
MAPK14	1.9	0.474		-	-2.0
MAPK3	3.2	0.148		-	-

MAPK8	**4.0**	**0.021**		1.6	2.0
MTCP1	0.9	0.553		-	-
MYD88	2.6	0.111		-	-
PABPC1	1.2	0.300		-	-
PAK1	**3.9**	**0.011**		-	1.7
PDGFRA	*NA*	*NA*		-	-
PDK1	2.1	0.087		-	-
PDPK1	**2.0**	**0.019**		-	-
PIK3CA	**3.0**	**0.004**		-	-
PIK3CG	*NA*	*NA*		-	-
PIK3R1	**5.7**	**0.040**		2.3	2.6
PIK3R2	2.0	0.210		-	-
PRKCA	0.4	0.276		-	-2.6
PRKCZ	3.1	0.124		2.0	-
PTEN	1.0	1.000		-	-
PTK2	1.6	0.088		-	-
PTPN11	0.9	0.684		-	-
RAC1	1.6	0.408		-	-
RAF1	1.4	0.689		-	-
RASA1	**4.5**	**0.003**		2.7	2.5
RBL2	1.2	0.198		-	-
RHEB	1.7	0.108		-	-
RHOA	0.9	0.572		-	-
RPS6KA1	0.8	0.776		-	-
RPS6KB1	1.1	0.804		-	-
SHC1	3.1	0.070		1.6	1.8
SOS1	1.1	0.423		-	-
SRF	2.1	0.150		-	-
TIRAP	1.1	0.860		-	-
TLR4	**40.3**	**0.019**		1.4	31.0
TOLLIP	1.4	0.255		-	-
TSC1	1.4	0.304		-	-
TSC2	**2.2**	**0.017**		-	-
WASL	1.5	0.353		-	-
YWHAH	2.2	0.050		-	-

Supplemental Table S2.3. Effects of Kinase Inhibitors on Poly(I-C)-Stimulated BE(2)-C/m-ISRE Cells.

-Values represent averages from two replicates - ranges are given due to limited titrations

-IC50 = concentrations producing 50% maximal inhibition

-CC50 = concentrations producing 50% cytotoxicity

-Active inhibitors, defined as IC50 values for either extracellular or transfected poly(I-C) <20, CC50 values >20, and no overlap in ranges, are indicated in bold italic type

Kinase inhibitor name	Target(s)	Extracellular poly(I-C) IC50	Transfected-poly(I-C) IC50	CC50
BML-257	***Akt***	***0.8-4***	***4-20***	***>100***
Triciribine	***Akt***	***0.8-4***	***0.8***	***100***
Perifosine	Akt, JNK, MAPK	100	20	100
Imatinib	BCL/ABL	0.8	0.8	20
Terreic acid	***BTK***	***4***	***100***	***>100***
LFM-A13	BTK	>100	100	>100
KN-93	CaMK II	<0.8	<0.8	<0.8
KN-62	CaMK II	100	100	>100
Olomoucine	CDK	20-100	4	0.8
N9-Isopropyl-olomoucine	CDK	>100	>100	100
Roscovitine	CDK	20	20-100	>100
Flavopiridol	***CDK 1,2,4***	***0.8-4***	***0.8-4***	***20-100***
BML-259	CDK5/p25	100	>100	>100
DRB (5,6-Dichloro-1-b-D-ribofuranosylbenzimidazole)	CK II	100	>100	>100
Apigenin	***CK-II***	***100***	***4-20***	***100***
GW 5074	cRAF	20-100	20-100	20
ZM 336372	cRAF	>100	100	>100
PI-103	***DNA-PK, PI3K p110α, mTOR***	***<0.8***	***<0.8***	***>100***
Tyrphostin 25	***EGFRK***	***20-100***	***4***	***>100***
Tyrphostin 51	***EGFRK***	***20-100***	***0.8-4***	***>100***
BML-265 (Erlotinib analog)	***EGFRK***	***4-20***	***0.8***	***100***
Tyrphostin 47	EGFRK	20-100	0.8-4	0.8
Lavendustin A	EGFRK	100	>100	>100
Tyrphostin 23	EGFRK	100	>100	>100
Tyrphostin AG 1478	EGFRK	>100	100	>100
RG-14620	EGFRK	20-100	100	>100
Erbstatin analog	EGFRK	20-100	20-100	20-100
Tyrphostin 46	EGFRK, PDGFRK	20-100	20	20-100
HDBA (2-Hydroxy-5-(2,5-dihydroxybenzylamino)benzoic acid)	EGFRK, CaMK II	4	<0.8	20
AG-494	EGFRK, PDGFRK	4-20	0.8-4	20
5-Iodotubercidin	***ERK2, Adenosine kinase, CK1, CK2,***	***4***	***20***	***100***
SU 4312	FLK1	100	4	0.8

SU1498	FLK1	20-100	100	>100
FLT3 Inhibitor	FLT3	>100	20-100	>100
PK412	***FLT3, SRC, ABL***	***0.8***	***<0.8***	***>100***
GSK3 Inhibitor XIII	***GSK3***	***0.8-4***	***0.8-4***	***100***
GSK3 Inhibitor VI	GSK3	0.8-4	0.8-4	4
SB-415286	GSK3	100	100	100
SB-216763	GSK3-α/β	100	20	100
Purvalanol A	***GSK3-α/β, CDK's***	***4-20***	***4-20***	***100***
Kenpaullone	GSK3β	4-20	0.8-4	20
Indirubin-3'-monoxime	GSK3β	4-20	0.8-4	20
Indirubin-3'-monoxime	GSK3β	100	4	20
Indirubin	GSK3β, CDK5	0.8	0.8	20
AG-825	HER1-2	100	100	>100
AG1024 IGF-IR	IGF-IR	100	20-100	>100
BAY 11-7082	IKK pathway	100	100	>100
SC-514	IKK2	100	20-100	>100
AG-126	IRAK	100	100	>100
HNMPA (Hydroxy-2-naphthalenylmethylphosphonic acid)	IRK	4-20	4-20	20-100
AG-490	JAK-2	20-100	20-100	100
ZM 449829	***JAK-3***	***100***	***4-20***	***100***
SP 600125	JNK	>100	100	>100
PD-98059	MEK	>100	>100	>100
U-0126	MEK	100	20-100	>100
ML-7	MLCK	20-100	20-100	>100
ML-9	MLCK	20-100	20-100	>100
Rapamycin	***mTOR***	***20***	***<0.8***	***20-100***
Daidzein	Negative control for genistein	20-100	20-100	100
iso-Olomoucine	Negative control for olomoucine	100	100	100
Tyrphostin 1	Negative control for TK inhibitors	20-100	4-20	20
AG-879	NGFRK	20-100	20-100	100
SB-203580	p38 MAPK	>100	>100	>100
SB-202190	p38 MAPK	20-100	20-100	>100
Damnacanthal	p56 LCK	4-20	0.8-4	20
2-Aminopurine	***p58 PITSLRE-b1***	***20-100***	***4-20***	***100***
Staurosporine	Pan-specific	0.8	<0.8	4
AG-370	PDGFRK	100	>100	>100
AG-1296	PDGFRK	100	100	>100
Tyrphostin 9	PDGFRK	4-20	0.8-4	4-20
LY 294002	***PI3K***	***4-20***	***4-20***	***>100***
Quercetin dihydrate	***PI3K***	***20-100***	***4***	***100***
Wortmannin	PI3K	4-20	4-20	20
PI3Kα Inhibitor 2	***PI3K p110α***	***0.8-4***	***0.8-4***	***100***

TGX-221	PI3K p110β	20-100	20-100	100
AS-252424	PI3K p110γ	20-100	20-100	100
AS-605240	PI3K p110γ	100	20-100	100
PIM1 Inhibitor II	PIMI	100	100	>100
Quercetagetin	PIMI	100	100	>100
H-89	PKA	100	100	>100
HA-1077	PKA, PKG	100	20-100	0.8
HA-1004	PKA, PKG	20-100	20-100	100
H-8	***PKA, PKG***	***4***	***4-20***	***20-100***
H-7	PKA, PKG, MLCK, and PKC.	20	4-20	20
H-9	PKA, PKG, MLCK, and PKC.	20-100	20-100	100
Hypericin	PKC	<0.8	<0.8	20
GF 109203X	PKC	100	100	100
Ro 31-8220	PKC	20-100	20-100	>100
Sphingosine	PKC	100	20-100	>100
Palmitoyl-DL-carnitine Cl	***PKC***	***4***	***20-100***	***20-100***
HBDDE (2,2',3,3',4,4'-Hexahydroxy-1,1'-biphenyl-6,6'-dimethanol dimethyl ether)	***PKCα, PKCγ***	***4-20***	***4-20***	***100***
Rottlerin	***PKCδ***	***4-20***	***4***	***20-100***
Sunitinib	Receptor tyrosine kinases	<0.8	<0.8	4
Y-27632	ROCK	100	>100	>100
PP2	Src family	>100	>100	>100
PP1	Src family	4-20	4-20	20-100
Piceatannol	Syk	20-100	20-100	>100
Tyrphostin AG 1295	Tyrosine kinases	100	20-100	>100
Genistein	Tyrosine Kinases	20-100	20-100	>100
Tyrphostin AG 1288	***Tyrosine kinases (TK)***	***4***	***0.8***	***>100***

Chapter III

IRF3 Mediates an Interferon-Independent Cytoprotective Response Against Neurotropic Arboviruses in Neurons

Early cellular innate immune responses are often vital for effective pathogen control, and an effective neuronal innate immune response may be crucial to prevent the essentially irreversible loss of critical central nervous system neurons by neurotropic arboviruses. To test this hypothesis, we used targeted, genetic approaches and a variety of neuronal culture models to study the influence of neuronal PRR pathway signaling on neurotropic arbovirus pathogenesis mainly using western equine encephalitis virus (WEEV) as a model neurotropic arbovirus. We found that WEEV activates neuronal PRR pathways in a replication dependent manner that requires IRF3, and abrogation of IRF3 enhanced virus-mediated neuronal cytopathogenicity for distinct neurotropic arboviruses including WEEV. Interestingly, IRF3-dependent protection of neurons from neurotropic arbovirus mediated cytopathology was independent of autocrine/paracrine type-I IFN activity and was likely due to direct IRF3-mediated induction of cell-intrinsic factors with cytoprotective properties. Importantly WEEV, and other neurotropic arboviruses, were found to potently and specifically block induction of neuronal antiviral PRR pathways at early times post infection. The antiviral PRR pathway inhibitory capacity of WEEV was mapped to the capsid gene, which blocked antiviral PRR signaling downstream of IRF3

activation. In addition, we determined that a WEEV structural gene, likely capsid, inhibited IRF3 nuclear translocation and host gene expression providing a potential dual mechanism for capsid-mediated inhibition of neuronal antiviral PRR signaling. Altogether, these data indicated that neuronal PRR pathways may be important determinants in neurotropic arbovirus pathogenesis.

Introduction

Viruses within several families preferentially infect CNS neurons, especially the neurotropic arboviruses which include but are not limited to West Nile virus (*Flaviviridae*), St. Louis encephalitis virus (*Flaviviridae*), La Crosse virus (*Bunyaviridae*), and the equine encephalitic alphaviruses (*Togaviridae*). Neurotropic arboviruses are transmitted via insect vectors and are responsible for sporadic epidemics of viral encephalitis (29) in which the extent of virus-mediated destruction of CNS neurons is often an important determinant in the severity and clinical outcome after infection. Unfortunately, there are very few effective treatments or vaccines for these viral infections, which contributes to their classification as potential bioterrorism agents (54).

Early cellular innate immune responses are often vital for effective pathogen control (15-17, 19, 21, 28), and an effective neuronal innate immune response may be crucial to prevent the essentially irreversible loss of critical central nervous system neurons by neurotropic arboviruses. Innate immune responses are activated by pattern recognition receptors (PRRs) that bind ligands containing pathogen-associated molecular patterns, such as modified carbohydrate or nucleic acid structures (37, 47). Ligation of these receptors induces a signal transduction cascade resulting in the production of antiviral type-I IFNs, other proinflammatory cytokines, and cell-intrinsic factors important for the generation of an antiviral cellular microenvironment (47). In addition, PRR signaling is important for activating an appropriate adaptive immune response (1), which is required for the eventual clearance of most viral infections (9).

Thus, PRR-mediated innate immune pathway signaling serves a pivotal role in controlling viral infections and may protect neurons from neurotropic arbovirus mediated destruction.

There are three general steps in innate antiviral immune responses: activation, amplification, and effector production. Antiviral PRR signaling is initiated by a variety of receptors, including the transmembrane Toll-like receptor (TLR) proteins and the cytoplasmic retinoic acid inducible gene I (RIG-I)-like receptors (RLRs) RIG-I and melanoma differentiated-associated gene 5 (MDA5) (34). Due to differential expression, ligand specificity, and pathogen-mediated interference, PRRs respond to viral infections in both a pathogen and cell type-specific manner (34, 61). After PRR ligation, PRR signal transduction is mediated by several adaptor proteins, including MyD88, TIR-domain-containing adapter-inducing IFN-β (TRIF), and IFN-β promoter stimulator protein 1 (IPS-1) (also referred to as Cardif, MAVS, and VISA) (34, 61). These adaptor protein complexes mediate the downstream activation of kinases such as TANK-binding kinase 1 (TBK1), several IκB kinases, and PI3K, which subsequently activate the transcription factors NFκB and IFN regulatory factor 3 (IRF3) (5, 8, 10, 11). Activated NFκB and IRF3 upregulate the expression of many genes important for mounting a robust antiviral response, including type-I IFNs, which function in either a paracrine or autocrine manner to induce IFN-stimulated genes (ISGs) (52). There are several ISGs that act directly as antiviral effectors, but many are also components of antiviral PRR pathways, which provides a mechanism for positive feedback regulation and amplification (8).

Viral PRR pathways protect host cells and tissues against viral infections, yet many viruses including neurotropic arboviruses possess PRR pathway countermeasures (61). For instance, the NS2A and NS1 proteins of the neurotropic arbovirus West Nile virus (WNV) inhibit the activation of antiviral PRR pathways (18, 22, 38, 59) resulting in higher viral replication and enhanced virulence in a manner that may be both viral strain and cell type-dependent. In a similar fashion, the NSs protein of La Crosse virus (LACV) potently inhibits type-I IFN induction, and in its absence, mutant virus robustly induces type-I IFNs resulting in reduced virulence (7).

We and others have demonstrated that neurons possess active antiviral PRR pathways mediated by the receptors TLR3, RIG-I, and MDA5 which activate NFκB and require IRF3 for the induction of type-I interferons (11, 30, 35, 41, 42, 44, 49). However, relatively little is known about how neuronal PRR pathways influence neurotropic arbovirus pathogenesis, but important observations have been made. For instance, it is known that infection of neurons with several neurotropic arboviruses induces the expression of type-I interferons (15, 17, 20, 49, 51, 53) and West Nile virus replication is enhanced in cortical neurons isolated from IPS-$1^{-/-}$, TLR$3^{-/-}$, IRF$7^{-/}$, and IRF7/$3^{-/-}$ mice (15-17, 19, 57). Additionally, WNV is known to be recognized by both RIGI and MDA5 in non-neuronal cell types (19), and evidence exists for the recognition of old world alphaviruses, which are not naturally encephalitic, via RIGI or MDA5 depending on the cell type and virus (10, 48).

In this report, we used targeted, genetic approaches to study the influence of neuronal PRR pathway signaling on neurotropic arbovirus pathogenesis using western equine encephalitis virus (WEEV) as a model neurotropic arbovirus due to its natural neurotropism. We found that IRF3 mediates a cytoprotective response against WEEV that was likely due to IRF3-mediated induction of cell-intrinsic factors with cytoprotective properties and independent of autocrine/paracrine type-I IFN activity. Viral countermeasures to neuronal PRR pathways were also observed, where WEEV, and other neurotropic arboviruses, were found to potently and specifically block induction of neuronal antiviral PRR pathways at early times post infection. The antiviral PRR pathway inhibitory capacity of WEEV was mapped to the capsid gene, which inhibited neuronal antiviral PRR signaling in part by early inhibition of IRF3 nuclear translocation and late inhibition of host macromolecular synthesis. These data indicated that neuronal PRR pathways may be important determinants in neurotropic arbovirus pathogenesis and that neuronal PRR pathways and viral countermeasures to them may be exploited to develop more efficacious vaccines and anti-neurotropic arboviral treatments.

Materials and Methods

Plasmids and Cytokines

The dominant negative overexpression plasmids pDN-TLR3, pDN-TRIF(TIR), pDN-RIG-I(ΔN), and pDN-IRF3(ΔN), as well as the short-hairpin RNA overexpression plasmids pshRNA-MDA5, pGIPZ-shCD14, and pGIPZ-shPI3K110α are described elsewhere (44). The construction of the HA-tagged β-galactosidase in a pCMV-TnT (Promega, Madison, WI) backbone (pIVT-LacZ) has been previously described (55). The shRNA overexpression plasmid pGIPZ-shOASL was purchased from Open Biosystems (Huntsville, AL). The overexpression plasmids pUNO-IRF3, pUNO-saIRF3, pUNO-MDA5, pUNO-TLR3, and pUNO-saTRIF as well as the promoter-reporter constructs pISRE-SEAP and pNFκB-SEAP were purchased from InvivoGen (San Diego, CA). The WEEV and WNV gene expression constructs were generated by PCR-amplifying individual WEEV genes from the full length WEEV cDNA clone pWEE2000 (12) or the WNV cDNA non-structural protein clone pc-WNV (provided by Richard Kinney, CDC, Atlanta, GA) and inserting them into the expression vector pCMV-TnT. V5-tagged viral gene expression constructs were generated for the indicated genes by first subcloning viral gene PCR products into pMT/V5-HisA (31) prior to inserting them into pCMV-TnT. Recombinant human IFNα-A/D and poly(I-C) are described elsewhere (44). Murine IFNα/β □(NR-3082)□ human IFNα (NR-3078), and human IFNβ □(NR-3080) were obtained from the BEI repository (Manassas, VA). Cells pre-treated with type-I IFNs were washed twice with HBSS (Life Technologies) prior to viral infection unless otherwise noted.

Cell Culture

BE(2)-C and Vero cells were cultured as previously described (44). BHK21 and BHK21 cells stably overexpressing bacteriophage T7 RNA polymerase (BHK21-T7/C3) were cultured as for the Vero cells except cells were supplemented with non-essential amino acids (Life Technologies), and 10% fetal calf serum was used instead of bovine growth serum. To avoid potential confounding effects of cell differentiation on transfection efficiency, stable cell lines were generated prior to differentiation as previously described (44) using Lipofectamine 2000. Primary rat cortical neurons were isolated and cultured as previously described (44). Primary mouse cortical neurons were isolated from wild-type, IRF3$^{-/-}$ (15), MDA5$^{-/-}$ (27), and IFNAR$^{-/-}$ (19) C57BL/6 mice or IPS-I$^{-/-}$ (C57Bl/6 x 129Sv/Ev) (57) and wild-type litter mate control mice. Freshly dissected cortices were stored in Hibernate E, 2% B27, 0.5 mM L-Gln and shipped overnight on ice. Mouse cortical neurons were disassociated and cultured as described for rat cortical neurons except they were plated at a density of 5 x 10^5 cells per cm^2 on poly-D-lysine and laminin coated plates (15), washed once three hours after plating, and fed every 1-2 days until use at 10-12 days in culture at which point they were highly susceptible to glutamate excitotoxicity, a characteristic of differentiated cortical neurons.

Populations of human neurons were derived from the human embryonic stem cell line H7 (WiCell, University of Wisconsin Madison, Madison, WI) over the course of four weeks through the sequential development of embryoid bodies, neuroepithelial rosettes, and neuroprogenitor cell cultures based on

previously established techniques (39, 43, 62). Fully differentiated cultures were screened by immunuflourescence for the expression of neurofilament 200 and synaptophysin and analyzed by flow cytometry to assess culture purity. Our hESC-derived human neurons were routinely positive for the neuronal surface markers CD90 (94.52 $\pm$ 3.58), PSA-NCAM (97.76 $\pm$ 0.17), and NGFR (72.61 $\pm$ 2.40).

Cell viability was determined by an MTT assay (44) or a luminescent ATP assay (ATPlite, PerkinElmer, Waltham, MA) according to manufacturer instruction. Lipofection of BE(2)-C/m cells was accomplished using Lipofectamine 2000 (Invitrogen, Carlsbad, CA) according to manufacturer instructions except one-fourth the amount of total DNA by weight was used to transfect 60-75% confluent monolayers. For cotransfections involving 3 or more plasmids, 25% of the total DNA weight was the transfection control pIVT-LacZ, and the remaining 75% of total DNA weight was divided equally among the remaining plasmids. Transfection complexes were removed after 6-20 hours of incubation. Transfection of BHK cells was described previously (45).

Viruses

The Cba 87 WEEV strain generated from the cDNA WEEV clone, pWE2000, was used for all WEEV infections as previously described (12), except reconstitution of infectious virus was accomplished by transfecting BSR-T7/5 cells (45) and harvesting tissue culture supernatants 36 hours post transfection at which point most of the cells had rounded up and detached. Infectious tissue culture

supernatants were cleared by centrifuging at 1500 x g for 10 minutes and contained 1-10 x 10^6 pfu/ml when quantitated by plaque assay on Vero cell monolayers. Stocks were further expanded by passing them once in Vero cells for 48 hours at a low multiplicity of infection (MOI). This typically yielded a final stock of 1-10 x 10^6 pfu/ml that was stored at -80^o C in single use aliquots and used for all infections unless otherwise noted.

Generation of sucrose gradient purified WEEV was accomplished using infectious WEEV 2000 tissue culture supernatants generated previously (12). Supernatants containing infectious virions were precipitated overnight at 4^o C with stirring in sterile 7% polyethylene glycol (Fisher, Fair Lawn, NJ) and 2.3 % sodium chloride (Fisher, Fair Lawn, NJ). Virions were recovered by centrifuging at 3500 x g for 20 minutes, resuspended in HBSS (Life Technologies), loaded onto 15-45% linear sucrose gradients, and centrifuged at 35,000 x g for 60 minutes. Virion bands were readily visible at approximate 15-30% and 30-45% sucrose levels and were collected separately and diluted in HBSS. Virions were pelleted at 35,000 x g for 60 minutes, resuspended in HBSS, titered (typically 10^7-10^9 pfu/ml), and stored at -80^o C in single use aliquots.

St. Louis encephalitis virus (SLEV) strain TBH-23 was obtained from Robert Tesh (University of Texas at Galveston) and propagated once in BHK21 cells followed by propagation in Vero cells to generate viral stocks. LaCrosse virus (LACV) strain LACV/human/1960 was also provided by Robert Tesh and propagated in Vero cells. The GFP-tagged Sendai virus (SeV) is described elsewhere (44). Viral titers were determined via plaque formation on Vero cell

monolayers as previously described (44), except SLEV was titered using BHK21 monolayers. To inactivate virus, supernatants were treated with ultraviolet light for 15 minutes on ice using a Spectrolinker crosslinker (Spectronics Corporation, Westbury, NY), which reproducibly blocked the propagation of WEEV in Vero cells and failed to produce detectable levels of WEEV transcripts in neuronal cells infected for 20 hours. Viral attachment was carried out in complete culture media for 90 minutes followed by two washes and application of neutralizing antisera where indicated. Primary cortical neuronal cultures were exclusively infected with sucrose-gradient purified WEEV to avoid non-specific neurotoxicity of unpurified viral preparations observed at high MOIs in preliminary experiments and to control for potential virus-independent activation of PRR pathways in unpurified viral preparations.

Conditioned Supernatants

Supernants from BE(2)-C/m cells or media treated with IFNα-A/D were UV-inactivated as described above, spun at 100,000 x g for 1 hour at 4^0 C, sterile filtered, and stored at -80^o C.

Immunoblotting, Immunofluorescence, Antibodies, SEAP Assay, and RT-PCR Analysis

Immunoblotting, RT-PCR, and immunofluorescence analysis were carried out as previously described (44). All antibodies have been previously described (44) except V5, WEEV, and Oct-1 which were purchased from Sigma-Aldrich (St.

Louis, MO), ATCC (Manassas, VA), and BioVision (Mountain View, CA), respectively. Neutralizing antisera against IFNα and IFNβ were purchased from PBL Biomedical Laboratories (Piscataway, NJ) and used at 500 neutralizing units per mL. RT-PCR primer sequences are available upon request. Secreted alkaline phosphatase activity was measured by a Quanti-Blue assay as previously described (12).

Subcellular Fractionation and Protein Radiolabeling

Nuclear and cytoplasmic extracts were generated as previously described (36) with several modifications. Namely, aprotinin was not used, the first spin was at 1500 x g, and the nuclei were washed twice with PBS and centrifuged at 1500 x g for 5 minutes at 4^{o} C after each wash.

To measure total protein synthesis, we used metabolic incorporation of ^{35}S-labeled methionine and cysteine. Control and WEEV-infected cells were incubated with 50 µCi per ml PRO-MIX ^{35}S-cell labeling mix (Amersham) for 30 min, washed with TBS containing 100 µg cycloheximide per ml, and lysed in SDS-PAGE sample buffer (12). After electrophoresis, gels were fixed, impregnated with sodium salicylate, dried, exposed, and digitized images of radioactive protein bands were quantitated as described previously (13).

Results

WEEV Replication Induces IFNβ Transcription in Neurons

To begin studying the influence of neuronal PRR pathways on neurotropic arbovirus pathogenesis, we first asked if WEEV could induce IFNβ transcription, a hallmark of PRR pathway activation, in a variety neuronal culture models (**Fig 3.1**). The first model employed was the previously characterized BE(2)-C neuronal culture model (46). This neuroblastoma cell line can be differentiated into mature human neurons, designated BE(2)-C/m, using retinoic acid, and it has been used to demonstrate differentiation-dependent responses of human neuronal cells to type-I IFN stimulation and neurotropic virus infection (12). Infection of differentiated BE(2)-C/m neuronal cells with WEEV, or the positive control Sendai virus (SeV) (44), robustly induced IFNβ transcripts (**Fig 3.1.A**). However, treatment of BE(2)-C/m neuronal cells with UV-inactivated WEEV (see materials and methods) largely failed to induce IFNβ transcription (115 fold induction versus 4-fold induction respectively, $p < 0.003$), suggesting that viral replication was required and that mere cell surface exposure of virus was largely insufficient to induce IFNβ transcription in human neuronal cells (**Fig 3.1.A**). Similarly, human embryonic stem cell-derived neurons induced IFNβ transcripts in response to both SeV and WEEV infection (**Fig 3.1.B**). Finally, rat primary cortical neurons induced IFNβ transcripts independent of the WEEV inoculating dose (**Fig 3.1.C**). These data suggest that human neuronal PRR pathways respond to WEEV.

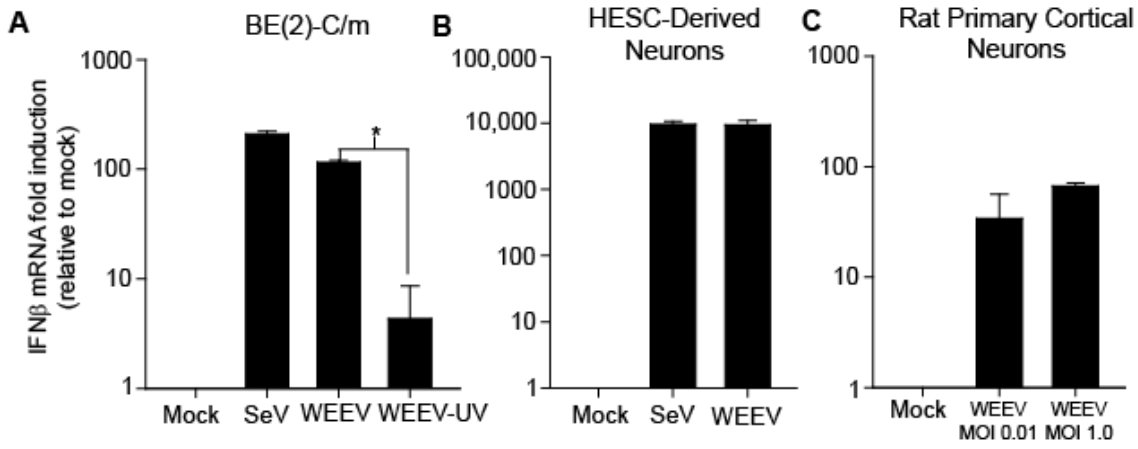

Figure 3.1. WEEV induction of IFNβ transcription in neurons. A. BE(2)-C/m cells were infected with SeV MOI 5.0 for 30 hours, WEEV MOI 1.0 for 20 hours, or UV-treated WEEV MOI 1.0 for 20 hours, and IFNβ transcript levels were assessed via qRT-PCR. **B.** Human embryonic stem cell-derived neurons were infected with SeV MOI 0.1 for 72 hours or WEEV MOI 0.1 for 24 hours, and IFNβ transcript levels were assessed. **C.** Rat primary cortical neurons were infected with WEEV at the indicated MOI, and IFNβ transcript levels were assessed 20 hours later. Data represent averages and SEMs from three independent trials for A and B and two independent trials for C. **p*-value < 0.05.

IRF3 mediates a neuronal cytoprotective response against WEEV

To further characterize the neuronal innate immune response to WEEV, we tested the functional impact of known PRR pathway signaling components on neuronal responses to WEEV. PRR pathway signaling components were genetically disrupted by stably overexpressing specific dominant negative mutants to the central PRR pathway transcription factor IRF3, the cytoplasmic PRR RIG-I, and the required TLR3 adaptor TRIF in BE(2)-C/m cells (see (44) for validation and pertinent controls). The IRF3 mutant lacks a DNA binding domain such that it competes for activation signals but does not induce transcription; the RIG-I mutant lacks the N-terminal CARD domains required for signal transduction; and the dominant negative TRIF mutant contains only a TIR domain and blocks downstream signal transduction. Overexpression of the dominant negative IRF3 and RIG-I mutants in BE(2)-C/m cells reduced WEEV-mediated induction of IFNβ transcripts (**Fig 3.2.A**); whereas no reduction was observed when the dominant negative TRIF mutant was overexpressed. These results indicated that RIG-I and IRF3 mediated a neuronal transcriptional response to WEEV and that a TLR3-TRIF-mediated pathway was largely dispensible. In further support of this, BE(2)-C/m cells stably expressing an shRNA targeting PI3K p110α, which we previously demonstrated influences TLR3 signaling in neuronal cells (44), showed no reduction in IFNβ transcripts following WEEV infection (**Supplemental Fig S3.1.A**).

Next, we tested the significance of PRR pathway signaling components on cell viability and viral titers following WEEV infection. Genetic disruption of IRF3

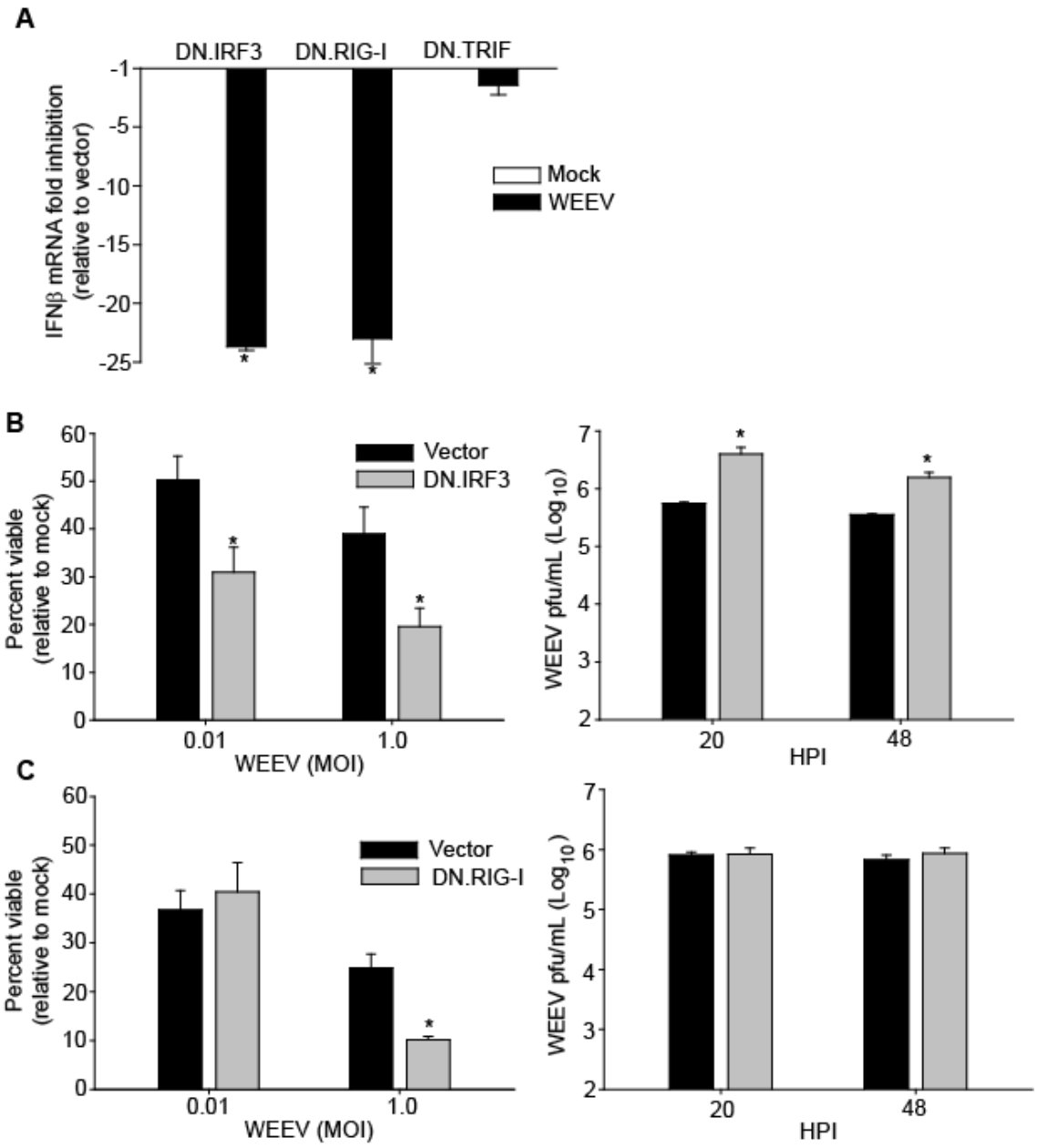

Figure 3.2. Neuronal PRR pathway component-dependent responses to WEEV. A. BE(2)-C/m cells stably overexpressing dominant negative forms of IRF3, RIG-I, or TRIF were mock infected or infected with WEEV MOI 1.0 for 20 hours, and IFNβ mRNA levels were measured by qRT-PCR. Results are expressed as the fold-change compared to similarly treated cells stably transfected with an empty vector. **B.** Control and dominant negative IRF3 overexpressing BE(2)-C/m cells were infected with WEEV at the indicated MOI and percent viability relative to mock infected controls was assessed via a MTT assay 48 hours post infection (HPI: left panel), or titers (MOI 1.0) were measured via plaque assay from supernatants harvested at the indicated times (right panel). Similar titers were observed for MOI 0.01 infections (data not shown). **C.** Control and dominant negative RIG-I overexpressing BE(2)-C/m cells were infected and analyzed as in B. Data represent averages and SEMs from at least three independent trials. **p*-value < 0.05.

rendered BE(2)-C/m neuronal cells more susceptible to WEEV-mediated cytopathic effect (CPE) and resulted in modestly higher WEEV titers independent of MOI (**Fig 3.2.B**). Expression of dominant negative RIG-I only impaired neuronal viability in response to a high WEEV inoculum and had no impact on viral titers (**Fig 3.2.C**). These results indicated that in neuronal cells IRF3 mediated a cytoprotective and potentially antiviral response to WEEV; however, RIG-I only mediated a cytoprotective response when the initial viral burden was high, suggesting that there may be redundancy for cytosolic detection of WEEV at the receptor level in neuronal cells or that the level of dominant negative RIG-I expression was insufficient to effect cell viability or viral replication following WEEV infection. Consistent with the dispensable role of a TLR3-TRIF pathway for transcriptional responses to WEEV in neuronal cells, no change in viability or WEEV titers was observed in cells stably overexpressing dominant negative TRIF (**Supplemental Fig S3.2.A**). Furthermore, transient overexpression of wild-type TLR3 or a dominant negative TLR3 mutant lacking a TIR domain failed to modulate neuronal viability following WEEV infection (**Supplemental Fig S3.2.B and C**). To demonstrate the functionality of transiently overexpressed wild-type and dominant negative TLR3, we verified the appropriate modulation of an ISRE promoter in neuronal cells when presented with the TLR3 ligand poly(I-C) (**Supplemental Fig S2.5**).

Since genetic disruption of RIG-I suggested that multiple cytoplasmic receptors may respond to WEEV in neurons, we examined the role of MDA5 in

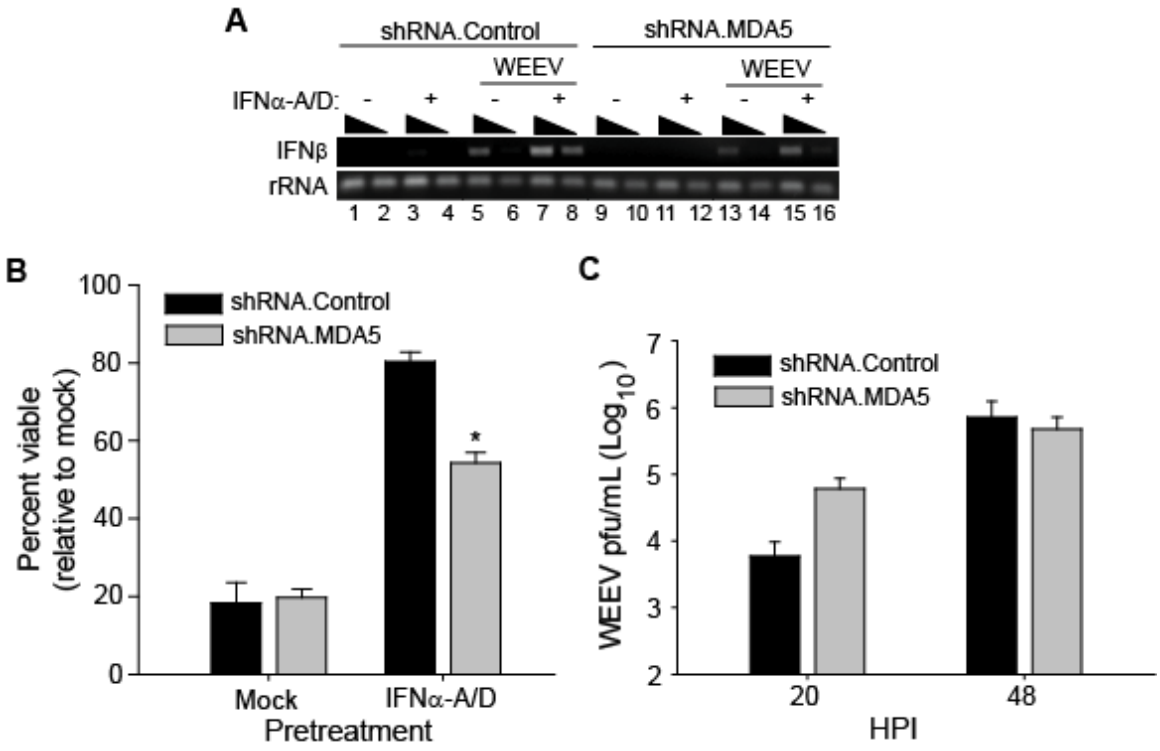

Figure 3.3. Neuronal cell MDA5-dependent response to WEEV. A. BE(2)-C/m cells stably overexpressing a control or MDA5-targeted shRNA were either mock-pretreated or pretreated with 1000 U/ml of IFNα-A/D for six hours, washed twice, and mock-infected or infected with WEEV MOI 1.0 for 20 hours. Samples were analyzed by RT-PCR for IFNβ and rRNA transcripts. Adjacent lanes for individual samples represent results using 10-fold dilutions of cDNA. **B.** Control BE(2)-C/m cells or cells stably overexpressing a MDA5-targeted shRNA were either mock-pretreated or pretreated with 1000 U/ml of IFNα-A/D for six hours, washed twice, and then mock-infected or infected with WEEV MOI 1.0. Cell viability relative to mock-infected controls was assessed 48 hours after infection via a MTT assay. **C.** Supernatants from WEEV-infected, IFNα-A/D-pretreated control or MDA5-depleted BE(2)-C/m cells were titered via plaque assay at the indicated times post infection. Data are representative of three independent trials for A. Averages and SEMs are displayed from three independent trials for B and two trials for C. **p*-value < 0.05.

neuronal responses to WEEV (**Fig 3.3**). To achieve this we generated stable BE(2)-C/m cells expressing a shRNA targeting MDA5. In these neuronal cells, MDA5 expression was reduced by approximately 50% (**Fig 2.4.B**) (44), but when pretreated with type-I IFNs, the difference in MDA5 expression between control cells and cells with an MDA5-targeted shRNA greatly increased (**Fig 2.4.B**) (44). We observed no difference in the IFNβ transcriptional response to WEEV in control neuronal cells versus cells expressing an shRNA targeting MDA5 (**Fig 3.3.A**) (compare lane 5 to 13), but when the difference in MDA5 expression was accentuated by pretreating with type-I IFNs, WEEV activated IFNβ transcription in control neuronal cells to a greater extent than in MDA5-depleted neuronal cells, which trended towards a significant difference (average density of lane 8 versus 16, *p*-value 0.15) (**Fig 3.3.A**). Targeting MDA5 expression in mock pretreated cells had no impact on neuronal cell viability following WEEV infection (**Fig 3.3.B**), but pretreating control versus MDA5-depleted neuronal cells with type-I IFNs significantly rendered the MDA5-depleted neuronal cells more susceptible to a WEEV-mediated CPE (**Fig 3.3.B**) and trended towards higher WEEV titers at 20 hours post infection (**Fig 3.3.C**) when the difference in MDA5 expression was still greatly accentuated by the type-I IFN pretreatment (**Supplemental Fig S3.3**). Pretreating the neuronal cells with type-I IFNs could have given them the capacity to produce functional amounts of autocrine/paracrine antiviral type-I IFN protein following WEEV infection, a finding that would be in contrast with our previous observations in mock pretreated neuronal cells (44). To assess this possibility, we tested the ability of

type-I IFN neutralizing antibodies to modulate neuronal viability following WEEV infection. To accomplish this, we incubated IFN-pretreated BE(2)-C/m cells with type-I IFN neutralizing antibodies following WEEV attachment, and observed no difference in WEEV-mediated CPE compared to matched cells in which no neutralizing antibody was given (see the far right bar of **Fig 3.3.B** for reference). Altogether, these data indicated that MDA5 may detect WEEV in neuronal cells and mediate a cytoprotective and potentially antiviral response independent of antiviral autocrine/paracrine type-I IFN signaling.

In addition to the loss-of-function studies described above, we also attempted gain-of-function studies for neuronal PRR pathway signaling components, but we were unable to isolate neuronal cells stably overexpressing wild-type IRF3, RIG-I, or MDA5. However, transient overexpression of IRF3 or RIG-I did protect neuronal cells from WEEV-mediated CPE, and transient overexpression of IRF3 or, as a positive control, a constitutively active IRF3 mutant reduced viral titers (**Supplemental Fig S3.4.A and B**). However, subsequent analysis revealed that transient overexpression of wild-type RIG-I or IRF3 constitutively induced type-I IFNs (**Supplemental Fig S3.4.C and D**), which we have previously shown decreases WEEV titers and enhances WEEV-infected neuronal cell viability (12). Therefore, we could not confidently interpret the role these over expression constructs played in neuronal responses to WEEV given the confounding ability of the constructs to constitutively activate neuronal antiviral PRR pathways.

IRF3 Mediates a Cytoprotective Response to WEEV in Primary Cortical Neurons

PRR pathway responses can be both cell type- and species-specific (34). To determine if our observations were unique to neuroblastoma-derived human neurons, we examined neuronal responses to WEEV in primary cortical neurons derived from wild-type, IRF3$^{-/-}$, MDA5$^{-/-}$, and IPS-1$^{-/-}$ mice. Consistent with results from neuroblastoma-derived human neurons, IRF3$^{-/-}$ and MDA5$^{-/-}$ cortical neurons were deficient in transcriptional induction of IFNβ when infected with WEEV (**Fig 3.4.A and B**). In addition, IRF3$^{-/-}$ cortical neurons were significantly more susceptible to WEEV-mediated CPE independent of MOI but showed no difference in WEEV titers (**Fig 3.4.C and D**). In contrast to the differentiated neuronal BE(2)-C/m cells, MDA5$^{-/-}$ and IPS-1$^{-/-}$ primary cortical neurons were as susceptible to WEEV-mediated CPE as wild-type cortical neurons (**Fig 3.4.C**), and WEEV titers from MDA5$^{-/-}$ primary neurons were no different than controls (**Fig 3.4.D**). These results suggested that neuronal IRF3 mediated a cytoprotective response to WEEV and that the influence of individual PRRs on this neuron-protective response may be complex, redundant, unique to immortalized human neuronal cells, or a combination of these factors. Accordingly, we focused further studies on the role of IRF3 in neuronal responses to neurotropic arboviruses.

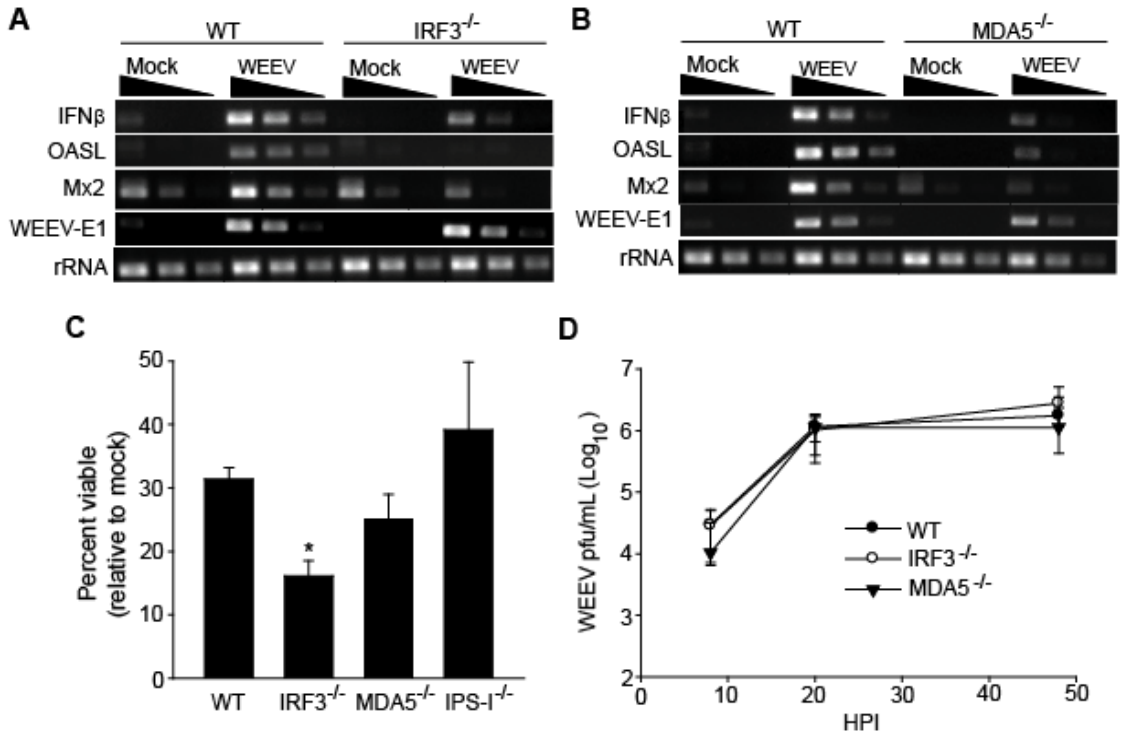

Figure 3.4. PRR pathway component-dependent responses to WEEV in primary neurons. A and B. Wild-type, IRF3$^{-/-}$ (A), or MDA5$^{-/-}$ (B) primary neurons were mock infected or infected with WEEV MOI 1.0 for 20 hours, and transcript expression was assessed via RT-PCR for the indicated genes. **C.** Primary cortical neurons derived from C57BL/6 wild-type, IRF3$^{-/-}$, MDA5$^{-/-}$, and IPS-1$^{-/-}$ mice were infected with WEEV MOI 1.0, and cell viability relative to mock infected controls was analyzed via a luminescent ATP assay 48 hours later. Neurons infected at an MOI of 0.01 demonstrated a similar phenotype (data not shown). **D.** WEEV titers from supernatants harvested from C were determined via plaque assay. Neurons infected at an MOI of 0.01 demonstrated a similar phenotype (data not shown). Data are representative of two independent trials for A and one trial for B. Data represent averages and SEMs from three independent trials for C and two for D. *p-value < 0.05.

Neuronal Cell PRR Responses to Diverse Neurotropic Arboviruses

Pattern recognition receptor pathway responses are often both pathogen- and cell type-specific. To determine if neuronal PRR pathways broadly respond to neurotropic viral infection, we examined neuronal cell responses to the neurotropic arboviruses St. Louis encephalitis virus (SLEV) and La Crosse virus (LACV). Both SLEV and LACV induced IFNβ transcription in neuronal cells, albeit SLEV did so to a greater extent than LACV 20 hours post infection. In addition, dominant negative IRF3 overexpression reproducibly reduced neuronal IFNβ transcription induced by SLEV and may have had a minor effect on LACV-induced IFNβ transcription, but the ability of dominant negative IRF3 to inhibit LACV-mediated induction of IFNβ was not reproducible (**Fig 3.5.A**). Next we assessed the effect of genetic disruption of the central PRR pathway transcription factor IRF3 on neuronal responses to SLEV and LACV, and we observed that neuronal cells overexpressing dominant negative IRF3 were significantly more susceptible to SLEV-mediated CPE independent of MOI (**Fig 3.5.B**). These data indicated that IRF3, like in the case of a WEEV infection, may influence neuronal survival following a SLEV infection. In contrast, overexpression of dominant negative IRF3 had no effect on LACV-mediated CPE, indicating that IRF3 may be dispensable for neuronal survival following LACV infection or that the extent of dominant negative IRF3 overexpression was insufficient to affect LACV-mediated CPE (**Fig 3.5.C**) (note that end points for each viral infection were adjusted to give viabilities within typical linear death curves for BE(2)-C/m cells). The differing influence of IRF3 in neuronal

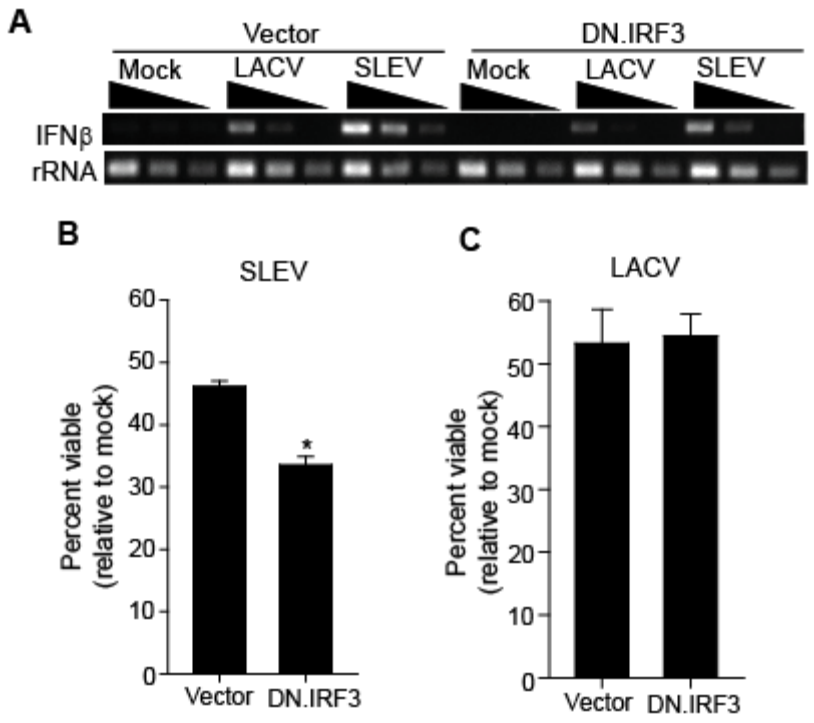

Figure 3.5. IRF3-dependent neuronal cell response to St. Louis and La Crosse viruses. A. BE(2)-C/m cells stably overexpressing a dominant negative IRF3 or a vector control were mock infected, infected with SLEV MOI 1.0, or infected with LACV MOI 1.0 for 20 hours followed by IFNβ and rRNA RT-PCR. **B and C.** Control or dominant negative IRF3 overexpressing BE(2)-C/m cells were infected with SLEV (B) or LACV (C) MOI 1.0, and cell viability relative to mock infected controls was assessed 48 (B) and 24 (C) hours later via a MTT assay. Neuronal cells infected at an MOI of 0.01 with either SLEV (B) or LACV (C) demonstrated similar phenotypes (data not shown). Data are representative of two independent trials for A. Averages and SEMs are displayed from three independent trials for B and C. **p*-value < 0.05.

responses to WEEV, SLEV, and LACV suggests that neuronal PRR responses are indeed complex and pathogen-dependent, but not without some level of overlap.

Neuronal IRF3-Dependent Cytoprotective Response to WEEV is Independent of Type-I IFN Autocrine/Paracrine Signaling

The observation that a dominant negative IRF3 mutant lacking a DNA binding domain accentuated WEEV-mediated CPE in neuronal cells suggested that IRF3 transcriptional activity was involved in the IRF3-dependent cytoprotective response to WEEV. To begin to understand what factors downstream of IRF3 were required for this response, we first assessed whether induction of antiviral type-I IFNs might mediate the IRF3-dependent cytoprotective response. Previous attempts to identify type-I IFNs in supernatants of WEEV-infected neuronal cells via ELISAs failed to detect any measurable amount of type-I IFNs, and treatment of WEEV-infected neuronal cells with type-I IFN neutralizing antibodies failed to increase WEEV-mediated CPE (12). In addition, WEEV failed to activate IFNβ-dependent ISRE reporter neuronal cells (data not shown). However, these assays may not have been sensitive enough to detect low levels of biologically relevant autocrine IFN signaling. Therefore, we developed an alternative assay that measured accumulation of the interferon-stimulated gene, RIG-I, following viral infection. When neuronal cells were infected with the positive control SeV, RIG-I protein accumulated (**Fig 3.6.A**, compare lane 1 and lane 6) in a manner dependent on autocrine IFNβ signaling because an IFNβ

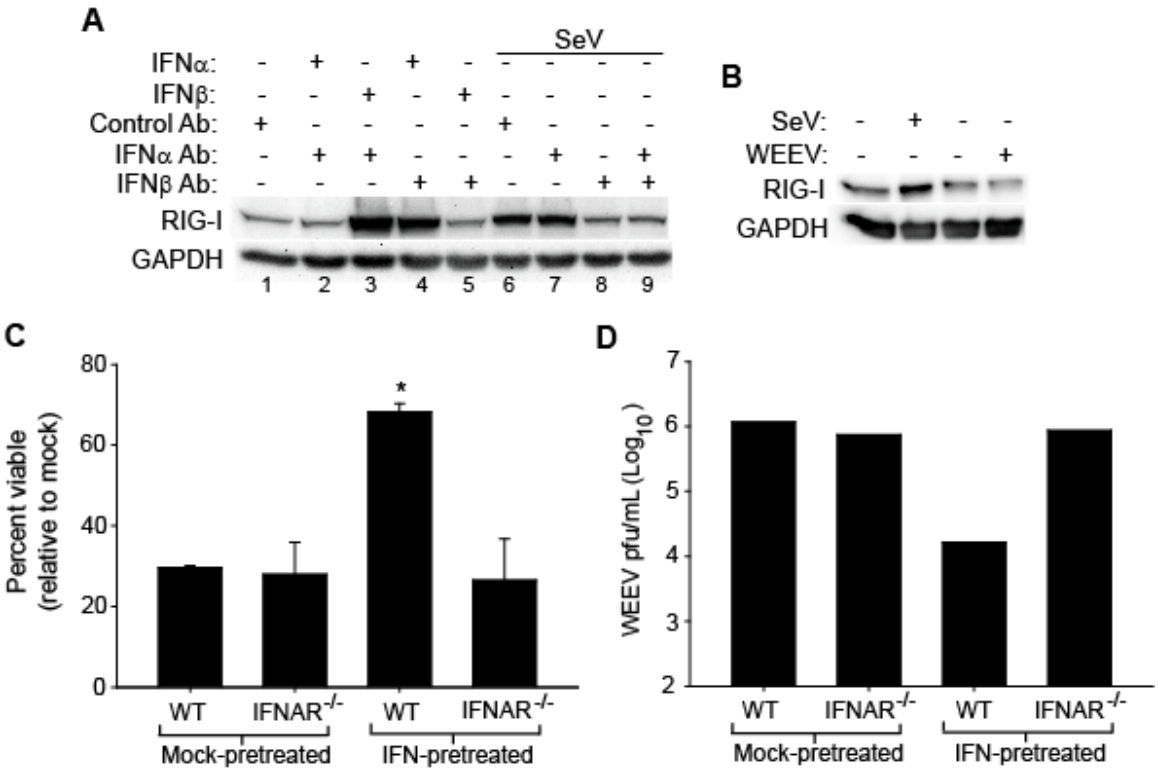

Figure 3.6. Neuronal response to WEEV is independent of type-I IFN autocrine/paracrine signaling. A. BE(2)-C/m cells were mock infected or infected with SeV MOI 5.0 and then incubated with 500 neutralizing units of control, IFNα, IFNβ, or IFNα and IFNβ neutralizing antibodies. As positive controls for IFN neutralization, indicated mock-infected, neutralizing antibody-treated cells were stimulated with 20 U/ml IFNα or 10 U/ml IFNβ 28 hours post infection. Whole cell lysates were collected 48 hours post infection and analyzed by western blot for RIG-I and GAPDH. **B.** BE(2)-C/m cells were mock-infected or infected with SeV MOI 5.0 for 48 hours, or mock infected or infected with WEEV MOI 1.0 for 24 hours. Lysates were analyzed by western blot for RIG-I and GAPDH. **C.** C57Bl/6 wild-type or IFNAR$^{-/-}$ cortical neurons were mock-pretreated or pretreated with 100 U/ml of mouse IFNα/β for 24 hours followed by WEEV MOI 1.0. Cell viability relative to mock infected controls was assessed 48 hours post infection via a luminescent ATP assay. Similar results were observed with WEEV MOI 0.01 (data not shown). **D.** WEEV titers from supernatants collected from neurons infected for 20 hours described in C were determined via plaque assay. Similar results were observed with WEEV MOI 0.01 (data not shown). No difference in titers was observed between wild-type or IFNAR$^{-/-}$ neurons at 8 or 48 hours post infection (data not shown). Data are representative of three independent trials for A and B. Averages and SEMs are displayed from three independent trials for C and one for D. *p-value < 0.05.

neutralizing antibody blocked the SeV-mediated induction of RIG-I (compare lane 6 to lane 8). Treatment with an IFNα neutralizing antibody had no effect on SeV-mediated induction of RIG-I (compare lane 6 to lane 7). Activity of the neutralizing antibodies was verified by demonstrating the specific ability of each antibody to potently and selectively block IFNα- or IFNβ-mediated induction of RIG-I (see lanes 1-5). To assess the neutralizing capacity of the type-I IFN antibodies throughout the experiment, exogenous IFN delivered to the antibody specificity control samples was added 28 hours after addition of neutralizing antibodies. In addition, SeV increased global expression of IRF3 and expression of a slower migrating form of IRF3, often indicative of phosphorylated, transcriptionally-active IRF3 (**Supplemental Fig S3.5**). Interestingly, WEEV failed to upregulate RIG-I expression in BE(2)-C/m cells (**Fig 3.6.B**) despite optimization of both MOI and assay end point. As a further test for WEEV-mediated induction of functional, antiviral type-I IFNs in neurons, we compared responses of primary cortical neurons derived from wild-type and interferon receptor (IFNAR) knock-out mice. No difference in cell viability (**Fig 3.6.C**) or WEEV titer (**Fig 3.6.D**) from $IFNAR^{-/-}$ versus wild-type primary neurons was observed. As a control for IFNAR function, primary neurons were pretreated with murine IFNα/β which, as expected, protected neurons from WEEV-mediated CPE and decreased WEEV titers 20 hours after infection of wild-type neurons, while $IFNAR^{-/-}$ primary neurons were refractory to this treatment. Altogether these data indicated that the IRF3-dependent, neuron-protective response to WEEV was independent of type-I IFN signaling.

After ruling out type-I IFN signaling, we asked if the IRF3-dependent, cytoprotective response to WEEV was mediated by cell-intrinsic or -extrinsic factors other than type-I IFNs. To accomplish this, we set up a bioassay to determine if conditioned supernatants from WEEV-infected BE(2)-C/m cells could transfer any modulatory capacity to a subsequent neuronal, WEEV-mediated cytopathic response. Control conditioned supernatants, with exogenous IFNα-A/D added to them prior to conditioning, protected target neurons from a WEEV-mediated CPE; however, conditioned supernatants from WEEV-infected producer neurons had no modulatory capacity on a subsequent WEEV-mediated CPE (**Supplemental Fig S3.6**). These data suggested that the IRF3-dependent, cytoprotective response to WEEV may be independent of cytoprotective, soluble, secreted factors. However, we could not rule out the possibility that our bioassay was insufficient to detect low levels of biologically relevant cell-extrinsic factors because we did observe a reduction in the protective capacity of type-I IFN-treated conditioned media relative to that of media with fresh, unconditioned type-I IFN. Therefore, we chose to directly test our alternate hypothesis that cell-intrinsic factor(s) downstream of IRF3 were responsible for the IRF3-dependent, cytoprotective response to WEEV.

WEEV-Induced, IRF3-Dependent Genes Which are Cytoprotective Against Neurotropic Arboviruses

Many antiviral effector genes are directly induced by IRF3 (2, 58), some of which have known antiviral activity against alphaviruses, although most have not been

tested against WEEV (6, 63). To test our hypothesis that the IRF3-dependent, cytoprotective response to WEEV in neuronal cells was mediated by cell-intrinsic factors, we searched for IRF3-dependent, WEEV-induced, antiviral effector genes. We looked for the WEEV-mediated induction of several of these genes in BE(2)-C/m cells at both ten and twenty hours post infection via RT-PCR using IFNβ and rRNA as positive and loading controls, respectively (**Fig 3.7**). The antiviral effectors oligoadenylate synthetase-like protein (OASL), myxoma resistance gene-B (MxB), MxA, and interferon inducible transcript-2 (IFIT2) were all reproducibly induced by WEEV, albeit to differing extents. In contrast, the expression of the IRF3-inducible antiviral effectors IFIT1, viperin, ISG20, ISG15, and zinc finger antiviral protein (ZAP) were unresponsive to WEEV infection. We verified that the two most responsive putative effectors, OASL and MxB (Mx2 is the mouse homologue), were dependent on not only IRF3, but also MDA5 in primary cortical neurons (**Fig 3.4.A and B**). WEEV envelope protein-1 transcripts were similar under each condition indicating that viral RNA burden between samples was equal. These data demonstrated that WEEV induces cell-intrinsic, IRF3-dependent, antiviral effector genes that may mediate an IRF3-dependent, cytoprotective response.

To determine if IRF3-dependent antiviral effector genes might mediate the neuronal-protective response to neurotropic arboviruses, we assessed whether shRNA-mediated depletion of the most responsive putative effector, OASL, rendered neuronal cells more susceptible to neurotropic arbovirus-mediated

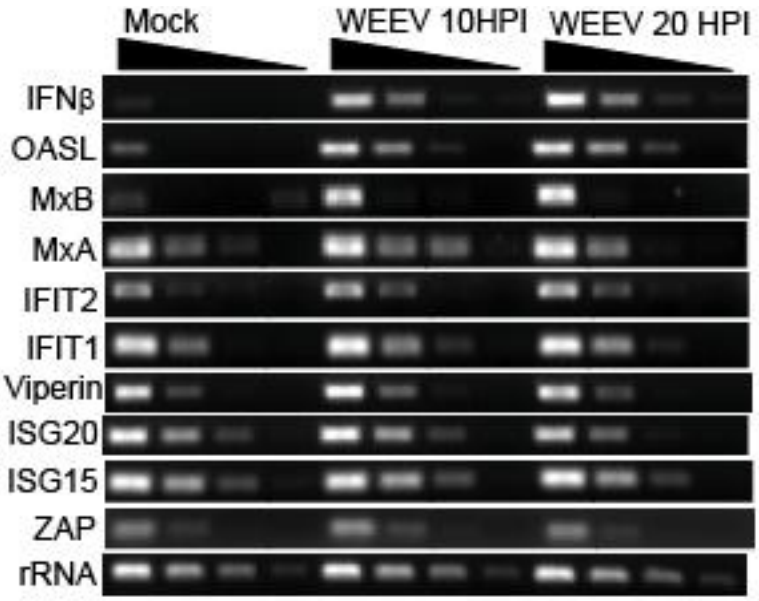

Figure 3.7. WEEV-induced genes in neuronal cells. BE(2)-C/m cells were mock infected or infected with WEEV MOI 1.0 for 10 or 20 hours, and transcription of the indicated genes was analyzed by RT-PCR. Data are representative of three independent trials.

CPE. For this purpose, we generated stable neuronal cell lines expressing control- or OASL-targeting shRNAs. Targeted depletion of OASL was verified by RT-PCR from mock-, WEEV-, and LACV-infected BE(2)-C/m cells in relation to cells stably expressing a control shRNA (**Fig 3.8.A**). Figure 3.8.A also demonstrates that LACV induces OASL mRNA. Decreased expression of OASL had no effect on a neuronal WEEV- (**Fig 3.8.B**) or SLEV-mediated CPE (**Fig 3.8.D**), but did modestly enhance a LACV-mediated cytopathic response (**Fig 3.8.C**). This finding indicated that OASL may mediate a neuronal response to LACV that could potentially be independent of IRF3, as cells stably overexpressing a dominant negative mutant of IRF3 responded normally to LACV (**Fig 3.5.C**). Given that depletion of OASL had no effect on a neuronal response to WEEV, but did affect the response to LACV, we concluded that OASL was not likely to be involved in the IRF3-dependent, cytoprotective response to WEEV. However, OASL depletion may have been insufficient to affect a neuronal response to WEEV. Nevertheless, these results suggested that cell-intrinsic factor(s) downstream of IRF3 may be responsible for the IRF3-dependent, cytoprotective response to WEEV, and that further study of other IRF3-dependent, putative cytoprotective genes, such as MxB, may identify genes which are protective against WEEV and possibly SLEV. In addition, non-biased methods, such as transcriptional arrays, may identify alternative WEEV-induced, IRF3-dependent cytoprotective genes in neuronal cells.

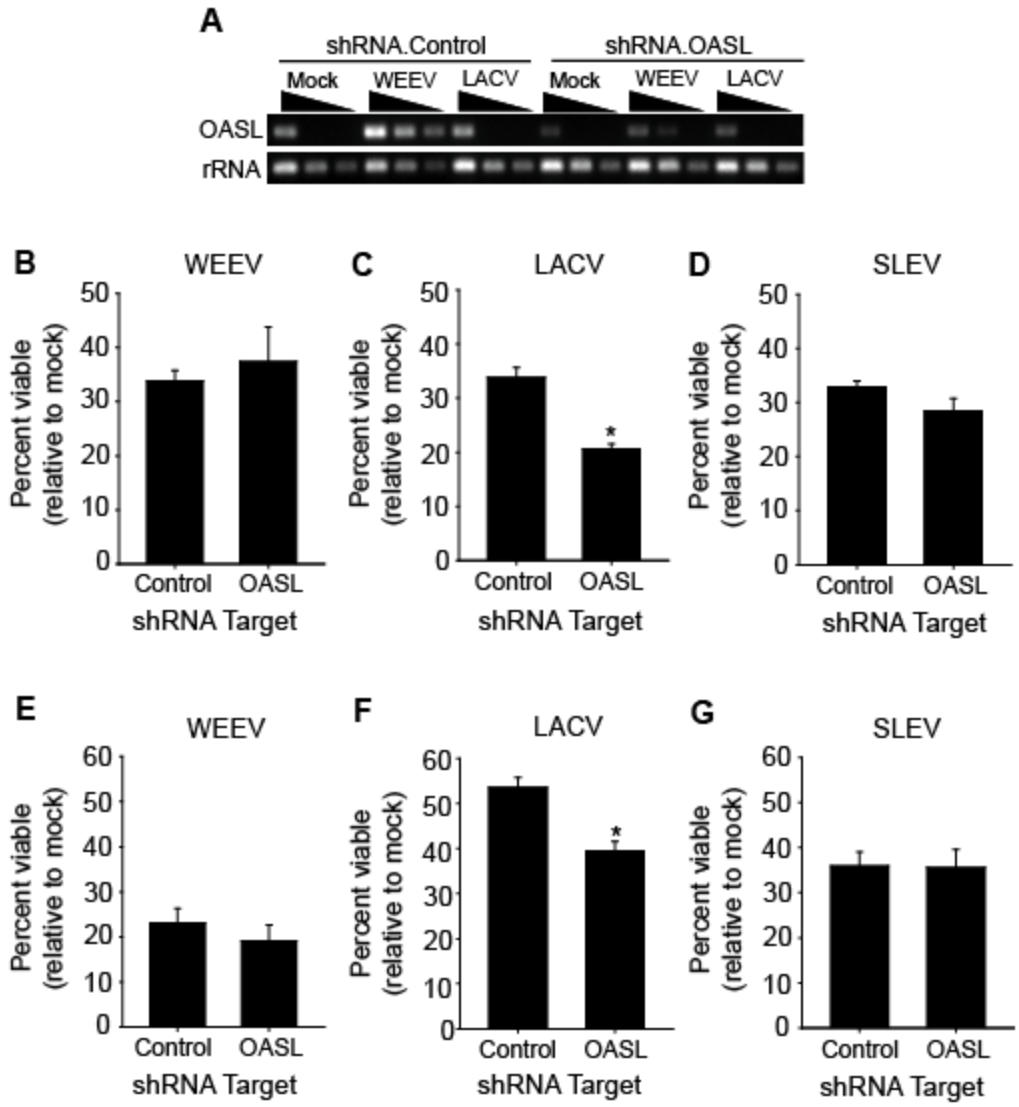

Figure 3.8. OASL protects neuronal cells from a LACV-mediated cytopathic effect. A. BE(2)-C/m cells stably overexpressing a control shRNA or a shRNA directed against OASL were mock-infected or infected at a MOI of 1.0 with WEEV or LACV for 20 hours and analyzed by RT-PCR for the transcription of OASL and rRNA. **B-G.** Cells described in A were infected with WEEV (B and E), LACV (C and F), or SLEV (D and G) at a MOI 0.01 (B-D) or 1.0 (E-F), and viability relative to mock-infected controls was assessed via a MTT assay at 24 (F), 48 (B, C, E, and G), or 72 (D) hours post infection. Data are representative of one trial for A. Averages and SEMs are displayed from four independent trials for B-G. *p-value < 0.05.

WEEV Impairs Poly(I-C)-Induced activation of ISRE and NFκB Reporter Neuronal Cells

Time course studies in neuronal cells revealed that IFNβ transcription was not robustly activated until ten or more hours post WEEV infection (**Supplemental Fig S3.7**) despite measurable amounts of viral RNA, protein, and viral particles at times as early as six hours post infection (12). Furthermore, WEEV induced IFNβ transcription, but we failed to observe any antiviral type-IFN protein production (**Fig 3.6**). Together, these observations suggested that WEEV may impair antiviral PRR pathway signaling at early times post infection, which is a hypothesis that others have formed and subsequently confirmed based on similar observations of West Nile virus (WNV) (23). To test this hypothesis, we determined if WEEV could inhibit poly(I-C)-mediated induction of neuronal antiviral PRR signaling. We either pre-infected (**Fig 3.9.A and Supplemental Fig S3.8.A**) or pre-stimulated (**Fig 3.9.B and Supplemental Fig S3.8.B**) IFNβ-dependent ISRE or NFκB reporter neuronal cells (44) with the TLR3 ligand, poly(I-C) (pIC); the MDA5 ligand, transfected-poly(I-C) (T-pIC); IFNα-A/D; or TNFα and measured SEAP reporter production 20 hours later. To control for non-specific effects of viral-mediated CPE, we monitored neuronal cell viability. WEEV impaired pIC- and T-pIC-mediated induction of ISRE and NFκB reporter neuronal cells independent of order of infection (**Fig 3.9.A and B**), albeit the reduction in reporter signal was greater in pre-infected cells. Under these conditions WEEV did not affect type-I IFN signaling, but when cells were pre-infected for at least four hours prior to IFN

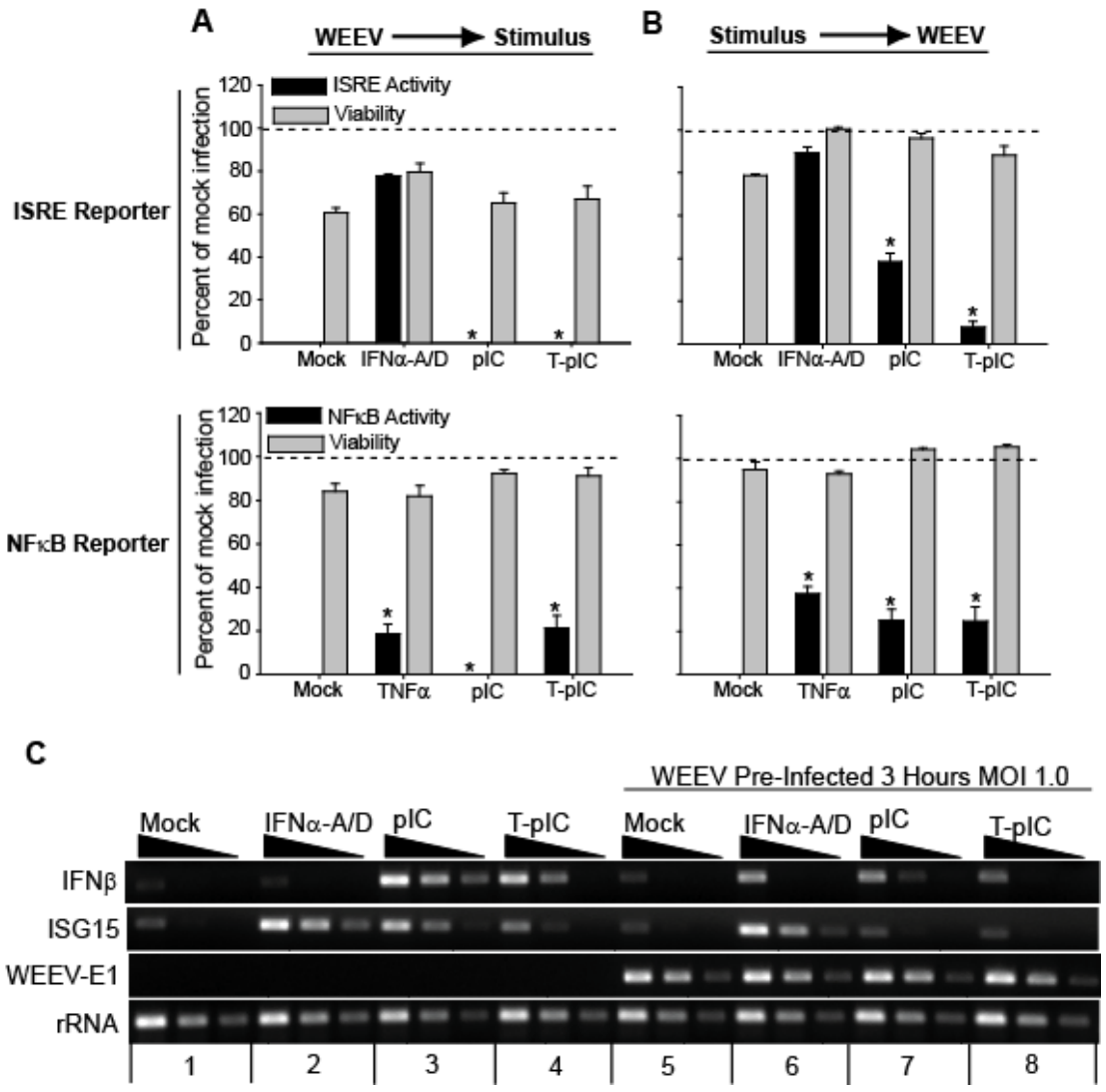

Figure 3.9. WEEV inhibition of neuronal cell antiviral PRR pathways. A. BE(2)-C/m ISRE (top panel) or NFκB (bottom panel) reporter cells were mock pre-infected or pre-infected with WEEV MOI 1.0 for 90 minutes followed by mock-stimulation or stimulation with 100 U/ml IFNα-A/D, TNFα (25 ng/ml), 50 μg/ml poly(I-C) (pIC), or 500 ng/ml transfected-poly(I-C) (T-pIC) as indicated. Secreted alkaline phosphatase (SEAP) reporter activity and cell viability were measured 20.5 hours post infection and expressed as percents of mock-infected controls. **B.** Cells were treated as in A except they were pre-stimulated for 3 hours and analyzed 16 hours post infection. **C.** BE(2)-C/m cells were pre-infected with WEEV MOI 1.0 for 3 hours followed by a 4 hour mock, IFNα-A/D, pIC, or T-pIC stimulation. The indicated transcripts were analyzed by RT-PCR. Averages and SEMs are displayed from three independent trials for A and B. Data are representative of three independent trials for C. *p-value < 0.05 compared to either percent viability or matched mock-infected percent reporter activity.

stimulation, ISRE reporter levels decreased in parallel with cell viability, indicating that the impaired type-I IFN response by a well-established WEEV infection was likely due to a non-specific mechanism (**Supplemental Fig S3.8.A**). WEEV also inhibited TNFα-mediated activation of NFκB reporter cells (**Fig 3.9.A and B**), suggesting that WEEV inhibits a common factor between PRR and TNFα signaling pathways.

WEEV Impairs Transcription of Poly(I-C)-Induced Endogenous Genes in Neuronal Cells

To validate that WEEV specifically blocks neuronal PRR signaling at early times post infection, we examined whether WEEV could block poly(I-C)-mediated induction of endogenous transcripts. As expected, pre-infection of BE(2)-C/m cells with WEEV decreased the induction of IFNβ transcripts by a four hour treatment of either pIC (compare group 3 to 7) or T-pIC (compare group 4 to 8) (**Fig 3.9.C**). Importantly, WEEV was unable to block the IFN-mediated induction of ISG15 (compare group 2 to 6), but it did inhibit the poly(I-C)-mediated induction of ISG15 (compare group 3 to 7 and 4 to 8) (**Fig 3.9.C**). A similar phenotype to that of ISG15 was observed for MxB, OASL, and Viperin and, which like ISG15, are responsive to both type-I IFN and PRR pathway signaling (**Supplemental Fig S3.9**). WEEV envelope protein-1 transcripts were similar under each condition indicating that viral RNA burden between samples was equal. These data demonstrated WEEV's ability to specifically block neuronal antiviral PRR signaling at early times post infection.

Diverse Neurotropic Arboviruses Inhibit Poly(I-C)-Induced Activation of ISRE Reporter Neuronal Cells

To determine if neuronal antiviral PRR pathway inhibition might be a general feature of neurotropic arboviruses, we assessed the ability of LACV and SLEV to inhibit poly(I-C)-mediated induction of ISRE reporter cells. Both viruses, when co-administered with poly(I-C) or IFNα-A/D, inhibited both exogenous poly(I-C) and transfected poly(I-C) stimulations, but had no effect an IFNα-A/D stimulation (**Fig 3.10.A and B**). Pre-infection for ten hours with LACV or SLEV did decrease type-I IFN-induced ISRE activity, but the reduction in ISRE activity was paralleled by a reduction in neuronal viability, indicating that the impaired type-I IFN response by a well-established LACV or SLEV infection was likely due to a non-specific mechanism (**Supplemental Fig S3.10**). Based on previous work (7), we expected LACV to block PRR signaling, but to our knowledge this is the first demonstration of SLEV inhibiting PRR signal transduction. Given that WNV (22), WEEV, LACV, and SLEV inhibit antiviral PRR signal transduction, we postulate that this may be a common virulence mechanism of many neurotropic arboviruses.

Exogenous Expression of WEEV Capsid Inhibits Neuronal Antiviral PRR Signaling

To determine which WEEV gene was responsible for antiviral PRR pathway inhibition, we individually placed the WEEV genes non-structural protein-1 (pnsP1), nsP2 (pnsP2), nsP3 (pnsP3), capsid (pCapsid), and the entire structural

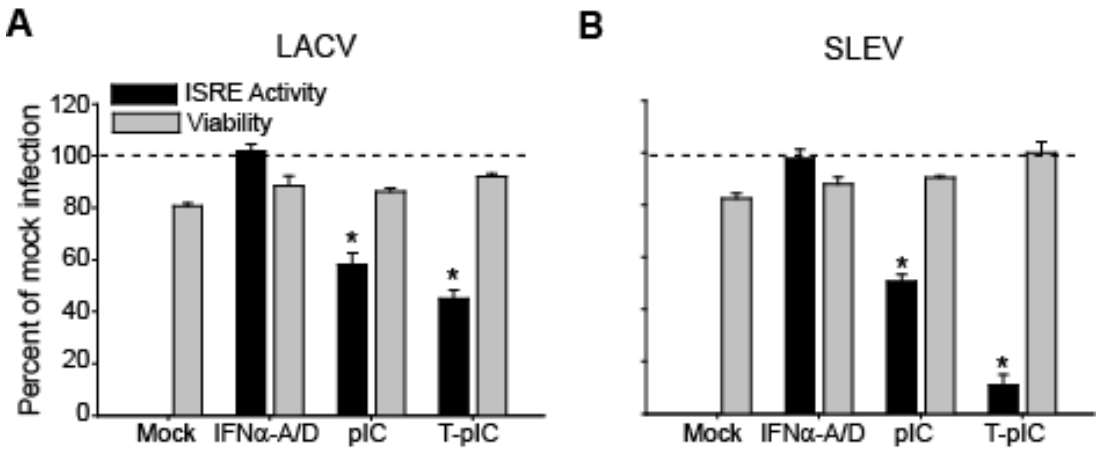

Figure 3.10. LACV and SLEV inhibit neuronal antiviral PRR pathways. A and B. BE(2)-C/m ISRE reporter neurons were infected with LACV MOI 1.0 (A) or SLEV MOI 1.0 (B) and co-stimulated with IFNα-A/D (100 U/ml), pIC (50 ug/ml), or T-pIC (700 ng/ml). SEAP reporter activity and cell viability were measured 22 hours later and expressed as percents of mock infected controls. Averages and SEMs are displayed from three independent trials. **p*-value < 0.05.

protein ORF (pStructural) under the control of a nuclear promoter. Repeated attempts to clone full-length nsP4 under the control of a mammalian promoter failed as did attempts to express nsP4 in bacterial cells. This was likely due to the short half-life observed for alphavirus nsP4 and is consistent with the relatively low amount of nsP4 expressed by cells infected with whole virus (56). A construct harboring the complete ORF for the nsP123 poly-protein did not express any detectable nsP123 in neuronal cells. As positive controls for antiviral PRR pathway inhibition, WNV NS1 and NS2A were also cloned (pNS2A and pNS1) (18, 22, 38, 59). Each viral gene was transfected into ISRE and NFκB reporter neuronal cells and, 48 hours later, were mock-stimulated or stimulated with pIC, T-pIC, IFNα-A/D, or TNFα. Neuronal viability was monitored following stimulation via an MTT assay to control for potential toxicity; none was observed. Twenty-four hours after stimulation, SEAP reporter activity was assessed, and the results are shown in **Figure 3.11.A and B**. Importantly, pCapsid and pStructural inhibited pIC and T-pIC-mediated ISRE activation without affecting an IFNα-A/D stimulation. pnsP1, pnsP2, and pnsP3 had no inhibitory activity, and the WNV genes pNS2A and pNS1 only inhibited a T-pIC stimulation. TNFα and pIC-mediated NFκB activation were inhibited by both pCapsid and pStructural, whereas pnsP1, pnsP2, and pnsP3 had no NFκB-inhibitory capacity. The WNV genes pNS2A and pNS1 only inhibited pIC-mediated NFκB activation. T-pIC-mediated activation of NFκB reporter cells previously transiently transfected with viral gene constructs was not assessed because we were unable to obtain sufficient T-pIC-mediated activation of

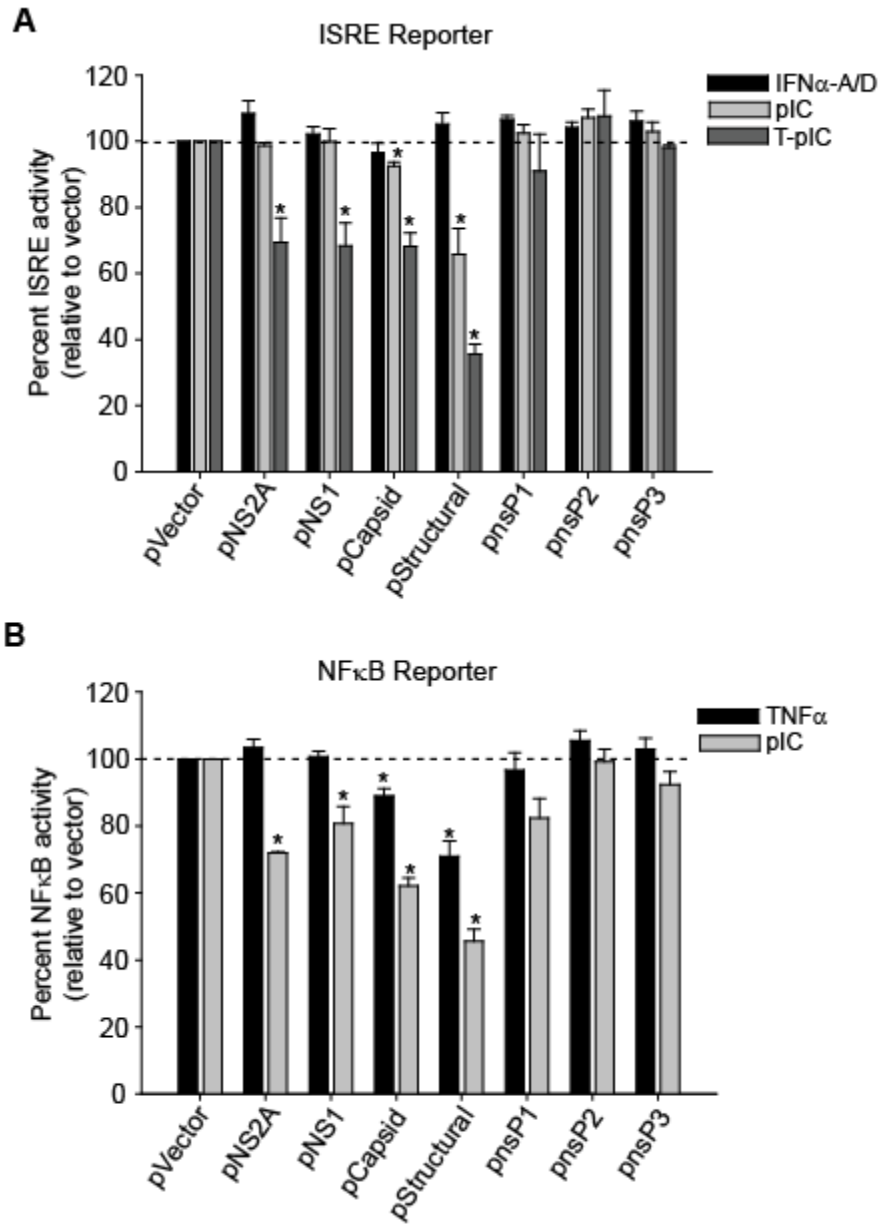

Figure 3.11. WEEV capsid inhibits neuronal PRR signaling. A and B. BE(2)-C/m ISRE (A) and NFκB (B) reporter cells were transfected with a vector control or expression constructs containing the WNV genes pNS2A and pNS1, or the WEEV genes pCapsid, pStructural, pnsP1, pnsP2, or pnsP3. 48 hours post transfection cells were mock-stimulated or stimulated for 24 hours with IFNα-A/D (100 U/ml) (A only), TNFα (25 ng/ml) (B only), pIC (50 μg/ml), or T-pIC (700 ng/ml) (A only), and SEAP reporter activity was assessed and presented as percent of vector-transfected control cells. Mock stimulations did not induce SEAP activity and were omitted from the figure. Averages and SEMs are displayed from three independent trials. *p-value < 0.05.

previously transiently-transfected NFκB reporter cells. The inability of WNV NS2A and NS1 to inhibit pIC-mediated induction of a neuronal ISRE, while still inhibiting a T-pIC stimulation and a pIC-mediated activation of neuronal NFκB, is in contradiction with previous work. One explanation for the ISRE phenotype may be that the dose of pIC given was too strong to observe NS1- or NS2A-mediated inhibition. This is consistent with the fact that the T-pIC stimulation is a much less efficacious activator of neuronal ISRE than the pIC stimulation (44), and may have been a weak enough stimulation to observe inhibition mediated by NS2A and NS1. In addition, the ability of NS1 to inhibit TLR3 signaling has recently come into question (5). Since pCapsid and pStructural essentially mimicked the antiviral PRR pathway inhibitory capacity of live WEEV, we concluded that WEEV capsid was likely responsible for antiviral PRR pathway inhibition.

Viral gene expression from the cloned constructs was verified in a variety of ways. pNS1, pNS2A, pnsP1, pnsP2, and pnsP3 all contained a C-terminal V5 epitope tag, and their expression in neuronal cells was verified via western blotting (**Fig 3.12.A**). Transfection efficiency was monitored by co-transfection of a HA-tagged β-galactosidase and western blotting for HA (**Fig 3.12.A**). We were unable to find commercially-available antibodies sufficiently sensitive to detect any of the untagged WEEV structural genes in BE(2)-C/m cells at 24 or 48 hours post transfection, nor were we able to detect expression of a V5-tagged version of pCapsid in BE(2)-C/m cells. Importantly, the V5-tagged version of pCapsid also inhibited neuronal PRR pathways (**Supplemental Fig S3.11**). However, we

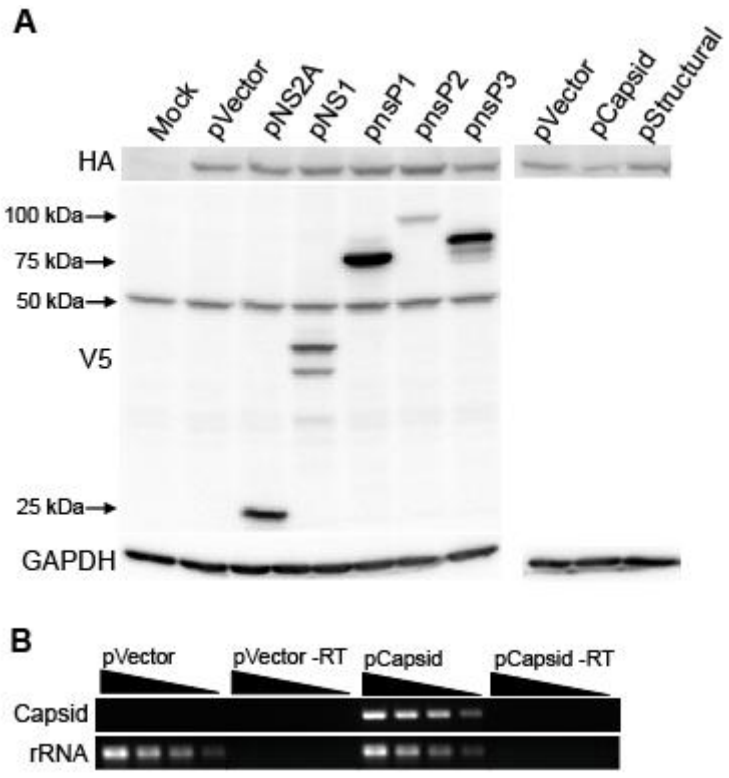

Figure 3.12. Viral gene expression analysis. **A.** Lysates from cells transfected for 48 hours, as described in figure 11, were analyzed by western blot for HA-tagged B-galactosidase, V5-tagged viral gene expression constructs, and GAPDH. **B.** BE(2)-C/m cells were transfected for 24 hours with an empty vector or an expression construct containing WEEV capsid. Samples were analyzed via RT-PCR for WEEV capsid or rRNA transcripts. "-RT" denotes controls where reverse-transcriptase was omitted. Data are representative of three independent trials for A and one for B.

did verify plasmid-mediated expression of WEEV capsid transcripts in BE(2)-C/m cells (**Fig 3.12.B**). These data indicated that plasmid-mediated capsid expression in neuronal cells was poor, but, despite the poor expression of WEEV capsid protein, transfection of pCapsid was sufficient to inhibit PRR signaling.

WEEV Capsid-Mediated Inhibition of Host Gene Expression

It is well documented that the capsid protein of the new world alphavirus Venezuelan equine encephalitis virus (VEEV), a close relative to WEEV, inhibits host gene expression (25, 26). Given our inability to visualize plasmid-mediated WEEV capsid protein expression in neuronal cells, we began to suspect that WEEV capsid may auto inhibit its own expression when under the control of a host-dependent promoter. To test this, we asked if capsid expression from pCapsid, which also contains a T7 promoter, could be enhanced in cells expressing bacteriophage T7 RNA polymerase. To accomplish this, BHK21 and BHK21 cells stably expressing a T7 bacteriophage RNA polymerase (BHK21-T7/C3) were transfected with an empty vector, pCapsid, pStructural, or a T7-driven WEEV replicon with the N-terminal 27 residues of capsid fused to YFP (pWEErep-YFP) which served as a positive control for our capsid antibody and T7 function. Whole cell lysates were collected 24 and 48 hours later and immunoblotted with a mouse ascites fluid generated from a WEEV-infected animal that we had previously determined recognized capsid. Transfection efficiency was monitored by co-transfecting a HA-tagged β-galactosidase and western blotting for HA. Surprisingly, WEEV capsid (approximately 30 kDa) was

visualized in both BHK21 and BHK21-T7/C3 cells transfected with pCapsid or pStructural at 24 hours with slightly more capsid being expressed from pCapsid than pStructural, whereas replicon-driven expression of capsid was appropriately observed only in BHK21-T7/C3 cells (**Fig 3.13.A**). However, by 48 hours post transfection, capsid expression was undetectable or extremely reduced in BHK21 cells. In contrast, capsid expression 48 hours post transfection in BHK21-T7/C3 cells was maintained (**Fig 3.13.A**), suggesting that capsid undergoes autoinhibition when controlled by mammalian nuclear promoters. In agreement with this, HA-tagged β-galactosidase expression, which was controlled by the same hybrid promoter region as pCapsid and pStructural, was reduced by capsid expression, but β-galactosidase expression was relatively even for matched transfections between BHK21 and BHK21-T7/C3 cells at 24 hours post transfection. In comparison to the 24 hours time point, expression of β-galactosidase 48 hours post transfection in BHK21 cells co-transfected with pCapsid or pStructural was undetectable or extremely reduced, whereas in the BHK21-T7/C3 cells, levels of β-galactosidase were significantly higher than in the identically transfected parental BHK21 cells 48 hours post transfection. Furthermore, sustained, high-level expression of capsid induced a cytopopathic effect observed 48 hours after pCapsid transfection of BHK21-T7/C3 cells (**Supplemental Fig S3.12**). These data indicated that pCapsid is capable of producing WEEV capsid protein and that WEEV capsid is capable of inhibiting the expression of genes controlled by mammalian nuclear promoters. These

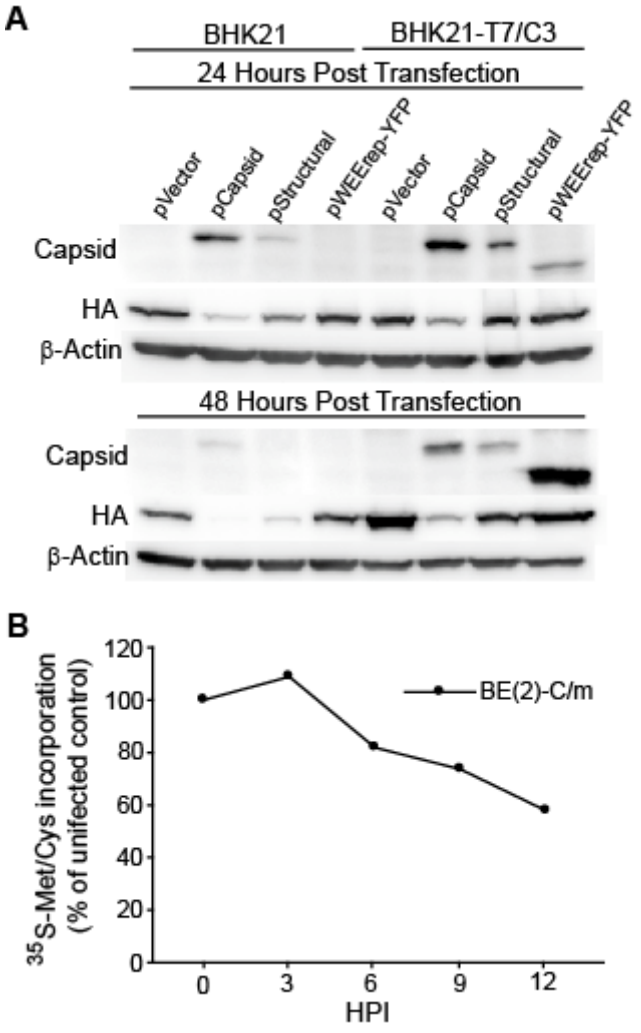

Figure 3.13. WEEV capsid-mediated inhibition of host gene expression. A. Identical numbers of BHK21 or BHK21 cells stably expressing T7 RNA polymerase (BHK21-T7/C3) were seeded overnight followed by transfection with a vector control, pCapsid, pStructural, or a T7-controlled WEEV replicon (pWEErep-YFP). Whole cell lysates were collected 24 and 48 hours post transfection and subjected to western blot analysis. Transfection efficiency was approximately 65% in both lines 24 hours post transfection with a GFP reporter (data not shown). **B.** BE(2)-C/m cells were infected with WEEV at an MOI of 10, labeled with 50 µCi per ml ^{35}S-Met/Cys for 30 min prior to harvesting at 3, 6, 9, and 12 hpi, and lysates were analyzed by SDS-PAGE and fluorography. Translation of a cellular protein at approximately 45 kDa was quantitated by densitometry, and results are expressed as the percentage of uninfected controls. Data are representative of two trials for A and four for B.

data, along with the fact that we could not detect capsid in BE(2)-C/m cells transfected with pCapsid, yet transfection with this construct inhibited neuronal PRR signaling, suggest that relatively little capsid expression was required to inhibit neuronal antiviral PRR signal transduction. The ability of small amounts of WEEV capsid to inhibit PRR signaling is consistent with the early inhibition of antiviral PRR signaling in WEEV-infected neurons (**Fig 3.9.C**), a time when capsid expression is relatively low.

The data in **Figure 3.13.A** suggested that WEEV capsid inhibits host gene expression. To determine if this may contribute to WEEV-mediated inhibition of PRR signaling, we first assessed, in neuronal cells, the kinetics of WEEV-mediated host translational shut down, which is often kinetically similar to alphavirus-mediated inhibition of host translation (14). To achieve this, BE(2)-C/m cells were labeled with ^{35}S-Met/Cys at varying times post WEEV infection (MOI 10), and analyzed by SDS-PAGE and fluorography. WEEV infection of neuronal cells suppressed host protein synthesis by just 25% compared to uninfected controls 9 hours post infection (**Fig 3.13.B**). However, WEEV suppressed antiviral PRR signaling by approximately 65% (**Fig 3.9.C** densitometry of IFNβ RT-PCR) at 7 hours post infection with a ten-fold lower inoculum, suggesting that host translational shut off was not likely to be the sole mechanism for capsid-mediated inhibition of antiviral PRR signaling.

Capsid Inhibits Neuronal Antiviral PRR Signaling After IRF3 Activation

To further characterize at what point WEEV capsid inhibits antiviral PRR signal transduction, we tested the ability of capsid to inhibit neuronal PRR pathways activated by expression of PRR pathway components that drive signaling from distinct points within the PRR pathway. Specifically, ISRE reporter neuronal cells were stimulated by transfecting an empty vector (pEmpty), MDA5 (pMDA5), constitutively-active TRIF mutant (psa.TRIF), or a constitutively-active IRF3 mutant (psa.IRF3) along with either a vector control (pVector), pnsP1, pDN.IRF3, pCapsid, or pStructural and an HA-tagged β-galactosidase to monitor transfection efficiency (**Fig 3.14.A**). As predicted, co-transfection of pDN.IRF3 with psa.TRIF or pMDA5 inhibited ISRE activation, whereas co-transfection of pDN.IRF3 with psa.IRF3 was unable to inhibit ISRE induction. Co-transfection of either pCapsid or pStructural with either psa.TRIF, pMDA5, or psa.IRF3 inhibited ISRE activation, where pCapsid had greater PRR pathway inhibitory activity than pStructural when co-transfected with psa.TRIF or psa.IRF3. pNS1 and pnsP1 had no inhibitory activity. Expression of constitutively-active TRIF, MDA5, constitutively-active IRF3, and the transfection efficiency control β-galactosidase was confirmed by western blot analysis (**Fig 3.14.B**). Of note, transfection of psa.TRIF, pMDA5, or psa.IRF3 reduced expression of β-galctosidase with psa.IRF3 and pMDA5 having the most and least dramatic effect respectively. Transfection of capsid reduced expression of constitutively-active TRIF, MDA5, and constitutively-active IRF3 by 80, 50, and 10%, respectively, relative to an empty vector (compare lane 2 to 8, lane 3 to 9, and lane 4 to 10). In comparison,

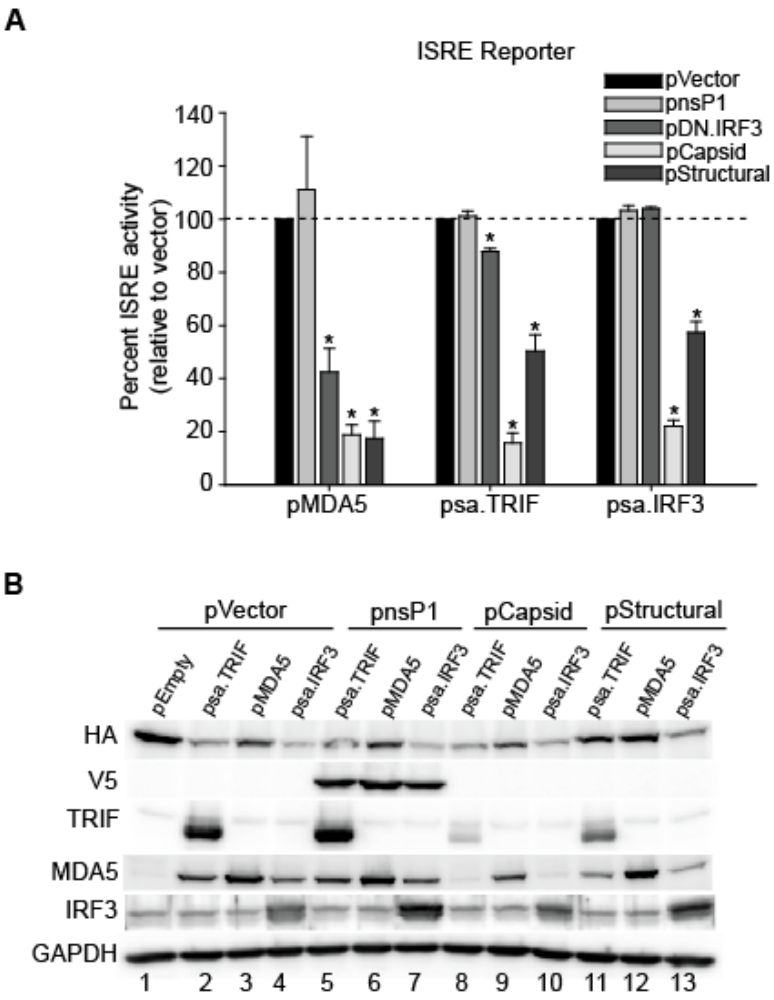

Figure 3.14. WEEV capsid inhibits neuronal antiviral PRR signaling after IRF3 activation. A. BE(2)-C/m ISRE reporter cells were co-transfected with a HA-tagged β-galactosidase to monitor transfection efficiency as well as an empty vector (pEmpty) or the PRR pathway signaling components constitutively active MDA5 (pMDA5), TRIF (psa.TRIF), and constitutively active IRF3 (psa.IRF3). To assess the ability of WEEV capsid to inhibit PRR signaling driven by the above PRR signaling components, cells were co-transfected with a negative vector control (pVector), pnsP1, the positive dominant negative IRF3 (pDN.IRF3) control, pCapsid, or pStructural. SEAP reporter activity was measured 48 hours later and expressed as percent of pVector-transfected controls. pEmpty-transfected cells failed to induce SEAP activity and were omitted from the figure. **B.** Lysates from the transfected cells described above were subject to western blot analysis for TRIF, MDA5, IRF3, HA, and GAPDH. Densitometry (44) was used to quantitate relative expression of proteins indicated in the text. Averages and SEMs are displayed from three independent trials for A. Data are representative of two trials for B. **p*-value < 0.05.

transfection of pStructural reduced expression of constitutively-active TRIF, MDA5, and constitutively-active IRF3 by 45, 5, and 0%, respectively, relative to an empty vector (compare lane 2 to 11, lane 3 to 12, and lane 4 to 13). Therefore, we cannot rule out a role for capsid-mediated inhibition of host gene expression as a mechanism for inhibition of PRR signaling, especially when PRR signal transduction was activated by constitutively-active TRIF overexpression; however, capsid-mediated reduction of 0-10% for constitutively-active IRF3 expression is unlikely to solely account for the capsid-dependent 80-90% inhibition of PRR signaling driven by constitutively-active IRF3 overexpression. These data further confirmed that WEEV capsid blocks antiviral PRR signaling and that it does so after IRF3 activation.

A WEEV Structural Gene, Likely Capsid, Inhibits IRF3 Nuclear Translocation

Venezuelan equine encephalitis virus capsid was recently shown to inhibit nuclear translocation by disrupting nuclear pore function (3, 4), and attenuated strains of VEEV blocked pores less efficiently (3). In addition, strong VEEV capsid-mediated blockade of nuclear translocation was observed just 4 hours post infection, whereas strong inhibition of cellular transcription was delayed until 10-24 hours post infection (3). These data correlate nicely with our results regarding WEEV inhibition of antiviral PRR signaling and host gene shut off (**Figures 3.9.C and 3.13.B**). To determine if disruption of nuclear translocation contributes to WEEV capsid-dependent inhibition of PRR signaling, we asked if

WEEV capsid inhibited nuclear translocation of IRF3 following a poly(I-C) stimulation. To achieve this, BE(2)-C/m cells were transfected with an empty vector or pStructural. pStructural was used as opposed to pCapsid because pStructural had a greater inhibitory capacity against a poly(I-C) stimulation and affected host gene expression less than pCapsid (**Figures 3.11 and 3.14**), which may be due to different dynamics for capsid expression and autoinhibition mediated by capsid expressed from pStructural versus pCapsid. As before, cells were co-transfected with a HA-tagged β-galactosidase to monitor transfection efficiency. Forty-eight hours post transfection, BE(2)-C/m cells were mock stimulated or stimulated with pIC for 2.5 or 5 hours, separated into cytosolic and nuclear fractions, and analyzed by western blotting (**Fig 3.15.A**). Immunoblotting for HA revealed uniform transfections and, as expected, a predominantly cytosolic localization of β-galactosidase. In contrast, the nuclear marker Oct-1 was primarily present in the nuclear fractions, and β-actin expression was present in both the cytosolic and nuclear fractions. Throughout the time-course, IRF3 expression was predominantly cytosolic, but upon poly(I-C) stimulation, IRF3 accumulated in the nucleus of vector-transfected cells but not pStructural-transfected cells. These data suggested that a WEEV structural gene, possibly capsid, inhibits IRF3 nuclear translocation.

To test if WEEV capsid, expressed in the absence of WEEV envelope proteins, inhibited IRF3 nuclear translocation, we co-transfected BE(2)-C/m cells

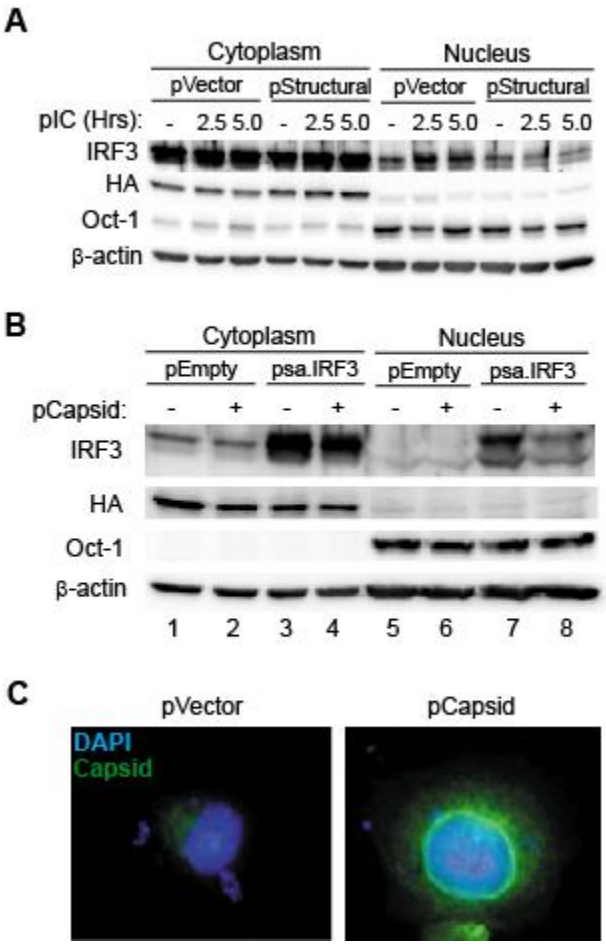

Figure 3.15. A WEEV structural gene, possibly capsid, inhibits IRF3 nuclear translocation. A. BE(2)-C/m cells were transfected with a vector control or pStructural for 48 hours followed by mock stimulation or stimulation with pIC (50 μg/ml) for 2.5 or 5 hours. Cells were also co-transfected with an HA-tagged β-galactosidase transfection control. Samples were separated into cytosolic and nuclear fractions and subjected to western blot analysis for IRF3, HA, β-actin, and Oct-1. Blots were visualized via chemiluminescence using HRP-conjugated secondary antibodies; however, assessment of IRF3 was achieved by amplifying with a biotin-conjugated antibody and visualized using HRP-conjugated streptavidin. **B.** BE(2)-C/m cells were transfected with a vector control or pCapsid along with an empty vector or psa.IRF3. Cells were also co-transfected with an HA-tagged β-galactosidase transfection control. 24 hours later cells were processed and analyzed as in A. **C.** BHK21-T7/C3 cells were transfected with a vector control or pCapsid and stained for WEEV capsid via immunofluorescence. Total magnification is 1000X. Data are representative of one trial for A, four for B, and one for C.

with either an empty vector or psa.IRF3 along with either a control vector or pCapsid. We used psa.IRF3 as a PRR stimulus as opposed to psa.TRIF or pMDA5 because pCapsid inhibited constitutively active IRF3 expression the least (**Fig 3.14.B**). Twenty-four hours post transfection, lysates were harvested, separated into cytosolic and nuclear fractions, and analyzed by western blotting (**Fig 3.15.B**). Transfection of pCapsid reduced the expression of constitutively active IRF3 by 20% relative to a vector control (densitometry of lane 4 versus 3). However, transfection of pCapsid reduced the nuclear accumulation of constitutively active IRF3 by 40% relative to a vector control (densitometry of lane 8 versus lane 7: $p < 0.05$ when comparing the ratio of IRF3 in the cytoplasmic fraction to that in the nuclear fraction). These data indicated that WEEV capsid may inhibit IRF3 nuclear translocation in neuronal cells.

To assess where capsid is expressed in cells and to begin asking if it might also inhibit nuclear pore function, we performed immunofluorescence staining for WEEV capsid in BHK21-T7/C3 cells transfected with a vector control or WEEV capsid. We viewed cells via epifluorescence, and in most transfected cells, we observed cytoplasmic capsid staining with more intense punctuate staining in a region surrounding nuclei. In approximately 25% of cells, we also observed intense nuclear staining. Importantly, an intense signal surrounding DAPI-stained nuclei was observed in approximately 30% of transfected cells (**Fig 3.15.C**), a pattern which is reminiscent of VEEV capsid localization to the nuclear pore complex (3). Together these data demonstrated that a WEEV structural gene, likely capsid, inhibits IRF3 nuclear translocation potentially by disabling

nuclear pores, and that this activity, along with suppression of host gene expression, may account for the ability of WEEV to inhibit neuronal cell antiviral PRR signaling.

Discussion

Early cellular innate immune responses are often vital for effective pathogen control and may ameliorate the destruction of CNS neurons by neurotropic arboviruses, the extent of which is often an important determinant in the severity and clinical outcome of these infections. In this report, we examined the functional impact of previously identified neuronal PRR pathways (44) on neurotropic viral infections primarily using WEEV as a model neurotropic arbovirus, whose primary target cell type within the CNS is the neuron. We drew five main conclusions which are graphically represented in **Figure 3.16**. First, WEEV activated neuronal PRR pathways via recognition by RIG-I and/or MDA5 and subsequent induction of an IRF3-dependent transcriptional response. Second, IRF3 mediated a neuronal cytoprotective response to WEEV which was likely dependent on IRF3-mediated induction of cell-intrinsic factors with cytoprotective properties and independent of autocrine/paracrine antiviral type-I IFN signaling. Third, the neurotropic arboviruses, WEEV, SLEV, and LACV all specifically inhibited neuronal antiviral PRR pathways at early times post infection. Fourth, WEEV capsid was the main WEEV gene responsible for inhibition of neuronal antiviral PRR pathways. Fifth, WEEV capsid likely inhibited neuronal antiviral PRR signaling by a combination of early inhibition of IRF3 nuclear translocation and late inhibition of host macromolecular synthesis. These results indicated that neuronal PRR-pathway responses may be important determinants of neurotropic arbovirus pathogenesis.

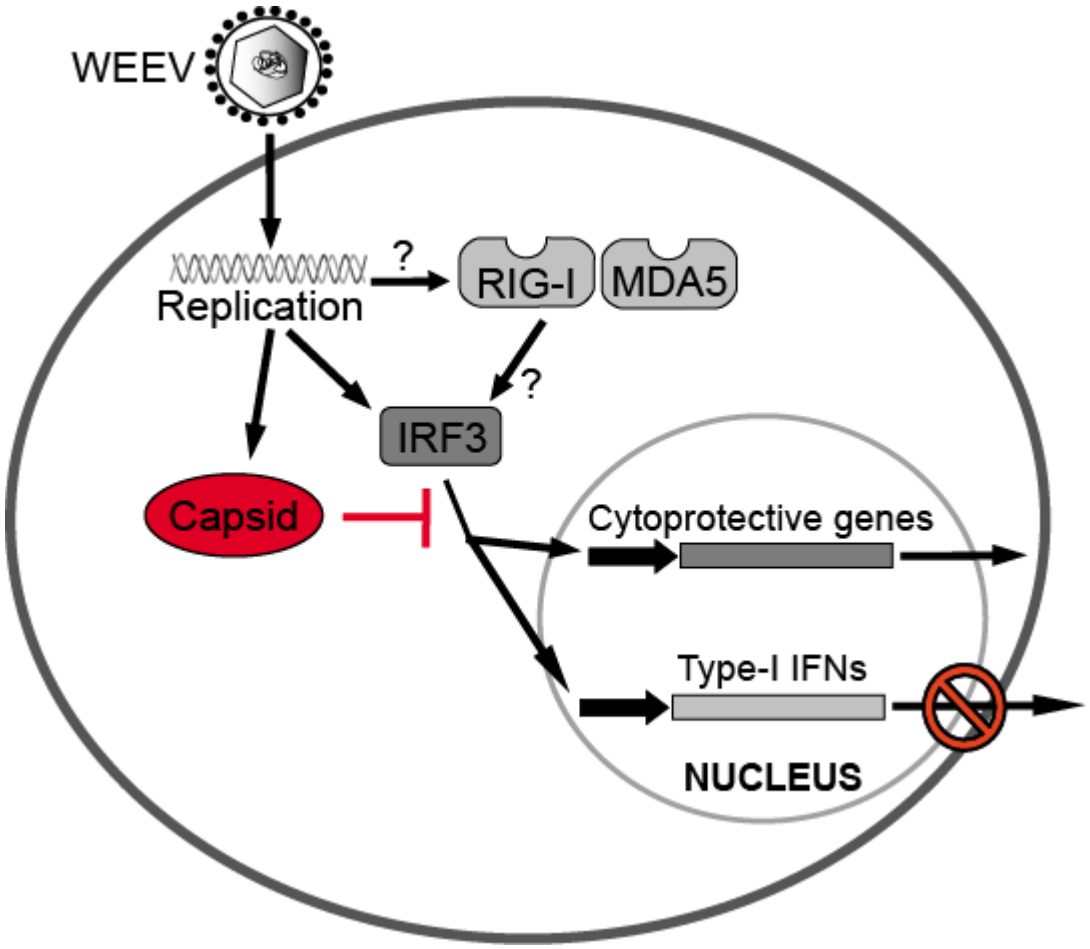

Figure 3.16. Interactions of neuronal PRR pathways with WEEV. Following infection and replication of neuronal cells, WEEV may be recognized by RIG-I and MDA5, which mediate a transcriptional and cytoprotective response, depending on the neuronal culture model. Future work using alternative neuronal models will have to definitively assess the role these two proteins play in neuronal PRR responses to WEEV. On the other hand, IRF3 mediates both a transcriptional and cytoprotective response to WEEV in neurons. Importantly, WEEV capsid inhibits antiviral PRR signaling in neurons possibly by inhibiting IRF3 nuclear translocation at early times post infection and shutting down host gene expression at late times post infection.

Previous studies investigating the role of PRR pathway signaling components on alphavirus infections suggested that old world alphaviruses, which are not naturally encephalitic, may be recognized by RIG-I (10) and MDA5 (48) and require TBK1 for activation of IRF3 (10). In contrast, the role of individual PRR signaling components on new world equine encephalitic alphaviruses has been much less studied, but it is known that equine encephalitic alphaviruses increase serum levels of type-I IFNs in mice (24, 33), and VEEV induces neuronal type-I IFN transcription (53, 60). In this report, we examined the role of previously identified neuronal PRR signaling components (44) on a WEEV infection and found that RIG-I, MDA5, and IRF3 mediate a neuronal transcriptional response; however, only IRF3 consistently mediated a cytoprotective response to WEEV in both human neuronal cells and primary neurons, suggesting that cytosolic recognition of WEEV resulting in neuronal protection is likely complex and possibly redundant. To clarify the role of individual neuronal PRR signaling components on neuron-protective responses to neurotropic arboviruses, future studies will require neuron-specific conditional knock-out mouse models to specifically analyze neuronal PRR responses in the neuron's natural environment.

In contrast to encephalitic alphaviruses, the neuronal PRR response to the neurotropic arbovirus WNV is fairly well characterized (15-17, 19, 57). Similar to what we observed with WEEV, $IRF3^{-/-}$ primary neurons showed reduced induction of type-I IFNs following WNV infection and only modest increases in titers at late time points (15); therefore, it would be interesting to determine if a

neuronal IRF3-dependent cytoprotective response to WNV exists, especially since its relative, SLEV, induced a greater CPE in dominant negative IRF3 overexpressing neuronal cells.

Many antiviral effector genes for old world alphaviruses have been identified (63), but to our knowledge, few have been tested for antiviral activity against intact new world alphaviruses (6). Here, we identified the WEEV-mediated, IRF3-dependent induction of several reported antiviral and potentially cytoprotective genes in neurons. shRNA-mediated depletion of the most induced putative effector, OASL, revealed that OASL protects neuronal cells from a LACV-mediated CPE, but not from a WEEV- or SLE-mediated CPE. To our knowledge, this is the first demonstration of an OASL-mediated cytoprotective effect in response to LACV, or any bunyavirus, in neuronal cells. Little is known about how OASL exerts its antiviral and potentially related neuronal cytoprotective effect, but the antiviral activity of OASL against encephalomyocarditis virus, a picornavirus, requires its ubiquitin-like domain. Furthermore, the OASL-mediated antiviral effect against encephalomyocarditis virus is thought to be drastically different than the classic OAS genes because it lacks any 2'-5' oligoadenylate synthetase activity (40). The next most WEEV-induced, IRF3-dependent, putative cytoprotective gene was MxB, which is currently being investigated for cytoprotective activity against neurotropic arboviruses. In humans, MxB, unlike MxA, does not appear to have antiviral activity. Moreover, MxB hasn't been tested against most neurotropic arboviruses, and the high similarity between MxA and MxB suggests that MxB

may have an unobserved antiviral role. MxA exerts its antiviral effect by disrupting the trafficking of viral components, which results in abrogated viral replication (50). In contrast, the best described cellular function of MxB is to enhance nuclear import (32). This suggests a particularly attractive hypothesis in which MxB may achieve a putative cytoprotective effect against WEEV by counteracting WEEV capsid's ability to inhibit nuclear translocation of IRF3. Regardless, future studies will be required to further clarify the neuronal cytoprotective effects of these genes in response to neurotropic arboviruses. These future studies should be done in vivo as much as possible because important differences between tissue culture and animal models have been observed for antiviral effector responses to old world alphaviruses (63).

Many viruses block antiviral PRR signaling including the neurotropic arboviruses WNV (18, 22, 38, 59) and LACV (7). Here we confirm the PRR pathway inhibitory capability of LACV and also demonstrate that WEEV and SLEV block neuronal antiviral PRR signaling. We are unaware of any documented ability of SLEV to inhibit antiviral PRR signaling, and future work will be required to determine how SLEV achieves this, and if it does so in a manner similar to the related flavivirus WNV.

Previous studies demonstrated that a panel of old and new world alphaviruses failed to induce type-I IFNs in MEFs and that the old world alphavirus, Sindbis virus, blocked SeV and poly(I-C)-mediated induction of type-I IFNs (10). However, the PRR pathway inhibition by Sindbis virus and WEEV are in conflict with reports documenting that many new and old world alphaviruses

increase serum levels of type-I IFNs in mice (14, 24). These conflicting data suggest that, in vivo, alphavirus antiviral PRR pathway countermeasures may not be completely effective in all cell types.

We mapped the WEEV-mediated inhibition of neuronal antiviral PRR signaling to the capsid gene, which in the related new world alphaviruses, VEEV and eastern equine encephalitis virus (EEEV), blocks host transcription (25, 26). VEEV capsid also blocks nuclear translocation by "clogging" nuclear pores, and an attenuated VEEV strain blocked nuclear pores less efficiently leaving others to postulate that capsid-mediated blockade of nuclear pores and inhibition of host transcription may inhibit antiviral pathways (3, 4). Accordingly, we tested and confirmed that a WEEV structural gene, likely capsid, inhibits IRF3 nuclear import and that WEEV capsid inhibits host gene expression, but future studies will have to definitively assess whether WEEV capsid localizes to and disrupts nuclear pores. Future studies will also have to rule out a role for WEEV envelope proteins in the WEEV-mediated disruption of IRF3 nuclear translocation. Since capsid expression had no effect on type-I IFN signaling and also blocked a TNFα-mediated activation of NFκB in neuronal cells, future studies will also have to determine the selectivity and specificity of WEEV-mediated inhibition of nuclear import.

Based on these data, we speculate that WEEV capsid blocks neuronal antiviral PRR signaling early by inhibiting nuclear translocation and late through a combined inhibition of nuclear translocation and inhibition of host gene expression. We base this hypothesis on the observation that IRF3 nuclear

translocation was robustly inhibited at early times post WEEV infection (**Fig 3.15.A**), and this correlated well with early inhibition of neuronal antiviral PRR signaling (**Fig 3.9.C**). In contrast, robust inhibition of host gene expression occurred much later (**Fig 3.13.B**).

Despite the ability of WEEV to inhibit neuronal antiviral PRR signaling, a functional cell-intrinsic, IRF3-dependent, type-I IFN- independent, neuronal cytoprotective response remained. One explanation for this paradox could be that the cytoprotective pathway is more responsive to low levels of PRR signal transduction reaching the nucleus than the antiviral type-I IFN-dependent pathway. However, this hypothesis will need to be specifically addressed. Finally, future studies should also confirm that neuronal PRR pathways are indeed inhibited from responding to a WEEV stimulus, as opposed to a poly(I-C) stimulus, by identifying WEEV capsid mutants or generating WEEV virus-like particles lacking structural genes that robustly induce antiviral type-I IFNs in neuronal cells. In conclusion, our data indicate that neuronal PRR pathways may be important determinants of neurotropic arbovirus pathogenesis and that neuronal PRR pathways, and viral countermeasures to them, may be exploited to develop more efficacious vaccines and anti-neurotropic arboviral treatments.

References

1. **Alsharifi, M., A. Mullbacher, and M. Regner.** 2008. Interferon type I responses in primary and secondary infections. Immunol Cell Biol **86:**239-45.
2. **Andersen, J., S. VanScoy, T. F. Cheng, D. Gomez, and N. C. Reich.** 2008. IRF-3-dependent and augmented target genes during viral infection. Genes Immun **9:**168-75.
3. **Atasheva, S., A. Fish, M. Fornerod, and E. I. Frolova.** 2010. Venezuelan equine Encephalitis virus capsid protein forms a tetrameric complex with CRM1 and importin alpha/beta that obstructs nuclear pore complex function. J Virol **84:**4158-71.
4. **Atasheva, S., N. Garmashova, I. Frolov, and E. Frolova.** 2008. Venezuelan equine encephalitis virus capsid protein inhibits nuclear import in Mammalian but not in mosquito cells. J Virol **82:**4028-41.
5. **Baronti, C., J. Sire, X. de Lamballerie, and G. Querat.** 2010. Nonstructural NS1 proteins of several mosquito-borne Flavivirus do not inhibit TLR3 signaling. Virology **404:**319-30.
6. **Bick, M. J., J. W. Carroll, G. Gao, S. P. Goff, C. M. Rice, and M. R. MacDonald.** 2003. Expression of the zinc-finger antiviral protein inhibits alphavirus replication. J Virol **77:**11555-62.
7. **Blakqori, G., S. Delhaye, M. Habjan, C. D. Blair, I. Sanchez-Vargas, K. E. Olson, G. Attarzadeh-Yazdi, R. Fragkoudis, A. Kohl, U. Kalinke, S. Weiss, T. Michiels, P. Staeheli, and F. Weber.** 2007. La Crosse bunyavirus nonstructural protein NSs serves to suppress the type I interferon system of mammalian hosts. J Virol **81:**4991-9.
8. **Borden, E. C., G. C. Sen, G. Uze, R. H. Silverman, R. M. Ransohoff, G. R. Foster, and G. R. Stark.** 2007. Interferons at age 50: past, current and future impact on biomedicine. Nat Rev Drug Discov **6:**975-90.
9. **Burdeinick-Kerr, R., J. Wind, and D. E. Griffin.** 2007. Synergistic roles of antibody and interferon in noncytolytic clearance of Sindbis virus from different regions of the central nervous system. J Virol **81:**5628-36.
10. **Burke, C. W., C. L. Gardner, J. J. Steffan, K. D. Ryman, and W. B. Klimstra.** 2009. Characteristics of alpha/beta interferon induction after infection of murine fibroblasts with wild-type and mutant alphaviruses. Virology **395:**121-32.
11. **Cameron, J. S., L. Alexopoulou, J. A. Sloane, A. B. DiBernardo, Y. Ma, B. Kosaras, R. Flavell, S. M. Strittmatter, J. Volpe, R. Sidman, and T. Vartanian.** 2007. Toll-like receptor 3 is a potent negative regulator of axonal growth in mammals. J Neurosci **27:**13033-41.
12. **Castorena, K. M., D. C. Peltier, W. Peng, and D. J. Miller.** 2008. Maturation-dependent responses of human neuronal cells to western equine encephalitis virus infection and type I interferons. Virology **372:**208-20.
13. **Castorena, K. M., S. A. Weeks, K. A. Stapleford, A. M. Cadwallader, and D. J. Miller.** 2007. A functional heat shock protein 90 chaperone is

essential for efficient flock house virus RNA polymerase synthesis in Drosophila cells. J Virol **81:**8412-20.

14. **Cruz, C. C., M. S. Suthar, S. A. Montgomery, R. Shabman, J. Simmons, R. E. Johnston, T. E. Morrison, and M. T. Heise.** 2010. Modulation of type I IFN induction by a virulence determinant within the alphavirus nsP1 protein. Virology **399:**1-10.
15. **Daffis, S., M. A. Samuel, B. C. Keller, M. Gale, Jr., and M. S. Diamond.** 2007. Cell-specific IRF-3 responses protect against West Nile virus infection by interferon-dependent and -independent mechanisms. PLoS Pathog **3:**e106.
16. **Daffis, S., M. A. Samuel, M. S. Suthar, M. Gale, Jr., and M. S. Diamond.** 2008. Toll-like receptor 3 has a protective role against West Nile virus infection. J Virol **82:**10349-58.
17. **Daffis, S., M. A. Samuel, M. S. Suthar, B. C. Keller, M. Gale, Jr., and M. S. Diamond.** 2008. Interferon regulatory factor IRF-7 induces the antiviral alpha interferon response and protects against lethal West Nile virus infection. J Virol **82:**8465-75.
18. **Daffis, S., M. S. Suthar, M. Gale, Jr., and M. S. Diamond.** 2009. Measure and countermeasure: type I IFN (IFN-alpha/beta) antiviral response against West Nile virus. J Innate Immun **1:**435-45.
19. **Daffis, S., M. S. Suthar, K. J. Szretter, M. Gale, Jr., and M. S. Diamond.** 2009. Induction of IFN-beta and the innate antiviral response in myeloid cells occurs through an IPS-1-dependent signal that does not require IRF-3 and IRF-7. PLoS Pathog **5:**e1000607.
20. **Delhaye, S., S. Paul, G. Blakqori, M. Minet, F. Weber, P. Staeheli, and T. Michiels.** 2006. Neurons produce type I interferon during viral encephalitis. Proc Natl Acad Sci U S A **103:**7835-40.
21. **Detje, C. N., T. Meyer, H. Schmidt, D. Kreuz, J. K. Rose, I. Bechmann, M. Prinz, and U. Kalinke.** 2009. Local type I IFN receptor signaling protects against virus spread within the central nervous system. J Immunol **182:**2297-304.
22. **Diamond, M. S.** 2009. Virus and host determinants of West Nile virus pathogenesis. PLoS Pathog **5:**e1000452.
23. **Fredericksen, B. L., and M. Gale, Jr.** 2006. West Nile virus evades activation of interferon regulatory factor 3 through RIG-I-dependent and -independent pathways without antagonizing host defense signaling. J Virol **80:**2913-23.
24. **Gardner, C. L., C. W. Burke, M. Z. Tesfay, P. J. Glass, W. B. Klimstra, and K. D. Ryman.** 2008. Eastern and Venezuelan equine encephalitis viruses differ in their ability to infect dendritic cells and macrophages: impact of altered cell tropism on pathogenesis. J Virol **82:**10634-46.
25. **Garmashova, N., S. Atasheva, W. Kang, S. C. Weaver, E. Frolova, and I. Frolov.** 2007. Analysis of Venezuelan equine encephalitis virus capsid protein function in the inhibition of cellular transcription. J Virol **81:**13552-65.

26. **Garmashova, N., R. Gorchakov, E. Volkova, S. Paessler, E. Frolova, and I. Frolov.** 2007. The Old World and New World alphaviruses use different virus-specific proteins for induction of transcriptional shutoff. J Virol **81:**2472-84.
27. **Gitlin, L., L. Benoit, C. Song, M. Cella, S. Gilfillan, M. J. Holtzman, and M. Colonna.** 2010. Melanoma differentiation-associated gene 5 (MDA5) is involved in the innate immune response to Paramyxoviridae infection in vivo. PLoS Pathog **6:**e1000734.
28. **Griffin, D. E.** 2003. Immune responses to RNA-virus infections of the CNS. Nat Rev Immunol **3:**493-502.
29. **Gubler, D. J.** 2002. The global emergence/resurgence of arboviral diseases as public health problems. Arch Med Res **33:**330-42.
30. **Jackson, A. C., J. P. Rossiter, and M. Lafon.** 2006. Expression of Toll-like receptor 3 in the human cerebellar cortex in rabies, herpes simplex encephalitis, and other neurological diseases. J Neurovirol **12:**229-34.
31. **Kampmueller, K. M., and D. J. Miller.** 2005. The cellular chaperone heat shock protein 90 facilitates Flock House virus RNA replication in Drosophila cells. J Virol **79:**6827-37.
32. **King, M. C., G. Raposo, and M. A. Lemmon.** 2004. Inhibition of nuclear import and cell-cycle progression by mutated forms of the dynamin-like GTPase MxB. Proc Natl Acad Sci U S A **101:**8957-62.
33. **Konopka, J. L., J. M. Thompson, A. C. Whitmore, D. L. Webb, and R. E. Johnston.** 2009. Acute infection with venezuelan equine encephalitis virus replicon particles catalyzes a systemic antiviral state and protects from lethal virus challenge. J Virol **83:**12432-42.
34. **Kumar, H., T. Kawai, and S. Akira.** 2009. Pathogen recognition in the innate immune response. Biochem J **420:**1-16.
35. **Lafon, M., F. Megret, M. Lafage, and C. Prehaud.** 2006. The innate immune facet of brain: human neurons express TLR-3 and sense viral dsRNA. J Mol Neurosci **29:**185-94.
36. **Lammerding, J., P. C. Schulze, T. Takahashi, S. Kozlov, T. Sullivan, R. D. Kamm, C. L. Stewart, and R. T. Lee.** 2004. Lamin A/C deficiency causes defective nuclear mechanics and mechanotransduction. J Clin Invest **113:**370-8.
37. **Lee, M. S., and Y. J. Kim.** 2007. Signaling pathways downstream of pattern-recognition receptors and their cross talk. Annu Rev Biochem **76:**447-80.
38. **Liu, W. J., X. J. Wang, D. C. Clark, M. Lobigs, R. A. Hall, and A. A. Khromykh.** 2006. A single amino acid substitution in the West Nile virus nonstructural protein NS2A disables its ability to inhibit alpha/beta interferon induction and attenuates virus virulence in mice. J Virol **80:**2396-404.
39. **Ma, W., T. Tavakoli, E. Derby, Y. Serebryakova, M. S. Rao, and M. P. Mattson.** 2008. Cell-extracellular matrix interactions regulate neural differentiation of human embryonic stem cells. BMC Dev Biol **8:**90.

40. **Marques, J., J. Anwar, S. Eskildsen-Larsen, D. Rebouillat, S. R. Paludan, G. Sen, B. R. Williams, and R. Hartmann.** 2008. The p59 oligoadenylate synthetase-like protein possesses antiviral activity that requires the C-terminal ubiquitin-like domain. J Gen Virol **89:**2767-72.
41. **McKimmie, C. S., and J. K. Fazakerley.** 2005. In response to pathogens, glial cells dynamically and differentially regulate Toll-like receptor gene expression. J Neuroimmunol **169:**116-25.
42. **Menager, P., P. Roux, F. Megret, J. P. Bourgeois, A. M. Le Sourd, A. Danckaert, M. Lafage, C. Prehaud, and M. Lafon.** 2009. Toll-like receptor 3 (TLR3) plays a major role in the formation of rabies virus Negri Bodies. PLoS Pathog **5:**e1000315.
43. **Pankratz, M. T., X. J. Li, T. M. Lavaute, E. A. Lyons, X. Chen, and S. C. Zhang.** 2007. Directed neural differentiation of human embryonic stem cells via an obligated primitive anterior stage. Stem Cells **25:**1511-20.
44. **Peltier, D. C., A. Simms, J. R. Farmer, and D. J. Miller.** 2010. Human Neuronal Cells Possess Functional Cytoplasmic and TLR-Mediated Innate Immune Pathways Influenced by Phosphatidylinositol-3 Kinase Signaling. J Immunol **184:**7010-21.
45. **Peng, W., D. C. Peltier, M. J. Larsen, P. D. Kirchhoff, S. D. Larsen, R. R. Neubig, and D. J. Miller.** 2009. Identification of thieno[3,2-b]pyrrole derivatives as novel small molecule inhibitors of neurotropic alphaviruses. J Infect Dis **199:**950-7.
46. **Peverali, F. A., D. Orioli, L. Tonon, P. Ciana, G. Bunone, M. Negri, and G. Della-Valle.** 1996. Retinoic acid-induced growth arrest and differentiation of neuroblastoma cells are counteracted by N-myc and enhanced by max overexpressions. Oncogene **12:**457-62.
47. **Pichlmair, A., and C. Reis e Sousa.** 2007. Innate recognition of viruses. Immunity **27:**370-83.
48. **Pichlmair, A., O. Schulz, C. P. Tan, J. Rehwinkel, H. Kato, O. Takeuchi, S. Akira, M. Way, G. Schiavo, and C. Reis e Sousa.** 2009. Activation of MDA5 requires higher-order RNA structures generated during virus infection. J Virol **83:**10761-9.
49. **Prehaud, C., F. Megret, M. Lafage, and M. Lafon.** 2005. Virus infection switches TLR-3-positive human neurons to become strong producers of beta interferon. J Virol **79:**12893-904.
50. **Reichelt, M., S. Stertz, J. Krijnse-Locker, O. Haller, and G. Kochs.** 2004. Missorting of LaCrosse virus nucleocapsid protein by the interferon-induced MxA GTPase involves smooth ER membranes. Traffic **5:**772-84.
51. **Roth-Cross, J. K., S. J. Bender, and S. R. Weiss.** 2008. Murine coronavirus mouse hepatitis virus is recognized by MDA5 and induces type I interferon in brain macrophages/microglia. J Virol **82:**9829-38.
52. **Ryman, K. D., and W. B. Klimstra.** 2008. Host responses to alphavirus infection. Immunol Rev **225:**27-45.
53. **Schafer, A., A. C. Whitmore, J. L. Konopka, and R. E. Johnston.** 2009. Replicon particles of venezuelan equine encephalitis virus as a reductionist murine model for encephalitis. J Virol **83:**4275-86.

54. **Sidwell, R. W., and D. F. Smee.** 2003. Viruses of the Bunya- and Togaviridae families: potential as bioterrorism agents and means of control. Antiviral Res **57:**101-11.
55. **Stapleford, K. A., D. Rapaport, and D. J. Miller.** 2009. Mitochondrion-enriched anionic phospholipids facilitate flock house virus RNA polymerase membrane association. J Virol **83:**4498-507.
56. **Strauss, J. H., and E. G. Strauss.** 1994. The alphaviruses: gene expression, replication, and evolution. Microbiol Rev **58:**491-562.
57. **Suthar, M. S., D. Y. Ma, S. Thomas, J. M. Lund, N. Zhang, S. Daffis, A. Y. Rudensky, M. J. Bevan, E. A. Clark, M. K. Kaja, M. S. Diamond, and M. Gale, Jr.** 2010. IPS-1 is essential for the control of West Nile virus infection and immunity. PLoS Pathog **6:**e1000757.
58. **Wang, N., Q. Dong, J. Li, R. K. Jangra, M. Fan, A. R. Brasier, S. M. Lemon, L. M. Pfeffer, and K. Li.** 2010. Viral induction of the zinc finger antiviral protein is IRF3-dependent but NF-kappaB-independent. J Biol Chem **285:**6080-90.
59. **Wilson, J. R., P. F. de Sessions, M. A. Leon, and F. Scholle.** 2008. West Nile virus nonstructural protein 1 inhibits TLR3 signal transduction. J Virol **82:**8262-71.
60. **Yin, J., C. L. Gardner, C. W. Burke, K. D. Ryman, and W. B. Klimstra.** 2009. Similarities and differences in antagonism of neuron alpha/beta interferon responses by Venezuelan equine encephalitis and Sindbis alphaviruses. J Virol **83:**10036-47.
61. **Yoneyama, M., and T. Fujita.** 2009. RNA recognition and signal transduction by RIG-I-like receptors. Immunol Rev **227:**54-65.
62. **Zhang, S. C., M. Wernig, I. D. Duncan, O. Brustle, and J. A. Thomson.** 2001. In vitro differentiation of transplantable neural precursors from human embryonic stem cells. Nat Biotechnol **19:**1129-33.
63. **Zhang, Y., C. W. Burke, K. D. Ryman, and W. B. Klimstra.** 2007. Identification and characterization of interferon-induced proteins that inhibit alphavirus replication. J Virol **81:**11246-55.

Appendix to Chapter III: Supplemental Data

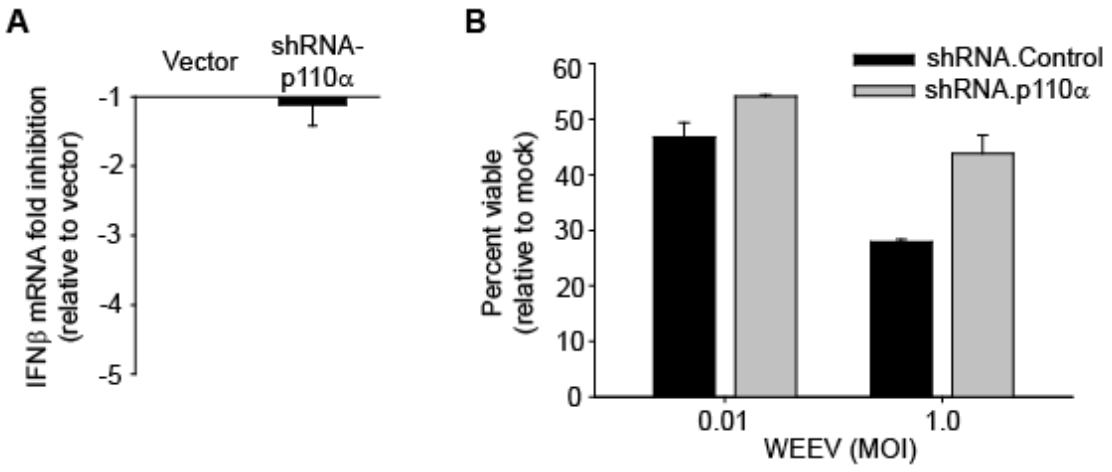

Supplemental Figure S3.1. Effect of PI3K p110α depletion on neuronal responses to WEEV. A. BE(2)-C/m cells stably expressing a vector control or shRNA targeting PI3K p110α were infected with WEEV (MOI 1) for 20 hours. RNA was harvested, and quantitative RT-PCR was used to assess IFNβ and rRNA transcript expression. **B.** BE(2)-C/m described in A were mock infected or infected with WEEV as indicated. 48 hours later cell viability was assessed by an MTT assay. Averages and SEMs are displayed from 2 trials for A and B.

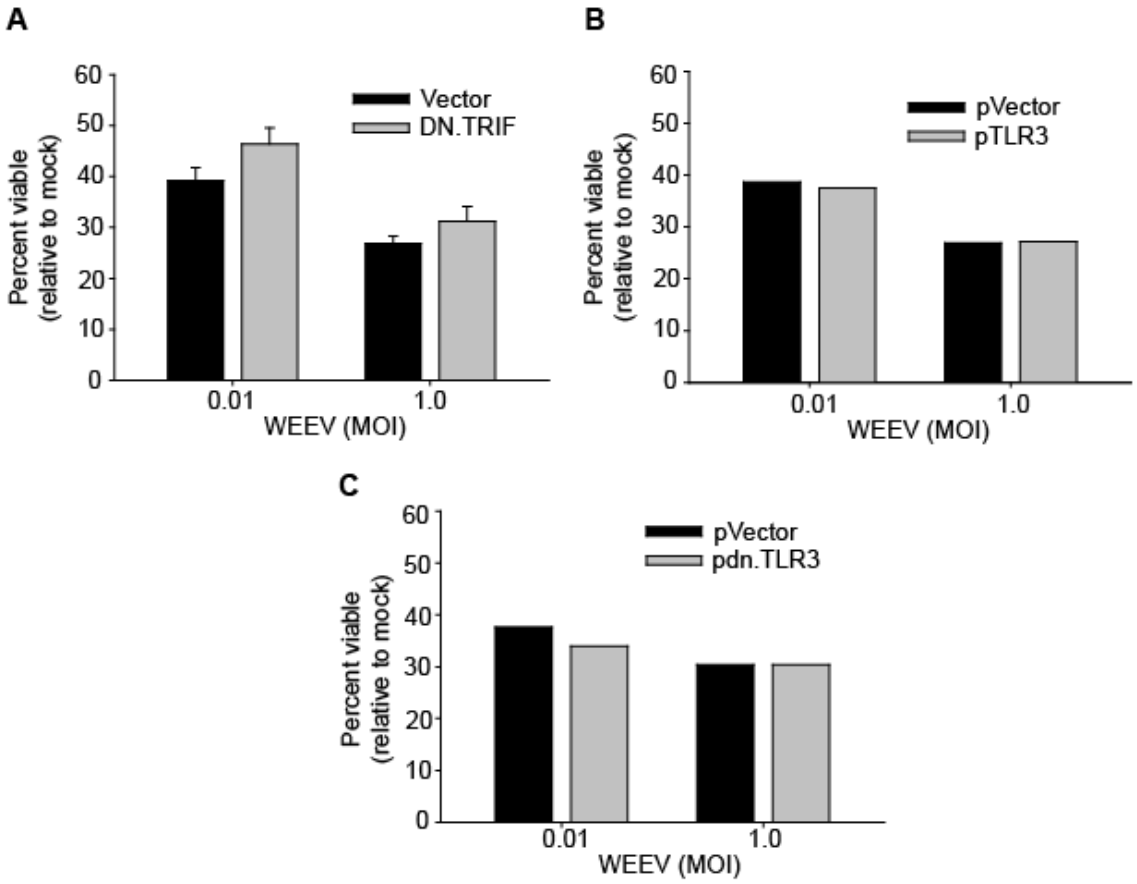

Supplemental Figure S3.2. TRIF and TLR3-independent neuronal response to WEEV. A. BE(2)-C/m cells stably overexpressing an empty vector or dominant negative TRIF were mock infected or infected with WEEV as indicated. Cell viability was assessed 48 hours later via an MTT assay. **B and C.** BE(2)-C/m cells were transfected with either a vector control (B and C), wild-type TLR3 (B), or dominant negative TLR3 (C). 48 hours after transfection cells were infected and analyzed as in A. Averages and SEMs are displayed from 3 independent trials for A. Representative experiments are displayed from 2 independent trials for B and C.

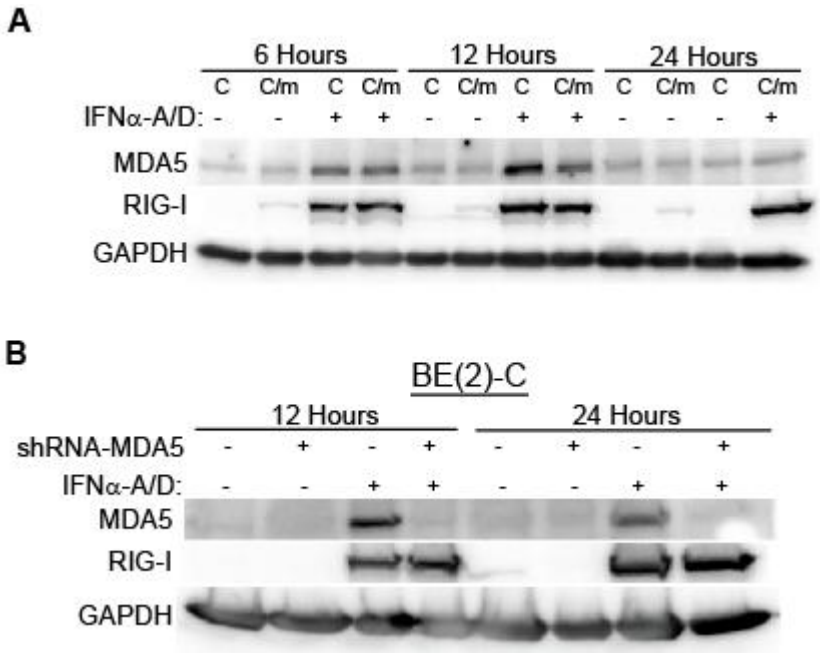

Supplemental Figure S3.3. IFN-mediated induction of MDA5 is transient relative to IFN-mediated induction of RIG-I in neuronal cells. A. BE(2)-C (C) or BE(2)-C/m (C/m) cells were mock stimulated or stimulated with IFNα-A/D (100 U/ml) for the indicated times. Lysates were collected and analyzed by Western blotting for MDA5, RIG-I, and GAPDH. **B.** BE(2)-C cells stably expressing a control shRNA or an shRNA targeting MDA5 were mock stimulated or stimulated with IFNα-A/D (1000 U/ml) for the indicated times. Lysates were collected and analyzed as in A. Data represent one trial.

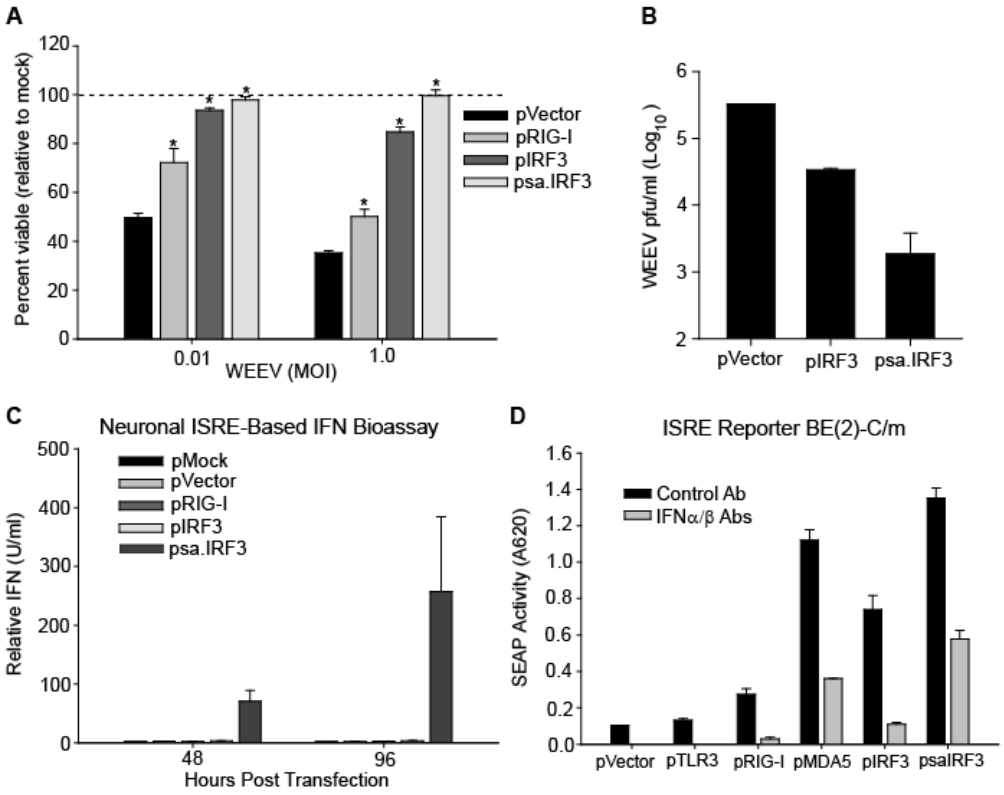

Supplemental Figure S3.4. Wild-type and constitutively active neuronal PRR pathway component-dependent responses to WEEV. A. BE(2)-C/m cells were transiently transfected with a vector control (pVector), wild-type RIG-I (pRIG-I), wilt-type IRF3 (pIRF3), or a constitutively active IRF3 (psa.IRF3) for 48 hours. Transfected cells were infected with WEEV as indicated, and viability was assessed 48 hours post infection via an MTT assay. **B.** BE(2)-C/m cells transiently overexpressing the indicated constructs were infected with WEEV (MOI 0.1). Supernatants were harvested 72 hours post infection, and WEEV titers were determined via a plaque assay. **C.** Supernatants from BE(2)-C/m cells transfected with the indicated constructs were harvested at the indicated times and stored at -80^{o} C. Thawed supernatants were serially diluted and used to stimulate BE(2)-C/m ISRE reporter cells. ISRE activation mediated by these supernatants was compared to a standard curve of IFNα-A/D-mediated activation of an ISRE in neuronal cells. Therefore, the amount of type-I IFNs in these supernatants harvested from PRR component-transfected neuronal cells are expressed in relative IFN units. **D.** BE(2)-C/m ISRE-SEAP reporter cells were transfected with the constructs listed in A as well as wild-type TLR3 (pTLR3) and wild-type MDA5 (pMDA5). Six hours after transfection, cells were washed and incubated with fresh media containing a control antibody or a mix of IFNα (500 neutralizing U/ml) and IFNβ (500 neutralizing U/ml) neutralizing antibodies. 48 hours after transfection, supernatants were harvested and SEAP activity was measured. Averages and SEMs are displayed from 3 trials for A and 2 trials for C and D. Data in B represent averages and standard deviations from duplicate wells for one trial. *$p < 0.05$.

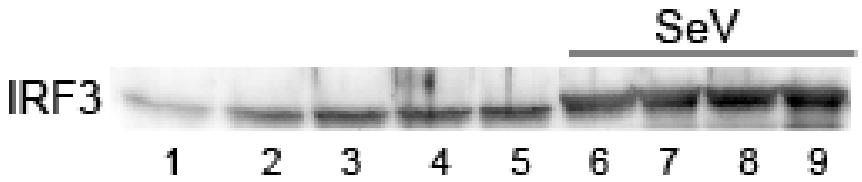

Supplemental Figure S3.5. SeV-mediated activation and induction of IRF3 in neuronal cells. Lysates from BE(2)-C/m cells described in Figure 3.6.A were analyzed by Western blot for IRF3. Data are representative of 3 independent trials.

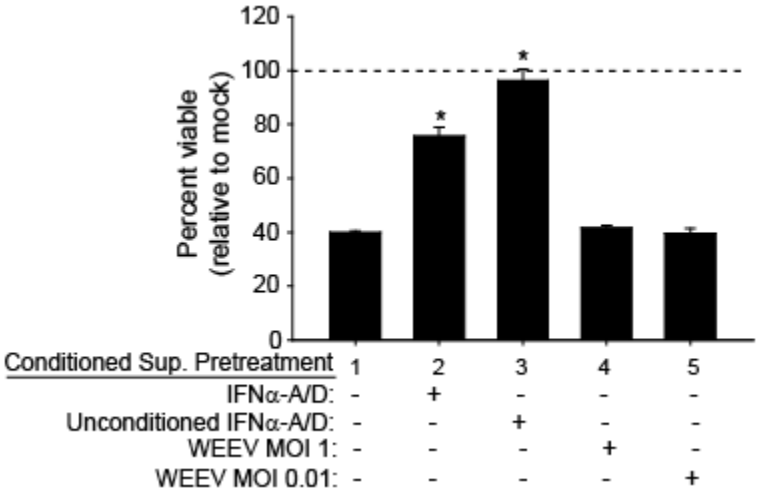

Supplemental Figure S3.6. Neuronal cell bioassay for viral-induced cell-extrinsic factors capable of modulating a WEEV-mediated CPE.
Supernatants from producer BE(2)-C/m cells mock infected, WEEV infected at the indicated MOI for 24 hours, or media treated with 80 U/ml IFNα-A/D were conditioned to inactivate and remove viral particles and used to pretreat target BE(2)-C/m cells (bars 1,2,4, and 5) for 18 hours. As a positive control, target BE(2)-C/m cells were pretreated with unconditioned media containing 80 U/ml IFNα-A/D (bar 3). Following pretreatment, target BE(2)-C/m cells were mock infected or infected with WEEV MOI 0.1 and cell viability relative to mock infected controls was assessed 48 hours post infection by a MTT assay. Averages and SEMs are displayed from three independent trials. *p-value < 0.05.

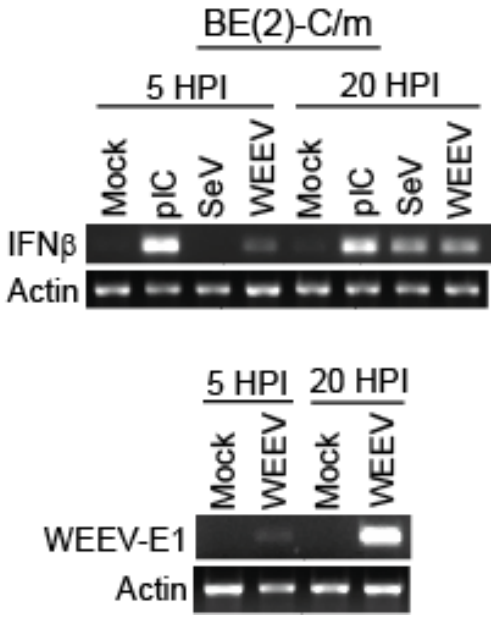

Supplemental Figure S3.7. Kinetics of WEEV-mediated induction of IFNβ mRNA in neuronal cells. BE(2)-C/m cells were mock infected or infected with WEEV MOI 5.0. RNA was isolated at five and twenty hours post infection, and IFNβ, WEEV envelope protein-1 (WEEV-E1), and actin transcript expression was assessed via RT-PCR. Data are representative of 2 independent trials.

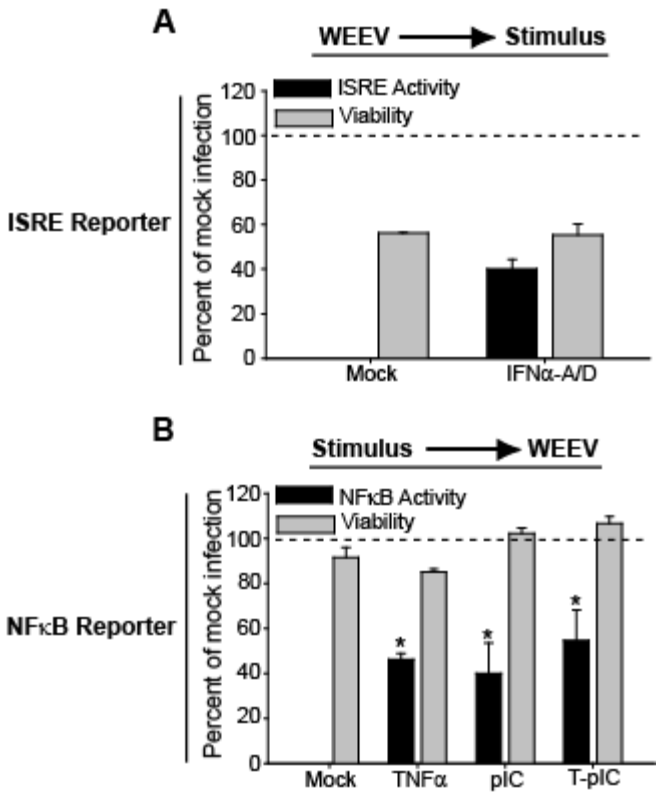

Supplemental Figure S3.8. WEEV inhibits PRR signaling but not type-I IFN signaling independent of its cytopathic effect in neuronal cells. A. ISRE-reporter BE(2)C/m cells were mock infected or infected with WEEV MOI 1.0 for 4.5 hours followed by mock stimulation or stimulation with IFNα-A/D (100 U/ml) for 15 hours. SEAP reporter activity and cell viability were assessed 15 hours after stimulation and presented as percents of mock infected controls. **B.** NFκB reporter BE(2)-C/m cells were treated and analyzed as in Figure 3.9.B except they were pre-stimulated for 7.5 hours. Averages and SEMs are displayed from three independent trials. **p*-value < 0.05 compared to either percent viability or matched mock-infected percent reporter activity.

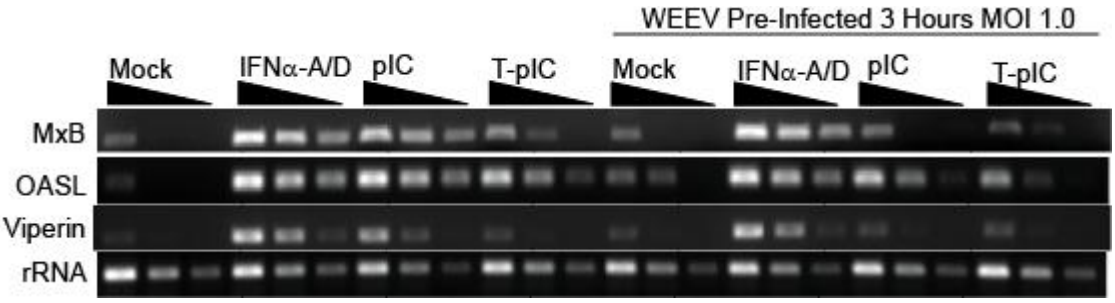

Supplemental Figure S3.9. WEEV inhibits neuronal cell PRR pathways but not type-I IFN pathways at early times post infection. BE(2)-C/m cells were treated and analyzed as in Figure 3.9.C except MxB, OASL, and Viperin transcripts were assessed via RT-PCR. Data are representative of 3 trials for Viperin, 2 for OASL, and 1 for MxB.

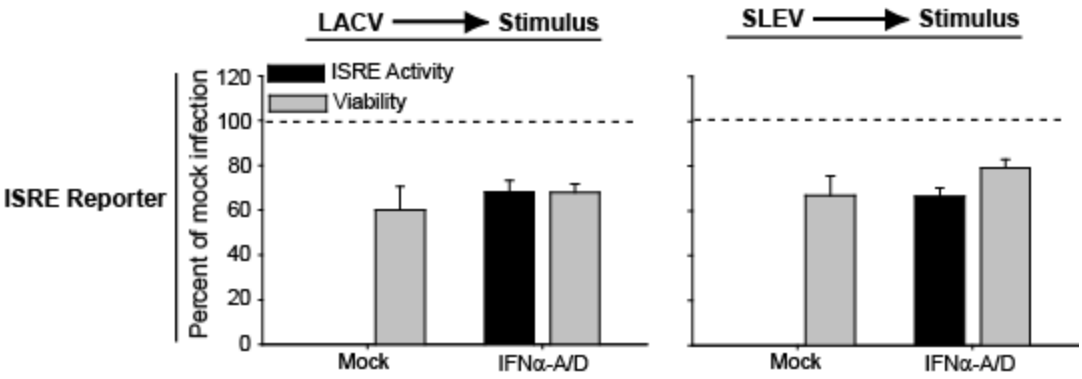

Supplemental Figure S3.10. LACV and SLEV-mediated inhibition of neuronal type-I IFN signaling parallels virus-mediated cytopathic effect. BE(2)-C/m ISRE reporter cells were infected with either LACV (left panel) or SLEV (right panel) at a MOI of 1.0 for 10 hours followed by mock stimulation or an IFNα-A/D (100 U/ml) stimulation. SEAP reporter activity and cell viability were assessed 15 hours after stimulation and presented as percents of mock infected controls. Averages and SEMs are displayed from three independent trials.

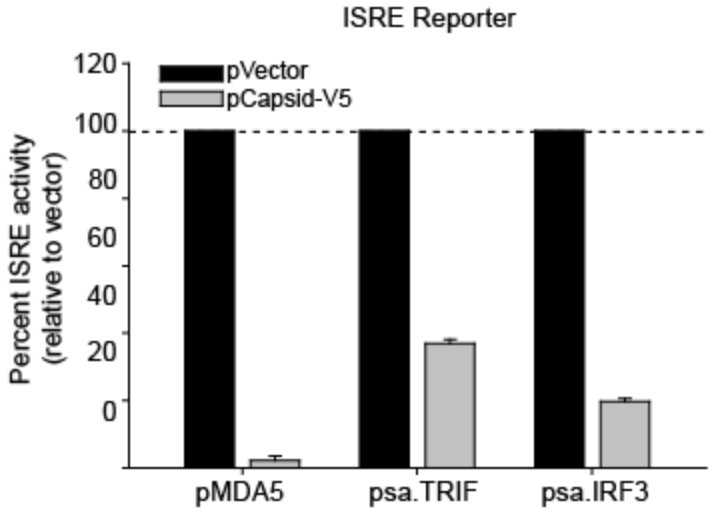

Supplemental Figure S3.11. V5-tagged WEEV capsid inhibits neuronal PRR pathway signaling. BE(2)-C/m ISRE reporter cells were treated and analyzed as in Figure 3.14.A except a C-terminal V5-tagged version of capsid was used. Averages and SEMs are displayed from 2 trials.

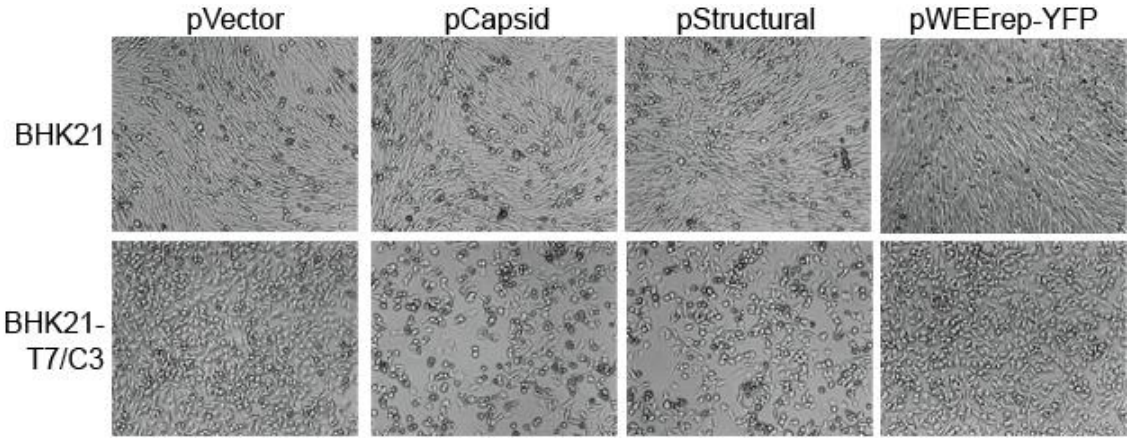

Supplemental Figure S3.12. WEEV capsid causes death of BHK21-T7/C3 cells. BHK21 or BHK21 cells stably expressing a bacteriophage T7 RNA-polymerase (BHK21-T7/C3) were transfected with the indicated constructs described in Figure 3.13.A. 100X, live-cell, phase-contrast images were acquired 48 hours post transfection using an Olympus IX70 inverted microscope. Data are representative of 2 trials.

Chapter IV

The Identification of Thieno[3,2-*b*]pyrrole Derivatives as Novel Small Molecule Inhibitors of Neurotropic Alphaviruses

Neurotropic alphaviruses such as western, eastern, and Venezuelan equine encephalitis viruses cause serious and potentially fatal central nervous system infections in humans and are high priority potential bioterrorism agents. There are currently no widely available vaccines or effective therapies for these virulent pathogens. To identify potential novel antivirals, we developed a cell-based assay with a western equine encephalitis virus replicon expressing a luciferase reporter gene and screened a small molecule diversity library of 51,028 compounds. We identified and validated a thieno[3,2-*b*]pyrrole compound with a 50% maximal inhibitory concentration of less than 10 μM, toxicity:activity ratio greater than 20, and potent activity against live virus in cultured neuronal cells. Furthermore, a structure-activity relationship analysis with twenty related compounds identified several with enhanced activity profiles, including six with submicromolar 50% maximal inhibitory concentrations. In conclusion, we have identified a novel class of promising inhibitors with potent activity against virulent neurotropic alphaviruses.

Introduction

The *Alphavirus* genus within the *Togaviridae* family contains about 30 mosquito-borne, enveloped, positive-stranded RNA viruses, one third of which cause significant diseases in human and animals worldwide (16). For example, neurotropic alphaviruses such as western, eastern, and Venezuelan equine encephalitis viruses (WEEV, EEEV, and VEEV, respectively) infect the central nervous system (CNS) and can lead to severe encephalitis in humans with fatality rates of up to 70%, and survivors often bear long-term neurological sequelae (7, 8). Neurotropic alphaviruses are also important members of the growing list of emerging or resurging public health threats (17) and are listed as CDC and NIAID category B bioterrorism agents, due in part to numerous characteristics that make them potential biological weapons: (i) high clinical morbidity and mortality; (ii) potential for aerosol transmission; (iii) lack of effective countermeasures for disease prevention or control; (iv) public anxiety elicited by CNS infections; (v) ease with which large volumes of infectious materials can be produced; and (vi) potential for malicious introduction of foreign genes designed to increase alphavirus virulence (38).

There are currently no licensed vaccines or antiviral drugs for alphaviruses. Formalin-inactivated vaccines for WEEV or EEEV and a live attenuated VEEV vaccine (TC-83 strain) are available on an investigational drug basis and are limited primarily to laboratory workers conducting research on these viruses (38). However, these vaccines have poor immunogenicity, require annual boosters, and have a high frequency of adverse reactions. The development of alternative

live attenuated, chimeric, and DNA-based alphavirus vaccines is being actively pursued, and several candidates have been tested in animal models (3, 9, 29, 37, 40, 41, 44, 46). Nevertheless, the broad clinical application of these newer generation vaccines is likely years away. Furthermore, combined active vaccination and antiviral therapy may be a more effective response to an outbreak due to either natural transmission or intentional exposure to a viral pathogen (4).

Several compounds have been reported to inhibit alphavirus replication, including the nucleoside analogs ribavirin and mycophenolic acid (27), (-)-carbodine (20), triaryl pyrazoline (35), and *seco*-pregnane steroids from the Chinese herbs *Strobilanthes cusia* and *Cynanchum paniculatum* (25). Nevertheless, there is still a pressing need to identify new antiviral drugs to treat these virulent pathogens. To this end, we developed a cell-based assay amenable to high-throughput screening (HTS) and analyzed a diversity library of >50,000 compounds for activity against WEEV RNA replication. We identified and validated several compounds with potent inhibitory activity against WEEV and related alphaviruses. Furthermore, we conducted limited structure-activity analyses with one of these compounds and identified a series of thieno[3,2-*b*]pyrrole derivatives as novel inhibitors of neurotropic alphaviruses.

Materials and Methods

Cells and Viruses

Human neuroblastoma (BE(2)-C), African green monkey kidney (Vero), and baby hamster kidney (BHK) cell lines were purchased from the American Type Culture Collection (ATCC, Manassas, VA) and cultured in Dulbecco's Modified Eagle Medium containing 5% bovine grown serum (HyClone, Logan, UT), 10 U/mL penicillin, and 10 μg/mL streptomycin. BSR-T7/5 cells, which are BHK cells that constitutively express bacteriophage T7 RNA polymerase (5), were generously provided by K. Conzelmann (Max von Pettenkofer-Institut, Munich, Germany) and were cultured in Glasgow Minimum Essential Medium containing 10% heat-inactivated fetal bovine serum, 10% tryptose phosphate broth, 1% sodium pyruvate, 0.1 mM non-essential amino acids, 10 U/mL penicillin, 10 μg/mL streptomycin, and 100-500 μg/mL G418 for selection. BHK cell lines VEErep/SEAP/Pac and EEErep/SEAP/Pac, which stably express double subgenomic VEEV or EEEV replicons with secreted alkaline phosphatase (SEAP) reporter and puromycin resistance genes (33), were generously provided by I. Frolov (UTMB, Galveston, TX) and were cultured in Dulbecco's Modified Eagle Medium containing 7% fetal bovine serum, 10 U/mL penicillin, 10 μg/mL streptomycin, and 5 μg/mL puromycin for selection. Infectious WEEV corresponding to strain Cba87 was generated as described (6), and all experiments that involved infectious WEEV were conducted under BSL-3 conditions in approved facilities at the University of Michigan. Fort Morgan virus (FMV) strain CM4-146 was purchased from ATCC, and SINV strain Toto64 was

generously provided by R. Kuhn (Purdue University, West Lafayette, IN). FMV and SINV stocks were prepared and quantified using Vero cells as described for WEEV (6).

WEEV Replicon

We generated the WEEV replicon plasmid pWR-LUC using the full-length genomic clone pWE2000 (37), generously provided by M. Parker (USAMRIID, Frederick, MD). This cDNA clone contains a T7 polymerase promoter to initiate precise transcription and produce viral RNA with authentic 5' termini. We amplified the firefly luciferase (fLUC) gene from pTRE2hyg-LUC (Clontech, Palo Alto, CA) by PCR without an ATG initiator codon but with engineered *AvrII* and *BstXI* sites and inserted the resultant fragment into the *AvrII-BstXI* site of pWE2000. This strategy replaced the majority of the WEEV structural genes with the fLUC reporter gene, but retained the first 27 amino acids of the capsid protein to preserve the predicted stem-loop region within the structural gene translation enhancer previously identified in alphaviruses (11). We further modified pWR-LUC by placing a hepatitis δ ribozyme and T7 terminator downstream of the polyadenylation region to ensure efficient transcription termination and produce authentic viral 3' termini (**Fig 4.1.A**). To generate the control replicon pWR-ΔLUC, we deleted the *NheI-NheI* fragment to remove the non-structural protein (nsP) coding region that included the majority of nsP2, 3, and 4.

Primary HTS, Dose-Response, and Secondary Validation of Candidate Compounds

BSR-T7/5 cells at approximately 60-70% confluence in 10 cm tissue culture plates (~2 x 10^6 cells/plate) were transfected with 15 μg pWR-LUC using 22 μL TransIT LT-1 (Mirus, Madison, WI) according to the manufacturer's instructions. Six hours after transfection cells were detached with 0.05% trypsin, diluted to 6.25 x10^5 cells/mL, and 20 μL cell suspension per well was dispensed into 384-well plates preloaded with individual compounds in 30 μL media at approximately 5-10 μM. All plates contained a series of 32 wells each of negative and positive controls, which consisted of dimethyl sulfoxide and 100 μM ribavirin, respectively. Plates were cultured at 37°C and 5% CO_2 for 18 h, 40 μL media was removed and replaced with 10 μL per well Steady-Glo luciferase reagent (Promega, Madison, WI), and luminescence was read on a PHERAstar multi-mode plate reader (BMG Labtech, Durham, NC). Individual compounds identified as primary hits as described below and in table 1 were validated by dose-response analyses using a similar 384-well format, but with 3.3-fold serial dilutions of compounds from 100 μM to 10 nM assayed in duplicate wells. Selected compounds were purchased from the original supplier and were further analyzed by repeat dose-response and toxicity studies using a 96-well format, where cell viability was quantitated by either 3-[4,5-dimethylthizol-2-yl]-2,5-diphenyltetrazolium bromide (MTT) assay as previously described (6) or with Alamar Blue (AbD Serotec, Oxford, UK) per the manufacturer's instructions. For secondary validation we used VEErep/SEAP/Pac and EEErep/SEAP/Pac cell lines cultured for 24 h with

compounds but without puromycin selection and measured SEAP reporter gene expression in supernatants using QUANTI-Blue (InvivoGen, San Diego, CA) per the manufacturer's instructions.

Final Verification of Candidate Compound Activity with Infectious Virus

Human BE(2)-C neuroblastoma cells were incubated simultaneously with candidate compounds and infectious WEEV, FMV, or SINV at a multiplicity of infection (MOI) of 1 or 0.1, and MTT viability assays, Northern blots, and infectious virus quantitation by plaque assay were done at 6 to 48 h after infection as previously described (6). For RT-PCR analyses, total RNA was isolated at 6 h after infection with TRIzol reagent (Invitrogen, Carlsbad, CA) according to the manufacturer's instructions, digested with RQ1 DNAse (Promega), and RNA concentrations and integrity were determined by spectrophotometry and denaturing agarose gel electrophoresis. First-strand cDNA synthesis was performed with the SuperScript First-Strand Synthesis System (Invitrogen) using equal amounts of total RNA with oligo(dT)12-16 primers. For semi-quantitative RT-PCR, we amplified 200-600 bp fragments of the WEEV nsP2 and E1 genes using cDNA serial dilutions and rRNA as the loading control, and analyzed products by agarose gel electrophoresis and ethidium bromide staining. For quantitative RT-PCR, we amplified ~200 bp fragments of the WEEV or FMV E1 gene and rRNA as an internal control using iQTM SYBR Green Supermix (BioRad, Hercules, CA) according the manufacturer's instructions in a 96-well format with triplicate wells. Amplification

and detection were done with an iCycler iQ system, and fluorescence threshold values were calculated using SDS 700 system software (Bio-Rad).

Results

Development and Validation of WEEV Replicon Cell-Based Assay for HTS

The alphavirus life cycle includes three general steps that are viable targets for antivirals: (i) attachment and entry; (ii) genome replication; and (iii) encapsidation and release. We focused on the second step, genome replication, in an attempt to identify novel alphavirus inhibitors. The alphavirus genome is an 11-12 kb single-stranded positive-sense RNA molecule that is divided into two major domains (16). The 5' two-thirds of the alphavirus genome encodes the non-structural proteins nsP1 through nsP4, which are initially synthesized as one or two polyproteins that undergo regulated autocatalytic processing to form an active replication complex. This enzymatic complex subsequently synthesizes via a negative strand intermediate both full-length genomic RNA and a 4 kb subgenomic RNA. The latter RNA segment encodes the structural capsid protein and envelope glycoproteins, which are not required for genome replication and therefore can be readily replaced by foreign genes to produce alphavirus vectors that are self-replicating, termed replicons (10).

To generate a WEEV replicon amenable to HTS, we replaced the majority of the structural genes in the full-length genomic clone pWE2000 (37) with the fLUC reporter gene (**Fig 4.1.A**). To facilitate the host cell transcription necessary to "launch" the WEEV replicon from a plasmid we used a highly transfectable

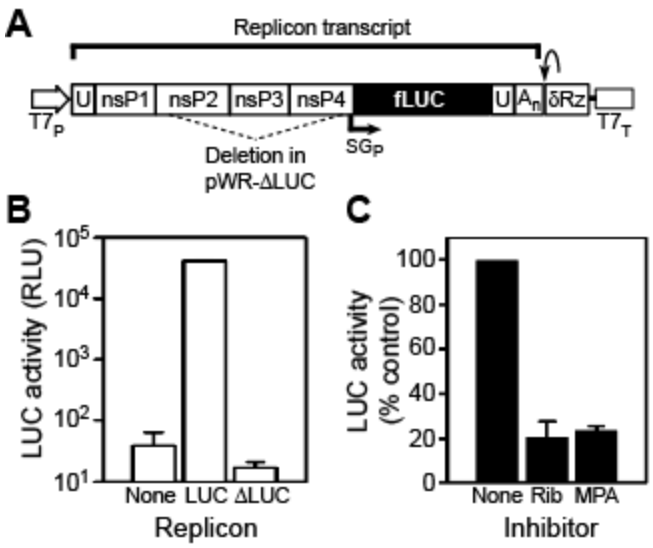

Figure 4.1. Cell-based WEEV replicon system for HTS. A. Schematic of WEEV replicon pWR-LUC. Authentic 5' and 3' viral termini are generated by precise placement of T7 polymerase promoter ($T7_P$) and hepatitis δ ribozyme (δRz)/T7 terminator ($T7_T$). The final composition of the replicon transcript is indicated by the bar above the schematic. Transcription of the fLUC reporter gene is controlled by the viral subgenomic promoter (SG_P). Region deleted for the control plasmid pWR-ΔLUC is indicated by the dashed lines. U, untranslated region; A_n, polyadenylated tail. **B.** fLUC reporter gene activity in BSR-T7/5 cells transfected with empty vector, pWR-LUC, or control pWR-ΔLUC. Results are expressed as relative luciferase units (RLU). **C.** BSR-T7/5 cells transfected with pWR-LUC were treated with no inhibitor, 50 μM ribavirin (Rib), or 5 μM mycophenolic acid (MPA), and fLUC activity was measured after 18 h. Results are expressed as percentage of fLUC activity relative to untreated control.

BHK cell line derivative, BSR-T7/5 cells, which constitutively express bacteriophage T7 RNA polymerase (5). One potential complication with using cell-based assays to identify antiviral compounds is the possibility that candidate compounds will induce type I interferon production and hence suppress virus replication indirectly. The use of BSR-T7/5 cells minimizes this potential complication as BHK cells are deficient in both the production and response to type I interferons (2, 22, 28).

BSR-T7/5 cells transiently transfected with the pWR-LUC replicon produced fLUC levels approximately three logs above background (**Fig 4.1.B**). Reporter gene expression was dependent on viral RNA replication, as essentially no fLUC expression was detected in cells transfected with pWR-ΔLUC, a control plasmid in which the majority of the nsP2-4 region had been deleted (**Fig 4.1.A and B**). Furthermore, both ribavirin and mycophenolic acid, which have previously been shown to inhibit alphavirus replication (27), suppressed fLUC expression in pWR-LUC transfected BSR-T7/5 cells by approximately 80% (**Fig 4.1.C**). We concluded from these results that the pWR-LUC:BSR-T7/5 system would function as a convenient and robust platform to identify small molecule inhibitors of WEEV RNA replication.

Primary HTS and Validation of Candidate Antivirals Against Neurotropic Alphaviruses

We initially optimized the pWR-LUC:BSR-T7/5 system to a 384-well HTS format and obtained Z'-scores greater than 0.6 (47), and subsequently used this

optimized system to screen a diversity library of 51,028 compounds at the University of Michigan Center for Chemical Genomics (CCG). This composite library consisted of compounds from four smaller collections: Chembridge (13,028 compounds), ChemDiv (20,000 compounds), Maybridge (16,000 compounds), and MS Spectrum 2000 (2,000 compounds), the latter of which included FDA-approved drugs. Table 4.1 provides a composite overview of the experimental systems, criteria, and results from the HTS and subsequent validation steps. For the primary HTS, we selected parameters to identify compounds with inhibitory activity that suppressed fLUC signal to at least 70% of the level obtained with the positive control ribavirin and obtained a hit rate of 0.4%. We further excluded 82 compounds that had activity in previous LUC-based screens run at the CCG, thus reducing the selection of toxic compounds or those with direct activity against the reporter gene. We subjected the remaining 114 compounds to dose-response analysis for primary validation, where 76% of these compounds had 50% maximal inhibitory concentration (IC_{50}) values of less than 100 μM.

We purchased new material from the original suppliers for 46 available compounds with the lowest IC_{50} values, and conducted secondary validation studies with cell-based replicons derived from VEEV or EEEV that incorporated a SEAP reporter gene rather than fLUC. This step allowed us to further exclude compounds that were active against fLUC but also increased the potential of identifying compounds with broad activity against neurotropic alphaviruses. Eleven compounds showed activity in the secondary validation assays and were

Table 4.1. Identification and validation steps in the discovery of novel small molecule compounds that inhibit neurotropic alphavirus replication.

Step	Experimental system/resource	Criteria	Number of compounds
	CCG chemical diversity library		51,028
HTS	pWR-LUC replicon and BSR-T7/5 cells	Reduction in fLUC activity either: 1) >2 S.D. per plate from negative control; or 2) >90% per plate of positive control	196
		No activity in previous CCG LUC-based screens	114
Primary validation	pWR-LUC replicon and BSR-T7/5 cells	Dose-response with IC_{50} <100 μM	87
Secondary validation	EEEV/VEEV-SEAP replicon-bearing BHK cells	Dose-response with IC_{50} <100 μM	11
Tertiary validation	Repeat dose-response with pWR-LUC replicon and BSR-T7/5 cells	Toxicity:activity ratio >5	4

evaluated in tertiary validation assays with repeat detailed dose-response and toxicity assessment to calculate precise 50% cytotoxicity concentration (CC_{50}) and IC_{50} values using the original pWR-LUC:BSR-T7/5 system. Four compounds had toxicity:activity (T:A) ratios (CC_{50}/IC_{50}) greater than 5 and were selected as candidates for further development as alphavirus inhibitors. One of these compounds, designated CCG32091, was particularly potent with a T:A ratio of greater than 20 (**Fig 4.2.A**). For comparison, ribavirin had an IC_{50} of 16.0 μM and T:A ratio of 19 with the pWR-LUC:BSR-T7/5 system. We chose CCG32091, which has a thieno[3,2-*b*]pyrrole core structure with a 4-fluorobenzyl R1 group attached to the pyrrole nitrogen and a 2-furanylmethylamine R2 group incorporated into the terminal carboxamide (IUPAC name, 1-({4-[(4-fluorophenyl)methyl]-4H-thieno[3,2-*b*]pyrrol-5-yl}carbonyl)-N-(furan-2-ylmethyl)piperidine-4-carboxamide), as our initial lead antiviral compound for final verification studies with live virus and structure-activity relationship (SAR) analysis (**Fig 4.2.B**).

Verification of CCG32091 Antiviral Activity with Live Virus and Cultured Neuronal Cells

The primary target cell of neurotropic alphaviruses is the CNS neuron (16), and thus we performed a final verification of the antiviral activity of CCG32091 using an in vitro model with human neuronal cells previously used to study WEEV pathogenesis (6). For initial experiments with infectious virus we used FMV, an alphavirus closely related to WEEV, and SINV, the prototypic alphavirus used to

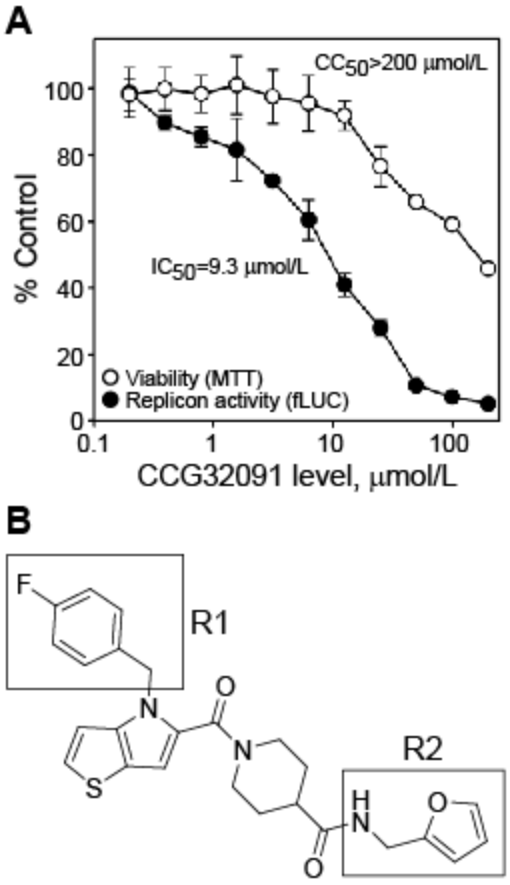

Figure 4.2. CCG32091 potently inhibits WEEV replicon activity with minimal cytotoxicity. A. Dose-response curves of BSR-T7/5 cells transfected with pWR-LUC and treated with increasing concentrations of CCG32091. fLUC reporter gene activity (closed circles) was measured by luciferase assay and viability (open circles) was measured by MTT assay. Results are expressed as percentage of untreated controls. Calculated concentrations that produced a 50% inhibition of fLUC activity (IC_{50}) or 50% cytotoxicity (CC_{50}) compared to untreated controls are shown. **B.** Structure of CCG32091. The R1 and R2 groups central to the SAR (see Table 4.2) are highlighted by boxes.

study pathogenesis (16). Both of these viruses can be handled safely under BSL-2 conditions. One characteristic of alphavirus replication in cultured mammalian cells is the rapid development of cytopathic effect (CPE), which is due in part to virus-mediated disruption of host cell transcription and translation (12, 13, 15). We infected BE(2)-C cells with FMV or SINV in the presence of 12.5 μM CCG32091 or 50 μM ribavirin and measured cell viability at 48 h after infection by MTT assay (**Fig 4.3.A**). Treatment with CCG32091 suppressed virus-induced CPE and increased cell viability from 20% in infected but mock-treated cells to 50% or 70% for SINV- or FMV-infected cells, respectively. Furthermore, CCG32091 effectively suppressed FMV-induced CPE at concentrations as low as 3 μM, the lowest concentration that we tested in this assay (data not shown).

We also directly assessed the ability of CCG32091 to inhibit virus replication by examining infectious virion production (**Fig 4.3.B**) and viral RNA replication (**Fig 4.3.C and D**). CCG32091 suppressed infectious FMV production by >90%, similar to the level of suppression seen with the positive control ribavirin (**Fig 4.3.B**). Furthermore, when we examined viral RNA replication by RT-PCR with either WEEV- or FMV-infected BE(2)-C cells, CCG32091 reduced the accumulation of viral RNAs encoding either nsP2 or E1 by 80-90% (**Fig 4.3C and D**). Northern blotting confirmed that CCG32091 reduced both genomic and subgenomic RNA accumulation after infection (data not shown). These results demonstrated that CCG32091 suppressed virus replication in infected neuronal

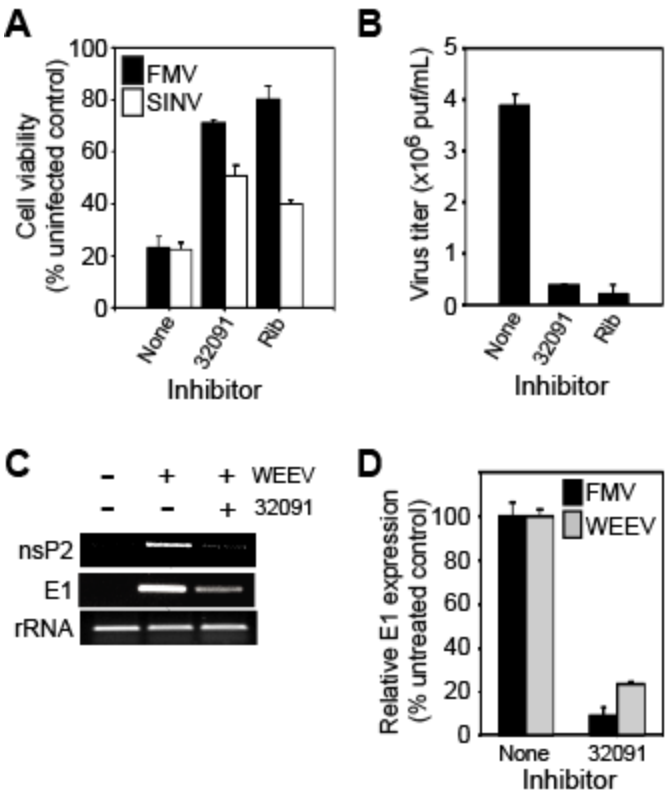

Figure 4.3. CCG32091 inhibits alphavirus replication in cultured human neuronal cells. A. Human BE(2)-C neuronal cells were infected with FMV (black bars) or SINV (white bars) at an MOI of 0.1 and simultaneously treated with no inhibitor, 12.5 μM CCG32091, or 50 μM ribavirin (Rib), and cell viability was determined at 48 h after infection by MTT assay. **B.** BE(2)-C cells were infected with FMV at an MOI of 1, treated with inhibitors as described above, and virus titers in culture supernatants were determined at 24 h after infection by plaque assay. **C.** BE(2)-C cells were infected with WEEV at an MOI of 1, treated with CCG32091, and viral RNA corresponding to nsP2 and E1 regions were analyzed by RT-PCR at 6 h after infection. rRNA levels are shown as a loading control. **D.** BE(2)-C cells were infected with FMV (black bars) or WEEV (grey bars) and treated with CCG32091 as described above, and viral RNA levels corresponding to the E1 gene were determined by quantitative RT-PCR.

cells, inhibited virus-induced CPE, and had broad activity against several alphaviruses.

SAR Analysis with CCG32091

To optimize the therapeutic profile of candidate antivirals in anticipation of future in vivo animal studies, we compared the structure of CCG32091 (**Fig 4.2.B**) with those of compounds in the entire CCG library. We identified 20 compounds that contained a core thieno[3,2-*b*]pyrrole moiety but had different combinations of R1 and R2 groups compared to CCG32091 (**Table 4.2**). We had previously identified 6 of these compounds as "hits" in the primary HTS and had already completed dose-response analyses for validation (CCG32075, 32089, 32090, 32092, 32095, and 32096). We completed dose-response analysis of the remaining 14 compounds to obtain a limited SAR for CCG32091 (**Table 4.2**). This analysis revealed an approximate 250-fold range of IC_{50} values, from a high of 46.8 μM to a low of 0.2 μM, where 6 compounds had submicromolar IC_{50} values (CCG32084, 32087, 32088, 32093, 32094, and 32095). We also completed toxicity studies with these 20 compounds and found that 90% had CC_{50} values >100 μM, including 5 of the 6 compounds with submicromolar IC_{50} values (**Table 4.2**). Although the data set was limited, several aspects of the SAR could be elucidated. At R1, there appeared to be little difference between methyl and ethyl groups (compare the 4-methylbenzylamides CCG32055 and CCG32019). However, substantially better activity was observed when the small alkyl group at R1 was replaced with 4-fluorobenzyl (compare CCG32088 with

Table 4.2. CCG32091 structure-activity relationship (SAR) analysis

Compound No.	R1	R2	IC_{50} (μM)	Compound No.	R1	R2	IC_{50} (μM)
32001*	CH_3	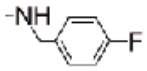	33.9	32087		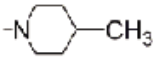	0.2
32009*	CH_3	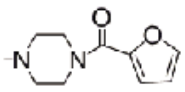	46.8	32088	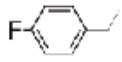	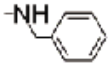	0.2
32052	CH_3	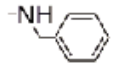	20.4	32089		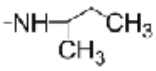	4.9
32055	CH_3	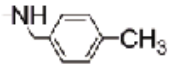	4.7	32090		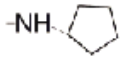	10.6
32075	CH_3	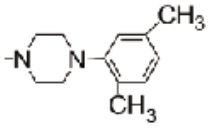	8.0	***32091***	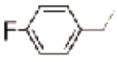	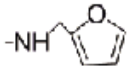	9.3
32084	CH_3	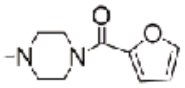	0.3	32092	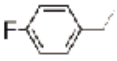	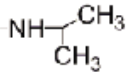	9.9
32019	CH_2CH_3	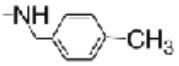	5.8	32093	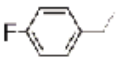	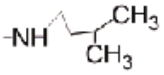	0.4
32023	CH_2CH_3	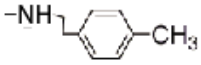	1.2	32094	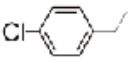		0.3†
32025	CH_2CH_3	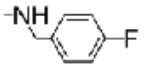	4.7	32095		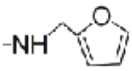	0.5
32044	CH_2CH_3		1.2	32096	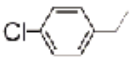	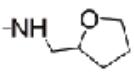	1.5†
32048	CH_2CH_3	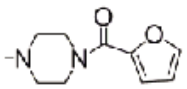	5.5				

*Compounds CCG32001 and 32009 have the R2 group attached to a piperidine-3-carboxamide in contrast to a piperidine-4-carboxamide for the remaining compounds in the table.

†Increased cytotoxicity compared to CCG32091 with CC_{50} values less than 100 μM.

CCG32052). A direct comparison between 4-fluorobenzyl and 4-chlorobenzyl at R1 (2-furanylmethyl amides CCG32091 and CCG32095) also suggested that 4-chlorobenzyl may represent a further optimization of R1. Among the amines incorporated at R2, none were clearly superior to the others. In fact, a variety of amines were seen with potent inhibitors, including 4-methylpiperidine (CCG32087), benzyl (CCG32088), isopentyl (CCG32093), and 4-(2-furanylcarboxy)piperazine (CCG32084). With regard to the internal piperidine carboxamide, the two 3-carboxamide analogs CCG32001 and CCG32009 had distinctly inferior activity compared to the closely related 4-carboxamide analogs CCG32025 and CCG32084, respectively. Overall, these results identified several additional compounds with enhanced potency but similar toxicity compared to the original lead compound CCG32091, and provide a useful initial dataset to begin targeted design for optimized antiviral compound synthesis based on the core thieno[3,2-*b*]pyrrole structure.

Discussion

The neurotropic alphaviruses represent emerging pathogens with the potential for widespread dissemination and the ability to cause substantial morbidity and mortality (17, 38), but for which no licensed therapies currently exist. In this report, we describe the identification of a novel class of thieno[3,2-*b*]pyrrole compounds with inhibitory activity against WEEV and several related alphaviruses. Heterocyclic compounds that contain a thieno[3,2-*b*]pyrrole core have been previously identified as possessing physiological activity with potential clinical applications, including uses as anti-inflammatory agents (23), glycogen phosphorylase inhibitors for diabetes treatment (45), and hepatitis C virus (HCV) inhibitors (30). The latter use is particularly relevant for the work presented in this report, as thieno[3,2-*b*]pyrroles were identified as allosteric inhibitors of the HCV RNA polymerase (30), which is a plausible potential mechanism of action for their activity against alphaviruses (see below). Significantly, the lead compound identified in this report, CCG32091 (**Fig 4.2**), is a PubChem registered compound (CID: 3240671) and part of the NIH Molecular Libraries-Small Molecule Repository (MLSMR), and has been identified as an active compound in only 5 of ~250 HTS assays conducted through the NIH Molecular Libraries Screening Center Network (MLSCN). This indicates that the spectrum of its biological activity is fairly narrow, which is a highly desirable attribute in a potential lead compound. In addition, Ilyin et al. recently described a solution-phase strategy for the synthesis of novel combinatorial libraries containing a thieno[3,2-*b*]pyrrole core (19), thus providing the opportunity to further explore

and potentially exploit these compounds as therapeutics for a range of human diseases, including infections with neurotropic alphaviruses.

The mechanism(s) underlying the antiviral activity of thieno[3,2-*b*]pyrroles against neurotropic alphaviruses is unknown, but the use of a replicon-based assay for the HTS and validation steps (**Fig 4.1 and Table 4.1**) implicates viral replicase proteins as potential targets. This hypothesis is supported by the observation that CCG32091 reduced viral RNA accumulation after infection of neuronal cells (**Fig 4.3**). Furthermore, the broad activity of CCG32091 against infectious virus or replicons derived from WEEV, EEEV, VEEV, FMV, and SINV suggests that a highly conserved viral enzymatic activity may be targeted. Alphavirus nsPs contain several distinct enzymatic activities, including methyltransferase (nsP1) (1), protease and helicase (nsP2) (14, 18), and RNA polymerase (nsP4) (34). In vitro assays have been developed for several of these activities (1, 39, 43), which provides a convenient approach to target identification. An alternative approach that takes advantage of the intrinsically high error rate of viral RNA polymerases previously used successfully for antiviral target identification is the isolation and characterization of viral escape mutants (24, 26, 36).

The preclinical utility of candidate novel antiviral agents rests on their ability to either prevent or treat established disease in animal models while exhibiting minimal toxicity. The treatment of CNS infections presents an additional hurdle to overcome, as the blood-brain-barrier (BBB) represents a formidable obstacle for drug penetration (32). The BBB is a highly effective physiologic barrier whose

primary function is to closely regulate access of blood stream components to the CNS. Although infectious and inflammatory CNS diseases often disrupt BBB function and increase permeability, drug penetration remains an important aspect to consider in the development of antiviral agents against neurotropic alphaviruses. Multiple physical-chemical factors influence CNS penetration of drugs, including lipophilicity, ionization properties, molecular flexibility, polar surface area (PSA), and size (31). The latter two properties are particularly important, where studies of marketed CNS and non-CNS drugs indicate that PSA values less than 60-90 $Å^2$ and MW less than 450 Da are required for adequate penetration (21, 42). The lead thieno[3,2-*b*]pyrrole compound identified in this report, CCG32091 (**Fig 4.2.B**), has a calculated PSA of 67.5 $Å^2$ and MW of 466 Da (PubChem database; http://pubchem.ncbi.nlm.nih.gov). Several of the compounds identified in the SAR (**Table 4.2**) had lower PSAs and MWs than CCG32091, and we are currently using the SAR results to refine the development of alphavirus inhibitors with reduced toxicity, enhanced potency, and optimal CNS penetration.

References

1. **Ahola, T., P. Laakkonen, H. Vihinen, and L. Kaariainen.** 1997. Critical residues of Semliki Forest virus RNA capping enzyme involved in methyltransferase and guanylyltransferase-like activities. J Virol **71:**392-7.
2. **Andzhaparidze, O. G., N. N. Bogomolova, Y. S. Boriskin, M. S. Bektemirova, and I. D. Drynov.** 1981. Comparative study of rabies virus persistence in human and hamster cell lines. J Virol **37:**1-6.
3. **Barabe, N. D., G. A. Rayner, M. E. Christopher, L. P. Nagata, and J. Q. Wu.** 2007. Single-dose, fast-acting vaccine candidate against western equine encephalitis virus completely protects mice from intranasal challenge with different strains of the virus. Vaccine **25:**6271-6.
4. **Bronze, M. S., and R. A. Greenfield.** 2003. Therapeutic options for diseases due to potential viral agents of bioterrorism. Curr Opin Investig Drugs **4:**172-8.
5. **Buchholz, U. J., S. Finke, and K. K. Conzelmann.** 1999. Generation of bovine respiratory syncytial virus (BRSV) from cDNA: BRSV NS2 is not essential for virus replication in tissue culture, and the human RSV leader region acts as a functional BRSV genome promoter. J Virol **73:**251-9.
6. **Castorena, K. M., D. C. Peltier, W. Peng, and D. J. Miller.** 2008. Maturation-dependent responses of human neuronal cells to western equine encephalitis virus infection and type I interferons. Virology **372:**208-20.
7. **Deresiewicz, R. L., S. J. Thaler, L. Hsu, and A. A. Zamani.** 1997. Clinical and neuroradiographic manifestations of eastern equine encephalitis. N Engl J Med **336:**1867-74.
8. **Earnest, M. P., H. A. Goolishian, J. R. Calverley, R. O. Hayes, and H. R. Hill.** 1971. Neurologic, intellectual, and psychologic sequelae following western encephalitis. A follow-up study of 35 cases. Neurology **21:**969-74.
9. **Fine, D. L., B. A. Roberts, S. J. Terpening, J. Mott, D. Vasconcelos, and R. V. House.** 2008. Neurovirulence evaluation of Venezuelan equine encephalitis (VEE) vaccine candidate V3526 in nonhuman primates. Vaccine **26:**3497-506.
10. **Frolov, I., T. A. Hoffman, B. M. Pragai, S. A. Dryga, H. V. Huang, S. Schlesinger, and C. M. Rice.** 1996. Alphavirus-based expression vectors: strategies and applications. Proc.Natl.Acad.Sci.U.S.A **93:**11371-11377.
11. **Frolov, I., and S. Schlesinger.** 1996. Translation of Sindbis virus mRNA: analysis of sequences downstream of the initiating AUG codon that enhance translation. J.Virol. **70:**1182-1190.
12. **Garmashova, N., R. Gorchakov, E. Frolova, and I. Frolov.** 2006. Sindbis virus nonstructural protein nsP2 is cytotoxic and inhibits cellular transcription. J Virol **80:**5686-96.
13. **Garmashova, N., R. Gorchakov, E. Volkova, S. Paessler, E. Frolova, and I. Frolov.** 2007. The Old World and New World alphaviruses use different virus-specific proteins for induction of transcriptional shutoff. J Virol **81:**2472-84.

14. **Gomez de Cedron, M., N. Ehsani, M. L. Mikkola, J. A. Garcia, and L. Kaariainen.** 1999. RNA helicase activity of Semliki Forest virus replicase protein NSP2. FEBS Lett **448:**19-22.
15. **Gorchakov, R., E. Frolova, and I. Frolov.** 2005. Inhibition of transcription and translation in Sindbis virus-infected cells. J Virol **79:**9397-409.
16. **Griffin, D. E.** 2001. Alphaviruses, p. 917-962. *In* D. M. Knipe, P. M. Howley, D. E. Griffin, R. A. Lamb, M. A. Martin, B. Roizman, and S. S. Straus (ed.), Fields Virology, Fourth ed. Lippincott Williams & Wilkins, Philadelphia.
17. **Gubler, D. J.** 2002. The global emergence/resurgence of arboviral diseases as public health problems. Arch Med Res **33:**330-42.
18. **Hardy, W. R., and J. H. Strauss.** 1989. Processing the nonstructural polyproteins of sindbis virus: nonstructural proteinase is in the C-terminal half of nsP2 and functions both in cis and in trans. J Virol **63:**4653-64.
19. **Ilyin, A. P., I. G. Dmitrieva, V. A. Kustova, A. V. Manaev, and A. V. Ivachtchenko.** 2007. Synthesis of heterocyclic compounds possessing the 4H-thieno[3,2-b]pyrrole moiety. J Comb Chem **9:**96-106.
20. **Julander, J. G., R. A. Bowen, J. R. Rao, C. Day, K. Shafer, D. F. Smee, J. D. Morrey, and C. K. Chu.** 2008. Treatment of Venezuelan equine encephalitis virus infection with (-)-carbodine. Antiviral Res **80:**309-15.
21. **Kelder, J., P. D. Grootenhuis, D. M. Bayada, L. P. Delbressine, and J. P. Ploemen.** 1999. Polar molecular surface as a dominating determinant for oral absorption and brain penetration of drugs. Pharm Res **16:**1514-9.
22. **Kramer, M. J., R. Dennin, C. Kramer, G. Jones, E. Connell, N. Rolon, A. Gruarin, R. Kale, and P. W. Trown.** 1983. Cell and virus sensitivity studies with recombinant human alpha interferons. J Interferon Res **3:**425-35.
23. **Kumar, P. R., S. Raju, P. S. Goud, M. Sailaja, M. R. Sarma, G. O. Reddy, M. P. Kumar, V. V. Reddy, T. Suresh, and P. Hegde.** 2004. Synthesis and biological evaluation of thiophene [3,2-b] pyrrole derivatives as potential anti-inflammatory agents. Bioorg Med Chem **12:**1221-30.
24. **Li, M. L., Y. H. Lin, H. A. Simmonds, and V. Stollar.** 2004. A mutant of Sindbis virus which is able to replicate in cells with reduced CTP makes a replicase/transcriptase with a decreased Km for CTP. J Virol **78:**9645-51.
25. **Li, Y., L. Wang, S. Li, X. Chen, Y. Shen, Z. Zhang, H. He, W. Xu, Y. Shu, G. Liang, R. Fang, and X. Hao.** 2007. Seco-pregnane steroids target the subgenomic RNA of alphavirus-like RNA viruses. Proc Natl Acad Sci U S A **104:**8083-8.
26. **Lin, Y. H., P. Yadav, R. Ravatn, and V. Stollar.** 2000. A mutant of Sindbis virus that is resistant to pyrazofurin encodes an altered RNA polymerase. Virology **272:**61-71.
27. **Malinoski, F., and V. Stollar.** 1981. Inhibitors of IMP dehydrogenase prevent sindbis virus replication and reduce GTP levels in Aedes albopictus cells. Virology **110:**281-289.

28. **Nagai, Y., Y. Ito, M. Hamaguchi, T. Yoshida, and T. Matsumoto.** 1981. Relation of interferon production to the limited replication of Newcastle disease virus in L cells. J Gen Virol **55:**109-16.
29. **Nagata, L. P., W. G. Hu, S. A. Masri, G. A. Rayner, F. L. Schmaltz, D. Das, J. Wu, M. C. Long, C. Chan, D. Proll, S. Jager, L. Jebailey, M. R. Suresh, and J. P. Wong.** 2005. Efficacy of DNA vaccination against western equine encephalitis virus infection. Vaccine **23:**2280-3.
30. **Ontoria, J. M., J. I. Martin Hernando, S. Malancona, B. Attenni, I. Stansfield, I. Conte, C. Ercolani, J. Habermann, S. Ponzi, M. Di Filippo, U. Koch, M. Rowley, and F. Narjes.** 2006. Identification of thieno[3,2-b]pyrroles as allosteric inhibitors of hepatitis C virus NS5B polymerase. Bioorg Med Chem Lett **16:**4026-30.
31. **Pajouhesh, H., and G. R. Lenz.** 2005. Medicinal chemical properties of successful central nervous system drugs. NeuroRx **2:**541-53.
32. **Pardridge, W. M.** 2005. The blood-brain barrier and neurotherapeutics. NeuroRx **2:**1-2.
33. **Petrakova, O., E. Volkova, R. Gorchakov, S. Paessler, R. M. Kinney, and I. Frolov.** 2005. Noncytopathic replication of Venezuelan equine encephalitis virus and eastern equine encephalitis virus replicons in Mammalian cells. J Virol **79:**7597-608.
34. **Poch, O., I. Sauvaget, M. Delarue, and N. Tordo.** 1989. Identification of four conserved motifs among the RNA-dependent polymerase encoding elements. Embo J **8:**3867-74.
35. **Puig-Basagoiti, F., M. Tilgner, B. M. Forshey, S. M. Philpott, N. G. Espina, D. E. Wentworth, S. J. Goebel, P. S. Masters, B. Falgout, P. Ren, D. M. Ferguson, and P. Y. Shi.** 2006. Triaryl pyrazoline compound inhibits flavivirus RNA replication. Antimicrob Agents Chemother **50:**1320-9.
36. **Scheidel, L. M., and V. Stollar.** 1991. Mutations that confer resistance to mycophenolic acid and ribavirin on Sindbis virus map to the nonstructural protein nsP1. Virology **181:**490-9.
37. **Schoepp, R. J., J. F. Smith, and M. D. Parker.** 2002. Recombinant chimeric western and eastern equine encephalitis viruses as potential vaccine candidates. Virology **302:**299-309.
38. **Sidwell, R. W., and D. F. Smee.** 2003. Viruses of the *Bunya-* and *Togaviridae* families: potential as bioterrorism agents and means of control. Antiviral Res. **57:**101-111.
39. **Tomar, S., R. W. Hardy, J. L. Smith, and R. J. Kuhn.** 2006. Catalytic core of alphavirus nonstructural protein nsP4 possesses terminal adenylyltransferase activity. J Virol **80:**9962-9.
40. **Turell, M. J., G. V. Ludwig, J. Kondig, and J. F. Smith.** 1999. Limited potential for mosquito transmission of genetically engineered, live-attenuated Venezuelan equine encephalitis virus vaccine candidates. Am.J.Trop.Med.Hyg. **60:**1041-1044.
41. **Turell, M. J., and M. D. Parker.** 2008. Protection of hamsters by Venezuelan equine encephalitis virus candidate vaccine V3526 against

lethal challenge by mosquito bite and intraperitoneal injection. Am J Trop Med Hyg **78:**328-32.

42. **van de Waterbeemd, H., G. Camenisch, G. Folkers, J. R. Chretien, and O. A. Raevsky.** 1998. Estimation of blood-brain barrier crossing of drugs using molecular size and shape, and H-bonding descriptors. J Drug Target **6:**151-65.
43. **Vasiljeva, L., L. Valmu, L. Kaariainen, and A. Merits.** 2001. Site-specific protease activity of the carboxyl-terminal domain of Semliki Forest virus replicase protein nsP2. J Biol Chem **276:**30786-93.
44. **Wang, E., O. Petrakova, A. P. Adams, P. V. Aguilar, W. Kang, S. Paessler, S. M. Volk, I. Frolov, and S. C. Weaver.** 2007. Chimeric Sindbis/eastern equine encephalitis vaccine candidates are highly attenuated and immunogenic in mice. Vaccine **25:**7573-81.
45. **Whittamore, P. R., M. S. Addie, S. N. Bennett, A. M. Birch, M. Butters, L. Godfrey, P. W. Kenny, A. D. Morley, P. M. Murray, N. G. Oikonomakos, L. R. Otterbein, A. D. Pannifer, J. S. Parker, K. Readman, P. S. Siedlecki, P. Schofield, A. Stocker, M. J. Taylor, L. A. Townsend, D. P. Whalley, and J. Whitehouse.** 2006. Novel thienopyrrole glycogen phosphorylase inhibitors: synthesis, in vitro SAR and crystallographic studies. Bioorg Med Chem Lett **16:**5567-71.
46. **Wu, J. Q., N. D. Barabe, D. Chau, C. Wong, G. R. Rayner, W. G. Hu, and L. P. Nagata.** 2007. Complete protection of mice against a lethal dose challenge of western equine encephalitis virus after immunization with an adenovirus-vectored vaccine. Vaccine **25:**4368-75.
47. **Zhang, J. H., T. D. Chung, and K. R. Oldenburg.** 1999. A Simple Statistical Parameter for Use in Evaluation and Validation of High Throughput Screening Assays. J Biomol Screen **4:**67-73.

Chapter V

General Discussion

Summary of Results

Neurotropic arboviruses cause severe and potentially fatal CNS infections where the extent of virus-mediated destruction of neurons is an important determinant in the severity and clinical outcome after infection. Early cellular innate immune responses mediated by pattern recognition receptors are often vital for effective pathogen control, and an effective neuronal innate immune response may be crucial to prevent the essentially irreversible loss of critical central nervous system neurons by neurotropic arboviruses. In this body of work I studied two complementary strategies of preventing death of neurotropic arbovirus-infected CNS neurons. The first approach investigated the interaction of neurotropic arboviruses with neuronal innate immune pattern recognition receptor pathways where the goal was to identify host and viral targets for the development of more effective neurotropic arbovirus vaccines and therapeutics. The second approach identified novel small molecules which inhibited neurotropic arbovirus replication and enhanced the viability of neuronal cells infected with neurotropic arboviruses. These studies significantly advance our knowledge of neuronal pattern recognition receptor signaling and neurotropic arbovirus biology by identifying specific, highly active PRR pathways in neurons

that mediate a neuron-protective response when challenged with neurotropic arboviruses. In addition, these studies demonstrate the potent countermeasures that neurotropic arboviruses deploy against neuronal antiviral PRR pathways, and advance our understanding of how a particular neurotropic arbovirus, WEEV, subverts these antiviral pathways. Finally, these studies identify a promising class of small molecules with anti-neurotropic arbovirus properties that may be clinically useful. In this chapter, I further summarize these studies and discuss their implications, significance, and potential future directions.

Neuronal Antiviral PRR Pathways

To investigate the hypothesis that neuronal PRR pathways influence neurotropic arbovirus pathogenesis, I first asked what PRR pathways are present and active in neurons. This was an important first step because PRR pathways are highly cell type-specific and few studies had investigated PRR signaling in neurons. Furthermore, the PRR signaling field progresses rapidly, suggesting that our knowledge of these pathways was, and likely still is, very incomplete. Thus, establishing a basic molecular framework for PRR signaling in neurons would greatly facilitate future studies aimed at investigating their impact on neurotropic viral infections. To accomplish this, I employed several neuronal culture models and used both global and targeted genetic and biochemical approaches to examine PRR expression and pathway activity in response to RLR and TLR ligands. I discovered that human CNS neurons selectively respond to TLR3-, TLR4-, MDA5-, and RIG-I-mediated stimulation (**Fig 5.1**) and failed to

observe any TLR7/8 or 9-mediated stimulation. TLR3, RIG-I and MDA5-mediated stimulation was dependent on the transcription factor IRF3 and activated NFκB resulting in the production of IFNβ and subsequent autocrine/paracrine ISRE activation mediated by the type-I IFN receptor. In contrast, TLR4-mediated stimulation failed to activate an ISRE but did produce a neuronal NFκB response. In comparison to neurons, LPS stimulation of TLR4 in the human monocytic cell line, U937, robustly activated both NFκB and an ISRE (**Supplemental Fig S2.4**), which suggested to us that neuronal TLR4 was unlikely to mediate a classical innate antiviral response and was not studied further. Finally, detailed genetic and pharmacologic studies revealed that TLR3- and possibly MDA5-mediated neuronal responses are positively regulated by the PI3K pathway, and in particular the PI3K p110α subunit. These results demonstrated that CNS neurons are immunologically active and possess specific and non-redundant functional PRR pathways. In particular, those pathways typically stimulated by viral pathogens via nucleic acid recognition are especially active in neurons, and therefore may play a protective role in neurotropic virus pathogenesis. In the time since these studies were conducted, several other viral PRRs were characterized including NOD2 (63) and DAI (67). Due to this, the model depicted in Figure 5.1 in no way defines an absolute set of viral PRRs in neurons, and future studies should investigate the neuronal relevance of these newly identified PRRs.

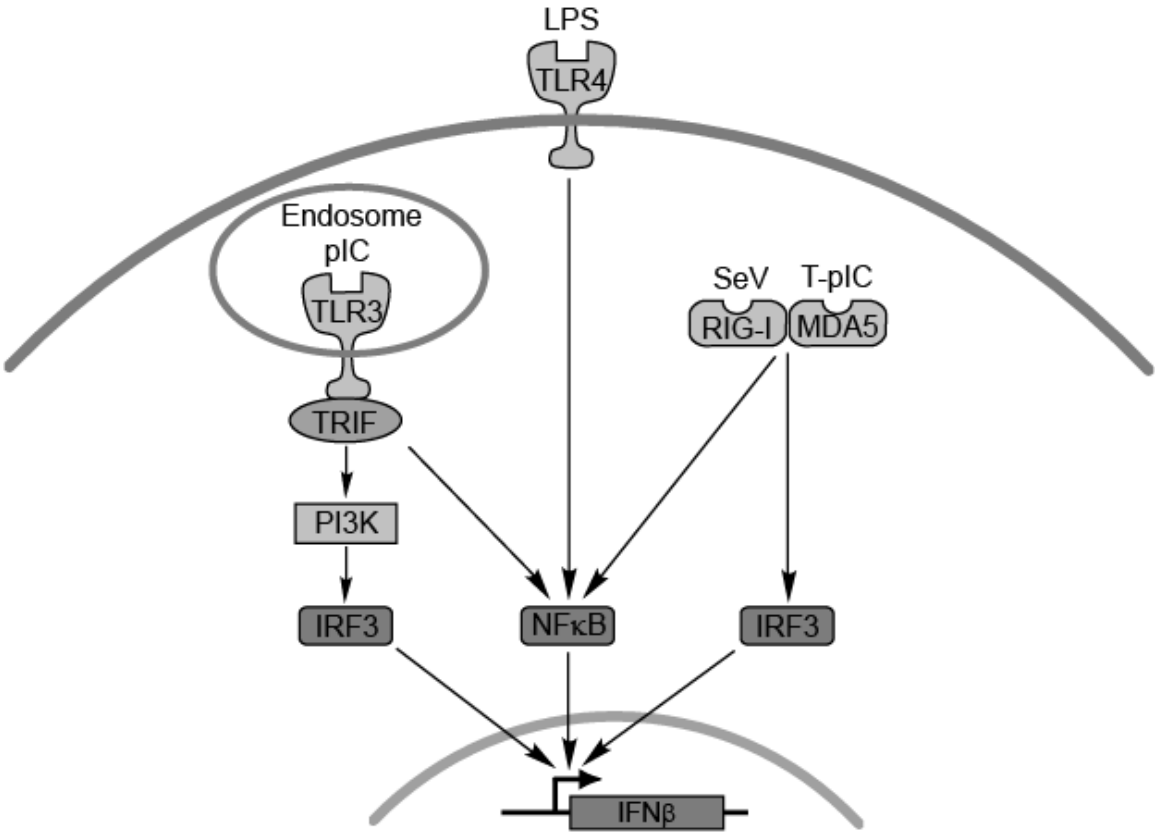

Figure 5.1. Neuronal PRR pathways. Neuronal PRR pathways identified by the studies in chapter II are depicted. Note that TLR4 does not appear to activate IRF3, and it is unclear if PI3Ks in neurons directly influence TLR3-dependent activation of IRF3. See text for further details. pIC-polyinosinic-polycytidylic acid, LPS-lipopolysaccharide, SeV-Sendai virus, T-pIC-transfected polyinosinic-polycytidylic acid.

Neuronal PRR Pathway Response to Neurotropic Arboviruses

After establishing a basic molecular understanding of neuronal PRR pathways, I then tested whether these PRR pathways influenced neuronal responses to neurotropic viral infections. To address this hypothesis I coupled targeted genetic and molecular techniques with several neuronal culture models including immortal neuronal cell lines, primary cortical neurons from mice with deletions in key PRR pathway component genes, and human embryonic stem cell-derived neurons. I began studying the interaction between neuronal PRR pathways and neurotropic arbovirus infections by first asking if WEEV could induce neuronal IFNβ transcription, a hallmark of PRR pathway activation. I found that replication-competent WEEV induced neuronal IFNβ transcription in a RIG-I/MDA5 and IRF3-dependent manner (**Fig 3.16**). These data are important because they greatly increase our knowledge of PRR pathway detection of encephalitic alphaviruses and subsequent downstream signaling in an appropriate target cell.

Next, I determined if neuronal PRR pathway components mediated a cytoprotective or antiviral effect when challenged with a neurotropic arbovirus. Interestingly, IRF3 consistently mediated a neuron-protective response to WEEV and SLEV, but had no effect on a LACV challenge (**Fig 3.16**). The differentiated human neuronal culture model, BE(2)-C/m, suggested that RIG-I and MDA5 also mediated a neuron-protective and possibly antiviral effect when challenged with WEEV, but these phenotypes were not recapitulated in the primary mouse neuronal culture model. This discrepancy between neuronal culture models will

ultimately require further experimentation to settle the potential neuron-protective and antiviral role of RIG-I and MDA5 in response to WEEV.

In differentiated human neuronal cells, IRF3 also appeared to have a small antiviral effect reflected by an approximate one-log_{10} reduction in WEEV titer, but this did not validate in primary cortical neurons derived from $IRF3^{-/-}$ mice. Due to these discrepancies between neuronal culture models, I focused further experiments on the consistent neuron-protective effect of IRF3 and found it to be independent of the induction of antiviral type-I IFNs and likely due to direct IRF3-dependent induction of cytoprotective genes. Candidate WEEV-induced, IRF3-dependent, cytoprotective genes included OASL and MxB, where depletion of the most induced candidate, OASL, enhanced a LACV-mediated CPE but had no effect on WEEV or SLEV. Curiously, OASL may mediate a neuronal response to LACV independent of IRF3, as cells stably overexpressing a dominant negative mutant of IRF3 responded normally to LACV. Nevertheless, these results suggested that cell-intrinsic factor(s) downstream of IRF3 may be responsible for the IRF3-dependent, cytoprotective response to WEEV. Further analysis of other neurotropic arbovirus-induced, IRF3-dependent, putative cytoprotective genes, such as MxB, may identify genes which are protective against WEEV and SLEV. With this in mind, MxB is an attractive candidate because it is closely related to the well characterized antiviral effector gene MxA, which has antiviral effects against old world alphaviruses, bunyaviruses, and flaviviruses (64). In contrast to MxA, which exerts its antiviral effect by disrupting the trafficking of viral nucleocapsids resulting in abrogated viral replication (60),

MxB is not known to be antiviral, but it has not been tested against many neurotropic arboviruses including WEEV. The best described cellular function of MxB is to enhance nuclear import (41). This suggests a particularly attractive hypothesis in which MxB may achieve a putative cytoprotective effect against WEEV by counteracting WEEV capsid's ability to inhibit nuclear translocation of IRF3. Future studies will be required to test this hypothesis.

As mentioned above, the ability of OASL to mediate a neuron-protective effect against LACV is somewhat puzzling because OASL is an IRF3-dependent gene (50), yet IRF3 appeared to have no effect on an LACV-mediated CPE (Chapter III). These results may indicate that in neurons infected with LACV, an alternate pathway independent of IRF3 induces OASL. The antiviral effects of OASL are poorly characterized in comparison to the classic OAS genes (49), and future studies will need to address the mechanism of OASL-mediated cytoprotection against LACV as well as clarify whether OASL's neuron-protective effects are direct or indirectly related to an antiviral effect. In addition, future studies should be done in vivo as much as possible because important differences between tissue culture and animal models have been observed for antiviral effector responses (76). In summary, these data extend the protective effect of OASL from picornaviruses (49) to now include a neurotropic arbovirus in *Bunyaviridae*. More broadly, these studies establish neuronal PRR pathways as potentially important determinants in neurotropic arbovirus pathogenesis.

Neurotropic Arbovirus Countermeasures to Neuronal PRR Pathways

Viral PRR pathways protect host cells and tissues against viral infections, yet many viruses, including the neurotropic arboviruses WNV and LACV, possess PRR pathway countermeasures allowing them to efficiently replicate, avoid immune detection, and cause disease (13, 51, 74). I suspected that WEEV may also potently block these pathways given that IFNβ transcription was not robustly induced until late in infection, and that I could not detect any WEEV-induced antiviral type-I IFN protein production. As suspected, WEEV, SLEV, and LACV all potently and specifically blocked induction of neuronal antiviral PRR pathways at early times post infection. To my knowledge this is the first demonstration of WEEV and SLEV inhibiting PRR signal transduction in a relevant cell type. It will be interesting to see if SLEV employs homologous mechanisms of PRR inhibition to that of other members of *Flaviviridae,* such as WNV and hepatitis C virus (4, 18). Since WNV, SLEV, LACV, and WEEV all inhibit PRR pathways, I postulate that this may be a general virulence mechanism for neurotropic arboviruses.

Alphavirus inhibition of antiviral signaling is often attributed to non-specific inhibition of host gene expression mediated by nsP2 for old world viruses and capsid for new world viruses (25). Recently, VEEV capsid has also been shown to inhibit nuclear translocation, and it was proposed that this may also contribute to the inhibition of antiviral signaling (3), although this hypothesis was not directly tested. I decided to systematically and directly explore how WEEV inhibits neuronal PRR signaling at a molecular level, and similar to VEEV, I mapped the antiviral PRR pathway inhibitory capacity of WEEV to the capsid gene. WEEV

capsid inhibited antiviral PRR signaling downstream of IRF3 activation, and a WEEV structural gene(s), likely capsid, inhibited IRF3 nuclear translocation. Further studies found that WEEV capsid also inhibited host gene expression, suggesting a dual mechanism for capsid-mediated inhibition of neuronal antiviral PRR signaling (**Fig 3.16**). Interestingly, this mechanism appears to be distinct from that of nsP2 for old world alphaviruses in which IRF3 efficiently reaches the nucleus in SINV (7) and Semliki Forest virus-infected cells (5). Altogether these studies examining the interaction of neuronal PRR pathways with neurotropic arboviruses indicated that neuronal PRR pathways are important determinants in neurotropic arbovirus pathogenesis. These studies also suggest that neuronal PRR pathways and viral countermeasures to them may be exploited to develop more efficacious vaccines and anti-neurotropic arboviral treatments.

It is somewhat paradoxical that WEEV activates neuronal IFNβ transcription, yet a functional cell-intrinsic, IRF3-dependent, type-I IFN-independent, neuronal, cytoprotective response remains. One explanation for this paradox could be that the cytoprotective pathway is more responsive to low levels of PRR signal transduction reaching the nucleus than the antiviral type-I IFN-dependent pathway. Adding to this paradox, new and old world alphaviruses increase serum levels of type-I IFNs (14, 24) in mice, suggesting that PRR pathway inhibition may be incomplete or ineffective in alternate cell types. Reassuringly, there is literature precedence for the simultaneous requirement for host antiviral signaling to effectively resolve infection of viruses that deploy potent countermeasures to the very same required host antiviral pathways (4), and one

well studied example is that of the neurotropic arbovirus WNV (19). Hence, it appears that there is an intense interplay between viruses and host antiviral PRR pathways possibly indicating that viruses and host PRR pathways generally co-evolve in a way that strikes a balance between the need to efficiently replicate yet not be overly burdensome on the host such that transmission remains efficient. Since humans are often dead end hosts for neurotropic arboviruses, it could be argued that neurotropic arboviruses and humans may have come into contact with each other relatively recently, and that over time host antiviral pathways and viral countermeasures to these antiviral pathways will reach an equilibrium such that neurotropic arboviruses are less pathogenic and that humans become natural participants in the transmission cycle of neurotropic arboviruses. Of course, these hypotheses will need to be specifically addressed. One way of testing these hypotheses would be to determine if WEEV is less able to inhibit PRR signaling in hosts that participate in its natural enzootic cycle. Additionally, future efforts should also confirm that neuronal PRR pathways are indeed inhibited from responding to a neurotropic arbovirus stimulus, as opposed to a poly(I-C) stimulus. For WEEV, this could be accomplished by identifying WEEV capsid mutants or generating WEEV virus-like particles lacking structural genes that robustly induce antiviral type-I IFNs in neuronal cells.

Neurotropic Alphavirus Replication Inhibitors

Finally, I took a different approach to preventing death of neurotropic arbovirus infected neurons by searching for small molecules that block neurotropic

arbovirus replication. To achieve this, ~51,000 small molecules were screened for the ability to inhibit a WEEV replicon harboring a luciferase reporter. I identified thieno[3,2-*b*]pyrrole derivatives as novel small molecule inhibitors of neurotropic alphaviruses. Importantly, these molecules decreased alphavirus titers and protected human neuronal cells from alphavirus mediated cytopathic effect. There is a great need for drugs to treat neurotropic arbovirus infections; therefore, these inhibitors are actively being pursued for clinical use by performing in vivo studies and optimizing the lead compound for reduced cytotoxicity, increased potency, increased efficacy, and greater CNS penetration. Perhaps small molecules derived from this screen will one day be partnered with small molecule modulators of PRR pathways to form a highly effective, anti-neurotropic arbovirus, multi-component therapy.

Unanswered Questions and Future Directions

The studies in this body of work give rise to many important questions including:

1. What is the mechanism and downstream factors of PI3K in neuronal antiviral PRR signaling?
2. What is the role of PI3K in neuronal responses to neurotropic arboviruses?
3. What other factors mediate the IRF3-dependent, neuron-protective response to WEEV?
4. How does a WEEV structural gene(s), likely capsid, inhibit IRF3 nuclear translocation?
5. What is the *in vivo* relevance of neuronal PRR signaling for WEEV pathogenesis?
6. How do neuronal PRR responses interact with PRR responses by other resident CNS cell types?
7. What is the mechanism of thieno[3,2-*b*]pyrrole derivatives' inhibition of alphaviruses?
8. Are neuronal PRR pathways and viral countermeasures to these pathways viable targets for development of therapeutics?

The following pages will discuss these questions and potential future directions that could be taken to address them.

What is the mechanism and downstream factors of PI3K in neuronal antiviral PRR signaling?

The PI3K pathway mediated by p110α and its receptor subunit p85α activate a number of downstream signaling molecules. One well characterized pathway activates the kinase Akt which has been linked not only to mTOR activation and subsequent enhancement of translation (15), but also to activation of NFκB (28, 53, 56). In addition, a PI3K/Akt/mTOR/S6-kinase pathway has been implicated in TLR9-mediated induction of IFNβ in dendritic cells (8). In chapter II I identified PI3Ks as important mediators of neuronal RLR and TLR pathways, but the mechanism of PI3K-mediated antiviral PRR signaling remains obscure. The majority of work investigating the role of PI3Ks in PRR signaling has focused on its effects during TLR-initiated signaling (32), where it appears to be necessary for full activation of IRF3. Other studies determined that PI3K/AKT pathways are essential for neuronal development and survival (11, 12, 35), suggesting a potential link between antiviral PRR pathway activation and the ability of neurons to overcome an infection until an adaptive immune response can be fully established. The kinase inhibitor library studies in chapter II suggested that Akt, mTOR, and glycogen synthase kinase 3 may be downstream of PI3K responses in neurons. All of these kinases participate in PI3K signaling and have been implicated in innate immunity in non-neuronal model systems (8, 10, 39, 40, 42, 55). Furthermore, preliminary studies demonstrated that poly(I-C) induced rapid phosphorylation of Akt and S6K in neuronal cells, and the mTOR inhibitor, rapamycin, demonstrated a similar neuronal PRR pathway inhibitory profile as

the PI3K inhibitor LY294002 suggesting that a common pathway was targeted by each drug (**Supplemental Fig S5.1**). Nevertheless, additional studies will be required to further delineate the precise PI3K pathway components involved in neuronal antiviral PRR activation.

Another potential hypothesis for how PI3K mediates antiviral PRR signaling is suggested by a recent interesting study demonstrating an antiviral PRR co-activator pathway. The authors of this study demonstrated that the host protein LRRFIP1 binds viral PAMPs and interacts with β-catenin, thereby promoting the interaction of IRF3 with its co-activator p300 (73). β-catenin is a known downstream target of PI3K/Akt signaling (21), suggesting that PI3K/Akt signaling may influence innate antiviral signaling via a similar co-activator pathway. In a co-activator-like pathway, PI3K-mediated signals would be transmitted in parallel to canonical IPS-I dependent antiviral signals until they united at the level of transcription. This hypothesis will need further study, but I have conducted a preliminary experiment consistent with a co-activator role for neuronal PI3K p110α. In this experiment, I asked if overexpression of a constitutively active p110α (61) could induce a neuronal ISRE. Interestingly, it did not induce a neuronal ISRE unless a PRR pathway stimulus was also given (**Supplemental Fig S2.5.B**). This is in stark contrast to most constitutively active direct PRR pathway signaling molecules (Chapter III). Furthermore, microarray analysis revealed that LRRFIP1 transcripts are elevated in PRR pathway competent differentiated versus PRR pathway incompetent undifferentiated neuronal cells (**Supplemental Table S2.1**). Altogether these data suggest that

the canonical IPS-I dependent pathway may be parallel to a co-activator-like, PI3K-dependent pathway in neuronal cells.

The PI3K pathway has been tentatively implicated in cytoplasmic RLR-initiated signaling (50), and in chapter II, I showed that PI3K inhibitors block MDA5-mediated signaling in neuronal cells. However, depletion of p110α in neuronal cells had no effect on induction of an MDA5-mediated stimulation. This may be due to insufficient depletion of p110α, redundancy among the p110s for MDA5-mediated signaling, or off target effects of these drugs. Because the PI3Ks are known druggable targets (33), the precise role of PI3K in RLR-mediated signaling would be worth determining, especially if modulation of RLR pathways proves beneficial for autoimmune or neuroinflammatory diseases. This could be accomplished in many ways, but one approach would be to explore RLR responses in animals with deletions of PI3K-components or attempting to deplete PI3K levels further.

In addition to PI3K inhibitors and associated downstream signaling molecules, the kinase inhibitor screen in chapter II also implicated several kinases not known to be involved in PRR signaling. Further investigation of these molecules and those kinases that showed preference to either a TLR3 or MDA5/RIG-I-mediated stimulus may provide novel insight for PRR signaling pathways.

What is the role of PI3K in neuronal responses to neurotropic arboviruses?

PI3K signaling dramatically affected neuronal PRR pathway signaling (Chapter II), yet depletion of PI3K expression had no effect on WEEV-mediated induction of IFNβ mRNA (Chapter III and **Supplemental Fig S3.1.A**). Curiously, depletion of PI3K expression slightly protected neurons from a WEEV-mediated cytopathic effect (**Supplemental Fig S3.1.B**). These preliminary data indicated that the dominant effect of neuronal PI3K signaling on a WEEV infection may not be to promote antiviral signal transduction. One alternative hypothesis consistent with the decreased WEEV-mediated CPE in PI3K-deficient neurons is that PI3K signaling may promote WEEV replication. In support of this alternative hypothesis, previous studies found that ribosomal protein S6, a target of PI3K/Akt/mTOR/S6K signaling, interacts with alphavirus nsP2 and mediates enhanced expression of alphavirus messages (52). While the observation that PI3K signaling may actually enhance WEEV replication in neurons was unexpected given the positive role PI3Ks play in neuronal antiviral PRR pathways, further examination of the interaction of alphaviruses and potentially other neurotropic arboviruses with PI3K-mediated pathways may provide novel insights about host factors involved in alphavirus replication.

What other factors mediate the IRF3-dependent, neuron-protective response to WEEV?

In chapter III I demonstrated an IRF3-dependent, neuron-protective response to WEEV that is independent of type-I interferons and likely due to direct, IRF3-

dependent induction of cytoprotective genes. IRF3 directly promotes an antiviral state independent of type-I IFNs (27), but very recently, a novel model for RLR- and IRF3-dependent but type-I IFN-independent signaling was presented. The authors of this model described an antiviral PRR pathway dependent on peroxisomal as opposed to mitochondrial IPS-I that is independent of type-I IFN induction (20), which provides a potential mechanism for the neuronal response I observed. While interesting, this potential model will need experimental verification in a neuronal system, and its dependence on IPS-I will have to be rectified with the apparent lack of dependence I observed for responses to WEEV in IPS-I$^{-/-}$ neurons. Nevertheless, this study highlights the complexity of antiviral PRR pathways and suggests that antiviral signaling independent of type-I IFNs is a relatively common phenomenon.

The innate antiviral effect of PRR pathways and the type-I IFN pathway are often dependent on multiple antiviral effector genes (2, 64, 72). In chapter III, I identified OASL and MxB as WEEV-induced, IRF3-dependent, putative cytoprotective genes against neurotropic arboviruses in neuronal cells. Depletion of the most induced candidate cytoprotective gene, OASL, rendered neuronal cells more susceptible to LACV but had no effect on neuronal responses to WEEV or SLEV. These data highlighted the pathogen-specific nature of antiviral effector genes and indicated that alternative cytoprotective genes mediate the neuronal cell response to WEEV and SLEV. One candidate cytoprotective gene is, as mentioned above, MxB, which is actively being investigated. However, other candidate genes may exist. One way of discovering these candidate genes

would be to perform a microarray experiment comparing WEEV-infected control and IRF3-deficient neurons, and then studying those genes with diminished induction in the IRF3-defective neurons. Of course, this approach assumes the IRF3-dependent response is transcriptional in nature. I believe this is a valid assumption given that the dominant negative IRF3 construct used to identify the IRF3-dependent phenotype lacked a DNA binding domain, thereby rendering it incapable of inducing transcription but still capable of receiving PRR pathway-mediated activation signals. The microarray approach outlined above is likely to identify several candidate genes, but rigorously and systematically characterizing the role these candidate genes play in the neuronal response to neurotropic arboviruses, including WEEV and SLEV, may be beneficial for future therapeutics development.

How does a WEEV structural gene(s), likely capsid, inhibit IRF3 nuclear translocation?

Work by others demonstrated that VEEV capsid localizes to nuclear pores and inhibits nuclear translocation (3), and other RNA viruses that do not require nuclei for their replication, including polio, rhino, rabies, and vesicular stomatitis viruses, have evolved mechanisms for efficient interference of nucleo-cytoplasmic trafficking (29, 34, 38, 71). In chapter III, I showed that a WEEV structural gene(s), likely capsid, inhibits IRF3 nuclear translocation in neuronal cells, and that WEEV capsid-staining in BHK cells showed intense capsid expression in a ring surrounding the nucleus. These data provided a potential

mechanism, in conjunction with shut off of host gene expression, for the ability of capsid to inhibit antiviral PRR signaling. Furthermore, these data supported the hypothesis that WEEV capsid, like VEEV capsid, inhibits nuclear pore function in neuronal cells. However, given that a construct harboring the WEEV structural genes inhibited IRF3 nuclear translocation and that WEEV capsid's ability to inhibit IRF3 nuclear accumulation could not be completely separated from its ability to inhibit host gene expression, future studies will have to rule out a role for WEEV envelope proteins in the WEEV-mediated disruption of IRF3 nuclear translocation.

The ability of WEEV capsid to disrupt nuclear pore function also needs to be directly tested. One approach would be to determine if WEEV capsid co-localizes or immunoprecipitates with nuclear pore machinery or nuclear transport receptors. In addition, the selectivity of the proposed capsid-mediated inhibition of nuclear translocation should also be tested given that an IFN-mediated transcriptional response, which also requires nuclear translocation of signal-activated transcription factors, was not susceptible to capsid-mediated inhibition at early times post infection. In a similar vein, TNFα-mediated activation of NFκB was inhibited by WEEV capsid, suggesting that a factor common to both pathways, potentially nuclear import of activated transcription factors, was inhibited by WEEV capsid. Finally, it is unclear whether WEEV capsid-mediated CPE, shut off of host macromolecular synthesis, and interference with type-I IFN induction are the result of one common mechanism (e.g. disruption of nuclear pore function) or are all independent functions of capsid. Efforts to identify

capsid mutants that differentially affect each of these functions may clarify this question.

What is the *in vivo* relevance of neuronal PRR signaling for WEEV pathogenesis?

While this question may seem intellectually trivial, its importance for this body of work could not be more paramount. The studies I conducted used *in vitro* or *ex vivo* neuronal cultures to ensure that all phenotypes could directly be attributed to neurons. However, these cultures do not perfectly mimic the natural environment of a CNS neuron. Furthermore, PRR pathway responses also vary between *in vitro* and *in vivo* models. For instance, DAI, a putative dsDNA sensor, was shown to detect cytosolic dsDNA and mediate an antiviral response *in vitro* (67), but when DAI was deleted, null mice responded normally to dsDNA (37). The function of LGP2 may also vary between *in vitro* and *in vivo* models, where *in vitro* it may negatively regulate RLR signaling, but *in vivo* it appears to be required for RLR signaling (65). Finally, important differences were observed between tissue culture and animal models for antiviral effector responses to old world alphaviruses (76). In support of innate antiviral responses of resident CNS cells being relevant *in vivo*, studies in conditional knockout mice that have disrupted type-I IFN receptor expression in neuroectodermal cells, which includes neurons, indicated that responses to type-I IFNs are important to control virus spread within the CNS (17). However, these responses may have been due to other neuroectoderm-derived cells such as astrocytes or

oligodendrocytes. For this reason, future studies investigating the role of neuronal PRR pathways *in vivo* should generate neuron-specific deletions of key PRR pathway components, such as IRF3, by crossing mice containing *loxP*-flanked alleles of interest (e.g. *IRF3*) with mice harboring the Cre-recombinase driven by the neuron-specific enolase promoter (43).

How do neuronal PRR responses interact with PRR responses by other resident CNS cell types?

The main target cell of neurotropic arboviruses in the CNS is the neuron, but this does not preclude other resident CNS cell types from eliciting an innate immune response. For example, glial cells (astrocytes, oligodendrocytes, and microglia) are capable of producing an innate response, and microglia, which are the myeloid-derived resident cell-type in the CNS, contain highly active TLR-mediated pathways (45, 62). Glial cell PRR signaling may mediate the neuropathology of several diseases including viral encephalomyelitis, Alzheimer's disease, amyotrophic lateral sclerosis, ischemic brain injury, and seizures (44, 62). In addition, innate immune signaling by glial cells mediates pathology of bystander neurons in several diseases including a neuro-adapted Sindbis virus model of encephalomyelitis (16, 36, 54, 58, 59). These studies suggest that PRR signaling by neurons and other resident cell types in the CNS may interact and be important for pathogenesis. A research program utilizing mice deficient in various PRR pathway components could easily be designed to investigate how PRR responses in different CNS cell-types interact because

there are established protocols for the isolation, culture, and co-culture of all resident cell types in the CNS (6, 22, 48, 75).

What is the mechanism of thieno[3,2-*b*]pyrrole derivatives' inhibition of alphaviruses?

The lack of antiviral medications and broadly approved vaccines highlights the urgent and pressing need for the development of broadly active antiviral agents against neurotropic arboviruses. To address this need, I identified a class of small molecules with a thieno[3,2-*b*]pyrrole core structure that inhibited neurotropic alphavirus replication and protected human neuronal cells from alphavirus-mediated CPE (Chapter IV). Although the mechanism underlying the antiviral activity of these molecules remains unknown, the fact that they were identified as inhibitors of neurotropic alphavirus replicons suggests that viral replicase proteins are potential targets, whereas early events in the viral life cycle, such as receptor engagement, internalization, and uncoating, are unlikely targets. In addition, the broad activity of the lead compound, CCG32091, against infectious virus or replicons derived from WEEV, EEEV, VEEV, Fort Morgan virus, and SINV suggests that a highly conserved viral enzymatic activity may be targeted. Alphavirus nsPs contain several distinct enzymatic activities, including methyltransferase (nsP1) (1), protease and helicase (nsP2) (26, 30), and RNA polymerase (nsP4) (57). In vitro assays have been developed for several of these activities (1, 69, 70), which provides a convenient approach for target identification. An alternative approach that takes advantage of the intrinsically

high error rate of viral RNA polymerases previously used successfully for antiviral target identification is the isolation and characterization of viral escape mutants (46, 47, 66). Finally, affinity purification and identification of viral or cellular proteins that physically interact with antiviral agents, as well as identifying the spectrum of viruses susceptible to the lead compound, may aid target deconvolution. All of these approaches, including optimizing the lead compound and testing its *in vivo* activity against diverse neurotropic arboviruses, are actively being pursued.

Are neuronal PRR pathways and viral countermeasures to these pathways viable targets for development of neurotropic alphavirus therapeutics?

Drug-resistant viral mutants quickly emerge due to intrinsically high error rates for viral RNA polymerases. Moreover, when used in combination, antiviral therapy is much more effective due to the decreased probability of generating multiply resistant viruses. One potential set of alternative antiviral drug targets are PRR pathways and viral countermeasures to these pathways. Recent evidence suggests that developing such medications may be fruitful. For instance, GSK983, a small molecule that induces a subset of ISGs independent of type-I IFN induction, inhibits replication of a wide array of viruses (31); and small molecules that block hepatitis C virus NS3/4A protease, a PRR pathway countermeasure, decrease viral replication and may be of clinical benefit (23, 68). Other examples include the TLR7 ligand imiquimod that is used topically to treat human papillomavirus, and the development of novel therapeutic platforms

that inhibit pandemic influenza replication such as gold nanorod delivery of the innate immune activator ssRNA (9). Existing therapeutics activating innate antiviral pathways could be immediately tested for activity against neurotropic arboviruses, but generation of inhibitors of neurotropic arbovirus PRR pathway countermeasures, such as those targeting WEEV capsid, would require extensive research and development. However, assays presented in chapter III could be easily modified and adapted for high throughput screening of small molecules that restore ISRE activation in neuronal cells transfected with WEEV capsid.

Overall Significance

The work presented here demonstrates that neurons are active players in the innate immune response to neurotropic arboviruses and that neuronal antiviral PRR pathways may be important determinants of neurotropic arbovirus pathogenesis. Specifically, I showed that human neurons posses a compliment of highly active antiviral PRR pathways and that these pathways mediate neuronal responses to neurotropic arboviruses. In addition, I demonstrated that neurotropic arboviruses posses PRR pathway countermeasures, and I determined that the neurotropic arbovirus WEEV subverts antiviral neuronal PRR pathways via inhibition of IRF3 nuclear translocation and host gene expression, both of which are likely mediated by WEEV-capsid. Finally, I identified a novel class of neurotropic alphavirus replication inhibitors which may be useful for mono-therapy or in combination with potential therapeutics designed to enhance the neuronal innate immune response or inhibit viral countermeasures to the innate immune response.

References

1. **Ahola, T., P. Laakkonen, H. Vihinen, and L. Kaariainen.** 1997. Critical residues of Semliki Forest virus RNA capping enzyme involved in methyltransferase and guanylyltransferase-like activities. J.Virol. **71:**392-397.
2. **Andersen, J., S. VanScoy, T. F. Cheng, D. Gomez, and N. C. Reich.** 2008. IRF-3-dependent and augmented target genes during viral infection. Genes Immun **9:**168-75.
3. **Atasheva, S., A. Fish, M. Fornerod, and E. I. Frolova.** 2010. Venezuelan equine Encephalitis virus capsid protein forms a tetrameric complex with CRM1 and importin alpha/beta that obstructs nuclear pore complex function. J Virol **84:**4158-71.
4. **Bowie, A. G., and L. Unterholzner.** 2008. Viral evasion and subversion of pattern-recognition receptor signalling. Nat Rev Immunol **8:**911-22.
5. **Breakwell, L., P. Dosenovic, G. B. Karlsson Hedestam, M. D'Amato, P. Liljestrom, J. Fazakerley, and G. M. McInerney.** 2007. Semliki Forest virus nonstructural protein 2 is involved in suppression of the type I interferon response. J Virol **81:**8677-84.
6. **Brewer, G. J., and P. J. Price.** 1996. Viable cultured neurons in ambient carbon dioxide and hibernation storage for a month. Neuroreport **7:**1509-12.
7. **Burke, C. W., C. L. Gardner, J. J. Steffan, K. D. Ryman, and W. B. Klimstra.** 2009. Characteristics of alpha/beta interferon induction after infection of murine fibroblasts with wild-type and mutant alphaviruses. Virology **395:**121-32.
8. **Cao, W., S. Manicassamy, H. Tang, S. P. Kasturi, A. Pirani, N. Murthy, and B. Pulendran.** 2008. Toll-like receptor-mediated induction of type I interferon in plasmacytoid dendritic cells requires the rapamycin-sensitive PI(3)K-mTOR-p70S6K pathway. Nat Immunol **9:**1157-64.
9. **Chakravarthy, K. V., A. C. Bonoiu, W. G. Davis, P. Ranjan, H. Ding, R. Hu, J. B. Bowzard, E. J. Bergey, J. M. Katz, P. R. Knight, S. Sambhara, and P. N. Prasad.** 2010. Gold nanorod delivery of an ssRNA immune activator inhibits pandemic H1N1 influenza viral replication. Proc Natl Acad Sci U S A **107:**10172-7.
10. **Colina, R., M. Costa-Mattioli, R. J. Dowling, M. Jaramillo, L. H. Tai, C. J. Breitbach, Y. Martineau, O. Larsson, L. Rong, Y. V. Svitkin, A. P. Makrigiannis, J. C. Bell, and N. Sonenberg.** 2008. Translational control of the innate immune response through IRF-7. Nature **452:**323-8.
11. **Cosker, K. E., and B. J. Eickholt.** 2007. Phosphoinositide 3-kinase signalling events controlling axonal morphogenesis. Biochem Soc Trans **35:**207-10.
12. **Cosker, K. E., S. Shadan, M. van Diepen, C. Morgan, M. Li, V. Allen-Baume, C. Hobbs, P. Doherty, S. Cockcroft, and B. J. Eickholt.** 2008. Regulation of PI3K signalling by the phosphatidylinositol transfer protein

PITPalpha during axonal extension in hippocampal neurons. J Cell Sci **121:**796-803.
13. **Crack, P. J., and P. J. Bray.** 2007. Toll-like receptors in the brain and their potential roles in neuropathology. Immunol Cell Biol **85:**476-80.
14. **Cruz, C. C., M. S. Suthar, S. A. Montgomery, R. Shabman, J. Simmons, R. E. Johnston, T. E. Morrison, and M. T. Heise.** 2010. Modulation of type I IFN induction by a virulence determinant within the alphavirus nsP1 protein. Virology **399:**1-10.
15. **Cully, M., H. You, A. J. Levine, and T. W. Mak.** 2006. Beyond PTEN mutations: the PI3K pathway as an integrator of multiple inputs during tumorigenesis. Nat Rev Cancer **6:**184-92.
16. **Darman, J., S. Backovic, S. Dike, N. J. Maragakis, C. Krishnan, J. D. Rothstein, D. N. Irani, and D. A. Kerr.** 2004. Viral-induced spinal motor neuron death is non-cell-autonomous and involves glutamate excitotoxicity. J Neurosci **24:**7566-75.
17. **Detje, C. N., T. Meyer, H. Schmidt, D. Kreuz, J. K. Rose, I. Bechmann, M. Prinz, and U. Kalinke.** 2009. Local type I IFN receptor signaling protects against virus spread within the central nervous system. J Immunol **182:**2297-304.
18. **Diamond, M. S.** 2009. Virus and host determinants of West Nile virus pathogenesis. PLoS Pathog **5:**e1000452.
19. **Diamond, M. S., E. Mehlhop, T. Oliphant, and M. A. Samuel.** 2009. The host immunologic response to West Nile encephalitis virus. Front Biosci **14:**3024-34.
20. **Dixit, E., S. Boulant, Y. Zhang, A. S. Lee, C. Odendall, B. Shum, N. Hacohen, Z. J. Chen, S. P. Whelan, M. Fransen, M. L. Nibert, G. Superti-Furga, and J. C. Kagan.** 2010. Peroxisomes are signaling platforms for antiviral innate immunity. Cell **141:**668-81.
21. **Fang, D., D. Hawke, Y. Zheng, Y. Xia, J. Meisenhelder, H. Nika, G. B. Mills, R. Kobayashi, T. Hunter, and Z. Lu.** 2007. Phosphorylation of beta-catenin by AKT promotes beta-catenin transcriptional activity. J Biol Chem **282:**11221-9.
22. **Fedoroff, S., and A. Richardson.** 2001. Protocols for Neural Cell Culture, 3 ed. Humana Press.
23. **Foy, E., K. Li, C. Wang, R. Sumpter, Jr., M. Ikeda, S. M. Lemon, and M. Gale, Jr.** 2003. Regulation of interferon regulatory factor-3 by the hepatitis C virus serine protease. Science **300:**1145-8.
24. **Gardner, C. L., C. W. Burke, M. Z. Tesfay, P. J. Glass, W. B. Klimstra, and K. D. Ryman.** 2008. Eastern and Venezuelan equine encephalitis viruses differ in their ability to infect dendritic cells and macrophages: impact of altered cell tropism on pathogenesis. J Virol **82:**10634-46.
25. **Garmashova, N., R. Gorchakov, E. Volkova, S. Paessler, E. Frolova, and I. Frolov.** 2007. The Old World and New World alphaviruses use different virus-specific proteins for induction of transcriptional shutoff. J Virol **81:**2472-84.

26. **Gomez, d. C., N. Ehsani, M. L. Mikkola, J. A. Garcia, and L. Kaariainen.** 1999. RNA helicase activity of Semliki Forest virus replicase protein NSP2. FEBS Lett. **448:**19-22.
27. **Grandvaux, N., M. J. Servant, B. tenOever, G. C. Sen, S. Balachandran, G. N. Barber, R. Lin, and J. Hiscott.** 2002. Transcriptional profiling of interferon regulatory factor 3 target genes: direct involvement in the regulation of interferon-stimulated genes. J Virol **76:**5532-9.
28. **Gustin, J. A., O. N. Ozes, H. Akca, R. Pincheira, L. D. Mayo, Q. Li, J. R. Guzman, C. K. Korgaonkar, and D. B. Donner.** 2004. Cell type-specific expression of the IkappaB kinases determines the significance of phosphatidylinositol 3-kinase/Akt signaling to NF-kappa B activation. J Biol Chem **279:**1615-20.
29. **Gustin, K. E.** 2003. Inhibition of nucleo-cytoplasmic trafficking by RNA viruses: targeting the nuclear pore complex. Virus Res **95:**35-44.
30. **Hardy, W. R., and J. H. Strauss.** 1989. Processing the nonstructural polyproteins of Sindbis virus: nonstructural proteinase is in the C-terminal half of nsP2 and functions both in cis and in trans. J.Virol. **63:**4653-4664.
31. **Harvey, R., K. Brown, Q. Zhang, M. Gartland, L. Walton, C. Talarico, W. Lawrence, D. Selleseth, N. Coffield, J. Leary, K. Moniri, S. Singer, J. Strum, K. Gudmundsson, K. Biron, K. R. Romines, and P. Sethna.** 2009. GSK983: a novel compound with broad-spectrum antiviral activity. Antiviral Res **82:**1-11.
32. **Hazeki, K., K. Nigorikawa, and O. Hazeki.** 2007. Role of phosphoinositide 3-kinase in innate immunity. Biol Pharm Bull **30:**1617-23.
33. **Hennessy, B. T., D. L. Smith, P. T. Ram, Y. Lu, and G. B. Mills.** 2005. Exploiting the PI3K/AKT pathway for cancer drug discovery. Nat Rev Drug Discov **4:**988-1004.
34. **Her, L. S., E. Lund, and J. E. Dahlberg.** 1997. Inhibition of Ran guanosine triphosphatase-dependent nuclear transport by the matrix protein of vesicular stomatitis virus. Science **276:**1845-8.
35. **Hu, J. Y., Y. Chen, and S. Schacher.** 2007. Protein kinase C regulates local synthesis and secretion of a neuropeptide required for activity-dependent long-term synaptic plasticity. J Neurosci **27:**8927-39.
36. **Irani, D. N., and N. A. Prow.** 2007. Neuroprotective interventions targeting detrimental host immune responses protect mice from fatal alphavirus encephalitis. J Neuropathol Exp Neurol **66:**533-44.
37. **Ishii, K. J., T. Kawagoe, S. Koyama, K. Matsui, H. Kumar, T. Kawai, S. Uematsu, O. Takeuchi, F. Takeshita, C. Coban, and S. Akira.** 2008. TANK-binding kinase-1 delineates innate and adaptive immune responses to DNA vaccines. Nature **451:**725-9.
38. **Ito, N., G. W. Moseley, D. Blondel, K. Shimizu, C. L. Rowe, Y. Ito, T. Masatani, K. Nakagawa, D. A. Jans, and M. Sugiyama.** 2010. The Role of Interferon-Antagonist Activity of Rabies Virus Phosphoprotein in Viral Pathogenicity. J Virol **84:**6699-710.

39. **Kaur, S., A. Sassano, B. Dolniak, S. Joshi, B. Majchrzak-Kita, D. P. Baker, N. Hay, E. N. Fish, and L. C. Platanias.** 2008. Role of the Akt pathway in mRNA translation of interferon-stimulated genes. Proc Natl Acad Sci U S A **105:**4808-13.
40. **Kaur, S., A. Sassano, A. M. Joseph, B. Majchrzak-Kita, E. A. Eklund, A. Verma, S. M. Brachmann, E. N. Fish, and L. C. Platanias.** 2008. Dual regulatory roles of phosphatidylinositol 3-kinase in IFN signaling. J Immunol **181:**7316-23.
41. **King, M. C., G. Raposo, and M. A. Lemmon.** 2004. Inhibition of nuclear import and cell-cycle progression by mutated forms of the dynamin-like GTPase MxB. Proc Natl Acad Sci U S A **101:**8957-62.
42. **Kroczynska, B., S. Kaur, E. Katsoulidis, B. Majchrzak-Kita, A. Sassano, S. C. Kozma, E. N. Fish, and L. C. Platanias.** 2009. Interferon-dependent engagement of eukaryotic initiation factor 4B via S6 kinase (S6K)- and ribosomal protein S6K-mediated signals. Mol Cell Biol **29:**2865-75.
43. **Kwon, C. H., J. Zhou, Y. Li, K. W. Kim, L. L. Hensley, S. J. Baker, and L. F. Parada.** 2006. Neuron-specific enolase-cre mouse line with cre activity in specific neuronal populations. Genesis **44:**130-5.
44. **Lehnardt, S.** 2010. Innate immunity and neuroinflammation in the CNS: the role of microglia in Toll-like receptor-mediated neuronal injury. Glia **58:**253-63.
45. **Li, J., Y. Liu, and X. Zhang.** 2010. Murine Coronavirus Induces Type I Interferon in Oligodendrocytes Through Recognition by RIG-I and MDA5. J Virol **84:**6472-82.
46. **Li, M. L., Y. H. Lin, H. A. Simmonds, and V. Stollar.** 2004. A mutant of Sindbis virus which is able to replicate in cells with reduced CTP makes a replicase/transcriptase with a decreased Km for CTP. J Virol **78:**9645-51.
47. **Lin, Y. H., P. Yadav, R. Ravatn, and V. Stollar.** 2000. A mutant of Sindbis virus that is resistant to pyrazofurin encodes an altered RNA polymerase. Virology **272:**61-71.
48. **Lund, S., K. V. Christensen, M. Hedtjarn, A. L. Mortensen, H. Hagberg, J. Falsig, H. Hasseldam, A. Schrattenholz, P. Porzgen, and M. Leist.** 2006. The dynamics of the LPS triggered inflammatory response of murine microglia under different culture and in vivo conditions. J Neuroimmunol **180:**71-87.
49. **Marques, J., J. Anwar, S. Eskildsen-Larsen, D. Rebouillat, S. R. Paludan, G. Sen, B. R. Williams, and R. Hartmann.** 2008. The p59 oligoadenylate synthetase-like protein possesses antiviral activity that requires the C-terminal ubiquitin-like domain. J Gen Virol **89:**2767-72.
50. **Melchjorsen, J., H. Kristiansen, R. Christiansen, J. Rintahaka, S. Matikainen, S. R. Paludan, and R. Hartmann.** 2009. Differential Regulation of the OASL and OAS1 Genes in Response to Viral Infections. J Interferon Cytokine Res **29:**199-207.

51. **Moisse, K., and M. J. Strong.** 2006. Innate immunity in amyotrophic lateral sclerosis. Biochim Biophys Acta **1762:**1083-93.
52. **Montgomery, S. A., P. Berglund, C. W. Beard, and R. E. Johnston.** 2006. Ribosomal protein S6 associates with alphavirus nonstructural protein 2 and mediates expression from alphavirus messages. J Virol **80:**7729-39.
53. **Nair, A. S., S. Shishodia, K. S. Ahn, A. B. Kunnumakkara, G. Sethi, and B. B. Aggarwal.** 2006. Deguelin, an Akt inhibitor, suppresses IkappaBalpha kinase activation leading to suppression of NF-kappaB-regulated gene expression, potentiation of apoptosis, and inhibition of cellular invasion. J Immunol **177:**5612-22.
54. **Nargi-Aizenman, J. L., M. B. Havert, M. Zhang, D. N. Irani, J. D. Rothstein, and D. E. Griffin.** 2004. Glutamate receptor antagonists protect from virus-induced neural degeneration. Ann Neurol **55:**541-9.
55. **Ohtani, M., S. Nagai, S. Kondo, S. Mizuno, K. Nakamura, M. Tanabe, T. Takeuchi, S. Matsuda, and S. Koyasu.** 2008. Mammalian target of rapamycin and glycogen synthase kinase 3 differentially regulate lipopolysaccharide-induced interleukin-12 production in dendritic cells. Blood **112:**635-43.
56. **Ouyang, W., J. Li, Q. Ma, and C. Huang.** 2006. Essential roles of PI-3K/Akt/IKKbeta/NFkappaB pathway in cyclin D1 induction by arsenite in JB6 Cl41 cells. Carcinogenesis **27:**864-73.
57. **Poch, O., I. Sauvaget, M. Delarue, and N. Tordo.** 1989. Identification of four conserved motifs among the RNA-dependent polymerase encoding elements. EMBO J. **8:**3867-3874.
58. **Prow, N. A., and D. N. Irani.** 2008. The inflammatory cytokine, interleukin-1 beta, mediates loss of astroglial glutamate transport and drives excitotoxic motor neuron injury in the spinal cord during acute viral encephalomyelitis. J Neurochem **105:**1276-86.
59. **Prow, N. A., and D. N. Irani.** 2007. The opioid receptor antagonist, naloxone, protects spinal motor neurons in a murine model of alphavirus encephalomyelitis. Exp Neurol **205:**461-70.
60. **Reichelt, M., S. Stertz, J. Krijnse-Locker, O. Haller, and G. Kochs.** 2004. Missorting of LaCrosse virus nucleocapsid protein by the interferon-induced MxA GTPase involves smooth ER membranes. Traffic **5:**772-84.
61. **Reif, K., B. M. Burgering, and D. A. Cantrell.** 1997. Phosphatidylinositol 3-kinase links the interleukin-2 receptor to protein kinase B and p70 S6 kinase. J Biol Chem **272:**14426-33.
62. **Rivest, S.** 2009. Regulation of innate immune responses in the brain. Nat Rev Immunol **9:**429-39.
63. **Sabbah, A., T. H. Chang, R. Harnack, V. Frohlich, K. Tominaga, P. H. Dube, Y. Xiang, and S. Bose.** 2009. Activation of innate immune antiviral responses by Nod2. Nat Immunol **10:**1073-80.
64. **Sadler, A. J., and B. R. Williams.** 2008. Interferon-inducible antiviral effectors. Nat Rev Immunol **8:**559-68.

65. **Satoh, T., H. Kato, Y. Kumagai, M. Yoneyama, S. Sato, K. Matsushita, T. Tsujimura, T. Fujita, S. Akira, and O. Takeuchi.** 2010. LGP2 is a positive regulator of RIG-I- and MDA5-mediated antiviral responses. Proc Natl Acad Sci U S A **107:**1512-7.
66. **Scheidel, L. M., and V. Stollar.** 1991. Mutations that confer resistance to mycophenolic acid and ribavirin on Sindbis virus map to the nonstructural protein nsP1. Virology **181:**490-499.
67. **Takaoka, A., Z. Wang, M. K. Choi, H. Yanai, H. Negishi, T. Ban, Y. Lu, M. Miyagishi, T. Kodama, K. Honda, Y. Ohba, and T. Taniguchi.** 2007. DAI (DLM-1/ZBP1) is a cytosolic DNA sensor and an activator of innate immune response. Nature **448:**501-5.
68. **Thomson, J. A., and R. B. Perni.** 2006. Hepatitis C virus NS3-4A protease inhibitors: countering viral subversion in vitro and showing promise in the clinic. Curr Opin Drug Discov Devel **9:**606-17.
69. **Tomar, S., R. W. Hardy, J. L. Smith, and R. J. Kuhn.** 2006. Catalytic core of alphavirus nonstructural protein nsP4 possesses terminal adenylyltransferase activity. J Virol **80:**9962-9.
70. **Vasiljeva, L., L. Valmu, L. Kaariainen, and A. Merits.** 2001. Site-specific protease activity of the carboxyl-terminal domain of Semliki Forest virus replicase protein nsP2. J.Biol.Chem. **276:**30786-30793.
71. **von Kobbe, C., J. M. van Deursen, J. P. Rodrigues, D. Sitterlin, A. Bachi, X. Wu, M. Wilm, M. Carmo-Fonseca, and E. Izaurralde.** 2000. Vesicular stomatitis virus matrix protein inhibits host cell gene expression by targeting the nucleoporin Nup98. Mol Cell **6:**1243-52.
72. **Wang, N., Q. Dong, J. Li, R. K. Jangra, M. Fan, A. R. Brasier, S. M. Lemon, L. M. Pfeffer, and K. Li.** 2010. Viral induction of the zinc finger antiviral protein is IRF3-dependent but NF-kappaB-independent. J Biol Chem **285:**6080-90.
73. **Yang, P., H. An, X. Liu, M. Wen, Y. Zheng, Y. Rui, and X. Cao.** 2010. The cytosolic nucleic acid sensor LRRFIP1 mediates the production of type I interferon via a beta-catenin-dependent pathway. Nat Immunol **11:**487-94.
74. **Yoneyama, M., and T. Fujita.** 2009. RNA recognition and signal transduction by RIG-I-like receptors. Immunol Rev **227:**54-65.
75. **Yoshida, T., and M. Takeuchi.** 1991. Primary culture and cryopreservation of mouse astrocytes under serum-free conditions. Cytotechnology **5:**99-106.
76. **Zhang, Y., C. W. Burke, K. D. Ryman, and W. B. Klimstra.** 2007. Identification and characterization of interferon-induced proteins that inhibit alphavirus replication. J Virol **81:**11246-55.

Appendix to Chapter V: Supplemental Data

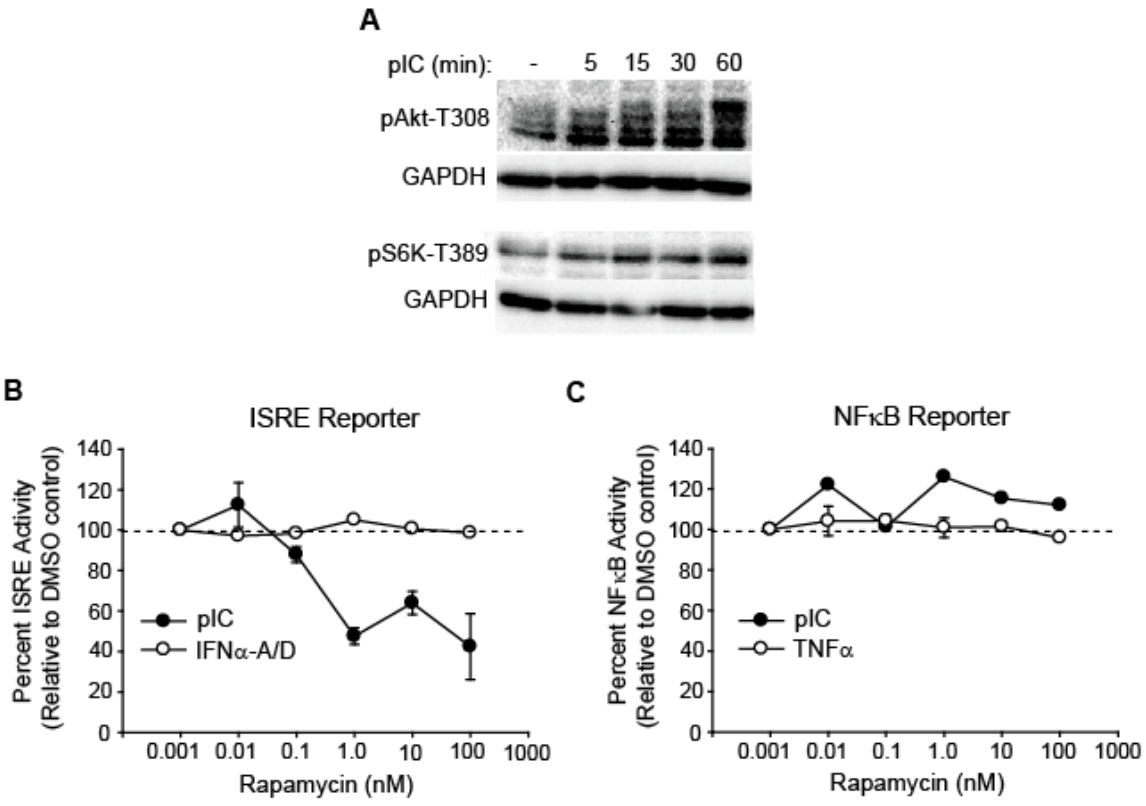

Supplemental Figure S5.1. Poly(I-C) induces Akt and S6K phosphorylation, and the mTOR inhibitor rapamycin disrupts neuronal PRR signaling. A. BE(2)-C/m cells were serum starved for 24 hours in media containing 0.5% BSA. Following serum starvation, cells were mock treated or treated with pIC (100 μg/ml) for 5, 15, 30, or 60 minutes. Then, lysates were collected and analyzed by Western blotting for phosphorylated Akt (pAkt-T308; Cell Signaling, Danvers, MA), phosphorylated S6K (pS6K-T389; Cell Signaling, Danvers, MA), or GAPDH. **B and C.** BE(2)-C/m ISRE (B) or NFκB (C) reporter cells were pre-treated with a DMSO control or serial dilutions of rapamycin (LC Laboratories, Woburn, MA) for 30 minutes followed by a mock stimulation or stimulation with 100 μg/ml pIC (B and C), 100 U/ml IFNα-A/D (B), or 50 ng/ml TNFα (C). 24 hours after stimulation, SEAP reporter activity and cell viability were assessed. Reporter activity is presented as a percent of DMSO controls. Rapamycin was not cytotoxic at any of the concentrations displayed (data not shown). Data in A represent 1 trial. Averages and SEMs from 2 trials are displayed for B and C except for the pIC stimulation of the NFκB reporter cells which represents 1 trial.